On the macromolecular dynamics of poly (dimethylamino)ethyl methacrylate in aqueous solution and its complex with polyacrylic acid.

The University Of Sheffield.

Peter James Aspinall

Submitted for the Degree of Doctor of Philosophy

Department of Chemistry, University of Sheffield

September 2010

Declaration

This thesis is submitted to the University of Sheffield for the degree of Doctor of Philosophy, having not been submitted to any other University for any degree. I declare that all work contained herein is my own work, except where referenced and acknowledged accordingly

.....

Peter Aspinall

September 2010

Acknowledgements:

I would like to thank my primary supervisor, Dr Linda Swanson for her invaluable guidance and support throughout the PhD and my secondary supervisors Professor Tony Ryan and Dr Stephen Rimmer without whom the project could not have gone ahead.

I would also like to thank Dr's Ramune Rutkaite, Benjamin Ryan and Rasika Fernando for their help in the early stages of the project and Kathryn Swindells and Katie Brown for acting as invaluable sounding boards. I would also like to thank Melanie Hannah for her much appreciated technical assistance.

I would like to thank everyone who I have worked with in the polymer labs over the past few years, there have been many and the advice, suggestions and friendly working environment I have got from each of you has been greatly appreciated.

The EPSRC is gratefully acknowledged for providing support in the form of finance for the project.

Finally, I would like to thank my family for their continuing support.

Abstract:

This project explored the aqueous solution dynamics of the polydimethylaminoethyl methacrylate (PDMAEMA) and polyacrylic acid (PAA) systems using fluorescence spectroscopy techniques.

PDMAEMA and PAA were synthesised several times using free radical polymerisation techniques with different fluorophore labels included in synthesis. The resulting polymers were explored with a selection of fluorescence techniques including time resolved anisotropy measurements, fluorescence decay lifetimes and steady state fluorescence studies.

Initial solution dynamics of these polymer systems indicate that the PDMAEMA exhibits a tightly coiled structure at high pH values and adopts an uncoiled conformation at low pH values. PAA exhibits a loose coil conformation at particularly low pH values but adopts an open extended conformation from around pH 4.5. The study also shows that the amine groups within PDMAEMA can affect the fluorescence of labels within the polymer.

Studies of the polymer samples in the presence of salts show that even small amounts of salts added to either system elicits a change in the polymer systems and these are generally most prominently shown to increase with small salt concentrations, with concentrations of over 1M often having a much lesser effect. It can generally be seen that the addition of salt to either system promotes the coiling of the polymer. In the case of PAA this is a much tighter coil and in PDMAEMA a lowering of the pH at which the polymer exhibits coiling is seen.

Studies of systems made up of both polymers show complicated behaviour in the systems with the main effects being shown when the pH of the system is such that one or the other polymer system is ionised and acting in a similar manner to that of the salts.

Table of contents:

Acknowledgements.....(i

Abstract.....(ii

Chapter 1: Introduction..... 1

1.1: Stimuli responsive polymers.....1

1.2: Polymer brushes.....8

1.3: Luminescence.....9

1.4: Fluorophores.....11

1.5: Energy Transfer.....13

1.6: Fluorescence Lifetime.....17

1.7: Time Resolved Anisotropy Measurements.....18

1.8: Studies of the interactions between two polymer systems.....22

1.9:Aims and objectives of the present work.....23

Chapter 2: Experimental.....25

2.1: Preparation and synthesis of materials for linear polymers.....25

2.1.1: Solvents.....25

2.1.2: General reagents.....25

2.1.3: Polymerisation initiator.....26

2.1.4: Fluorescent probes and labels.....26

2.1.4.1: acenaphthylene.....26

2.1.4.2: (9-anthryl)methyl methacrylate.....27

i) Reagent preparation.....27

ii) Synthesis.....27

2.1.5: Monomer preparation.....28

2.2: Polymer preparation.....29

2.2.1: poly-2-(dimethylamino)ethyl methacrylate preparation.....29

2.2.2: poly-acrylic acid preparation.....35

2.3: Characterisation.....37

2.3.1: Molecular weight determination.....37

2.3.2: Yield calculations.....37

2.3.3: Label content.....38

2.3.4: Polymer brushes.....45

2.3.4.1: Macroinitiator preparation.....45
2.3.4.2: Synthesis of labelled poly-2-(dimethylamino)ethyl methacrylate brushes.....45
*i)*Preparation of the initiator surface.....45
*ii)*Binding of macroinitiator to slide surface.....46
*iii)*Syntheis of AMMA labelled PDMAEMA brushes.....46
*iv)*Synthesis of ACE labelled PDMAEMA brushes.....48
*v)*Results of brush synthesis.....48
2.4: Fluorescence measurements.....49
2.4.1: preparation of samples for photophysics studies.....49
2.4.2: Instrumentation.....49
*i)*TRAMS.....49
ii) Fluorescence lifetime measurements.....50
iii) Steady state fluorescence.....51
Chapter 3: Fluorescence investigations of the solution behaviour of pH responsive polymers.....52
3.1: Fluorescence measurements of linear polydimethylaminoethyl methracrylate (PDMAEMA) polymers in aqueous solution.....52
3.1.1: Steady state spectra of linear PDMAEMA in aqueous solution.....52
3.1.2: Fluorescence lifetime measurements of linear PDMAEMA samples in aqueous solution.....62
3.1.3: Time Resolved Anisotropy Measurements on linear PDMAEMA samples in aqueous solution.....69
3.2: Fluorescence measurements of linear polyacrylic acid (PAA) in aqueous solution.....75
3.2.1: Steady state spectra of linear PAA polymers in aqueous solution.....75
3.2.2: Fluorescence lifetime measurements of linear PAA samples in aqueous solution.....82
3.2.3: Time Resolved Anisotropy Measurements on linear PAA samples in aqueous solution.....88
Chapter 4: Fluorescence investigation of pH responsive polymers in the prescence of various salts.....95
4.1.1: Steady state spectra of linear PDMAEMA polymers in aqueous solution in the presence of NaCl.....95

4.1.2: Fluorescence lifetime measurements of linear PDMAEMA samples in aqueous solution in the presence of NaCl.....101
4.1.3: Time Resolved Anisotropy Measurements on linear PDMAEMA samples in aqueous solution in the presence of NaCl.....108
4.1.4: Steady state spectra of linear PDMAEMA polymers in aqueous solution in the presence of $CaCl_2$.....111
4.1.5: Fluorescence lifetime measurements of linear PDMAEMA samples in aqueous solution in the presence of $CaCl_2$.....115
4.1.6: Time Resolved Anisotropy Measurements on linear PDMAEMA samples in aqueous solution in the presence of $CaCl_2$.....122
4.2.1: Steady state spectra of linear PAA polymers in aqueous solution in the presence of NaCl.....125
4.2.2: Fluorescence lifetime measurements of linear PAA samples in aqueous solution in the presence of NaCl.....129
4.2.3: Time Resolved Anisotropy Measurements on linear PAA samples in aqueous solution in the presence of NaCl.....136
4.2.4: Steady state spectra of linear PAA polymers in aqueous solution in the presence of $CaCl_2$.....139
4.2.5: Fluorescence lifetime measurements of linear PAA samples in aqueous solution in the presence of $CaCl_2$.....144
4.2.6: Time Resolved Anisotropy Measurements on linear PAA samples in aqueous solution in the presence of $CaCl_2$.....152
Chapter 5: Fluorescence investigation of potential complexation between polydimethylaminoethyl methacrylate and polyacrylic acid in aqueous solution.....158
5.1: Fluorescence Energy Transfer Measurements.....158
5.1.1: Steady state spectra of an aqueous solution of unlabelled PDMAEMA and ACE-AMMA labelled PAA at various pH values.....158
5.1.2: Fluorescence lifetime measurements of an aqueous solution of ACE-AMMA labelled PAA and unlabelled PDMAEMA at various pH values.....163
5.1.3: Time Resolved Anisotropy Measurements on an aqueous solution of ACE-AMMA labelled PAA and unlabelled PDMAEMA at various pH values.....166
5.2.1: Steady state spectra of an aqueous solution of ACE-AMMA labelled PDMAEMA and unlabelled PAA at various pH values.....169

5.2.2: Fluorescence lifetime measurements of an aqueous solution of ACE-AMMA labelled PDMAEMA and unlabelled PAA at various pH values.....175
5.3: Fluorescene Intermolecular Energy Transfer.....178
5.3.1: Steady state spectra of an aqueous solution of ACE labelled PAA and AMMA labelled PDMAEMA at various pH values.....178
5.3.2: Fluorescence lifetime measurements of an aqueous solution of ACE labelled PAA and AMMA labelled PDMAEMA at various pH values.....184
Chapter 6: Conclusions.....187
Chapter 7: Future work.....189
References.....190

Chapter 1: Introduction

1.1: Stimuli responsive polymers

Stimuli-sensitive [1], or 'smart' polymers, are a substantial class of polymer that undergo a conformational change when a particular condition is met. These can be defined as 'polymers that undergo relatively large and abrupt, physical or chemical changes in response to small external changes in the environmental conditions.' [2] Such polymers can be classified as environmentally-sensitive or intelligent but they all classify the same group.

The environmental changes mentioned above can be either physical or chemical in nature. Physical conditions that can alter the polymer conformation include a change in temperature, electric or magnetic field changes, or mechanical stress. Chemical stimuli include changes in pH, changes in ion concentrations of solutions or a direct response to another chemical agent. Regardless of the stimulus, the response is brought about by a change in the interaction between components of the polymer or by interactions between the polymer and the solvent environment.

The most commonly studied stimuli responsive polymer is poly(N-isopropyl acrylamide) or PNIPAM. PNIPAM is a temperature responsive polymer system which exhibits an open, uncoiled state at low temperatures and at temperatures above its Lower Critical Solution Temperature or LCST. For PNIPAM this occurs around 32°C at which it forms a collapsed coil-like conformation which aggregates together. This response comes about through a balance of backbone hydrophobic interactions and hydrophilic interaction of the pendant groups. PNIPAM has a drastic enough difference between its two stable states that a visual difference is seen. As the temperature is increased above PNIPAM's LCST a clear solution will turn visibly cloudy.

PNIPAM is studied extensively for a number of reasons: It is easy to synthesise but more importantly the LCST is easy to modify by addition of either hydrophobic or hydrophilic co-monomers which with lower or raise the LCST respectively. This is particularly useful with the

LCST already being relatively close to the physiological temperature of the human body. PNIPAM has for example been looked at as a controllable release system for drugs, using aspirin as the model for this release. [3] PNIPAM has not only been looked at using fluorescence systems,[4, 5] but also using microscopy and light scattering techniques.[6] There is interest in using PNIPAM as part of a system to track cell transplantation and migration in the treatment of diseases, using treatments such as application of stem cells. [7] PNIPAM has also been looked at in other forms from a linear polymer, notably that of polymer brushes[8] and as core/shell particles.[9]

Chemically responsive polymers are usually responsive to the pH of the surrounding environment.[10] Poly(methacrylic acid) or PMAA is a commonly studied pH responsive polymer[11-13] along with the related polymer poly(acrylic acid) or PAA[11, 14-17]. Both of these polymers are poly acids. A commonly studied poly base is poly(dimethylaminoethyl) methacrylate or PDMAEMA[18, 19].

PDMAEMA is often explored not only as a homopolymer system but also in systems that use the DMAEMA monomer in conjunction with other monomers as this is a way to readily incorporate tertiary amine groups in to a macromolecular system. This helps increase the compatibility with other polymer systems and improves the adhesion characteristics when incorporated into latex emulsions [20]. The amine groups impart a cationic nature to the macromolecule and because of this the polymer is pH responsive. There are several other structurally similar monomers with pendant amine groups that are less well studied including diethylaminoethyl methacrylate and dimethylaminoethyl acrylate.

Polymers with an ionic nature at certain pH values are said to be polyelectrolytic in nature[21]. They contain easily ionisable pendant groups which are able to lose or accept protons depending on the pH of the surrounding environment. pH responsive polymers fall into two categories; weak polyacids and weak polybases.

Polyacids such as PAA donate protons at high pH, above their pKa. At low pH values, below their pKa the polymer keeps its own protons and its conformation is usually that of a tight coil because of the hydrophobic nature of the polymer backbone promoting coiling to minimise unfavourable contact with the aqueous media. When the pH is increased above the pKa there is an increase in the number of ionised pendant groups which repel one another. The polymer chain consequently adopts an open, extended, structure to minimise these repulsions. Some poly-acids, mostly notably PMAA even adopt a hypercoiled state at low pH values.[22, 23]

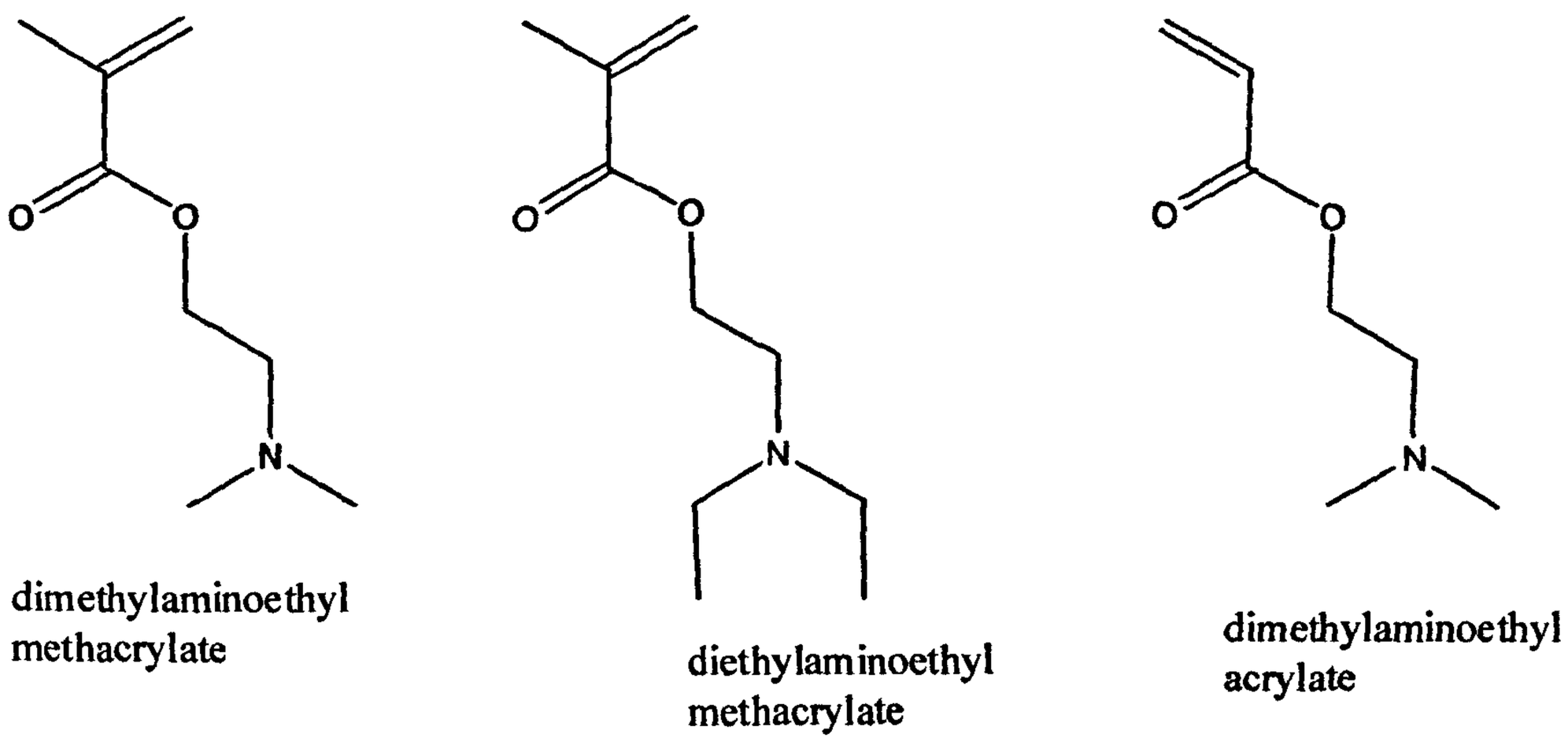

Figure 1: Chemical Structures for the monomers dimethylaminoethyl methacrylate, diethylaminoethyl methacrylate and dimethylaminoethyl acrylate.

Polybases based on monomers such as DMAEMA [18], are the opposite to the above case. At low pH, pendant side groups are protonated and the polymer chain expands to an open conformation minimising repulsive forces. At pH values above the pKa, pendant side chains are neutral and the polymer adopts a coiled conformation[19] (figure 2).

Polyacids and polybases, along with temperature-sensitive polymers, are often investigated for situations in which a part of a system needs to be responsive to an environmental change. Often these involve controlled release of a substance in a specific environment.[24-27]. For example; A number of smart polymers have been used to transport anti-cancer drugs to the site of a tumour. The drug-polymer systems tend to accumulate in the cancerous cells making them site specific. This behaviour is a consequence of the fact that these cells lack the normal waste disposal systems of bodily cells.[28-30]. The drugs transported in this way include, cisplatin [31] doxarubicin[32] adriamycin[33] and paclitaxel[34].

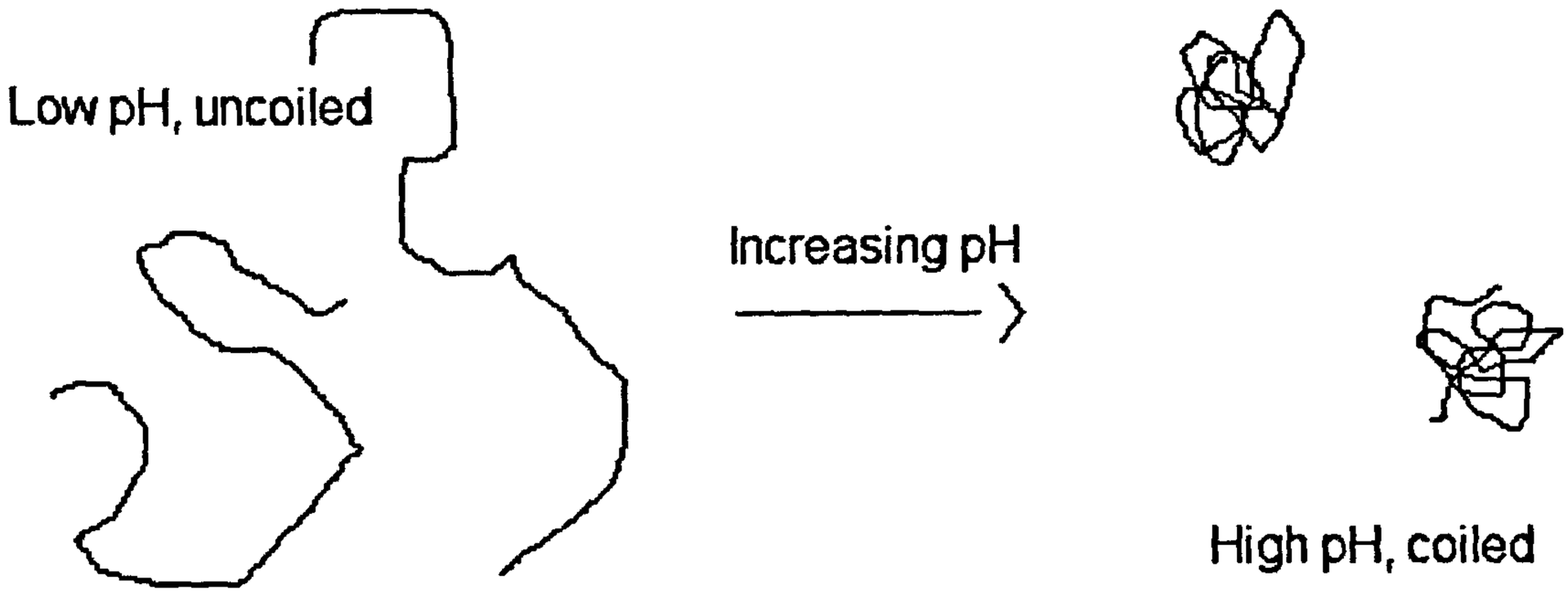

Figure 2: A schematic representation of the conformations of PDMAEMA at low and high pHs.

Polyelectrolyte polymers can also be partly ionised by dissolution in protic solvents. This can be helpful for analytical purposes and in many cases allows a fully extended polymer conformation to be adopted.

Although the pH at which the polymer conformation changes is directly related to polymer pKa this can change depending upon the ionic strength *I*,

Where $$I = \frac{1}{2}\sum_{i=1}^{n} c_i z_i^2$$ **(1.0)**

Ionic strength directly affects the observed pKa of a polymer [18, 19]. For example it is noticed that the reported pKa of PDMAEMA varies between 7.6 in a general situation[19] and 8.1, when the ion concentration is extrapolated to zero[18]. This means that with an increase in the salt concentration a small change in the pKa of PDMAEMA might be expected. This in turn will produce a slight shift in the pH at which PDMAEMA based polymers expand and contract.

It has also been shown that although PDMAEMA is pH responsive, there isn't always a defined point at which the conformation changes. [18] Despite this, the polymer also exhibits a Lower Critical Solution Temperature (LCST)[35, 36]. The LCST is the precise temperature at which the balance of hydrophilic and hydrophobic interactions in the system tips from holding the polymer in an extended open conformation to allowing the polymer to collapse into a tight coil.

This gradual change may be brought about by the same mechanism that results in a pKa for PDMAEMA of only 7.6 despite the fact that other amine containing polymers such as poly(vinylamine) have a pKa of around 9.4[37]. It has been reported that the long chains involving the amine groups in the DMAEMA repeat unit can interact in different cyclic conformations[19, 38] as shown in figure 3.

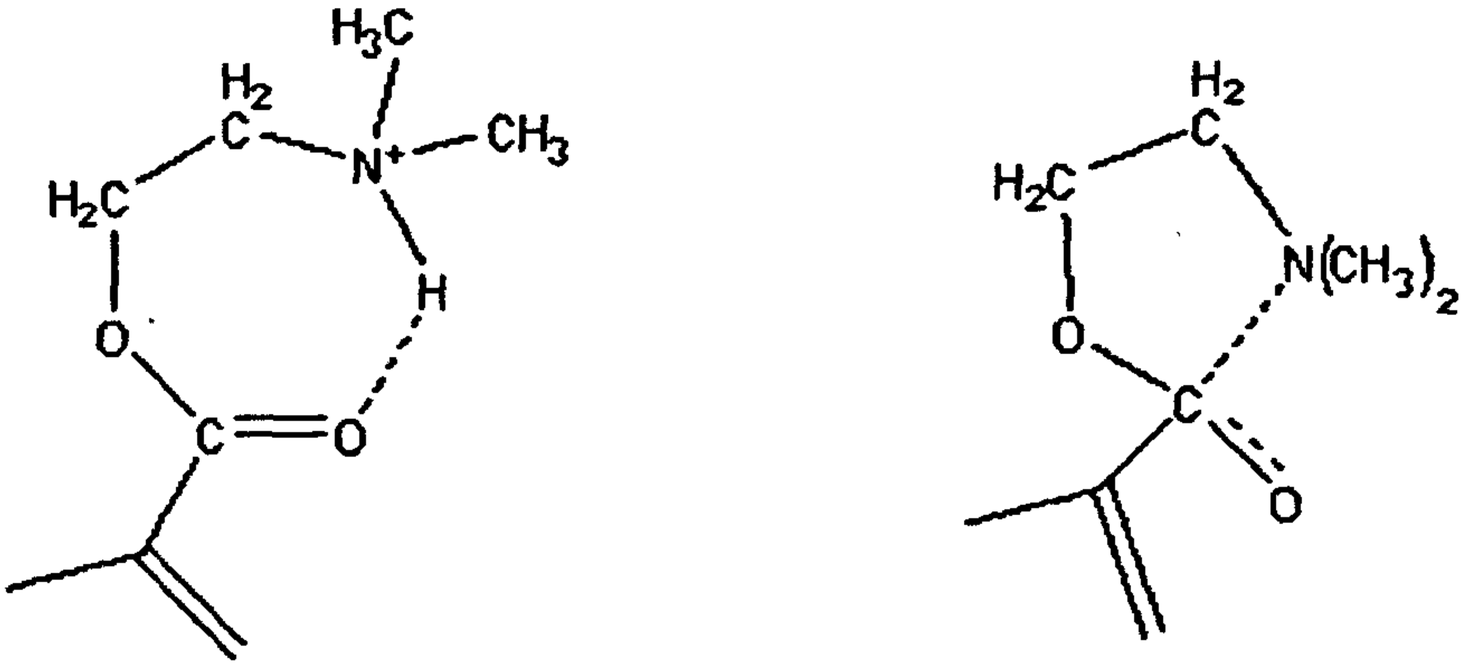

Conformation 1 Conformation 2

Figure 3: Possible conformations of the DMAEMA monomer side chains that show the potential for some stabilisation that could alter its pKa. In conformation 1 where the monomer is already protonated there is the potential for hydrogen bonding within the side chain stabilising the monomer electronic structure. Alternatively in conformation 2 interaction of the nitrogen lone pair with the carboxyl group could provide stabilisation of the electronic structure.

In conformation 1, the ionised form of the polymer would be stabilised through hydrogen bonding which raises the pKa. This does, however, require the side group to already be ionised. Conformation 2 on the other hand, delocalises the free electron pair of the amine making it unavailable for protonation and thus the pKa is instead lowered.

PDMAEMA is used in a variety of ways both as a homopolymer and as a part of a copolymer including applications in paper making, mineral processing[39], water treatment, modification of natural rubbers[40] and a number of applications related to environmental protection[41]. There are also a number of further potential applications under investigation such as using the polymer as a sensor [42] and drug delivery systems[43]. These drug delivery systems are often in the form of hydrogels which can protect their load from damaging environments until the conditions for release are met. This is particularly useful for administering sensitive proteins and peptides.[44-47]. These sorts of systems can even be used for delivery of insulin by coupling the polymer gel holding the Insulin to a glucose responsive enzyme to facilitate release.[47]

Copolymers involving DMAEMA have a number of further applications that make use of the synergistic effect between the monomers within the system. Often these are block copolymers that will form into micelles and they have uses as stabilisers in dispersion polymerisations [48]. These copolymers have also been investigated as nanoreactors and further drug delivery vehicles[49-54] as well as polymer brushes.[55, 56]

As mentioned before PAA is a commonly studied poly acid [57, 58]. Which has been the subject of variety of fluorescence studies. By way of example PAA has been studied using pyrene as a bound label for steady state measurements by Francoise Winnik and co[15]. Pyrene was also used by Vasilescu and Anghel as a probe to study PAA via steady state and time resolved quenching experiments. [59] Lindman and co again also use pyrene as a bound label and studied not only the steady state spectra of PAA but also the fluorescence decays.[60] PAA has also been extensively studied by Soutar and Swanson using multiple techniques such as time resolved anisotropy studies on an acenapthylene system in both aqueous [16] and methanolic [61] media.

Unfortunately complex interactions between water and PAA as well as the influence of intramolecular hydrogen bonding at partial ionisation complicates the fluorescence behaviour of this particular polymer system. This renders fluorescence decays none exponential as the result of the large number of microenvironments that can be created in the system[62, 63]

PAA already has a number of uses, including but not limited to acting as a dispersion agent for chemicals such as TiO2 and CaCO3, being used in super absorbent materials or as a part of thickening agents or adhesives.[64]. There has been particular study on the use of AA containing polymers as replacements for phosphate based detergents for the chelation of calcium. PAA is being considered over other replacements detergents as it also shows dispersion properties[65].

1.2: Polymer Brushes.

Polymer brushes are assemblies of macromolecules that are tethered by one end to a surface or interface[66, 67] as seen in figure 4 these systems are usually densely packed and can be grown from a number of surfaces. These assemblies can be useful in a number of applications many of which are related to the fact that when the brush is formed using a responsive polymer the thickness of the brush changes as the polymer is stimulated.[68]

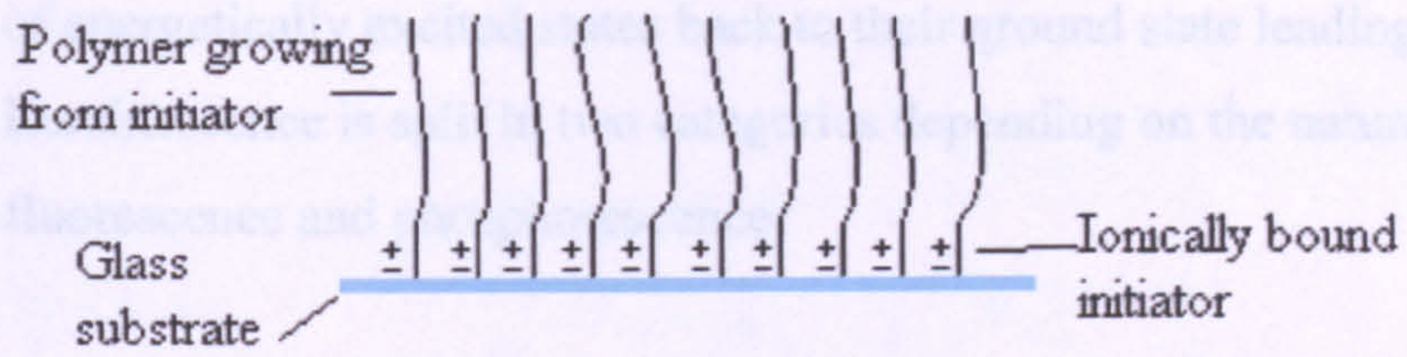

Figure 4: A diagrammatic representation of a polymer brush system using an initiator ionically bound to a glass substrate from which the polymer chains are then grown.

This can be exploited by layering the nanopores of a membrane with a pH responsive polymer brush, causing the permeability of the membrane to change. This same principle can be used on a larger scale by creating pH sensitive valves for manufacturing systems where a coated valve piece can swell to block any flow at a particular pH range. [69]

A second use of responsive polymer brushes makes use of the idea that a collapsed brush is a favourable surface for protein adsorption yet an expanded brush surface is not favourable. This leads to a system for programmable binding and release of proteins making them useful for growth of proteins and then easy release.[70] Further applications of polymer brushes also include colloidal stabilisation, lubrication, adhesion, emulsification and dispersion.

Brushes such as these are often made with polyelectrolytes [41, 71, 72] such as PDMAEMA or PAA and a proper understanding of the behaviour of these polymers in many situations is essential to understanding and predicting brush behaviour.

1.3: Luminescence

Any substance which emits light is said to be luminescent. Luminescence is caused by the decay of energetically excited states back to their ground state leading to the release of a photon. Luminescence is split in two categories depending on the nature of the excited state; these are fluorescence and phosphorescence.

Fluorescence occurs when after one electron in an electron pair has been excited from the ground state in to a higher energy state (excitation) the excited electron then decays back to the original ground state emitting energy of specific wavelengths depending on the energy gap between the two states. Excitation of a fluorophore is generally achieved by subjecting it to electromagnetic radiation with one of usually several wavelengths which will excite that particular molecule. This radiation causes the excitation of one or more electrons which are promoted from the ground state, S_0, to either the first or second electronic state, S_1 and S_2, respectively. These electrons usually relax down to the lowest level of S_1 through the processes of internal conversion and vibrational relaxation. When this then decays back to the ground state a photon of specific energy is released. This is a rapid process with typical emission rates of around $108s^{-1}$ with corresponding lifetimes of about 10 ns[73]. The internal conversion in this process means that the energy of emission is lower than the energy of excitation and so detectable at a longer wavelength, this is known as the Stokes shift.

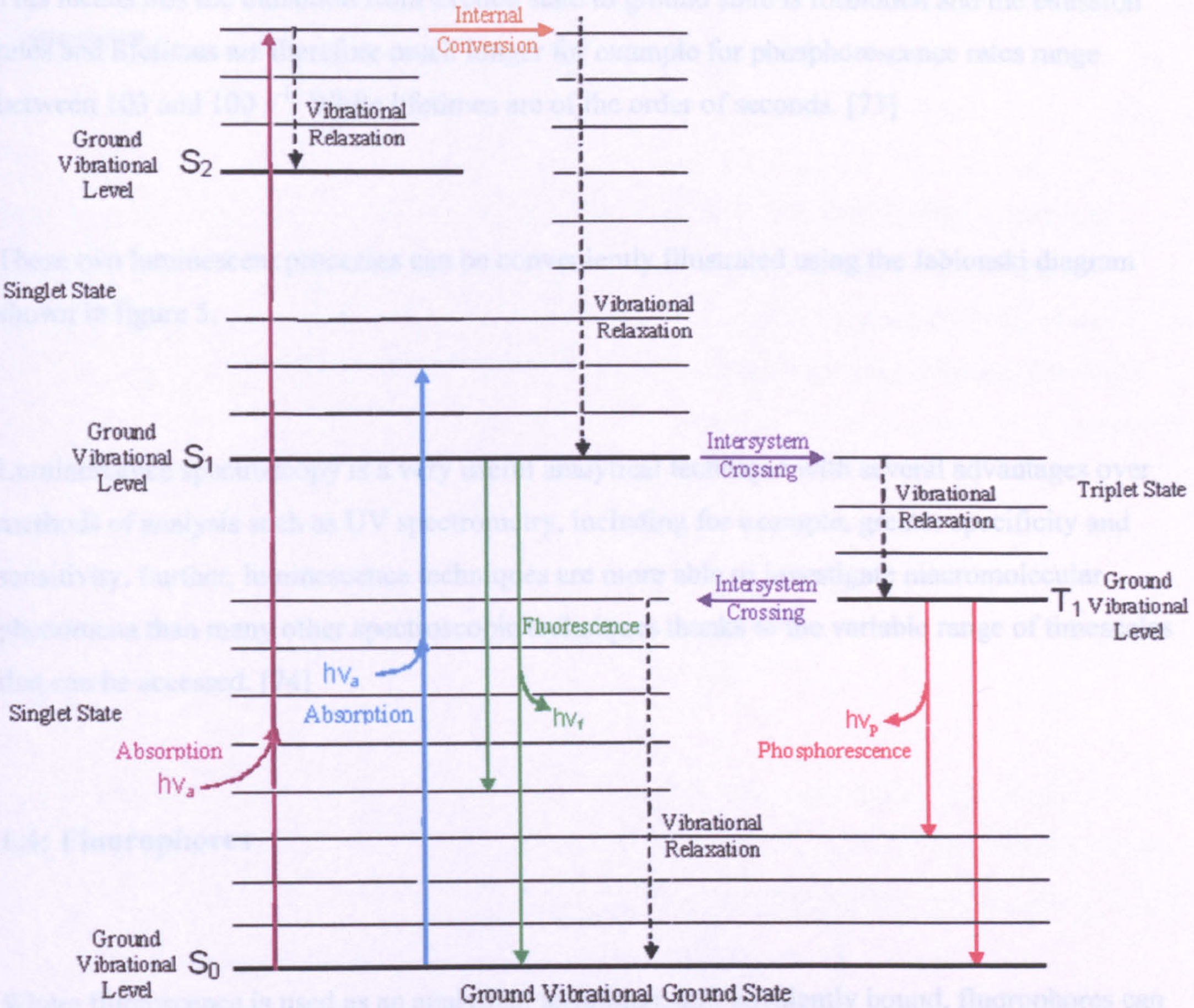

Figure 5: A simple Jablonski diagram showing the basic processes that can occur between the excitation of a fluorophore and its emission.

It is also possible for an electron in the S1 level to flip its spin and convert into a triplet excited state. It is from such species that phosphorescence emission results. This process is observed more readily in molecules containing heavy atoms such as bromine or iodine. The electron in the excited state has the same orientation as the electron remaining in the ground state where as in fluorescence, they have opposite orientations.

This means that the transition from excited state to ground state is forbidden and the emission rates and lifetimes are therefore much longer for example for phosphorescence rates range between 103 and 100 s^{-1}. While lifetimes are of the order of seconds. [73]

These two luminescent processes can be conveniently illustrated using the Jablonski diagram shown in figure 5.

Luminescence spectroscopy is a very useful analytical technique with several advantages over methods of analysis such as UV spectrometry, including for example, greater specificity and sensitivity. Further, luminescence techniques are more able to investigate macromolecular phenomena than many other spectroscopic techniques thanks to the variable range of timescales that can be accessed. [74]

1.4: Fluorophores

Where fluorescence is used as an analytical technique, non-covalently bound, fluorophores can be added to a system as a probe where the subject of the investigation is not fluorescent. These fluorophores are often able to bind in a non-covalent manner to the subject of investigation.

In polymer investigations however, it is common for one or more fluorophores to be covalently attached to the polymer during synthesis. [16] [61] This allows for the motions of individual parts of the polymer to be monitored directly. Acenaphthylene (ACE) (Figure 6) when bound to a polymer becomes a part of the backbone and its motion can therefore be considered to represent the segmental motion of the polymer. (9-anthryl) methyl methacrylate (AMMA) (Figure 6), on the other hand has a degree of rotational motion given that the part of the molecule

that is fluorescence is not directly bound to the backbone and thus can be considered to give some indication of the freedom sidechains within the polymer have.

Although it is common practice to use covalently bound fluorescent labels during polymer analysis, pyrene can also be used as a probe. [59] Pyrene is a molecule where the relative intensity of the first and third bands (at λ=373 nm and λ=384nm, respectively [75]) of its emission spectrum are dependent on the polarity of the surrounding solvent system [76, 77].

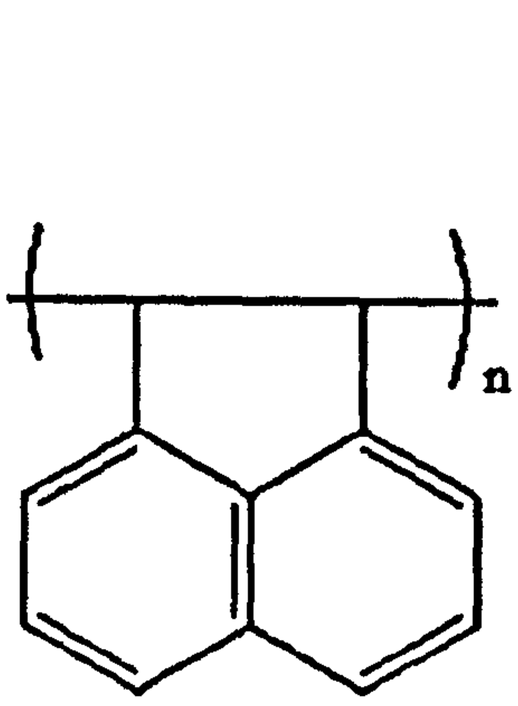

poly(acenaphthylene)

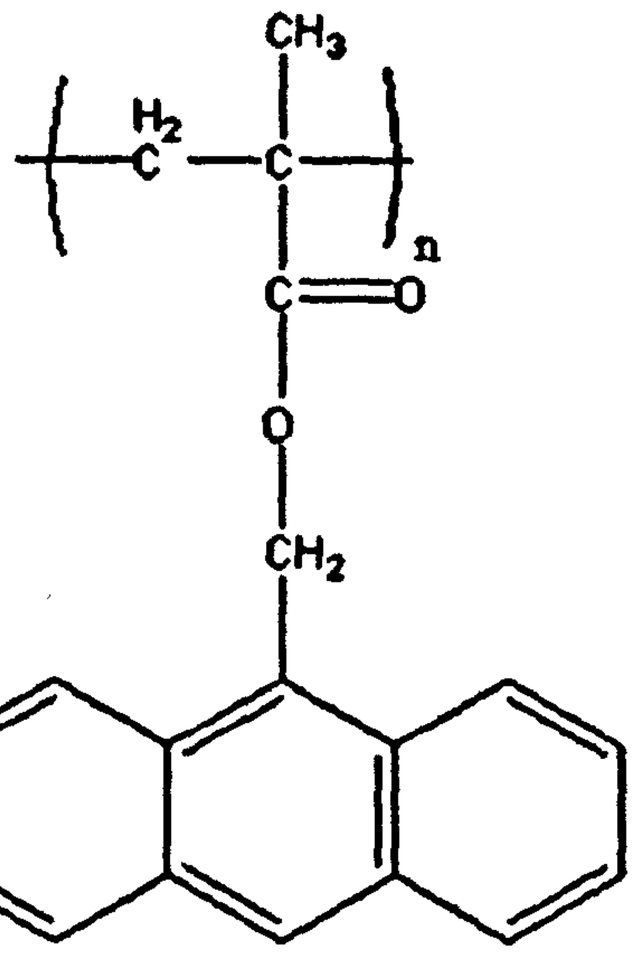

poly((9-anthryl)methyl methacrylate)

Figure 6: Chemical structures of the two common fluorescent labels to be used in this investigation, acenaphthylene and (9-anthryl)methyl methacrylate.

Pyrene can be solubilised by responsive polymers and so is a useful indication of conformation change in such systems. Poly(N-isopropylacrylamide) (PNIPAM) has been studied using pyrene. [78] The pyrene molecule can be released at the LCST of PNIPAM. The change in the pyrene's

relative intensities between being shielded in the coiled PNIPAM and being free in solution have been used to show the exact point of conformational change. Pyrene has also been used as was shown earlier in the study of poly acid systems such as PAA [59] where the pyrene is solubilised by the PAA when the polymer adopts a coiled state and is released when the polymer uncoils.

Although a possible analytical technique for use with PDMAEMA, small molecule solubilisation tests are usually used with dilute solutions of polymer. The compact nature of polymer brush systems may well mean that there is little or no change in the solubilisation of pyrene molecules whatever the pH of the system and hence bound fluorophores will be used.

1.5: Energy Transfer

One of the most used fluorescence techniques in the analysis of polymers is based on the idea of non-radiative energy transfer (NRET). This occurs whenever the emission spectrum of a donor fluorophore overlaps with the absorption spectrum of another fluorophore; the acceptor[79, 80] This is shown in general by equation (1.1)

$$D^* + A \rightarrow D + A^* \qquad \textbf{(1.1)}$$

Where D is the donor and A is the acceptor.

It is important to understand that there is no emission of radiation by the donor. Instead, in NRET the donor and acceptor interact through a dipole-dipole mechanism and the extent of the energy transfer is dependent on the distance this interaction covers.

This distance relationship proposed by Förster is related to the inverse 6th power of the physical distance between the donor and acceptor[79] as shown in equation (1.2).

$$E = \frac{R_0^6}{R_0^6 + r^6} \qquad \textbf{(1.2)}$$

Where R_0 is the Förster distance, a description of the spectral overlap between the donor and the acceptor fluorophores, E is the energy transfer efficiency, and r is the distance between the donor and acceptor molecules. The distances governed by this expression are in the range of 10-60Å, which are commonly found in macromolecules. This property of dual fluorophore systems is used analytically[79], and has been termed the 'Spectroscopic Ruler'.

As the relationship between the energy transfer is based on the distance between the donor and acceptor, when these fluorophores are bound to the polymer chain, changes in the efficiency of energy transfer give an indication of changes in the conformation of the polymer.

This relationship was extensively used by Guillet et al[81-85] in creating a new way to measure end group diffusion coefficients for a polymer, specifically PMAA. This was achieved by attaching a naphthalene donor label to one end of the polymer chains and an anthracene acceptor label to the other end of the chain. The distance between the two labels, and thus the length of the polymer is calculated to be much less than was calculated or obtained from other methods and this enhancement of the energy transfer between the two labels is attributed to end group diffusion. Guillet then later used this same 'spectroscopic ruler technique' to monitor the chain end distance in PMAA samples in dilute solutions as they underwent conformational changes through an alteration of the pH of the solution. [86]

The AMMA and ACE label combination is appropriate for the energy transfer process since there is an overlap between the donor emission and acceptors absorption spectrum (the ACE donor label undergoes excitation at 290 nm but emits at 340 nm whereas the AMMA acceptor molecule undergoes excitation at 340 nm and emits at 420 nm).

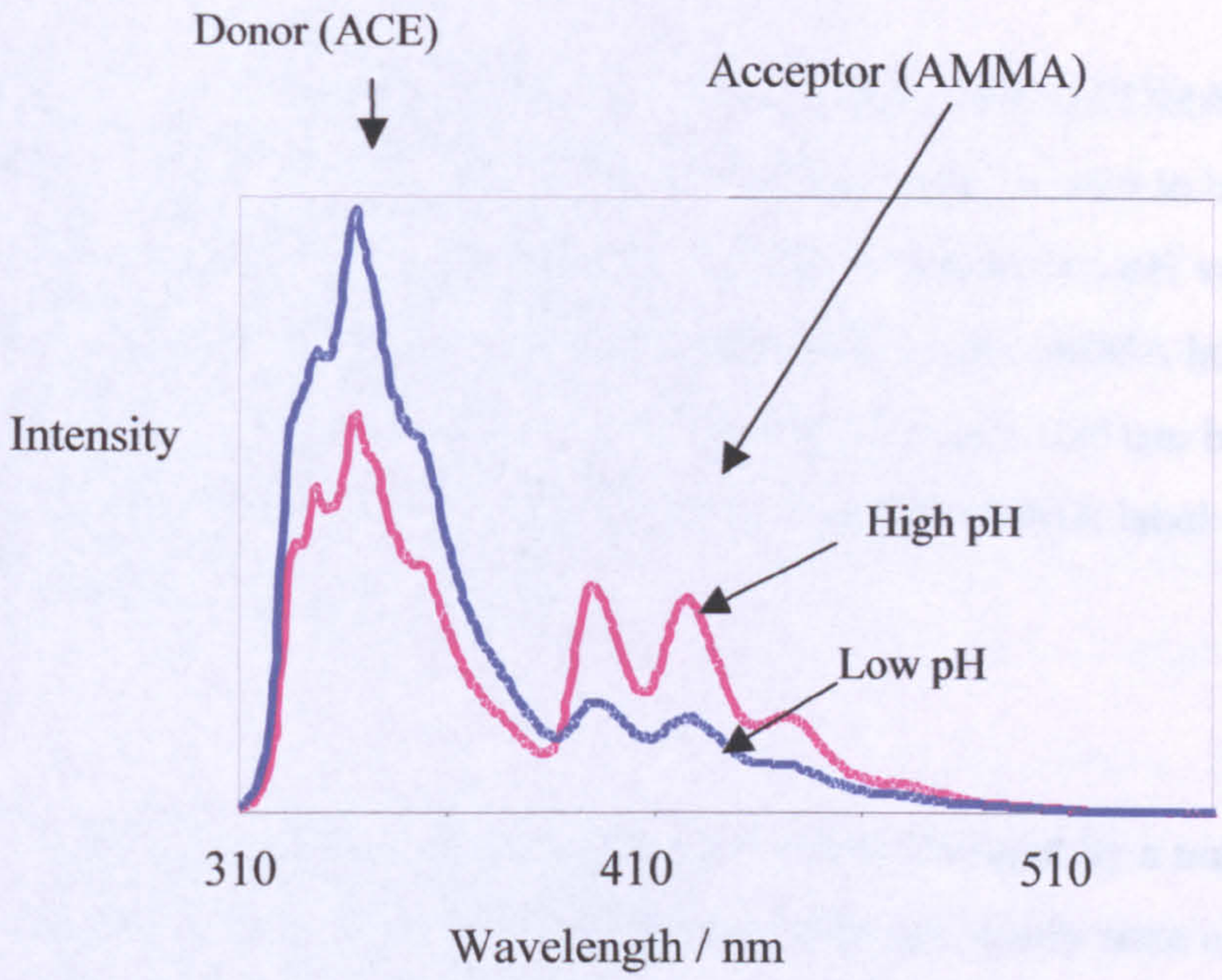

Figure 7: Spectra to show the changes that might be expected in the PDMAEMA system as the pH changes and the energy transfer between the chromophores increases. The opposite effect might be expected for the PAA sample, so greater energy transfer would be seen at low pH values where that system is likely to be in a coiled state.[87]

The energy transfer in figure 7 shows an emission from the AMMA label when the ACE label has been excited at 290 nm. This transfer of energy from the donor is a form of fluorescence quenching. The smaller the distance between the acceptor and donor fluorophores the greater the amount of energy transfer. In figure 7 the low pH blue line corresponds to an open extended

conformation as seen in the first conformation in figure 2, at high pH values the polymer chain coils up and the two fluorophores have a smaller distance separating them and energy transfer can take place. The result of energy transfer on the emission spectra is a drop in the emission from the ACE label and an increase in the emission from the AMMA label as the energy is transferred from ACE to AMMA as can be seen in the high pH line of figure 7. These readings are all done at low polymer concentrations such that the results can be considered to be those for an isolated polymer strand and changes with solution conditions can be considered to be between the polymer chain and the solution or interpolymer interaction and not intrapolymer.

The above situation is indicative of a polybase such as PDMAEMA. In the case of a poly acid such as PAA the pH values of the two lines could be seen to be reversed as the polymer responds in the opposite way to a polybase. In other words at low pH values it would be expected that the spectra shows energy transfer from the ACE to the AMMA label as the polymer has a coiled structure at this pH value. At high pH values a poly acid can be expected to adopt an uncoiled conformation and little to no emission from the AMMA label would be observed using steady state fluorescence spectroscopy.

Energy transfer can be inferred from the data obtained by a number of analytical techniques and because of this is widely used[88, 89]. Although steady state emission spectra can show NRET it also shows radiative energy transfer where the donor emission occurs and this is then absorbed by the acceptor. A second technique is required to confirm the presence of NRET in the system, the most useful is to use fluorescence energy lifetime spectra as described below.

As with the following experiments the steady state fluorescence spectroscopy measurements are taken for solutions with a low polymer concentration to limit any interpolymer interactions and instead provide a picture of what a single polymer chain conformation is likely to be at any given solution condition.

1.6: Fluorescence Lifetime

Fluorescence lifetime is the time taken from the excitation flash, the pulse of electromagnetic radiation used to excite the fluorophores, until a single fluorescent photon is detected. By creating a histogram of lifetime measurements and fitting to an exponential model the fluorescence decay lifetime can be derived. This exponential model can be single, double or even triple exponential and this is dependent on the number of environments that the fluorophore is in, the more complicated environments will give several different lifetimes. The equations follow the form

$$I_{(t)} = I_0 \exp(-t/\tau_1) + I_1 \exp(-t/\tau_2) + I_2 \exp(-t/\tau_3) \quad \textbf{(1.3)}$$

Where the fluorescence decay as a function of time, $I_{(t)}$, is related to 1 or more segments of the equation depending upon the exponential fit required. A single exponential being the first decay component (I_0), to the power of the time, t, over the lifetime, τ. And the above equation representing a triple exponential fit.

An average lifetime value can be calculated from multi-exponential fits using equation 1.4.

$$\tau = \sum_i B_i \tau_i^2 / \sum_i B_i \tau_i \quad \textbf{(1.4)}$$

The lifetime is directly related to the amount of quenching of the fluorophore; the shorter the lifetime the greater the amount of quenching. As energy transfer is a type of quenching related to

distance, a shortening of the fluorescence lifetime would indicate an increase in energy transfer and hence a coiling of the polymer's structure.

This can be directly related back to equation 1.2 as E, the energy transfer efficiency, can be said to be directly related to the lifetimes of the donor label in the presence and absence of the acceptor label, or

$$E = 1 - \frac{T_{DA}}{T_D} \tag{1.5}$$

where E equals energy transfer efficiency, T_{DA} is the lifetime of the donor label in the presence of the acceptor and T_D is the lifetime of the donor label in the absence of the acceptor.

For fluorescence investigations this means that for a suitable doubly labelled polymer a distance between the donor and acceptor labels can calculated for any given set of conditions and changes is this value with changing conditions can show a collapse or expansion of a polymer chain.

1.7: Time Resolved Anisotropy Measurements

Time Resolved Anisotropy Measurements, or TRAMS, is another widely used fluorescence technique when investigating polymer conformations. [16, 23, 61, 78, 90-96] TRAMS can be used to provide information about the rate at which artificially induced anisotropy of the chromophore is lost and thus the overall rate of motion of the chromophore, which can be directly related to the segmental motion of the polymer backbone[97].

TRAMS is based on the principle that fluorophores preferentially absorb photons whose electric vectors are aligned parallel to the transition moment of the fluorophore . This means that when polarised light is used as the excitation source, those fluorophores with an absorption transition dipole aligned parallel to the polarisation will become excited and any not aligned in this way do not absorb radiation.

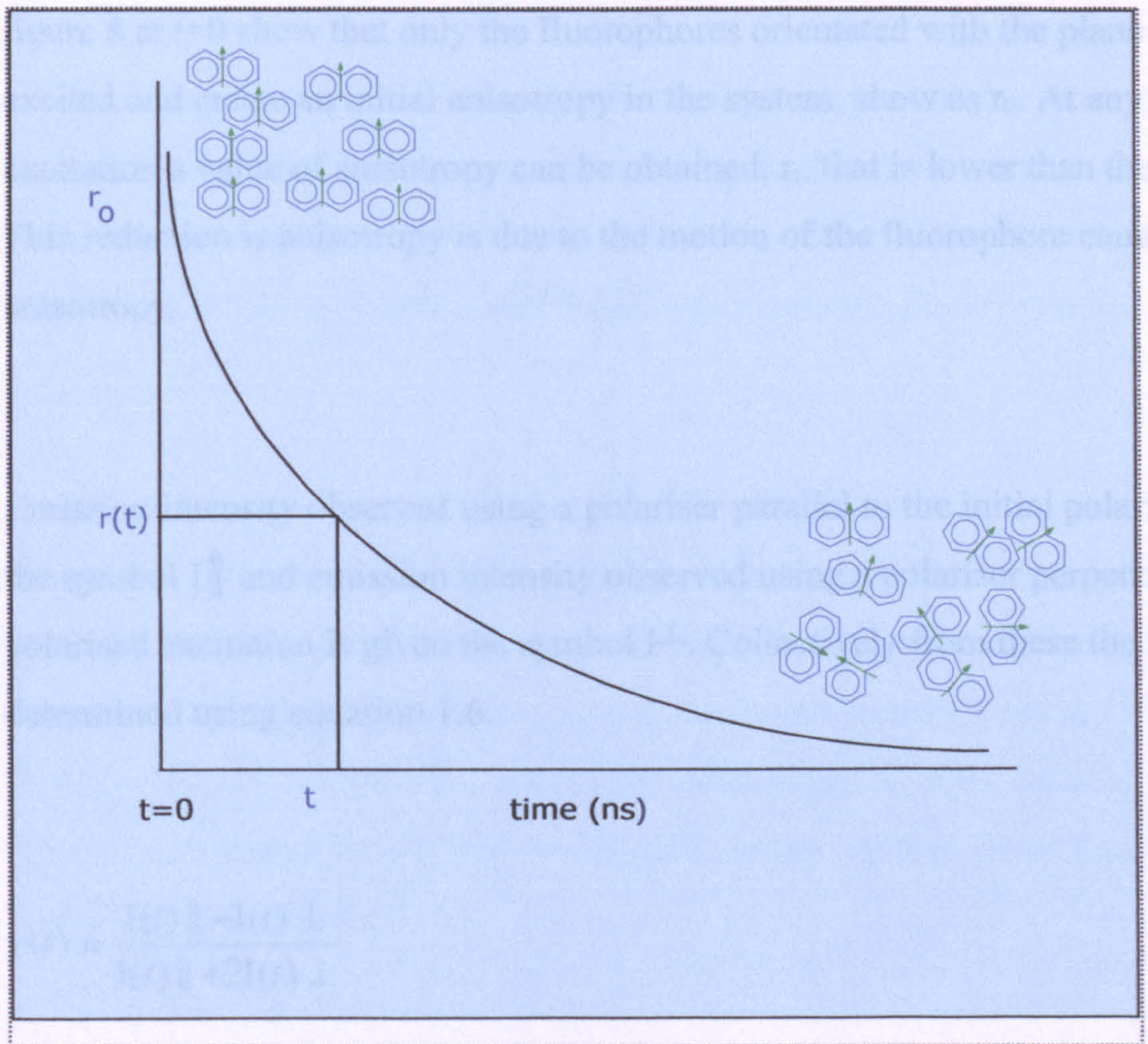

Figure 8: A schematic of the process of the TRAMS experiment.[87] The chromophore is excited at t=0 and the decay of this anisotropy is measured over time. When the chromophore is bound to a polymer chain the faster the decay the more freedom that segment of the polymer chain has.

Essentially an artificial anisotropy is created in the fluorophore population. Over time, these fluorophores will release an emission however the anisotropy will not be complete, the emission is not entirely polarised as the fluorophore population will have moved position because of the segmental motion of the polymer system. This change in anisotropy can be observed alternately

polarising the emission received by the spectrometer such that the emission and excitation polarisers are parallel or perpendicular to one another and using the relative intensities of observed emission to calculate an anisotropy value. This principle is shown diagrammatically in figure 8 above.

At t=0 polarised light is used to excited a polymer solution. The fluorophores represented in figure 8 at t=0 show that only the fluorophores orientated with the plane of the polarisation are excited and create an initial anisotropy in the system, show as r_0. At any given time, t, after the excitation a value of anisotropy can be obtained, r_t, that is lower than the original anisotropy. This reduction is anisotropy is due to the motion of the fluorophore causing the decay of anisotropy.

Emission intensity observed using a polariser parallel to the initial polarised excitation is given the symbol $I\parallel$ and emission intensity observed using a polariser perpendicular to the initial polarised excitation is given the symbol $I^{\perp}$. Collectively from these the anisotropy can be determined using equation 1.6.

$$r(t) = \frac{I(t)\parallel - I(t)\perp}{I(t)\parallel + 2I(t)\perp} \qquad \textbf{(1.6)}$$

Anisotropy, $r(t)$, is a dimensionless quantity and is independent of the overall intensity of the sample because the upper part of the equation, the intensity difference between parallel and perpendicular, is normalised by the lower part of the equation showing the overall intensity.

The most useful number obtained from TRAMS is the correlation time, τ_c, this is obtained through mathematically modelling the decay of anisotropy shown in figure 8 deriving the τ_c

value which gives a measure of the speed of segmental motion of the polymer as the fluorophores are bound to the polymer backbone. For a small molecule this value would be a representation of its rotational movement. So for example a polymer with a high degree of segmental motion, most likely to be seen when the polymer is in an open formation, would show a small correlation time. A polymer chain with a small degree of segmental motion, most likely seen when the polymer is in a coiled position would show a longer correlation time.

The mathematic principles behind the treatment of the raw data are complex and include successive iterations and compensations for systematic errors introduced by the hardware. The processing of the data is significantly reduced by using IBH software to analyse the information and this allows several methods of acquiring correlation times including impulse reconvolution. [97]

Generally data may be fitted using a single exponential curve as in equation 1.7. However in some cases not all fluorophores are in the same environment and this fit is inaccurate. For example a partially coiled polymer may hold some chromophores in a shielded, coiled, part of the polymer while others are a part of the extended areas of the polymer chain. Chromophores in these two areas will have different mobilities to one another. In such cases, a double exponential is used as in equation 1.8.

$$r(t) = a \exp\left(\frac{-t}{\tau_c}\right) \qquad (1.7)$$

$$r(t) = a_1 \exp\left(\frac{-t}{\tau_{c1}}\right) + a_2 \exp\left(\frac{-t}{\tau_{c2}}\right) \qquad (1.8)$$

This gives two correlation times relating to the two different environments that the chromophores are found in.

1.8 Studies of the interactions between two polymer systems.

Two polymer systems can complex together through hydrogen bonding although there is little difference generally between the strength of the hydrogen bonds between two polymers and between a single polymer and water molecules.

Despite a complicated fluorescence behaviour, the ease of PAA complexation has led to several fluorescence studies of the complexing of PAA with other polymers including PEO[62, 98-101].

One particular study by Wang and Morawetz[102] used a copolymer of dimethylacrylamide and acrylamide to complex with PAA to challenge the idea that polymer complexation requires two long areas of monomer residues available for hydrogen bonding that had previously been considered[103]. The degree of complexing they achieved was followed by the enhancement of the lifetime of the dansyl fluorescent label they used, a technique others had used before. [100, 104]

Complexation of PAA can lead to fluorescence decays which are even harder to interpret than for the already complex decays for a system composed solely of PAA in aqueous solution.

Despite this larger τc values for complexed PAA over that of uncomplexed PAA indicates that in such interpolymer complexes the freedom of motion for PAA is restricted as is suggested by other work [62] and further confirming that complexes do form.

It has also been shown that PAA will also complex with non-ionic polymeric surfactants in such a way that lifetime values for labels in the surfactant are also enhanced. [59]

1.9: Aims and objectives of the present work:

The literature regarding the conformational behaviour of PDMAEMA in aqueous solution is very sparse despite the fact that responsive polymers are investigated more and more for systems which can change configuration at specific environmental conditions so that they can be used as targeted small moleculare delivery sysems, responsive valves or sensors for other systems to name a few. Consequently the objective of this work is to gain a greater understanding as to the factors which affect the chain dynamics of the polymer as this directly affects what systems can make use of PDMAEMA and the degree of modification it would need for specific uses.

In order to achieve this fluorescence labels, acenaphthylene (ACE) and (9-anthryl)methyl methacrylate (AMMA) are incorporated in several different PDMAEMA samples during synthesis in order to monitor the polymer response to both the pH of the solution and the ionic strength of the solution via fluorescence spectroscopic methods.

TRAMS will be used to directly monitor polymer dynamics.

Steady state spectra and fluorescence lifetime measurements on a sample labelled with donor (ACE) and acceptor (AMMA) will be used to indicate the presence of nonradiative energy transfer, NRET, and from the lifetime measurements accurate distances between labelled segments can be derived.

Interpolymer complexation between PDMAEMA and PAA will also be investigated. TRAMS should reveal changes in the mobility of the PDMAEMA as it interacts with the polyacid.

This process will also be monitored using steady state and lifetime studies. Two distinct types of experiments will be attempted.

Intramolecular: - where the donor and acceptor are on the same polymer chain.

Intermolecular: - where the donor and acceptor are on separate chains.

Macromolecular aggregation will be detected by changes in the energy transfer efficiency.

The final stage of the project will be concerned with the synthesis of labelled PDMAEMA brushes grown from solid surfaces. The pH response of these species will be measured by fluorescence methodologies.

Chapter 2: Experimental

2.1: Preparation and synthesis of materials for linear polymers

2.1.1: Solvents

- toluene (Fischer HPLC grade)
- dioxane (Fischer general grade)
- methanol (Aldrich general and spectroscopic grade)
- water (double distilled)
- tetrahydrofuran (Fisher general and Aldrich Spectroscopic grades)
- diethyl ether (Aldrich general and spectroscopic grade)
- hexane (Fischer general and Aldrich spectroscopic grades)

2.1.2: General reagents

- sodium hydroxide (Lancaster)
- 9-anthracenemethanol (≥97%, Fluka)
- methacryloyl chloride (≥97%, Fluka)
- hydrochloric acid (≥37% Fluka)
- pyridine (BDH)
- triethylamine (99.5%, Aldrich)
- calcium hydride (BDH)
- calcium chloride

- sodium chloride

2.1.3: Polymerisation initiator

2,2'-azobisisobutyronitrile (AIBN) (BDH, 97%).

AIBN was recrystallised from methanol as follows. Over a water bath at 40°C, AIBN was dissolved in a minimum amount of methanol in a flask with stirring. The solution was filtered and left to cool before being put in the freezer overnight. The recrystallised material was then washed with a small amount of methanol and filtered under a vacuum before the entire process was repeated twice more. Following the final recrystalisation the AIBN was dried in a vacuum oven overnight at room temperature. The purified reagent was stored in the freezer at -10°C.

2.1.4 Fluorescent probes and labels

2.1.4.1 acenaphthylene (ACE) (Lancaster, 90%)

ACE was used as previously purified by the Swanson research group. ACE has one major impurity, acenaphthene, the hydrogenated form of acenaphthylene, which was removed by preparative liquid chromatography. A 60/40 vol% mixture of acetonitrile and water was used as the eluent. A LUNA ODS column was used with a UV detector set at 254nm and a flow rate of 1ml/min. The resulting solution was evaporated and dried overnight in a vacuum oven. The purity of the monomer was assessed via melting point determination using Gallenkampf apparatus with a heating rate of 5°C/min. The purity was judged to be 100% based on the documented ACE melt point of 86.5-87°C and the obtained melt point of 86.8°C.

2.1.4.2(9-anthryl)methyl methacrylate (AMMA)

i) Reagent preparation

9-anthracenemethanol (≥97%, Fluka) was dried overnight at 100°C in a vacuum oven. methacryloyl chloride (≥97%, Fluka) was used as received. Triethylamine was refluxed for 8 hours with 5wt% of anhydrous calcium hydride (BDH) then distilled on to molecular sieves. pyridine was refluxed for 3.5 hours with 5wt% of anhydrous calcium hydride and distilled onto molecular sieves. Tetrahydrofuran (THF) was kept over 10wt% of reagent of anhydrous calcium hydride for 16 hours then refluxed for 3 hours and distilled. 0.5M hydrocholoric acid solution was prepared using 48.6ml of ≥37% HCL and diluting to 1000ml with distilled water. A solution of water saturated with sodium hydrogen carbonate was prepared by dissolving a maximal amount of $NaHCO_3$ in distilled water and then filtering off any excess salt.

ii) Synthesis

The synthesis was carried out according to the literature [105] with a rough mechanism as below.

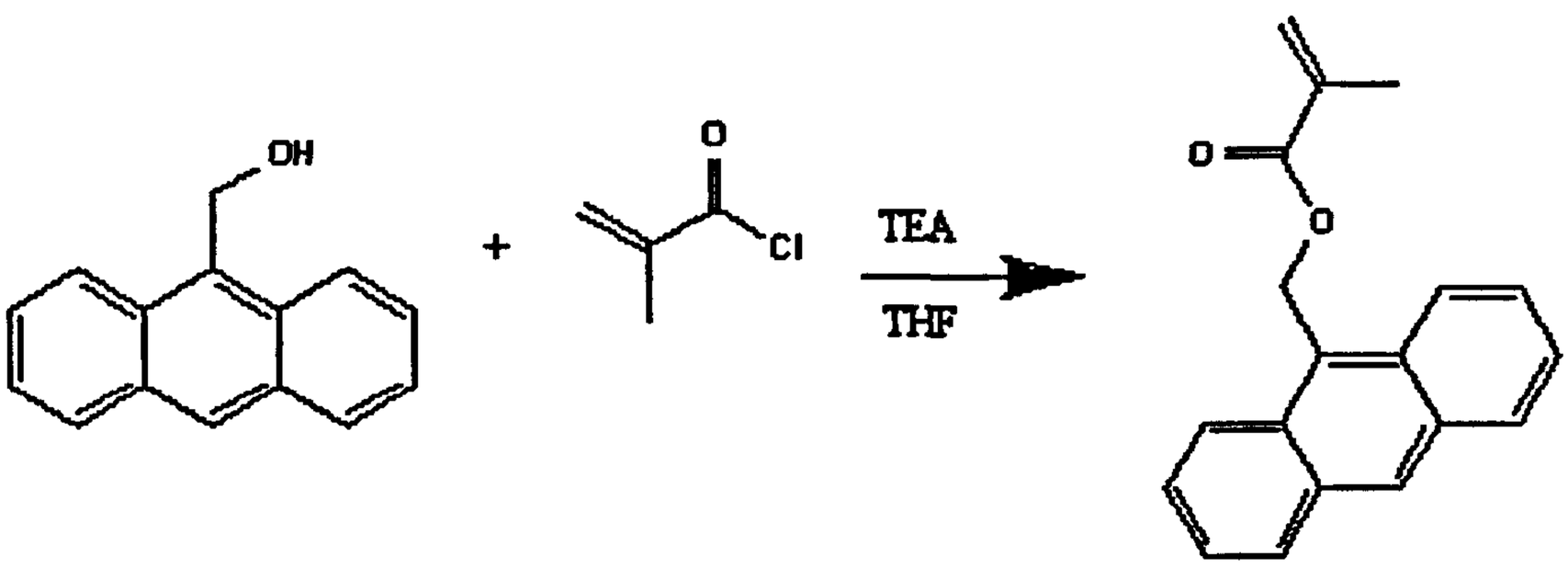

Figure 9: Basic mechanism for synthesis of AMMA from anthracene methanol.

A three necked round bottom flask (500ml) was heated and dried with nitrogen prior to the reaction. Into this 45.3g of 9-anthracenemethanol, 45ml of triethylamine and 30ml of pyridine were placed along with 260ml of THF. 35ml of methacryloyl chloride was added via a dropping funnel over 1.5 hours with stirring whilst the reaction mixture was kept at 0°C. After addition was complete the reaction was left to stir for a further hour while cooled and was allowed to warm to room temperature over the course of 3 hours.

An orange precipitate and solution were obtained from this process. Distilled water was added to the mixture, followed by diethyl ether to extract the organic product. The mixture was then separated using a separating funnel and the aqueous lower layer discarded. The orange ether extract was filtered and washed with 0.5ml HCL solution 3 times, with saturated $NaHCO_3$ solution 4 times and finally with distilled water 4 times before being dried over anhydrous magnesium sulphate. The ether was removed using a rotary evaporator and the product recrystallised 3 times from spectroscopic grade methanol. The monomer was then dried in a vacuum oven at 60°C for several days.

2.1.5 Monomer preparation

Both 2-(dimethylamino)ethyl methacrylate (98% Aldritch) and acrylic acid (99% Aldritch) were vacuum distilled to remove polymerisation inhibitor and then stored at -10°C

2.2: Polymer preparation

2.2.1: poly-2-(dimethylamino)ethyl methacrylate preparation

2-(dimethylamino)ethyl methacrylate was polymerised using an AIBN initiated free radical mechanism. This method was chosen because the free radical mechanism results in a polymer which does not contain any potential contaminants that will impede fluorescence investigations. Polymers were prepared with ACE label, AMMA label and with both ACE and AMMA labels. Solutions with a monomer to solvent weight ratio of roughly 1:3 were made using THF as the solvent.

The monomer mixes included either 0.5 wt% ACE, 1.0 wt% AMMA or 0.5 wt% ACE and 1.0 wt% AMMA. The AIBN was used at a concentration of 1g/litre.

The polymerisation solution was thoroughly degassed using a freeze-pump-thaw method and then polymerised at 60°C for not less than 16 hours.

As an example reaction mechanism the below series of figures (figures 10-16) shows the AIBN initiated free radical polymerisation of DMAEMA with ACE and AMMA labels.

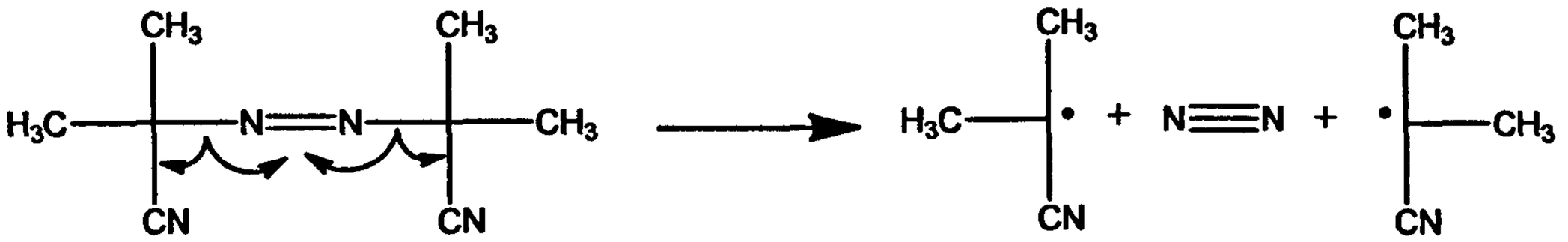

Figure 10: Heat or UV light causes the AIBN to break down in to radicals.

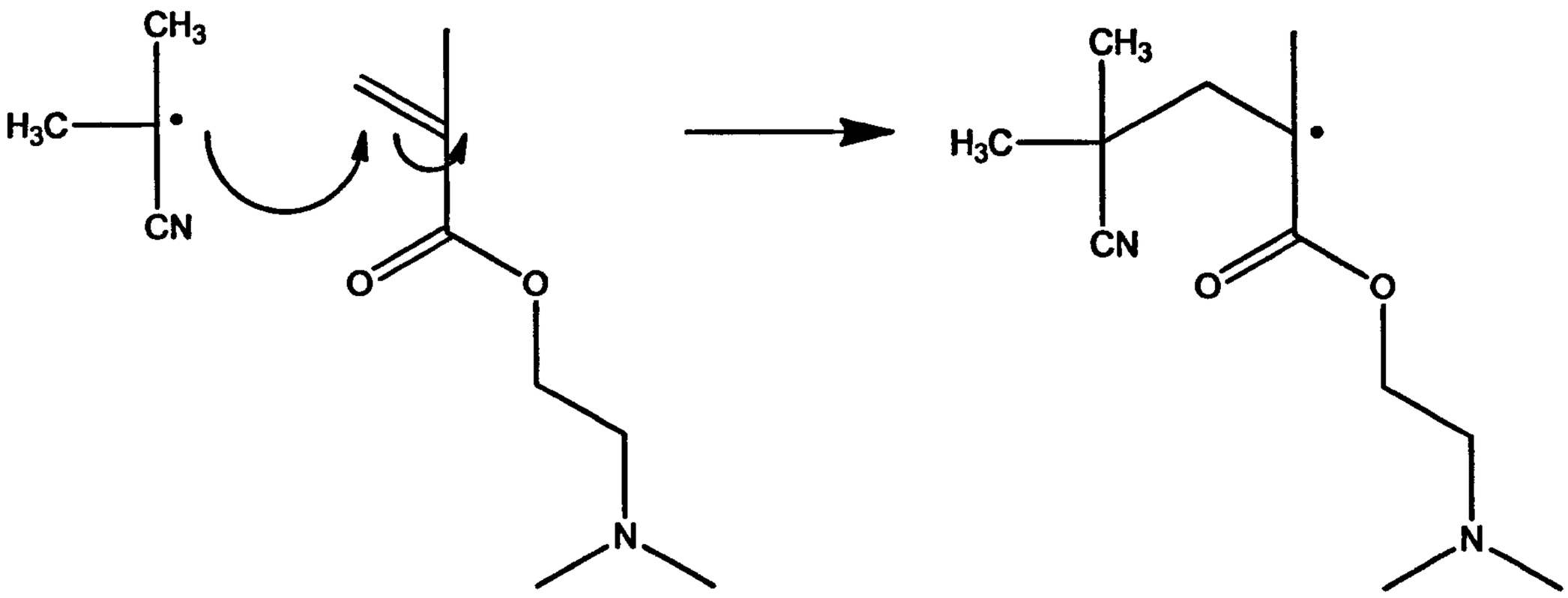

Figure 11: The radical formed from AIBN can initiate polymerisation with a DMAEMA molecule.

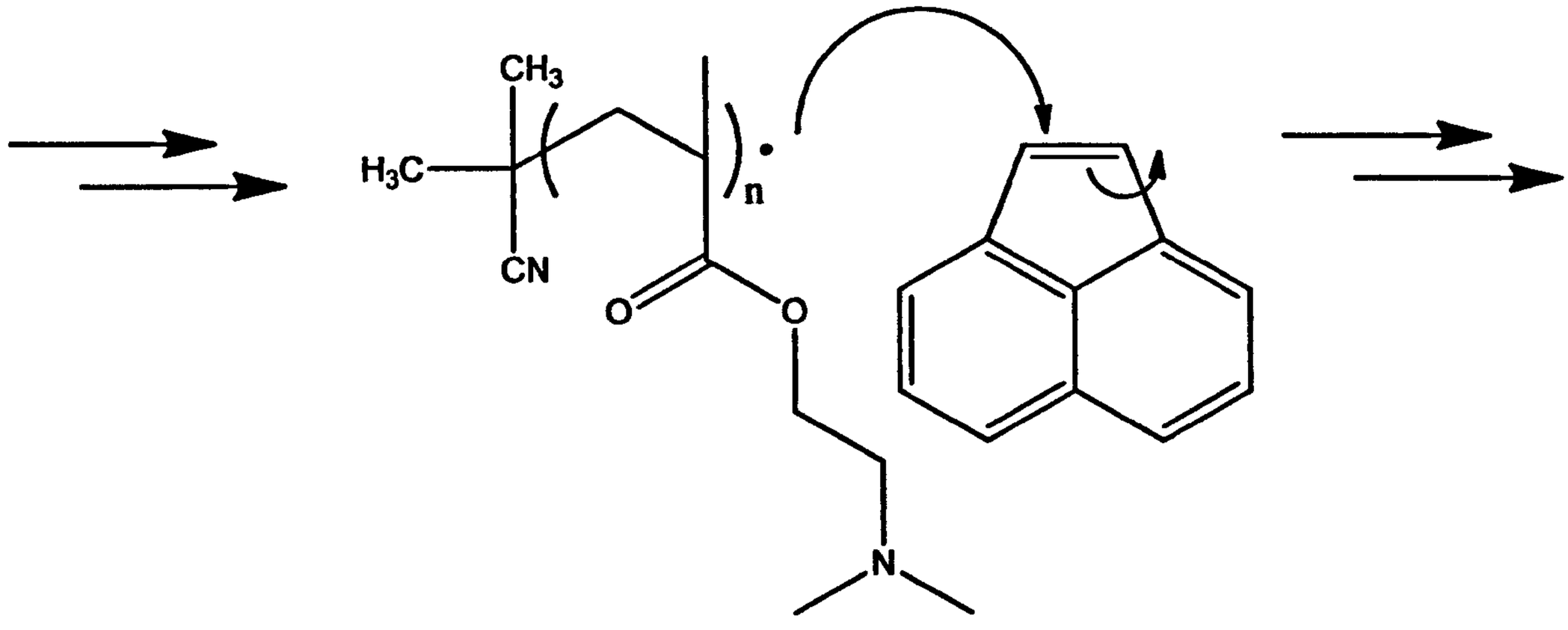

Figure 12: As polymerisation occurs addition of the ACE label can also occur as a propagation step

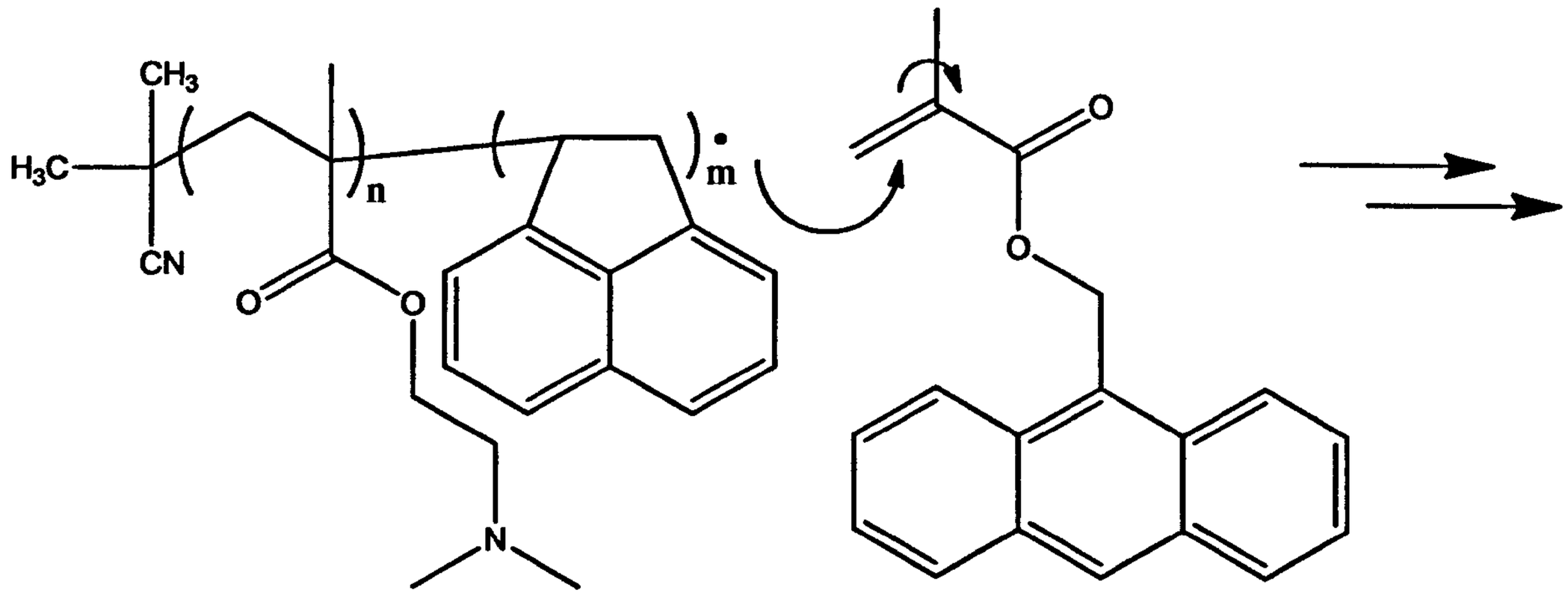

Figure 13: As can addition of the AMMA label.

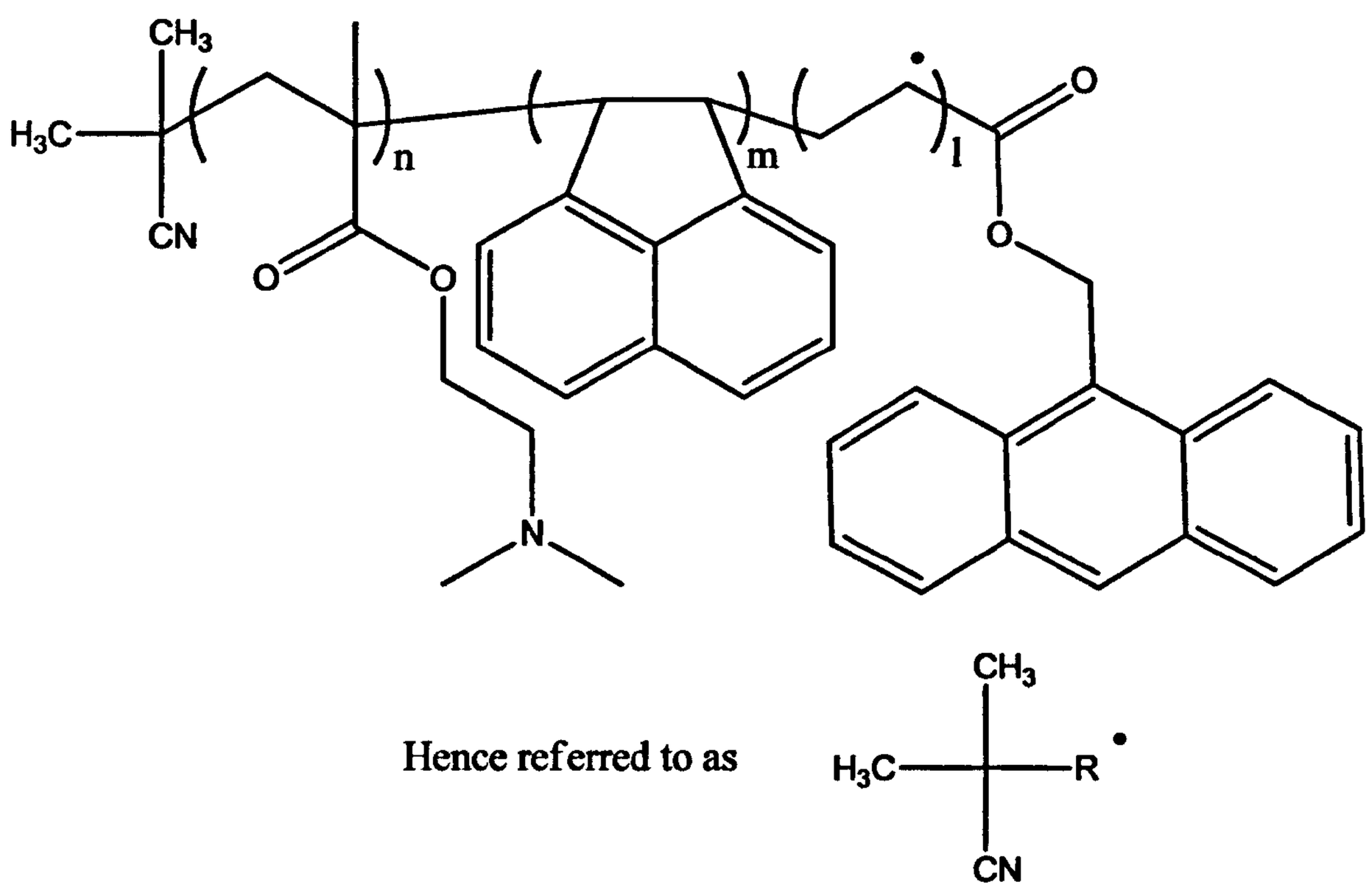

Figure 14: This leads to a species with varying numbers of molecules of DMAEMA, ACE and AMMA incorporated and the chain end being that of the initial radical formed from AIBN this is also then shown in a shortened form for ease of use in the following termination steps.

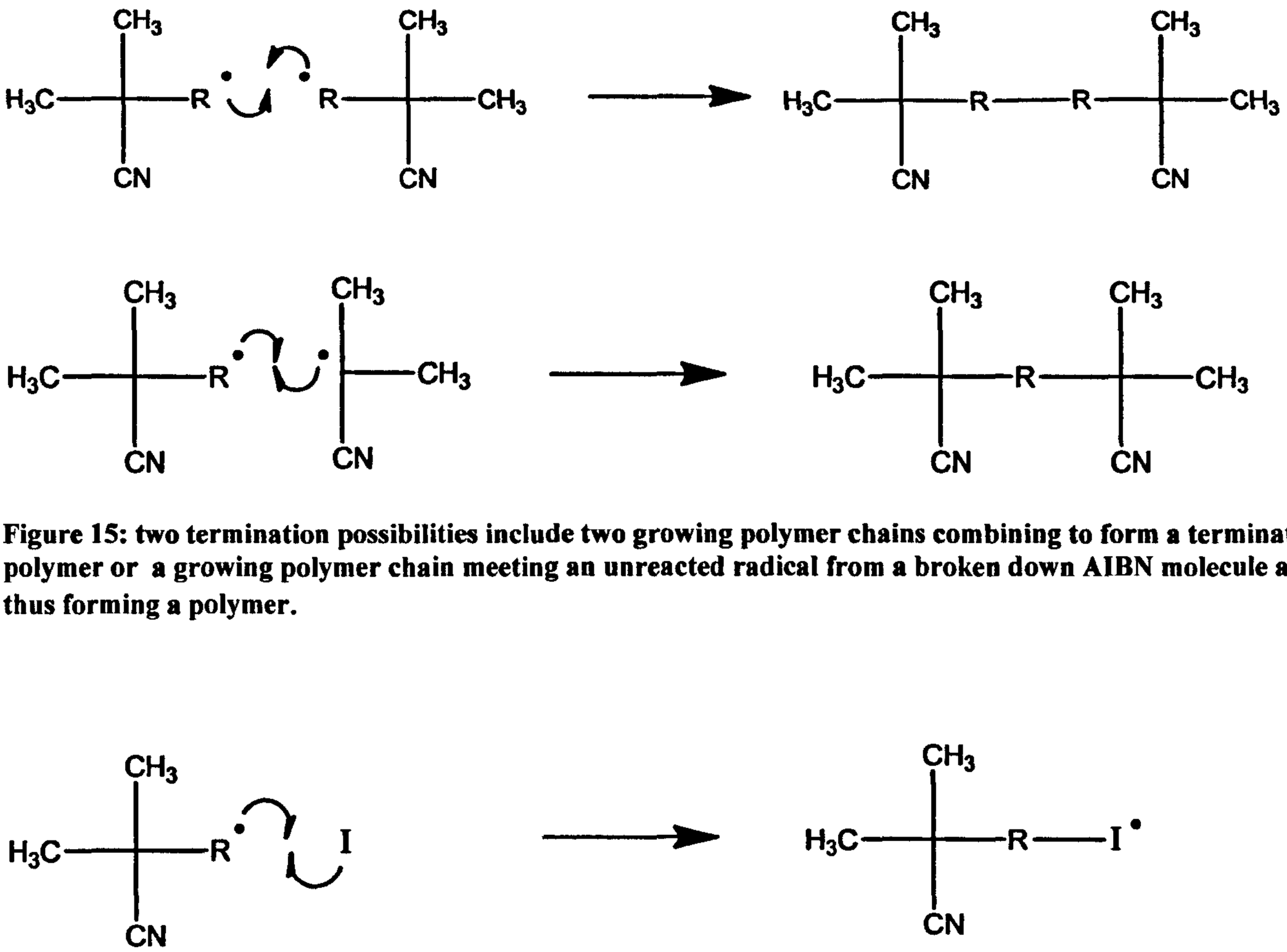

Figure 15: two termination possibilities include two growing polymer chains combining to form a terminated polymer or a growing polymer chain meeting an unreacted radical from a broken down AIBN molecule and thus forming a polymer.

Figure 16: A final termination possibility would be reaction with an inhibitor species, shown as I, which forms a much more stable radical species in effect stopping further polymerisation possible inhibitors could be oxygen molecules or large aromatic species both of which will form much less reaction radical species at the chain end.

The polymers were purified by multiple dissolutions (3 times) and subsequent precipitations using THF as the solvent and hexane as the non-solvent, this removes any unreacted monomer and labels which remain dissolved in the THF/hexane mix. The polymer was then dried in a vacuum oven over at least 24 hours before being weighed.

The resulting polymer can be said to reasonably have a structure represented as

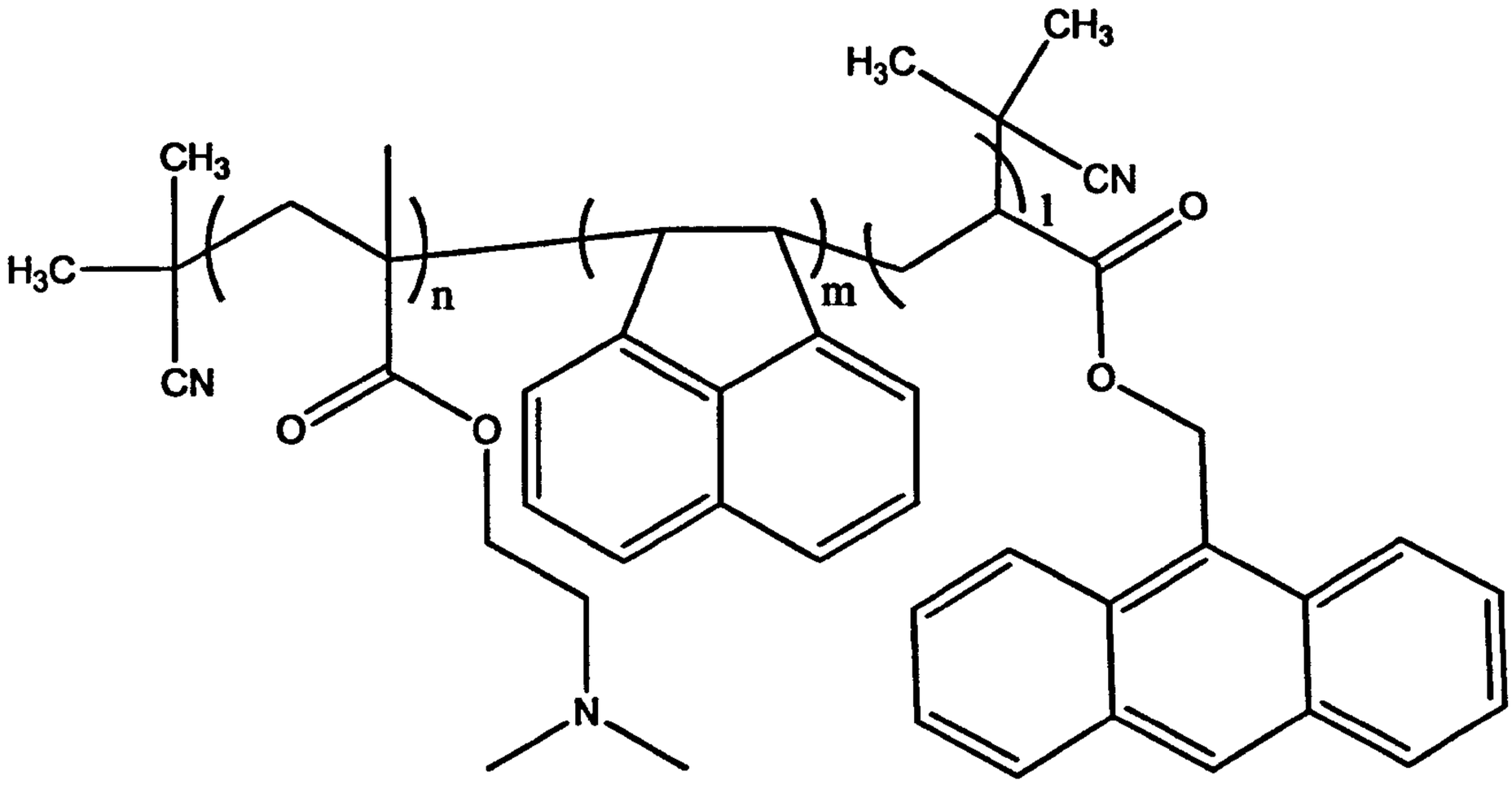

Figure 17: A representation of an ACE-AMMA-DMAEMA polymer where n would be much larger in value than m or l.

Or in the case of the other synthesised PDMAEMA samples.

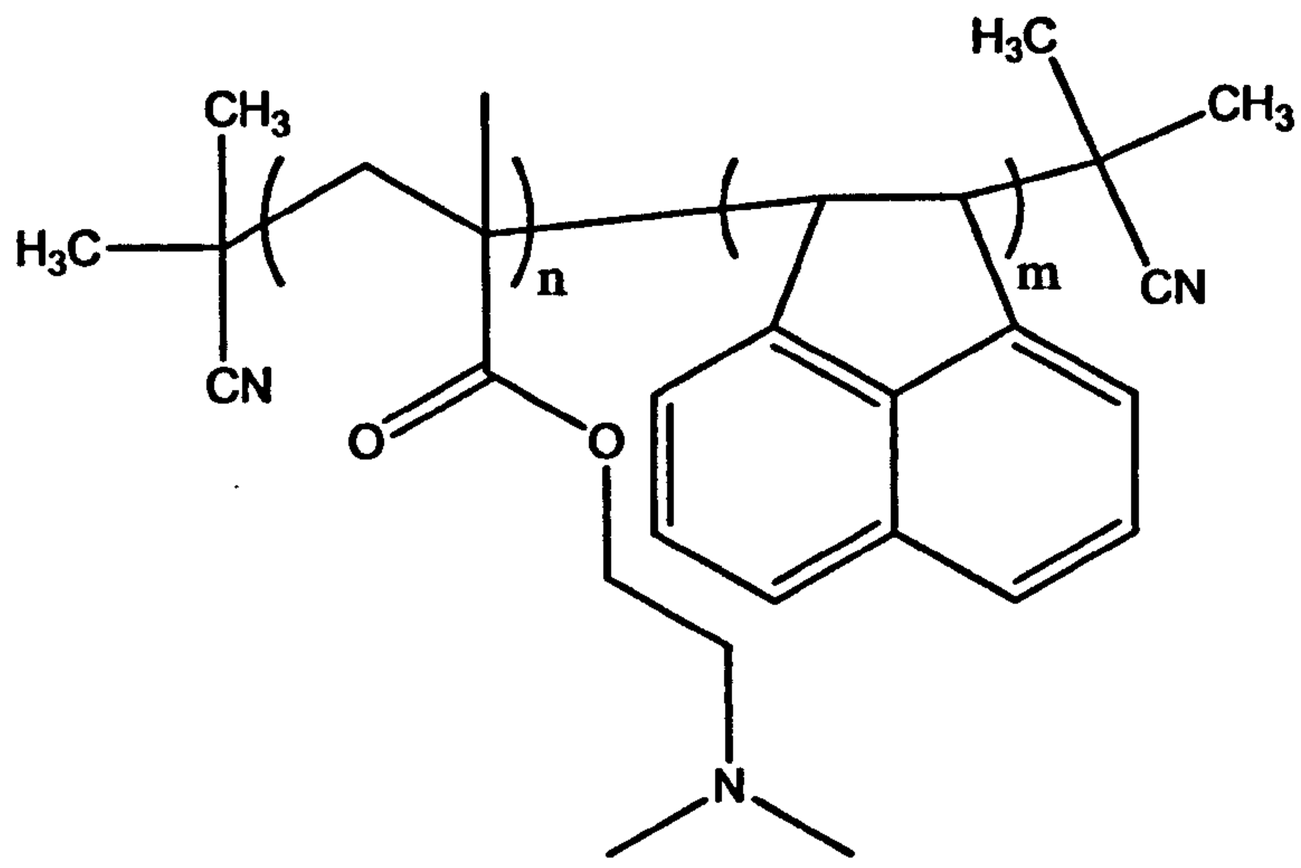

Figure 18: ACE labelled PDMAEMA where n would be significantly larger than m.

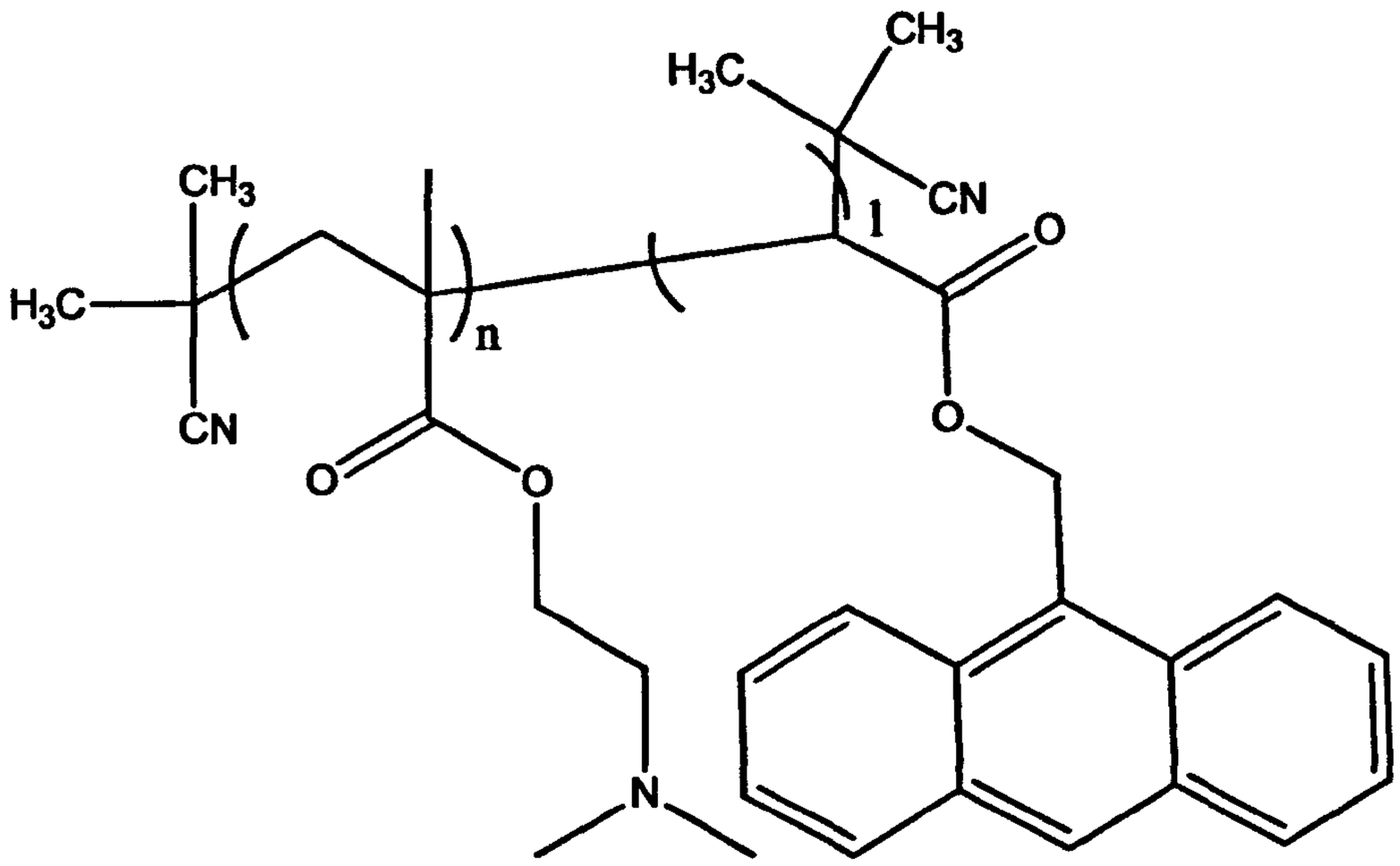

Figure 19: AMMA labelled PDMAEMA where n would be significantly larger than l

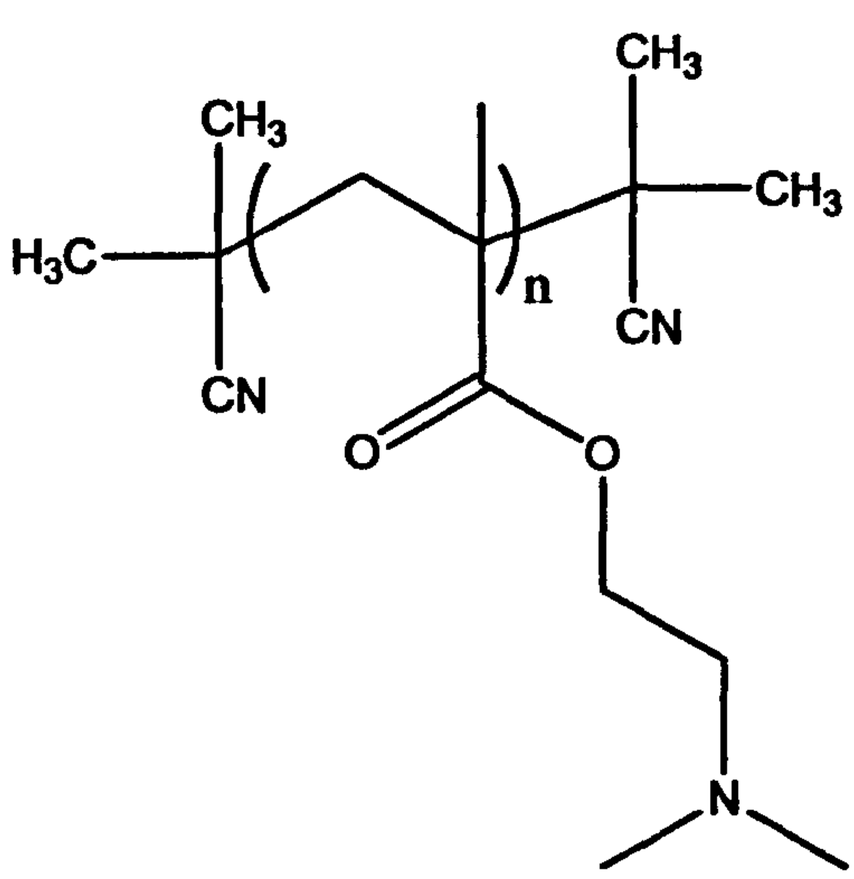

Figure 20: Unlabelled PDMAEMA

As a typical polymerisation below is listed the amounts of reagents used for the synthesis of the ACE labelled PDMAEMA sample and the resulting yield.

Solvent used: THF, 20ml

Monomer used: DMAEMA 5.8984g

Label used: ACE 29.64mg

Initiator: AIBN 30mg

The reaction was left at 60°C for 24 hours.

The resulting polymer, after reprecipitation 3 times as mentioned above, was dried and gave a final weight of 3.812g and thus a final yield of 64.3%

2.2.2: poly-acrylic acid preparation

Acrylic acid was polymerised using an AIBN initiated free radical mechanism in the same way that DMAEMA was. Polymers were prepared with ACE label, AMMA label and with both ACE and AMMA labels. Solutions with a monomer to solvent weight ratio of approximately 1:3 were made using methanol as the solvent.

The monomer mixes included either 0.5 wt% ACE, 1.0 wt% AMMA or 0.5 wt% ACE and 1.0 wt% AMMA. The AIBN was used at a concentration of 1g/litre.

The polymerisation solution was thoroughly degassed using a freeze-pump-thaw method and then polymerised at 60°C for not less than 2 hours.

The polymer was purified by multiple dissolutions (3 times) and subsequent precipitations using methanol as the solvent and diethyl ether as the non-solvent, this removes any unreacted monomer and labels which remain dissolved in the methanol/diethyl ether mix. .The produced polymer was then dried in a vacuum oven over at least 24 hours before being weighed.

The final polymers can be said to have structures and a reaction mechanism such as that for DMAEMA such that an ACE-AMMA labelled PAA sample can be shown as that in figure 21.

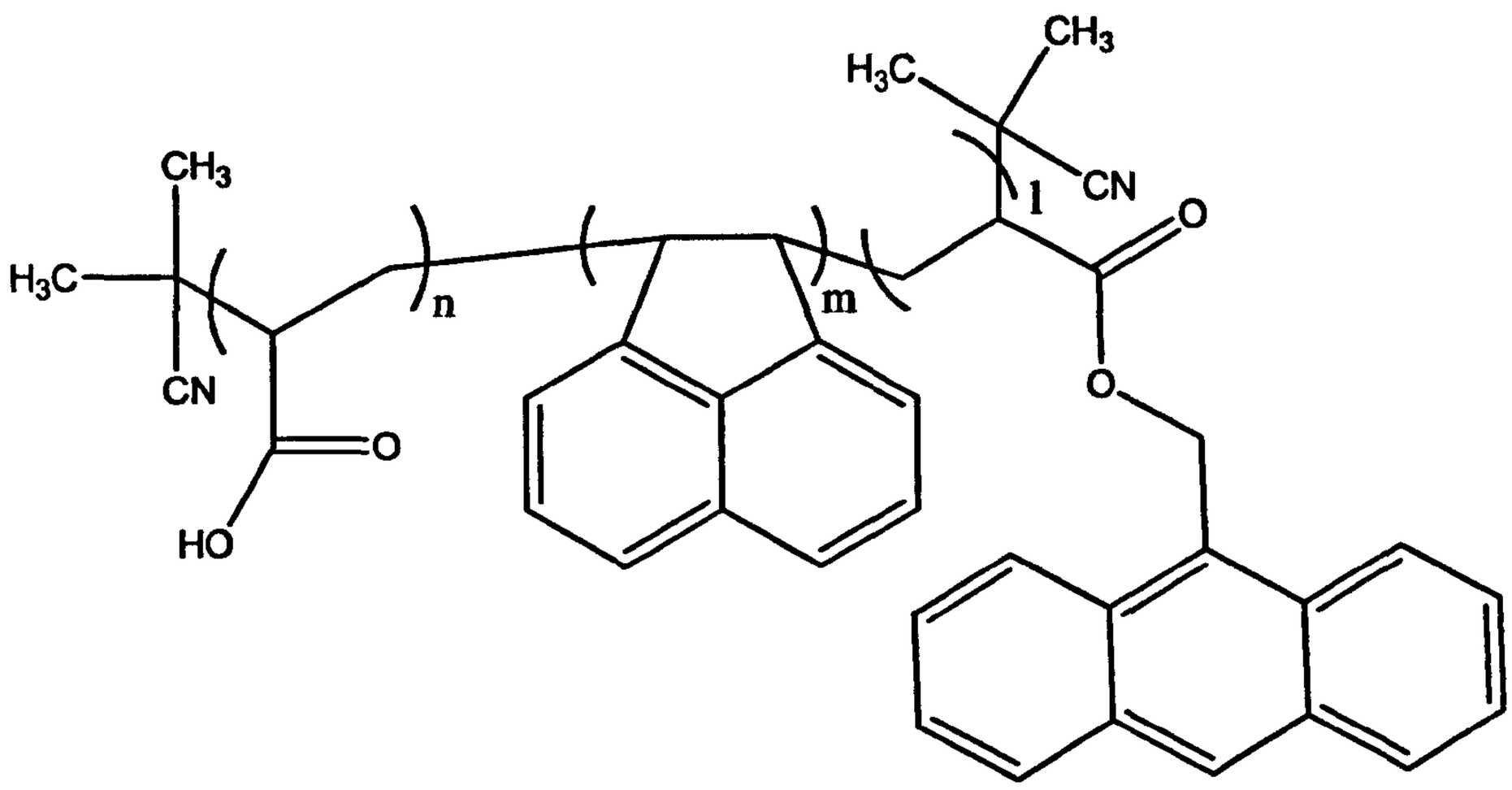

Figure 21: An ACE-AMMA labelled PAA representation where n is significantly larger than m or l when the polymerisation was initiated with AIBN.

As a typical polymerisation below is listed the amounts of reagents used for the synthesis of the ACE labelled PAA sample and the resulting yield.

Solvent used: Methanol, 20ml

Monomer used: DMAEMA 5.2523g

Label used: ACE 2.64mg

Initiator: AIBN 30mg

The reaction was left at 60°C for 24 hours.

The resulting polymer, after reprecipitation 3 times as mentioned above, was dried and gave a final weight of 2.75g and thus a final yield of 52.1%

2.3: Characterisation.

2.3.1 Molecular weight determination.

To determine the molecular mass of the resulting polymers a gel permeation chromatography (GPC) instrument was used. A refractive index detector on the Viscotek tda model 300 triple detector array was used. The system pump was an LC1150 hplc pump from Polymer Laboratories. The GPC column was stored at 70°C.

2.3.2 Yield calculations

Polymer yields were obtained through a simple calculation such that the mass of end material was expressed as a percentage relative to the mass of the monomer and label(s) used in the reaction mixture.

2.3.3 Label content

The label content of the polymers are expressed as a mole percent relative to the system which as a whole is representative of the moles of labels and monomer in the final polymer.

As the concentration of label within the polymer system is low a simple calibration plot was possible using the Beer-Lambert equation

$$A=\varepsilon cl \qquad (3.1)$$

where A is the absorbance value for a label at a particular wavelength obtained from a UV spectrometer; c is the concentration of label in the solution, l is the path length of the cell, in this case 1cm, and ε is the molar absorptivity.

The two fluorescent labels used in the polymer system cannot themselves be used for calibrations as they are insoluble in the methanol used for the spectra and also do not accurately represent the emissions of the labels in the polymer system as the polymerisation step breaks a double bond. Instead for acenaphthylene, acenapthene was used as a model compound and for 9-anthrylmethyl methacrylate, methylanthracene was used.

By plotting A against c for models of the two fluorescent label models, where A is measured at 290 nm and 370 nm for the ACE and AMMA models respectively, an ε value can be obtained for each. (These graphs are show in figures 22 and 23 and give ε values of 5930.3 mol $L^{-1}cm^{-1}$ and 26664 mol $L^{-1}cm^{-1}$ for the ACE and AMMA models respectively) Using this value, absorbance values for the labels from samples of the polymers can then be used to express the concentration of label in the system, an example of which is shown below.

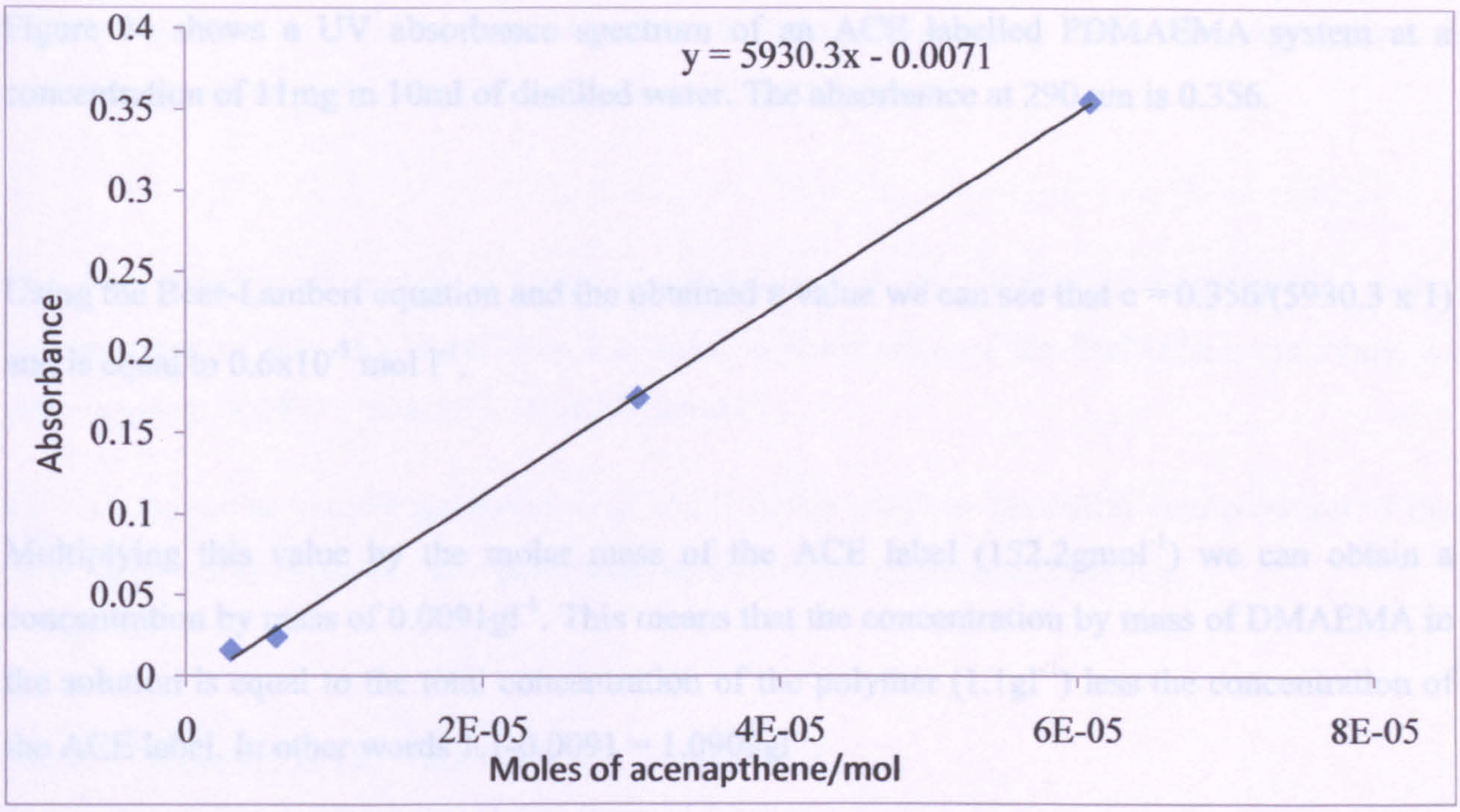

Figure 22. A calibration plot of absorbance values of an acenapthene model for the ancenaphthylene fluorophore in small molar amounts. The value before the x in the equation is the ε value required.

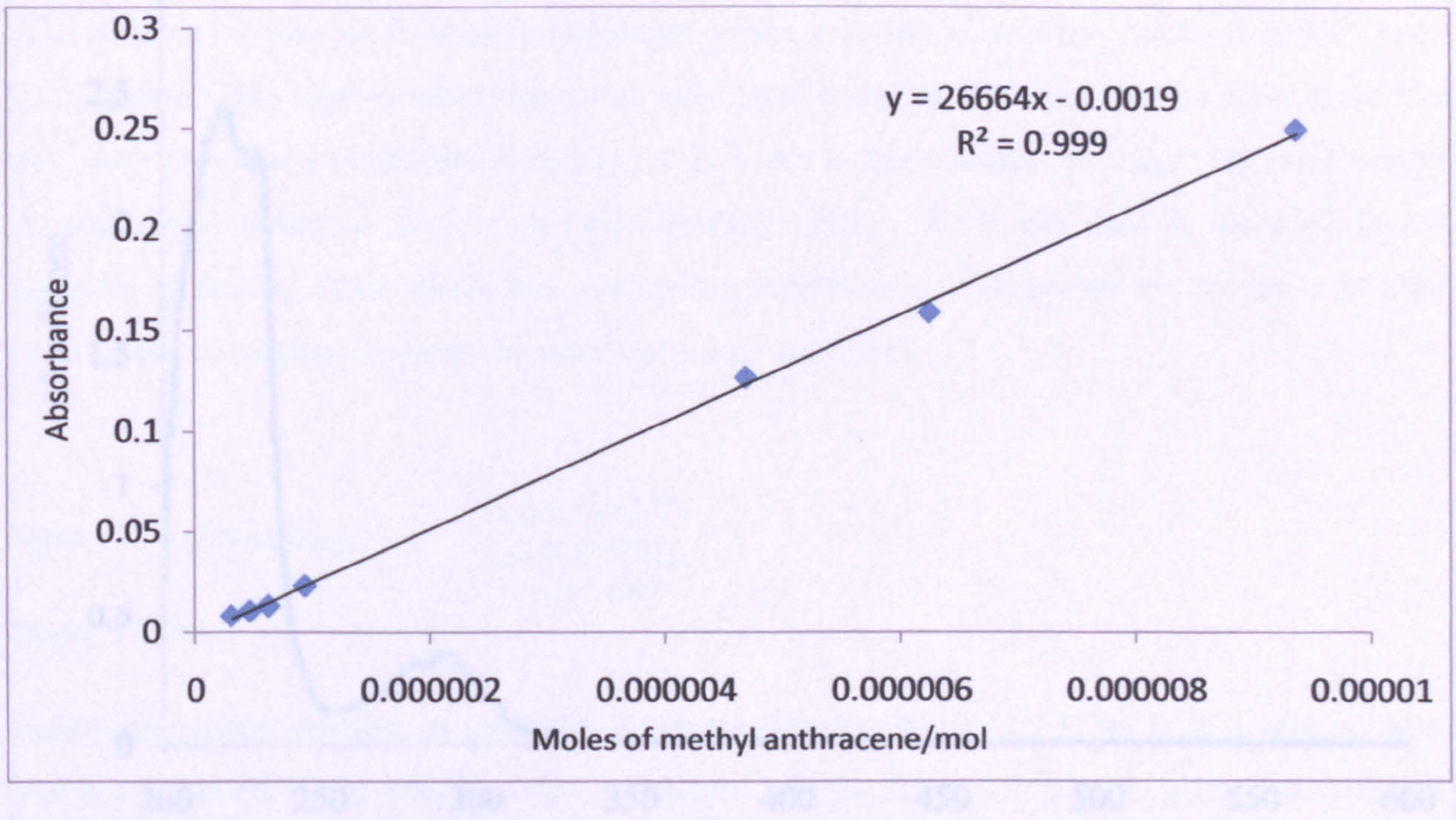

Figure 23. A calibration plot of absorbance values of a methyl anthracene model for the (9-anthryl methyl)methacrylate fluorophore in small molar amounts. The value before the x in the equation is the ε value required.

Figure 24 shows a UV absorbance spectrum of an ACE labelled PDMAEMA system at a concentration of 11mg in 10ml of distilled water. The absorbance at 290 nm is 0.356.

Using the Beer-Lambert equation and the obtained ε value we can see that c = 0.356/(5930.3 x 1) and is equal to 0.6×10^{-5} mol l^{-1}.

Multiplying this value by the molar mass of the ACE label (152.2gmol^{-1}) we can obtain a concentration by mass of 0.0091gl^{-1}. This means that the concentration by mass of DMAEMA in the solution is equal to the total concentration of the polymer (1.1gl^{-1}) less the concentration of the ACE label. In other words 1.1-0.0091 = 1.0909gl^{-1}.

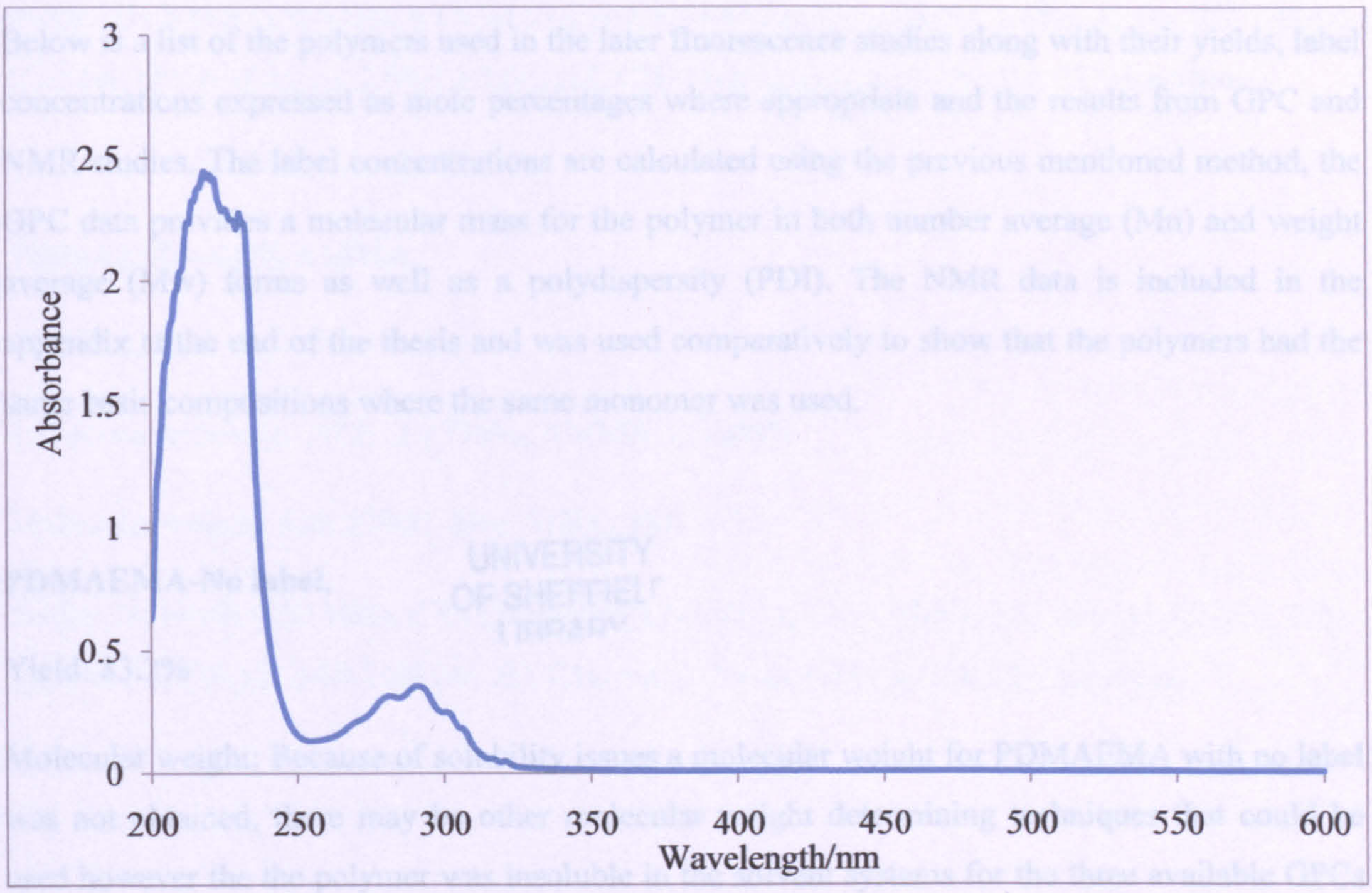

Figure 24. A UV absorbance spectrum across a wavelength range of 200 – 600 nm for an ACE labelled PDMAEMA sample in aqueous media and a concentration of 11mg in 10ml.

Converting this to a molar concentration of DMAEMA using the molecular mass of 157.2126gmol^{-1} we get a molar concentration of 0.006939mol l^{-1}.

The total number of moles of polymer substituents in the system is therefore the molar concentration of the ACE label plus the molar concentration of the DMAEMA monomer, in other words 0.006939 + 0.6x10^{-5} = 0.006999mol l^{-1} .

To find the molar percentage therefore of ACE in the polymer the molar concentration of the ACE label can be expressed as a percentage of the overall molar concentration.

(0.6x10^{-5}/0.006999)x 100 = 0.8583%

Below is a list of the polymers used in the later fluorescence studies along with their yields, label concentrations expressed as mole percentages where appropriate and the results from GPC and NMR studies. The label concentrations are calculated using the previous mentioned method, the GPC data provides a molecular mass for the polymer in both number average (Mn) and weight average (Mw) forms as well as a polydispersity (PDI). The NMR data is included in the appendix at the end of the thesis and was used comparatively to show that the polymers had the same basic compositions where the same monomer was used.

PDMAEMA-No label.

Yield: 83.2%

Molecular weight: Because of solubility issues a molecular weight for PDMAEMA with no label was not obtained, there may be other molecular weight determining techniques that could be used however the the polymer was insoluble in the solvent systems for the three available GPCs at the concentrations required. While this prevents a molecular weight determination for the

polymer it is still soluble in aqueous solutions at the masses required for the fluorescence studies and so may still be used.

NMR: 1H NMR (250 MHz, *D_2O*) δ ppm 4.18 (m, 2H, CH_2N), 2.68-2.41 (m, 2H, CH_2O), 2.25 (m, 6H, N-$(CH_3)_2$), 1.64-1.46 (m, 2H, CH_2 main chain), 1.26-0.96 (m, 3H, CH_3 backbone)

PDMAEMA-ACE

Yield: 64.3%

Label concentration: ACE: 0.8583 %

Molecular weight: Mn: 19000, Mw: 40900, PDI: 2.16

NMR: 1H NMR (250 MHz, *$CDCl_3$*) δ ppm 4.23-3.83 (m, 2H, CH_2N), 2.68-2.41 (m, 2H, CH_2O), 2.25 (m, 6H, N-$(CH_3)_2$), 2.08-1.62 (m, 2H, CH_2 main chain), 1.02 (m, 3H, CH_3 backbone)

PDMAEMA-ACE-AMMA

Yield: 43.8%

Label concentration: ACE: 1.1739%, AMMA: 0.2080%

Molecular weight: Mn: 27900, Mw: 37800, PDI: 1.35

NMR: 1H NMR (250 MHz, *$CDCl_3$*)δ ppm 4.19-3.89 (m, 2H, CH_2N), 2.53 (m, 2H, CH_2O), 2.25 (m, 6H, N-$(CH_3)_2$), 2.04-1.69 (m, 2H, CH_2 main chain), 1.02 (m, 3H, CH_3 backbone)

PDMAEMA-AMMA

Yield: 59.7%

Label concentration: AMMA: 0.2388%

Molecular weight: Mn: 16600, Mw: 38400, PDI: 2.31

NMR: 1H NMR (250 MHz, *$CDCl_3$*) δ ppm 4.15-3.91 (m, 2H, CH_2N), 2.60-2.46 (m, 2H, CH_2O), 2.31-2.19 (m, 6H, N-$(CH_3)_2$), 1.97-1.71 (m, 2H, CH_2 main chain), 1.12-0.96 (m, 3H, CH_3 backbone)

PAA-No label

Yield: 92.1%

Molecular weight: Mn: 5.900, Mw: 10.700, PDI: 1.83

NMR: 1H NMR (250 MHz, *D_2O)*δ ppm 2.36 (m, 1H, CH), 1.70 (m, 2H, CH_2 backbone)

PAA-ACE

Yield: 52.1%

Label concentration: ACE: 0.8792%

Molecular weight: Mn: 26400, Mw: 36700, PDI: 1.39

NMR: 1H NMR (250 MHz, *D_2O)*δ ppm 2.58-2.12 (m, 1H, CH), 2.03-1.00 (m, 2H, CH_2 backbone)

PAA-ACE-AMMA

Yield: 23.4%

Label concentration: ACE: 1.52.144%, AMMA: 0.0424%

Molecular weight: Mn: 19200, Mw: 26800, PDI: 1.39

NMR: 1H NMR (250 MHz, $CDCl_3$)δ ppm 2.67 (m, 1H, CH), 1.49 (m, 2H, CH_2 backbone)

PAA-AMMA

AMMA labelled PAA was synthesised however the yield was extremely low and the polymer was insoluble in any of the deuterated solvents available as well as being methanol insoluble so no characterisation was obtained and the polymer was not used.

Other polymers

Poly(dimethylaminoethyl)acrylate and poly(diethylaminoethyl)methacrylate were both attempted however synthesis of these polymers was problematic and final polymers were never obtained in a purity sufficient to undertake fluorescence studies. It proved to be impossible to precipitate the polymers in a none solvent system and the only form of isolation from the reaction mixture was through rotary evaporation of the solvent which would leave impurities such as unreacted monomer and label in the recovered polymer.

2.3.4: Polymer brushes.

2.3.4.1: Macroinitiator preparation. (Prepared by a member of Prof Steve Armes' research team.)

Two ATRP macroinitiators with cationic sites to bind to the substrate were used in the brush synthesis, to provide brushes with two different polymer binding densities. An initiator that provides a lower polymer density allows more room for the polymers to alter conformation over varying pH and has a higher binding affinity to the substrate surface. The macroinitiator that provides a higher density therefore restricts the room available for polymer strand motion as pH varies and is bound slightly less tightly to the substrate surface.

Of the two macroinitiators the first was used in surface initial polymerisations of both particles, and planar surfaces. (The second is a newer initiator and the synthesis has yet to be published.)

The macroinitiator was prepared in a three-step synthesis as shown in the literature.[106]

2.3.4.2: Synthesis of labelled poly-2-(dimethylamino)ethyl methacrylate brushes.

i) Preparation of the initiator surface.

Standard surfaces for brush synthesis are single pieces of silica crystal however for the purposes of fluorescence experiments this was impractical as emission from any labels included in the polymer brush are obliterated by the reflection of the excitation source from the silica substrate. For the purpose of this study quartz slides were used as the substrate, as these are optically pure at the wavelengths looked at for the labels used in the system.

Brush synthesis is extremely susceptible to grease present on the surface of the substrate. To eliminate this, the substrate was thoroughly degreased by multiple washing with acetone, isopropyl alcohol and finally distilled water and all equipment used in the synthesis was cleaned, the substrates were then handled only with tweezers.

Following this, the surface was rendered hydrophilic by cleaning the slides with a mixture of peroxide, ammonia and water at a ratio of 1:5:5. This was heated to 75°C and the slides immersed in the liquid for approximately 15 minutes or until the mixture stopped effervescing. Care was taken to ensure the mixture did not drop to the level of the slides as this would etch the surface making them unsuitable for brush synthesis.

To prevent etching when removing the slides from the cleaning solution, distilled water was added until the solution flowed over the sides of the vessel to dilute the mixture to sufficient levels to stop any etching of the slides upon removal. The cleaned slides were then rinsed with methanol and distilled water before being dried with compressed air.

ii) Binding of macroinitiator to slide surface.

Slides were carefully immersed in a solution of the macroinitiator and distilled water and ($1 mg ml^{-1}$). As the slides are for use in fluorescence experiments and are therefore transparent, both sides of the slide will be seen. To prevent any unusual formations on the slide surfaces, the area which will be analysed was elevated away from the surface during initiator binding by being propped up away from the surface of the container they were in.

The slides were left covered in solution overnight for the initiator to bind to the surface. Following this each slide was washed several times with distilled water and then dried. They were then stored until needed

iii) Synthesis of AMMA labelled PDMAEMA brushes.

The synthesis of polymer brushes using ATRP requires a system devoid of oxygen. When precise control isn't required treatment of the solvents by bubbling through with nitrogen is sufficient.

The solvent system for this synthesis is a methanol/water mix in the ratio of 4.1:0.9. The precise amount of solvent required depends upon the amount of reaction mixture needed to cover the surfaces of each slide on which a polymer is wanted to form. Half the total volume of the reaction mixture was made up of the solvent mixture. In this case 30ml of solution was required therefore a solvent system of 12.3ml methanol and 2.7ml distilled water was used. As well as degassing the solvents degassing any liquid monomer solution was needed and this was done while solid reagents are weighed out.

The amounts of reagents were determined using the ratio:

32 moles of monomer, to 1 mole of CuCl 0.05 mole of $CuBr_2$ and 2.1 mole of bpy.

The total monomer volume was approximately the same as that for the solvent system; in this case a total volume of 15ml.

As the resulting polymer brush was to be analysed using fluorescence techniques the total monomer amount included 0.1 mole % of AMMA.

Once all the liquid components of the polymerisation mixture were degassed they were added together along with the solid components of the catalyst. The reaction mixture was then stirred until all the solid has dissolved, while still under a flow of nitrogen.

While the solution was stirring the slides were placed in a vessel which was then sealed and degassed using repeated applications of a vac-line and nitrogen. The vessel was then left under a constant nitrogen pressure.

The reaction mixture was then injected into the sealed vessel through a rubber septum and the reaction left, at room temperature, for a time period varying between an hour and 24 hours.

As each ATRP polymerisation can require different lengths of time for adequate polymerisation the first polymerisation used several slides and each of the individual vessels were opened and

the reaction stopped at a variety of times. The resulting brushes showed a relatively long time indicating a polymerisation time close to 24 hours as optimal for brush grown [illegible] system. Following syntheses therefore used fewer substrates to obtain a usable brush by using this reaction length. The reason for such specific timing is that unlike the free radical mechanism which continues to polymerise until a termination occurs the ATRP mechanism makes use of a reversible termination so addition of monomer units occurs in a stepwise method and the total length of polymers is controllable and poly dispersity is limited.

To stop the reaction as soon as the vessel is opened to the air a substantial quantity of methanol was added to the vessel which was then emptied and again methanol added. The polymer brushes were then washed several times with methanol and water before being dried using compressed air.

iv) Synthesis of ACE labelled PDMAEMA brushes

The synthesis of ACE labelled PDMAEMA brushes followed the same route as the AMMA labelled brush but with 0.05 mol% of ACE replacing the AMMA.

v) Result of brush synthesis

Although a visual determination of brush synthesis showed polymer growth on the glass substrate, a coloured sheen such as a layer of oil on water is visible, attempted fluorescence readings on the polymer brushes showed data that did not conform to any recognisable pattern of emission. It is assumed that there were problems with reflected light from the excitation sources obliterating any detail of fluorescence from the brushes. Further investigation in to a method of achieving polymer brushes on which fluorescence measurements can be taken on is needed.

2.4: Fluorescence measurements

2.4.1: Preparations of samples for photophysics studies.

To obtain a consistent polymer concentration in solutions for photophysics studies a stock solution of polymer in distilled water at a concentration of 0.1g in 100ml was made. Each time a solution was required for fluorescence studies 1ml of this solution was removed to make up to 10ml to give a concentration of 10^{-2}wt%. The pH of these solutions was controlled by addition of HCL and NaOH.

The pHs of the polymer brushes were set by immersing the solid supports in a solution of the appropriate pH.

2.4.2: Instrumentation.

i) **TRAMS:**

All the time resolved anisotropy measurements were made on an Edinburgh Instruments 199 Fluorescence Spectrometer with a computer controlled toggling polariser. The instrument's excitation source is an IBH nanoLED pulsed diode controller. A 298nm source was used to excite ACE and a 370nm source was used to excite AMMA. TRAMS data was obtained using a time correlated single photon counting method. Individual time dependant emission intensity components were collected with the polariser alternating between the vertical position [$I_{\parallel}$] and the horizontal position [$I_{\perp}$] with the memory quarter in the Multi-channel Analyser (MCA) being alternated at the same time.

The anisotropy curve was then calculated from the vertical and horizontal data components using the following equation:

$$r(t) = \frac{I(t)\parallel - I(t)\perp}{I(t)\parallel + 2I(t)\perp} \qquad \textbf{(1.6)}$$

Where r is anisotropy and the I values are the intensities of the fluorescence polarised in the parallel and horizontal positions relative to the analyser's polariser. Resulting data was then analysed using an IBH software package.

ii) Fluorescence lifetime measurements:

Fluorescence lifetime readings were taken on an IBH system 5000 fluorescence spectrometer with an emission monochromator. The instrument's excitation source is an IBH nanoLED pulsed diode controller. A 298nm source was used to excite the ACE label. The data was obtained using a single photon counting method and was displayed on a computer using IBH datastation200 software. Fluorescence lifetime was then calculated from this data using another IBH software package.

iii) **Steady state fluorescence:**

Steady state measurements were recorded on a Perkin Elmer LS50 Luminescence spectrometer. The excitation source was a Xenon flash tube triggered at 50 or 60Hz, or line frequency, to produce intense short duration pulses of radiation across the instruments operating range. The remainder of the system consists of 2 reflection grating monochromators, a series of mirrors and both reference and sample photomultiplier detectors. The resulting spectra were displayed on a PC after processing by the instrument electronics.

Chapter 3: Fluorescence investigations of the solution behaviour of pH responsive polymers.

3.1.0: Fluorescence measurements of linear polydimethylaminoethyl methacrylate (PDMAEMA) polymers in aqueous solution.

3.1.1: Steady state spectra of linear PDMAEMA in aqueous solution.

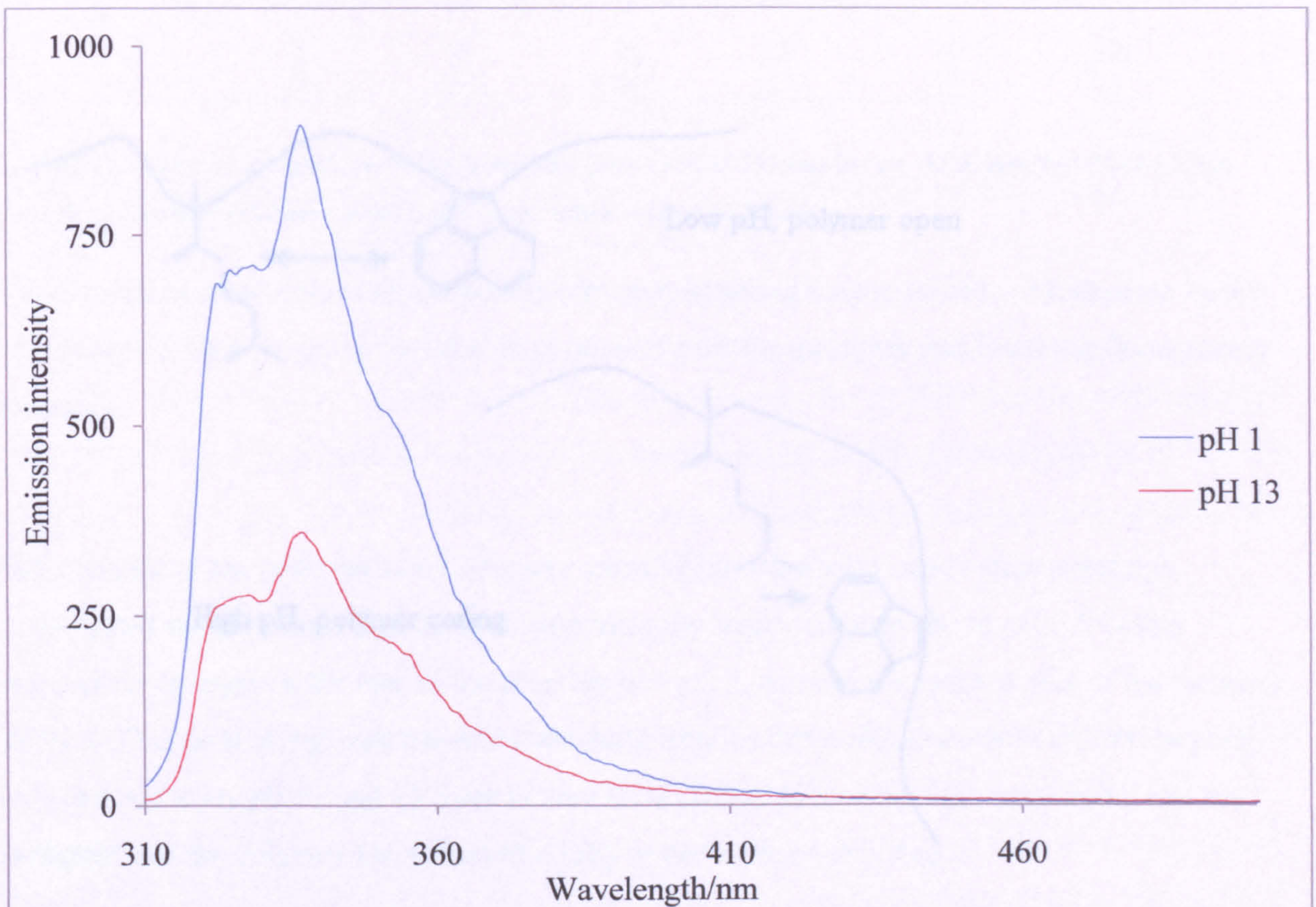

Figure 25: Example steady state emission spectra for an ACE labelled PDMAEMA sample in aqueous solution at two extreme pH values when excited at 290nm.

Steady state spectroscopy on an ACE labelled PDMAEMA sample across a pH range shows a decrease in the intensity of emission of the sample when excited at 290nm as the pH increases. This is most notable above pH 8 where the intensity drops markedly as shown in figure 27. Presumably this is an indication that fluorescence quenching occurs in the system.

The aqueous environment may quench the fluorescence from the label; however for PDMAEMA it would be expected that the polymer would adopt a coiled conformation at high pH which would prevent access of water molecules to the fluorophore and instead would reduce quenching from this source. Therefore the quenching of the ACE emission must come from within the polymer system itself. Presumably the pendant amine groups of the polymer could quench the fluorescence of the ACE label and this is what is observed at high pH.[107]

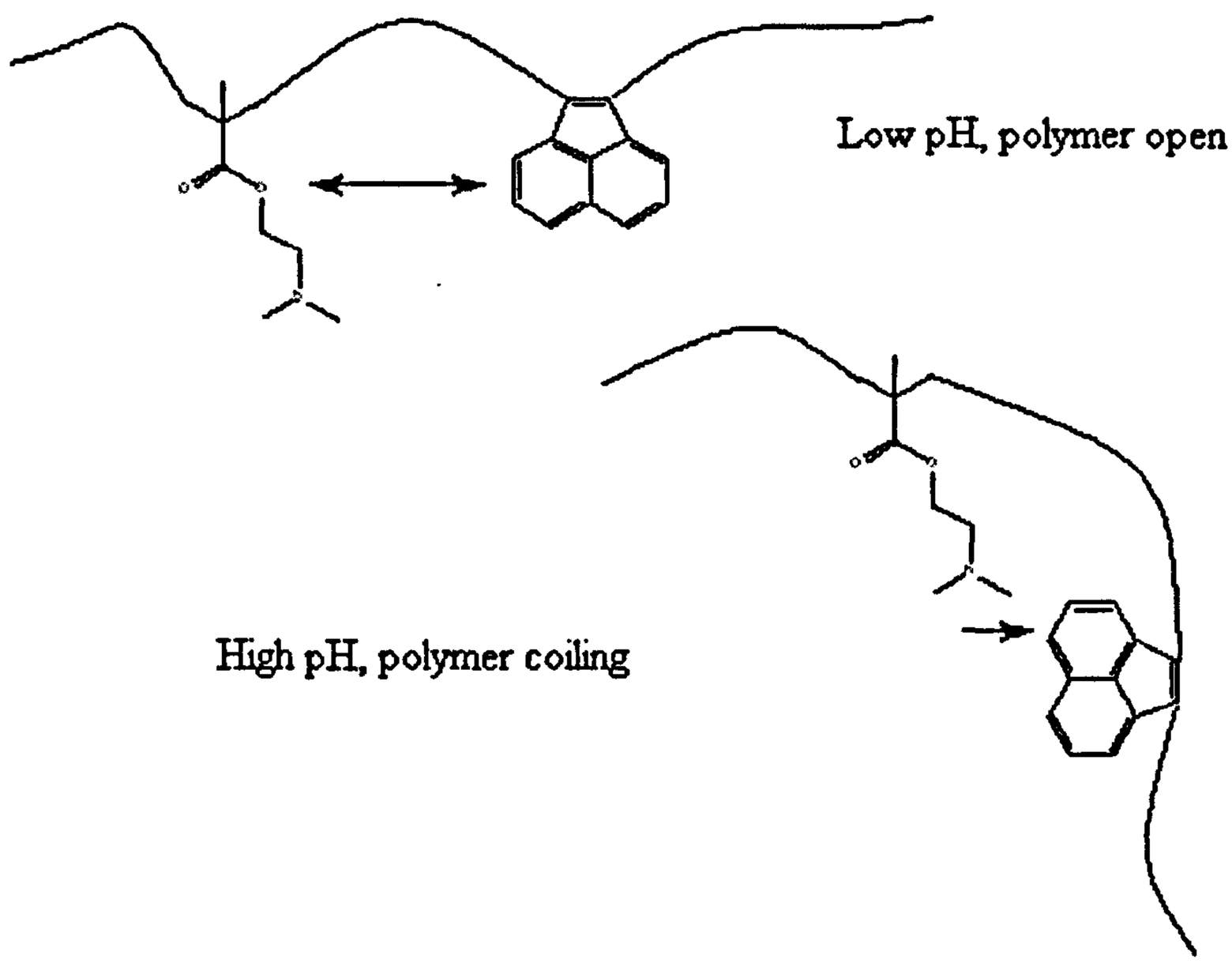

Figure 26: At low pH when uncoiled the amine groups are far enough away to not quench the ACE label. At high pH when the polymer is coiled amine groups may be close enough to quench the ACE label.

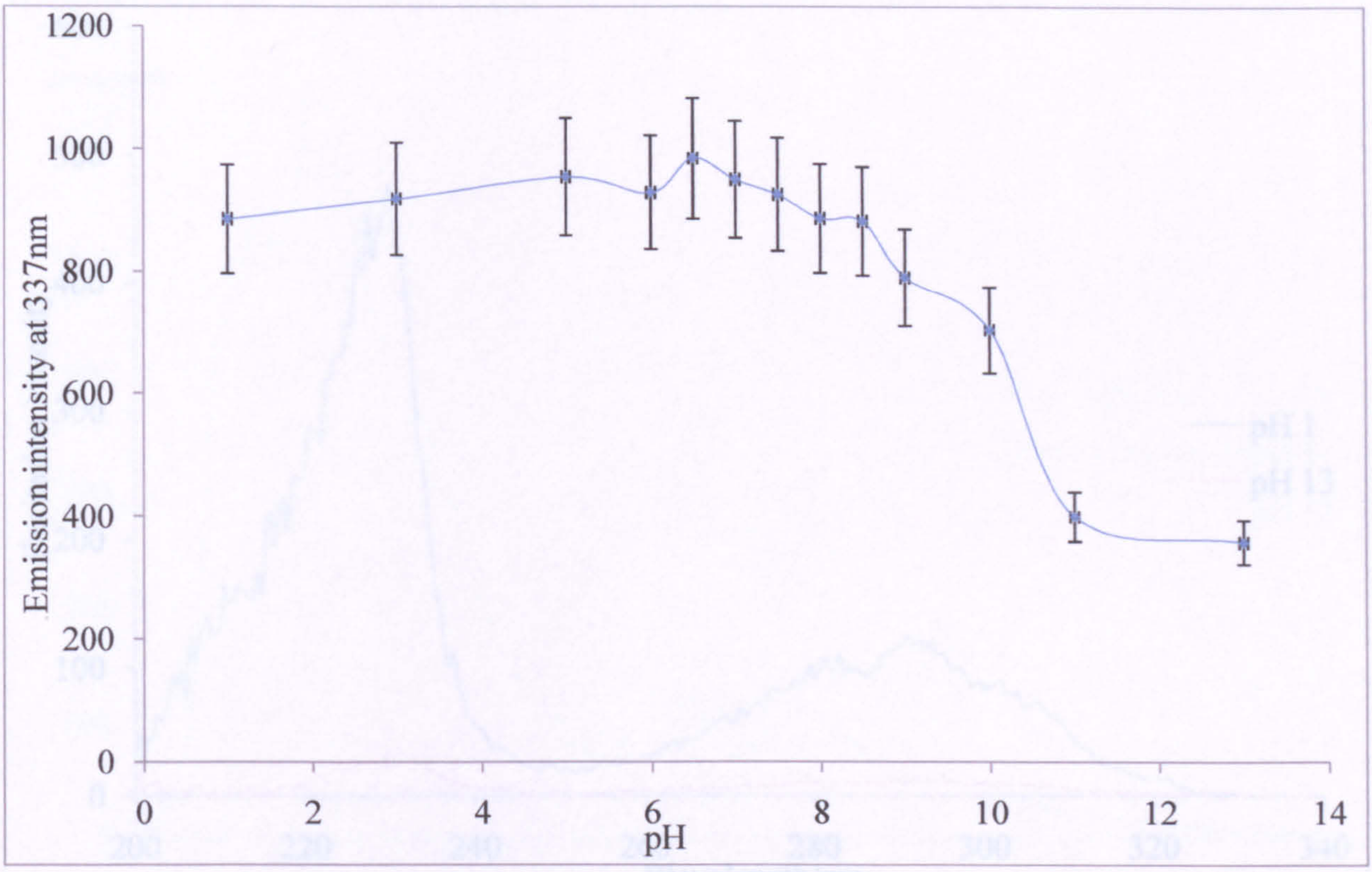

Figure 27: A plot of the peak emission intensities (observed at 337nm) for an ACE labelled PDMAEMA sample in aqueous solution across a pH range when excited at 290nm.

This would be consistent with the polymer system adopting a more coiled conformation as the pH increases, thus bringing the label in to contact with the quencher and lowering fluorescence intensity.

When a plot of the peak emission intensity values from the above steady state spectra is constructed it can be seen that the emission intensity begins to drop above pH 6.5 with a substantial increase in the rate of the drop beyond pH 9, above the expected pKa of the polymer system. This drop along with internal quenching implies that coiling becomes tightest beyond this pH. Between pH 11 and 13 there is very little change in emission intensity and it can be assumed that the polymer has achieved a fully coiled state by this stage.

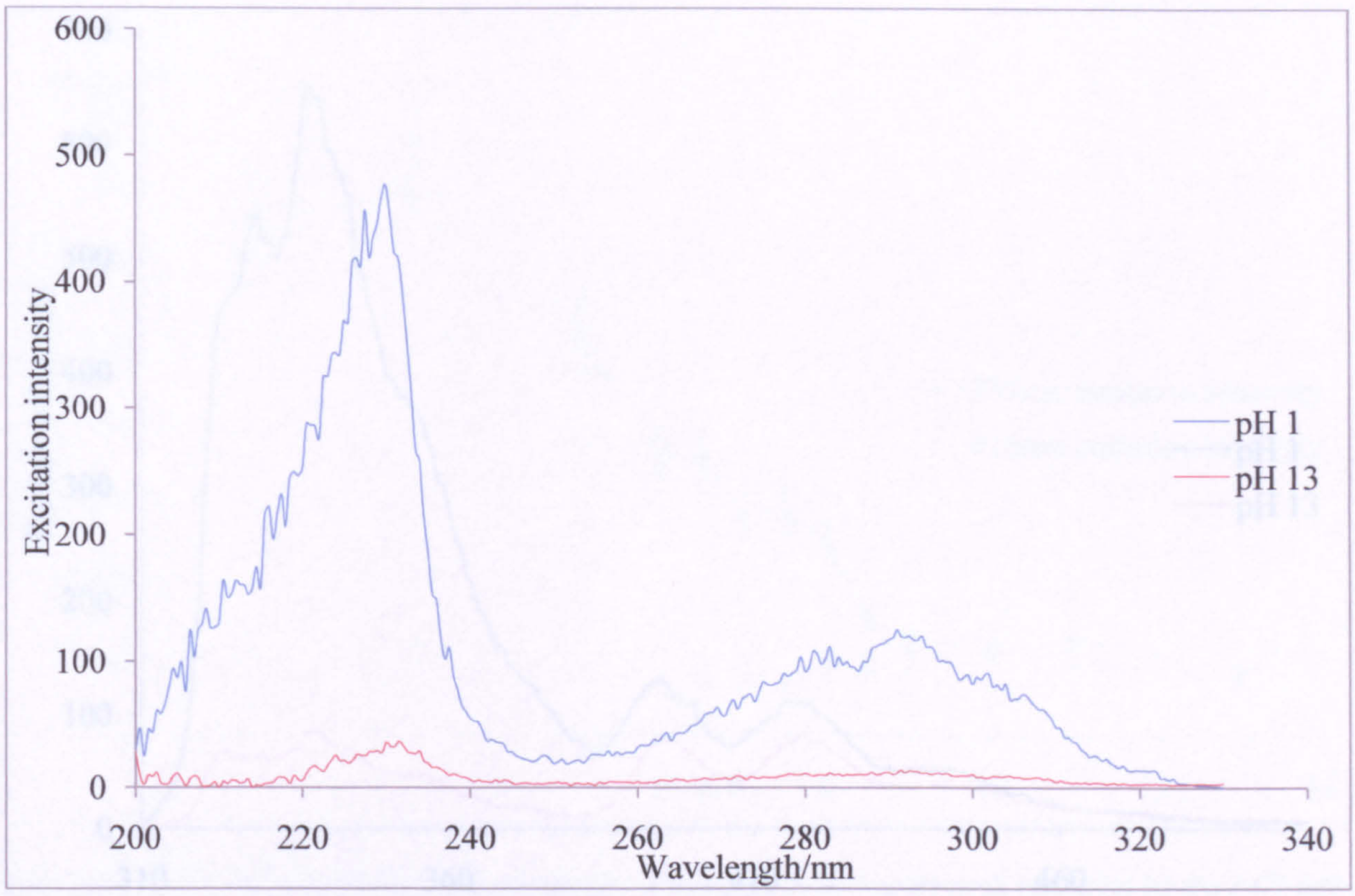

Figure 28: Example steady state excitation spectra for an ACE labelled PDMAEMA sample in aqueous solution at two extreme pH values when observed at 340nm.

It can be seen in figure 28 above that there is also a drop in the excitation of the ACE label of PDMAEMA as the solution pH increases. This drop matches the drop in intensity of the emission, supporting the theory that the fluorescence in the system is being quenched under these conditions.

Steady state spectra were measured from PDMAEMA samples labelled with both ACE, acting as a donor, and an AMMA, acting as an acceptor, in aqueous solution (See figure 29). From the two extreme pH values it can be seen that there is a substantial drop in the emission intensity of the ACE label observed at 340nm, there is however a much smaller drop in the intensity of the AMMA label emission intensity at 420nm.

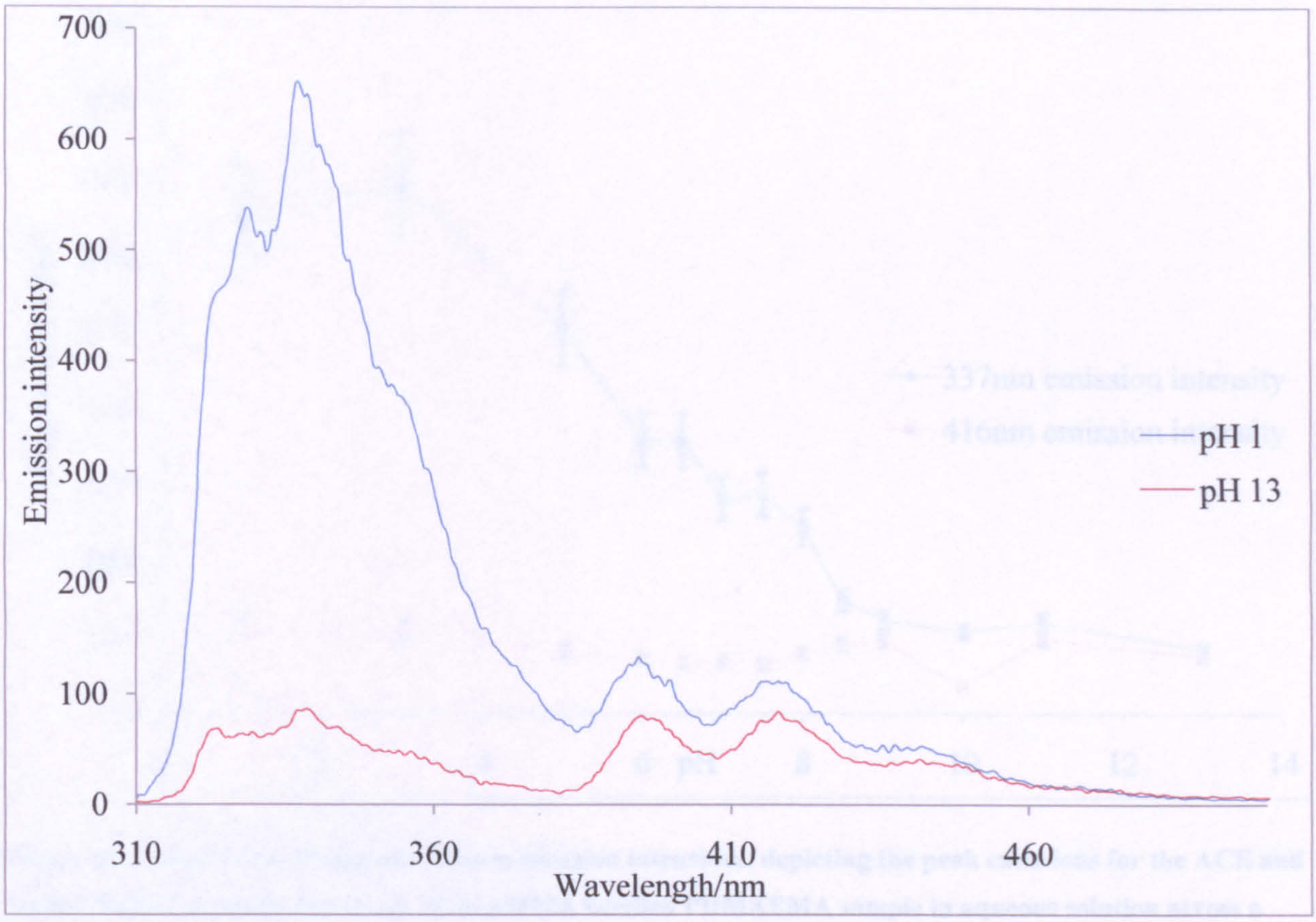

Figure 29: Example steady state emission spectra for an ACE-AMMA labelled PDMAEMA sample in aqueous solution at two extreme pH values when excited at 290nm.

This infers that energy is being transferred from the ACE label to the AMMA label as quenching from the internal amine groups of the polymer should affect both labels to the same extent.

When the peak emission intensities for the ACE and AMMA labels (sampled at 337 nm and 416 nm respectively) are plotted one can see clearly that the emission intensity of the naphthyl fluorescence begins to drop from pH5 and plateaus at around pH 8.5. This is the same pH value that the ACE labelled PDMAEMA sample began to drop in emission intensity. The peak emission of the AMMA label shows very little decrease across the entire range, with an anomalous drop in emission intensity visible at pH 10.

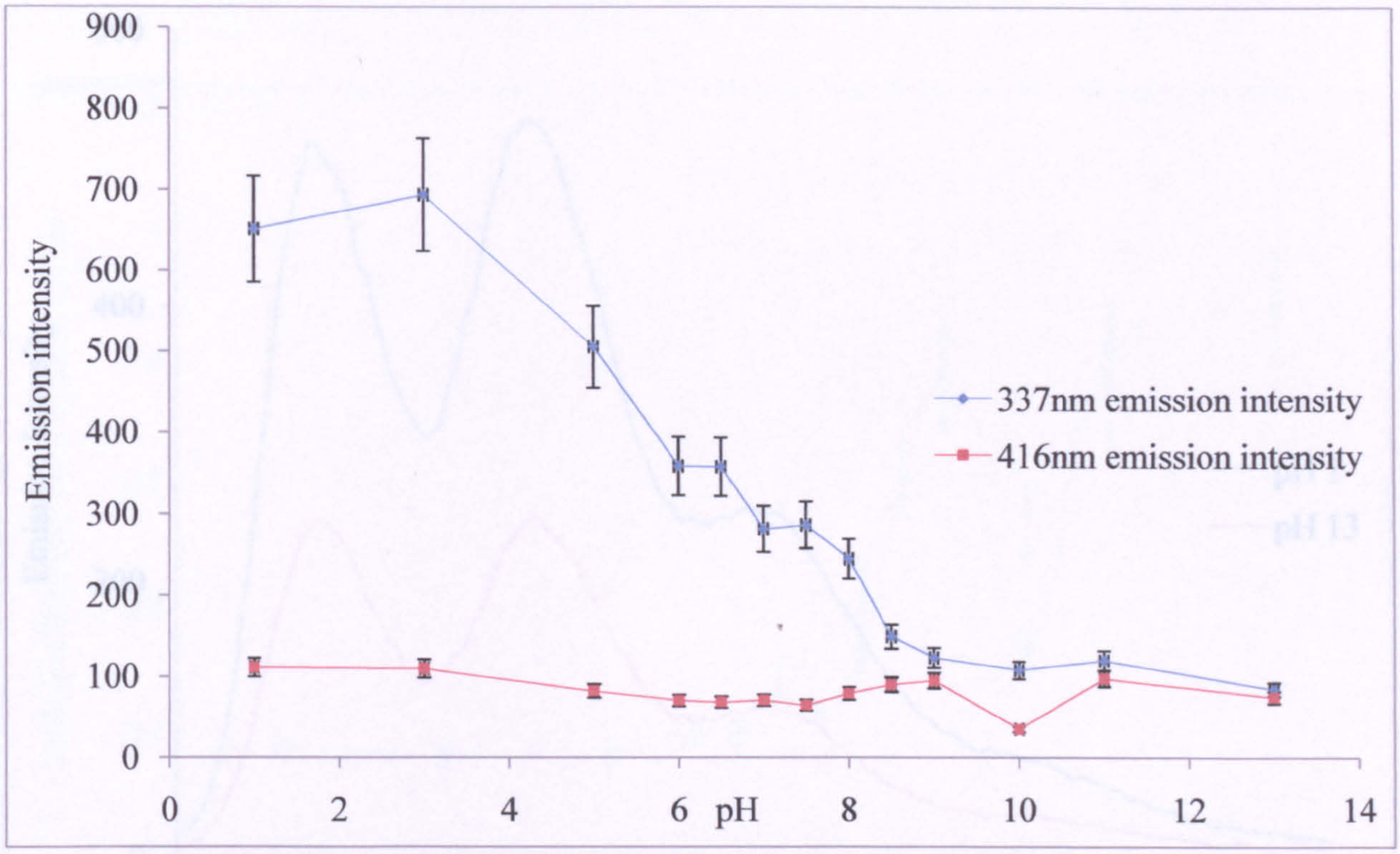

Figure 30: A plot of the 337nm and 416nm emission intensities, depicting the peak emissions for the ACE and AMMA labels respectively, for an ACE-AMMA labelled PDMAEMA sample in aqueous solution across a range of pH values when excited at 290nm.

When the polymer sample is excited at 370nm the AMMA label can be stimulated directly. In figure 30 the emission intensity for the fluorescence from the anthryl decrease in going from high to low pH in a manner similar to that of the ACE labelled sample.

This provides further evidence that the deprotonated amine unit must act as quencher of fluorescence at higher pH values. This would be indicated because despite the fact that PDMAEMA should in theory coil as the pH value of the solution increases there is a decrease in the emission intensity of a directly excited AMMA label, which is not quenched by ACE. This means that with the aqueous media being more excluded in this conformation something in the polymer chain itself must act as a quencher, most likely the amine group.

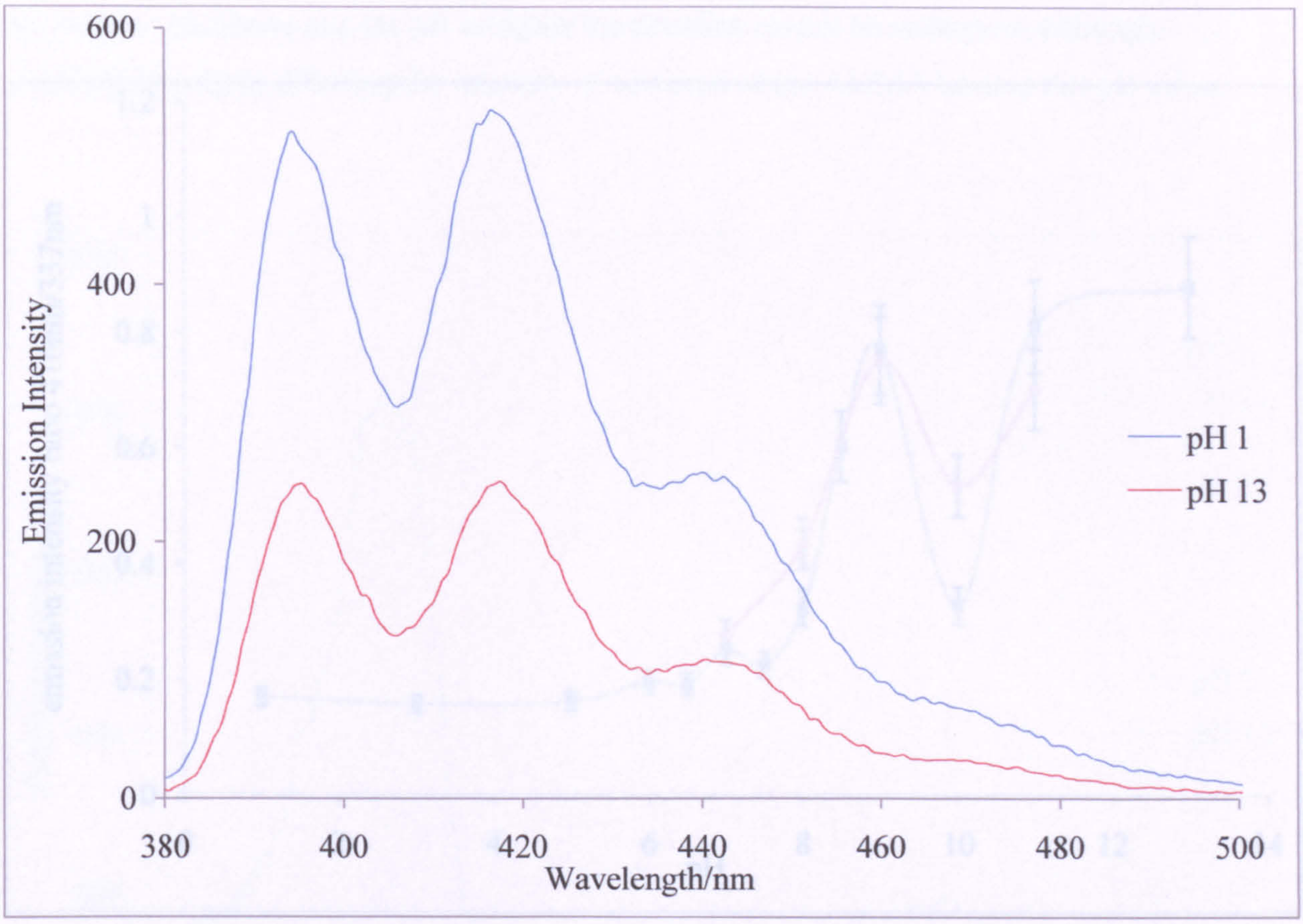

Figure 31: Example steady state emission spectra for an ACE-AMMA labelled PDMAEMA sample in aqueous solution when excited at 370nm at two extreme pH values.

There is no shallow change and plateau in the AMMA emission when directly excited is seen in the AMMA emission when the entire system is excited at 290nm. This further indicates that something is affecting the AMMA emission when the ACE label is excited.

Figure 32 shows a plot of the ratio of the intensity of emission samples at 461 nm (AMMA) and 337 nm (ACE) upon excitation at 290 nm.

Changes in the ratio can be taken as further evidence for energy transfer in the system although any distinction between non radiative and radiative forms of energy transfer are not possible from these ratios.

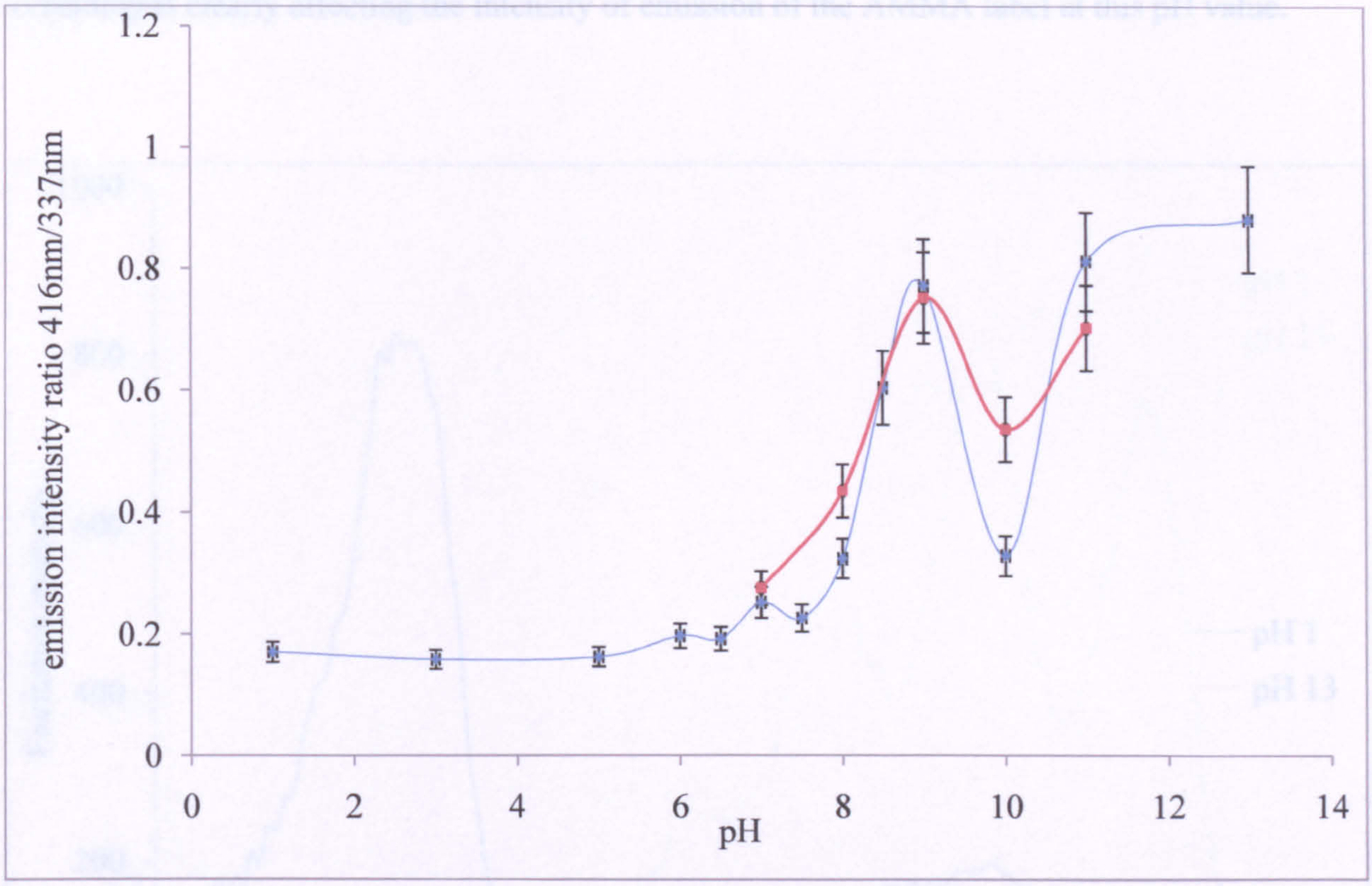

Figure 32: A plot of the ratio between the emission intensity of the AMMA label as observed at 416nm and the ACE label as observed at 337nm for an ACE-AMMA labelled PDMAEMA sample in aqueous solution when excited at 290nm. The second set of data, shown in red, is a repeat of several pH values which while showing the rise expected in the ratio also show an unexpected decrease.

The AMMA:ACE emission intensity ratio begins to increase from pH 7, around the pKa of the PDMAEMA system. The small drop in the emission intensity of the AMMA label at pH 10 is compounded here with the ratio and a significant drop in the ratio occurs at pH 10. A change in a system involving PDMAEMA over a very short pH range has been previously reported by Takagishi et al[18]. It was shown that methyl orange has a significantly higher binding constant with PDMAEMA at pH 8 than might be expected and this was attributed to a crossover of the ionic charge of polymer which aids binding at low pH values, and the enhanced affinity for small molecules that a coiled polymer system has. As the fluorophores in this situation are bound to

the polymer backbone and the pH is higher the situation cannot be analogous, although something is clearly affecting the intensity of emission of the AMMA label at this pH value.

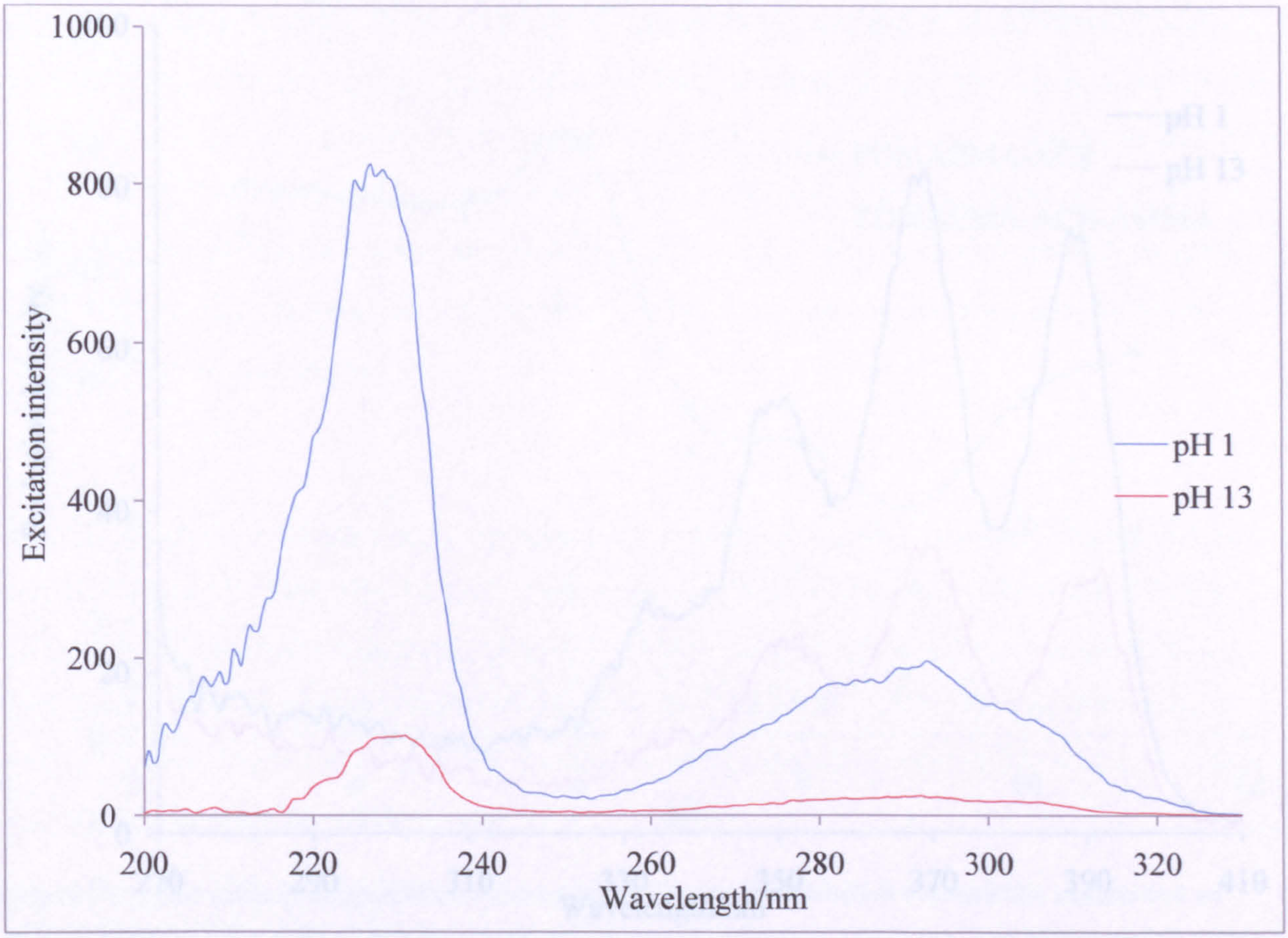

Figure 33: Example excitation spectra for an ACE-AMMA labelled PDMAEMA sample in aqueous solution when observed at 340nm at two extreme pH values.

Excitation spectra of the ACE-AMMA labelled sample (see figure 34) when observed at 420 nm show a significant drop in excitation intensity between the pH extremes corresponding to the same decrease observed in the emission intensity of the ACE label. The excitation spectra of the polymer sample when observed at 420nm, within the emission range of the AMMA label, also shows a consistent decrease in excitation intensity across the entire range of pH values matching

the same decrease observed in the emission spectra of the sample when excited at 370nm to directly excite the AMMA label.

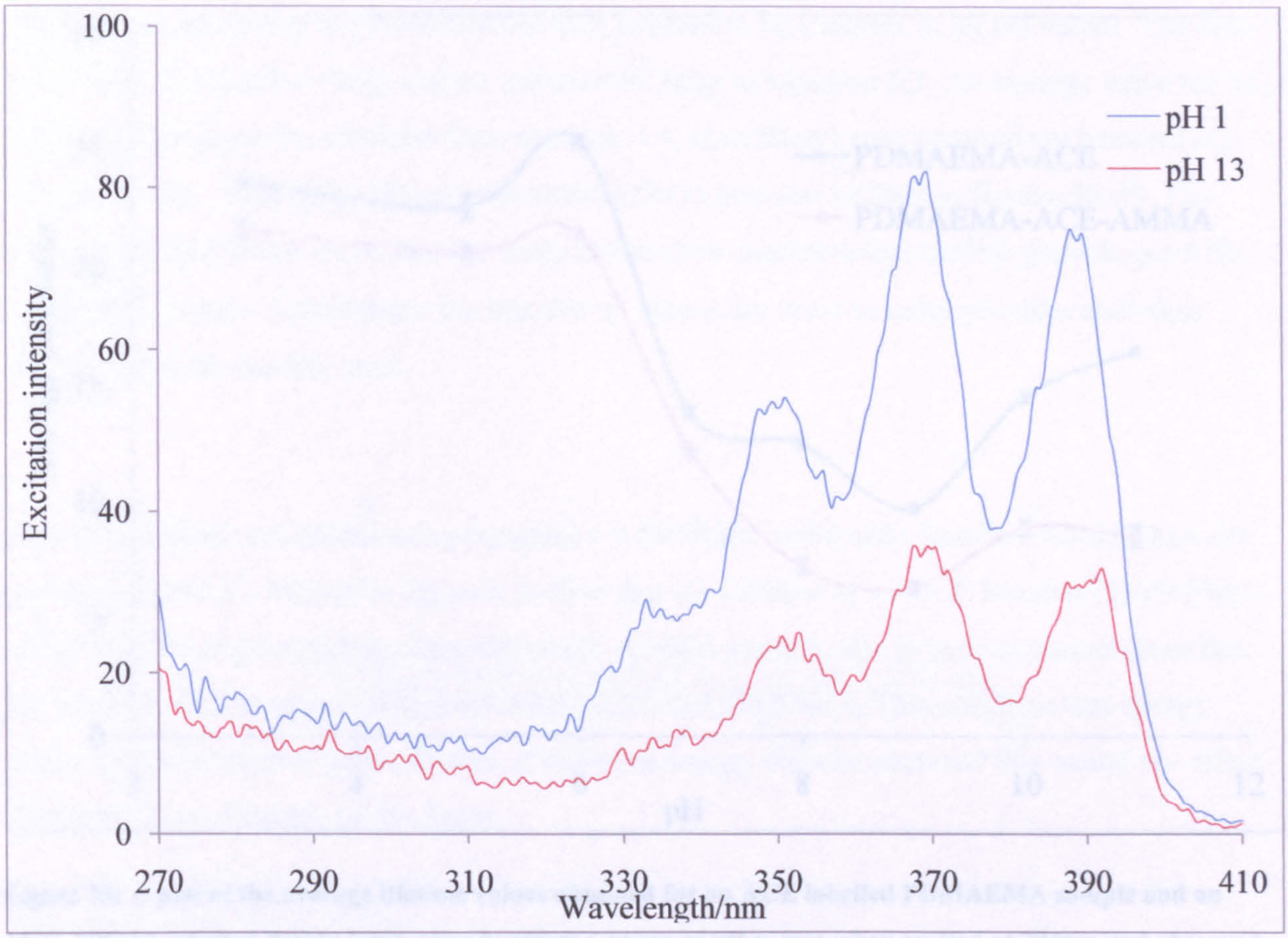

Figure 34: Example excitation spectra for an ACE-AMMA labelled PDMAEMA sample in aqueous solution when observed at 420 nm at two extreme pH values.

Upon further examination of figure 34 there is little change in the excitation intensity at 290 nm yet a substantial decrease in the intensity at 370 nm. This suggests that although the increased pH and the quenching from the polymer amine groups affects the excitation intensity as would be expected there is a relative increase in the excitation intensity centred at 290 nm relative to that at 420 nm. This provides further evidence of energy transfer between the two fluorophores.

3.1.2: Fluorescence lifetime measurements of linear PDMAEMA samples in aqueous solution.

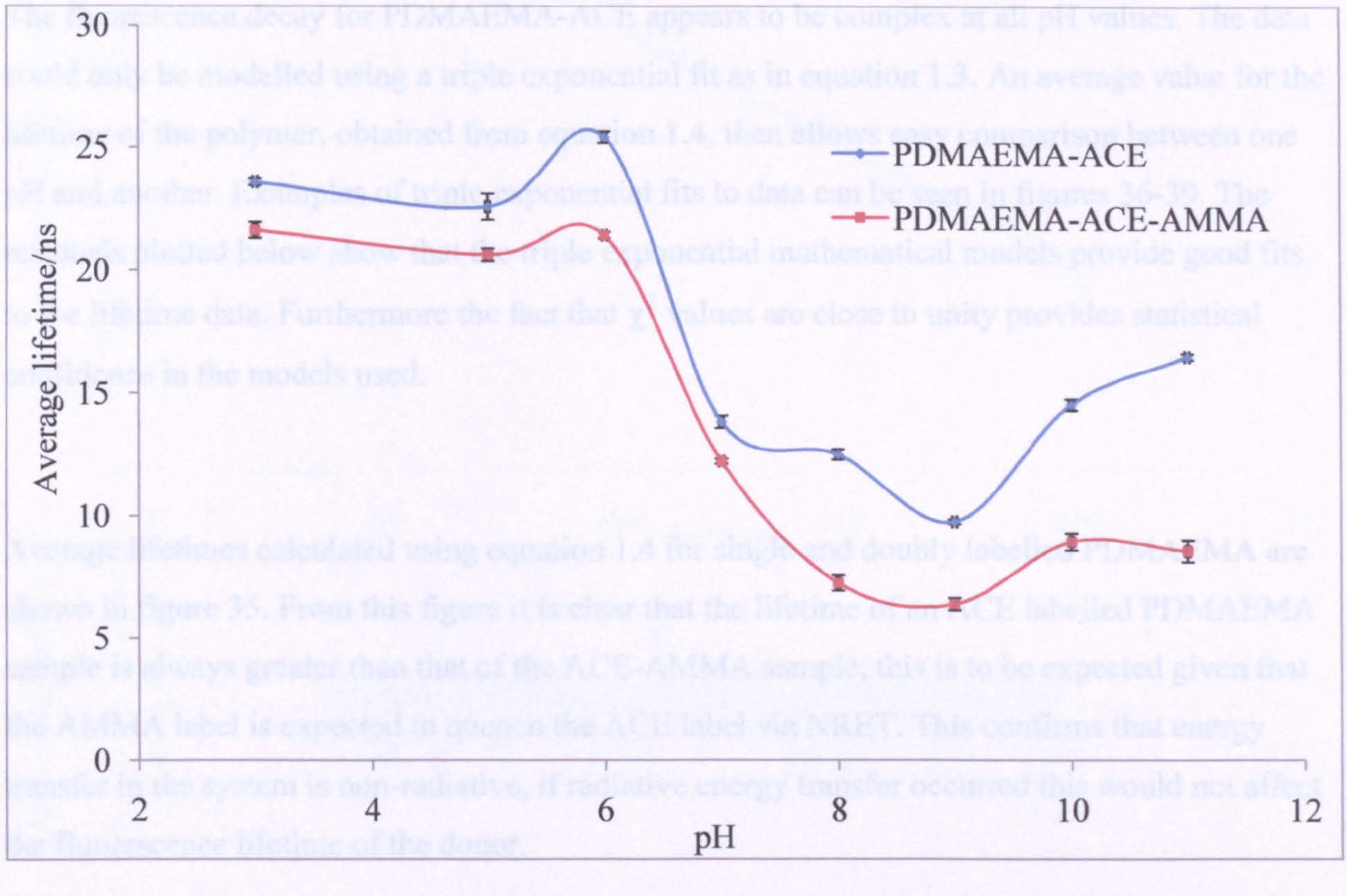

Figure 35: A plot of the average lifetime values obtained for an ACE labelled PDMAEMA sample and an ACE-AMMA labelled PDMAEMA sample across a range of pH values when excited at 284nm and observed at 340nm.

It has been show previously that the lifetime of an excited ACE label in aqueous media is sensitive to the polymer conformation[108]. As it is unlikely that the label will exist in only one environment as the polymer conformation changes it would therefore not be expected that a simple, single exponential model would describe the fluorescence decay. For example in a PMAA-ACE system the fluorescence lifetime of the ACE label can be modelled by a single exponential at high pH when the polymer adopts an open, expanded, conformation. At low pH

on the other hand the polymer forms a coiled structure and the decay models are much more complex.

The fluorescence decay for PDMAEMA-ACE appears to be complex at all pH values. The data could only be modelled using a triple exponential fit as in equation 1.3. An average value for the lifetime of the polymer, obtained from equation 1.4, then allows easy comparison between one pH and another. Examples of triple exponential fits to data can be seen in figures 36-39. The residuals plotted below show that the triple exponential mathematical models provide good fits to the lifetime data. Furthermore the fact that χ^2 values are close to unity provides statistical confidence in the models used.

Average lifetimes calculated using equation 1.4 for single and doubly labelled PDMAEMA are shown in figure 35. From this figure it is clear that the lifetime of an ACE labelled PDMAEMA sample is always greater than that of the ACE-AMMA sample, this is to be expected given that the AMMA label is expected to quench the ACE label via NRET. This confirms that energy transfer in the system is non-radiative, if radiative energy transfer occurred this would not affect the fluorescence lifetime of the donor.

Furthermore, by considerations of the data shown in figure 18 it is tempting to conclude that the labels must interact (ie be within 10 nm) across the entire pH range. The interaction appears to be greater at pH values in excess of 6. It could be that PDMAEMA adopts a partially contracted coil conformation at low pH which collapses into a tighter coil at pH values in excess of the pKa.

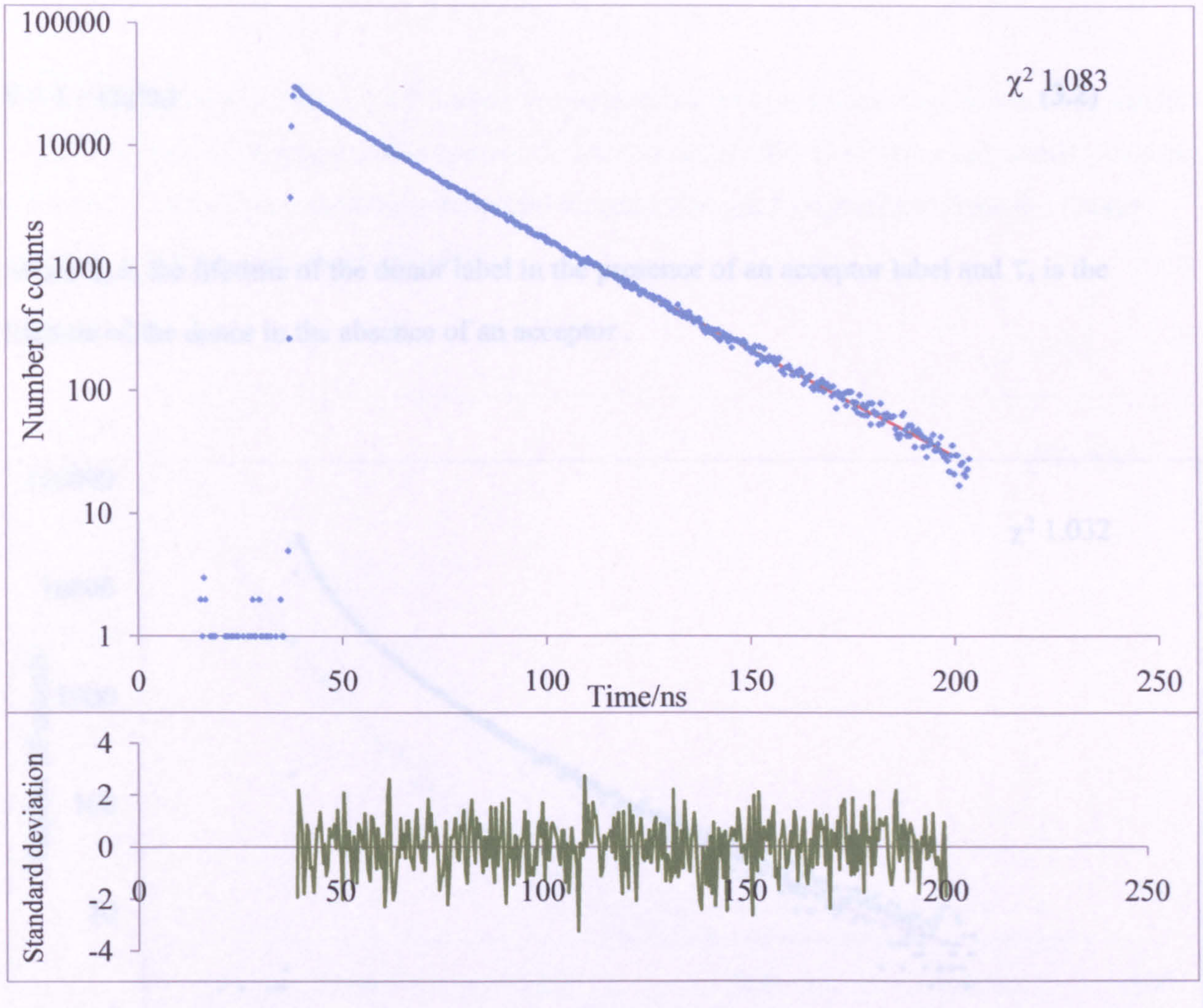

Figure 36: A fluorescence decay with corresponding mathematical fit (shown in red) and a plot of the resulting residuals for an ACE labelled PDMAEMA sample of pH 3.

As the lifetime results are indicative of a non radiative energy transfer system then equation 3.1 can be used to calculate distance between the ACE and AMMA labels as the pH changes.

$$E = \frac{R_0^6}{R_0^6 + r^6} \qquad \textbf{(3.1)}$$

Where R_0 represents the Forster transfer distance, and r is the average distance between D and A. E, or the energy transfer efficiency is represented by equation 3.2 below.

$$E = 1 - (\tau_d/\tau_s) \quad \textbf{(3.2)}$$

where τ_d is the lifetime of the donor label in the presence of an acceptor label and τ_s is the lifetime of the donor in the absence of an acceptor .

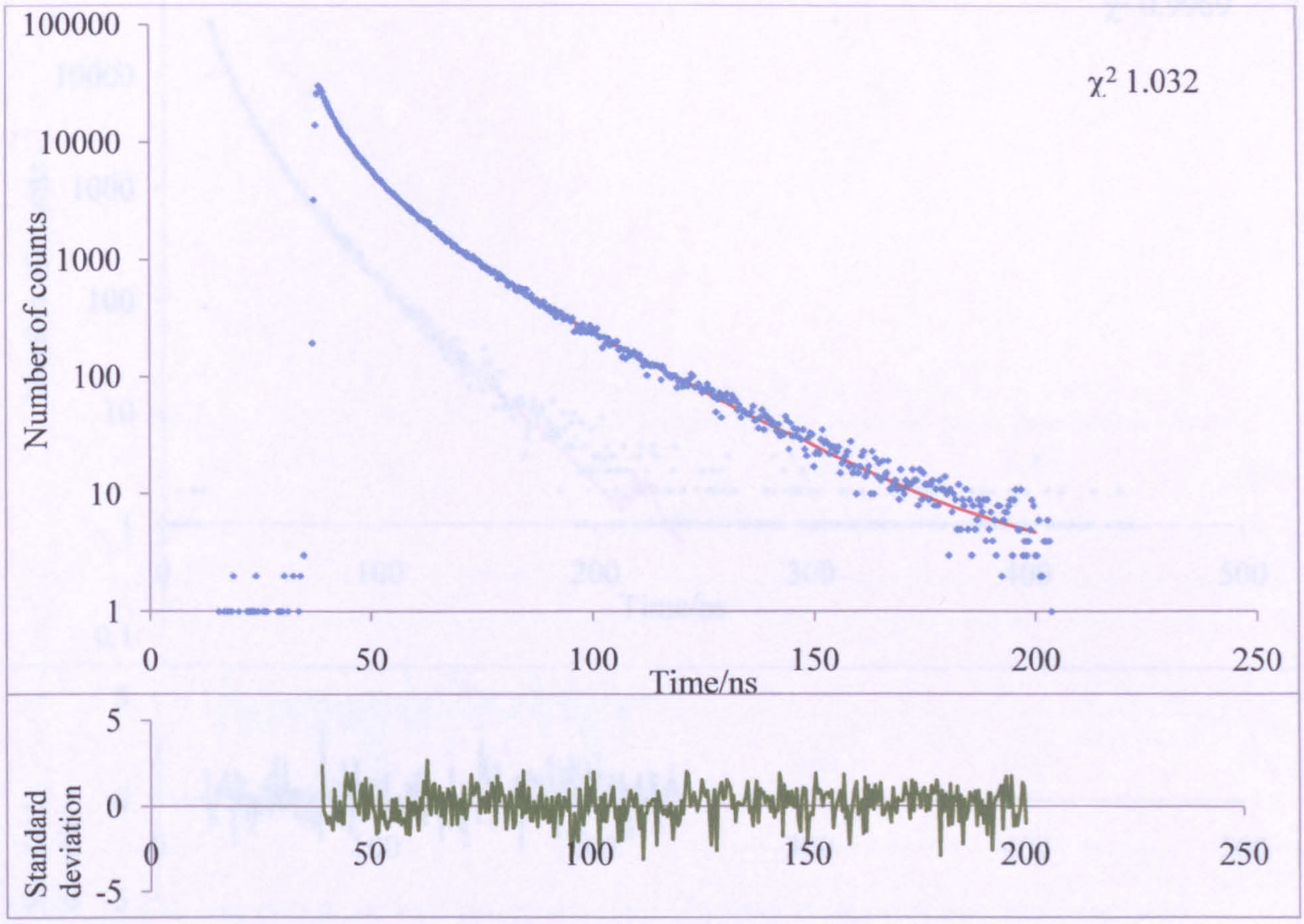

Figure 37: A fluorescence decay with corresponding mathematical fit (shown in red) and a plot of the resulting residuals for an ACE labelled PDMAEMA sample of pH 10.

For an ACE AMMA system the R_0 value, the measure of the spectral overlap between the labels is 2.3 according to literature and is commonly used as such.[109] The r value calculated was then converted to angstroms. Generally the useful distance that can be considered from the Förster equation is between 10 and 60 angstroms.

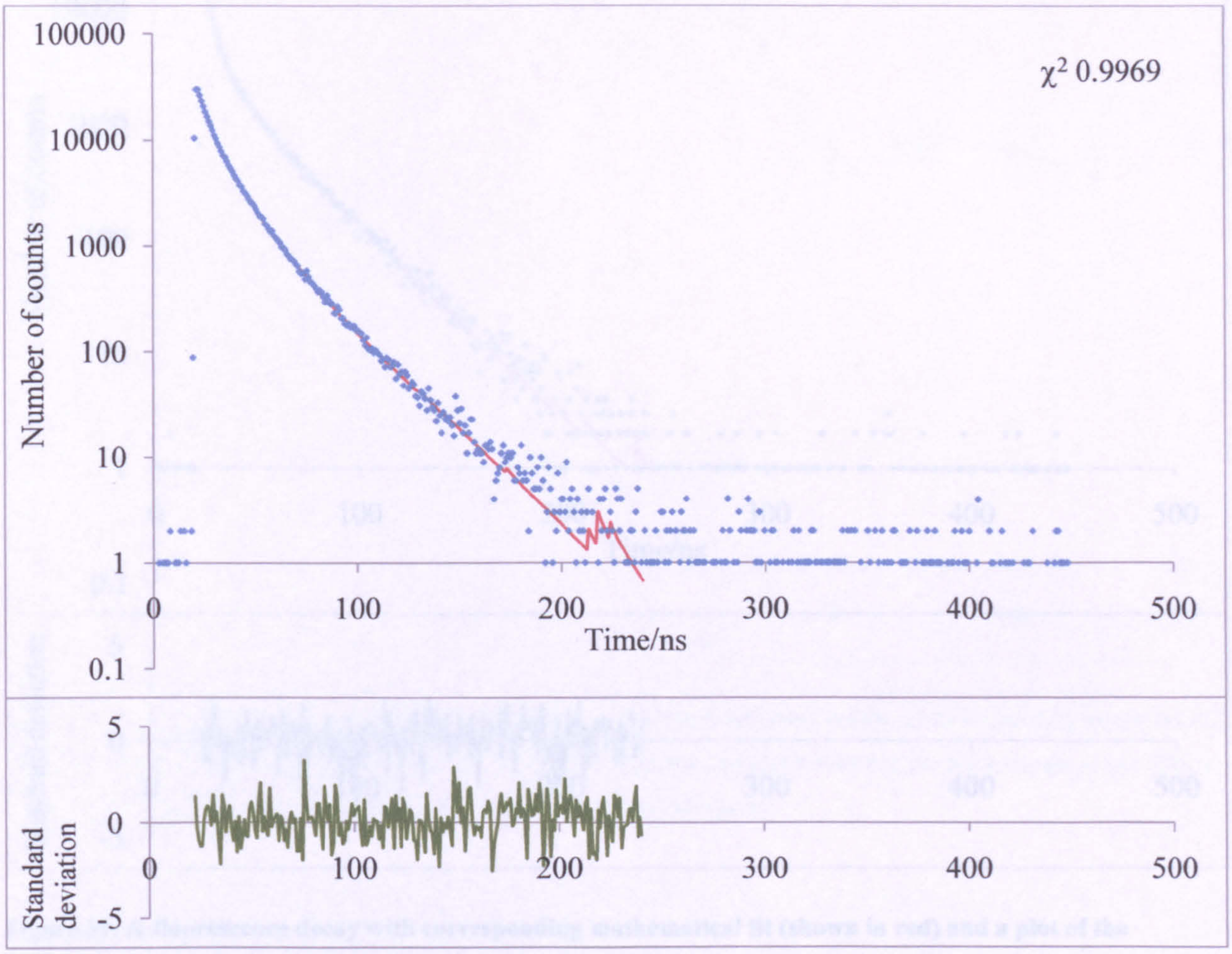

Figure 38: A fluorescence decay with corresponding mathematical fit (shown in red) and a plot of the resulting residuals for an ACE-AMMA labelled PDMAEMA sample of pH 3.

The lifetimes shown in figure 35 used with the above equations give distances between the ACE and AMMA labels of between 34 and 23 angstroms as can be seen in figure 40. When the error

in the lifetimes is taken in to account then the distance between the ACE and AMMA labels can be shown to be constant at both low and high pH values and show a reduction in distance between pH 7 and 8 corresponding to the PDMAEMA pKa as was expected.

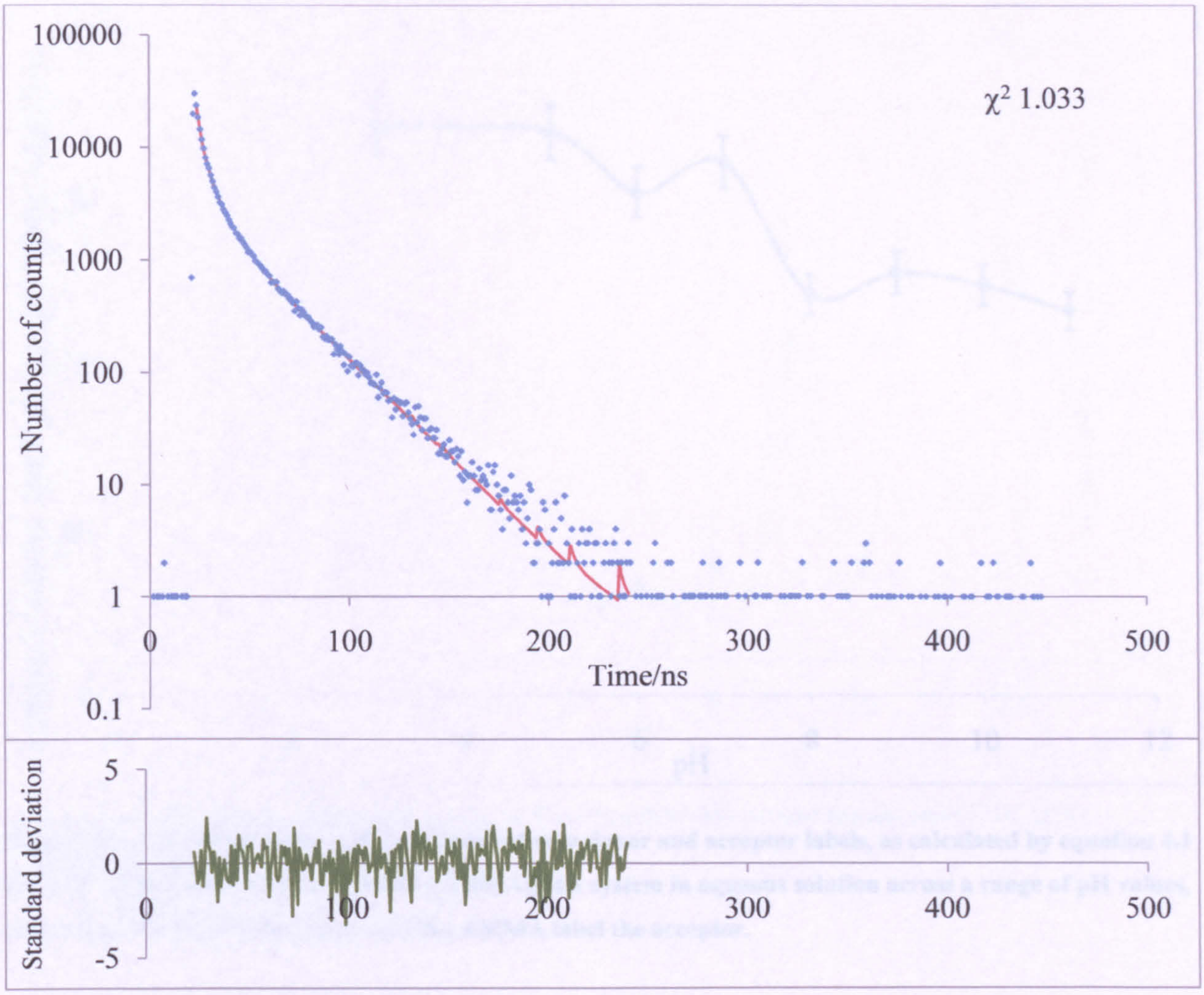

Figure 39: A fluorescence decay with corresponding mathematical fit (shown in red) and a plot of the resulting residuals for an ACE-AMMA labelled PDMAEMA sample of pH 9.

Note that both the polymer systems show the rise in lifetime at pH 10 and there is no apparent change in the distance between the two labels in the double label system so the energy transfer is independent of the strange rise in lifetime.

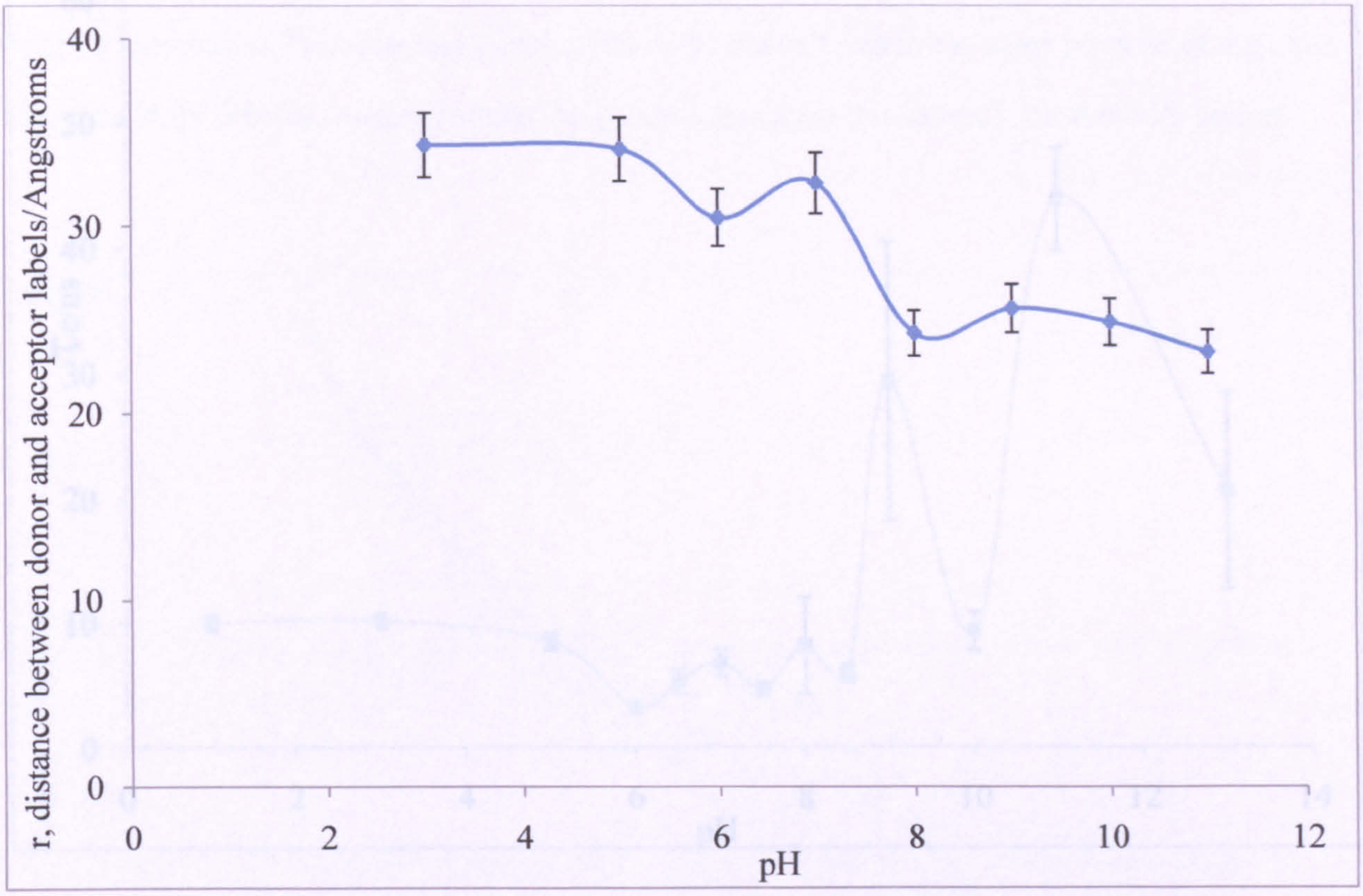

Figure 40: A plot of the value r, the distance between donor and acceptor labels, as calculated by equation 4.1 for ACE PDMAEMA and ACE-AMMA PDMAEMA system in aqueous solution across a range of pH values, where the ACE label is the donor and the AMMA label the acceptor.

3.1.3: Time Resolved Anisotropy Measurements on linear PDMAEMA samples in aqueous solution.

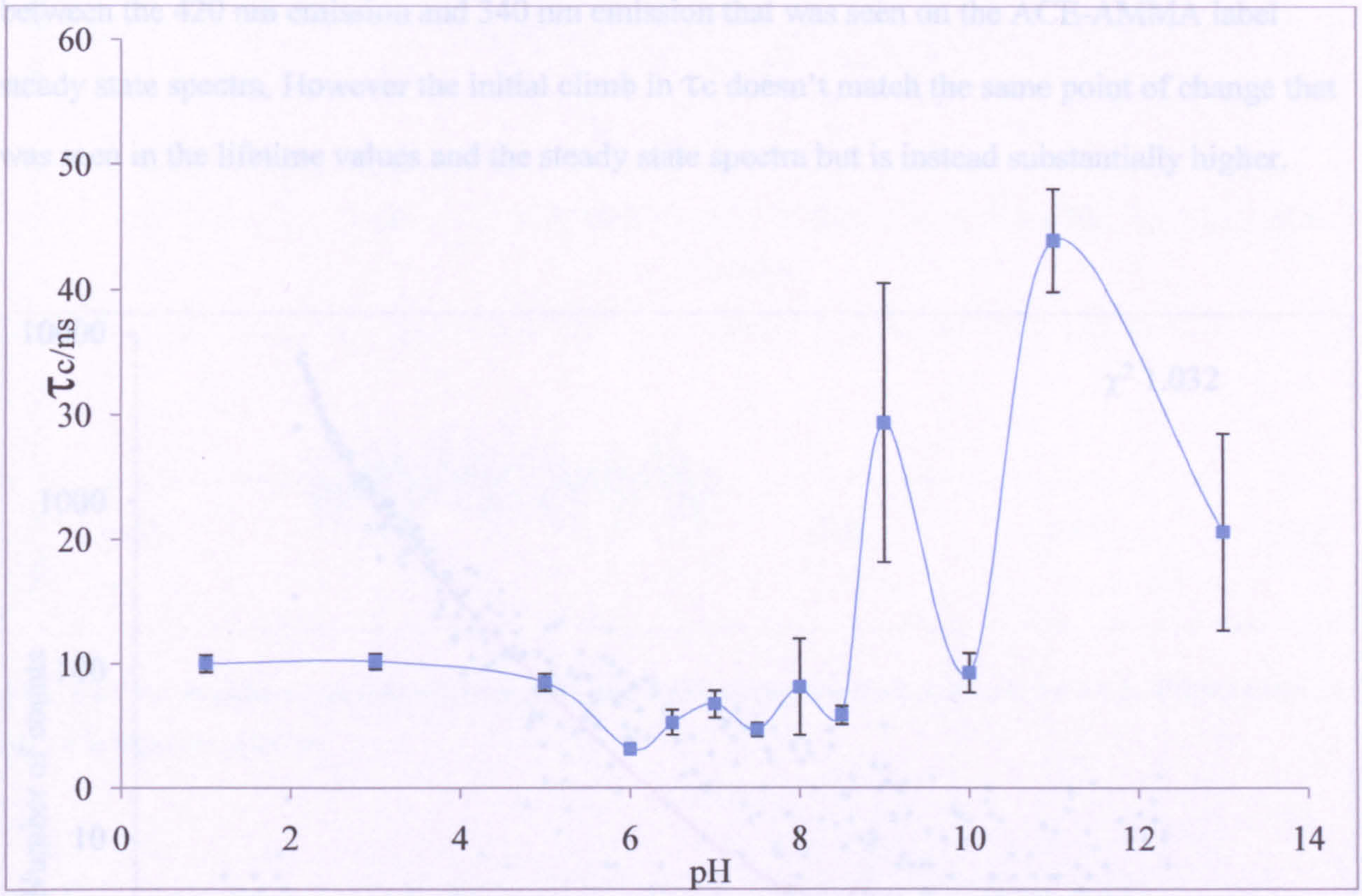

Figure 41: A plot of the τ_c values obtained from Time Resolved Anisotropy Measurements on ACE-PDMAEMA across a range of pH values.

Time resolved anisotropy measurements of the PDMAEMA samples provided a τc value that is indicative of the segmental motion of the polymer backbone. For the ACE labelled PDMAEMA system a single exponential fit using an impulse reconvolution method, leaving the r^{∞} varying, shows a good statistical fit to the data at each pH examples of which can be seen in figures 42 and 43.

Figure 41 shows a plot of the τc values obtained for this polymer system. There is a general consistency in the τc up to around pH 8.5 where the τc rises rapidly before dropping between pH 9 and 10 and rising once again prior to pH 11. This sudden drop matches the drop in the ratio between the 420 nm emission and 340 nm emission that was seen on the ACE-AMMA label steady state spectra. However the initial climb in τc doesn't match the same point of change that was seen in the lifetime values and the steady state spectra but is instead substantially higher.

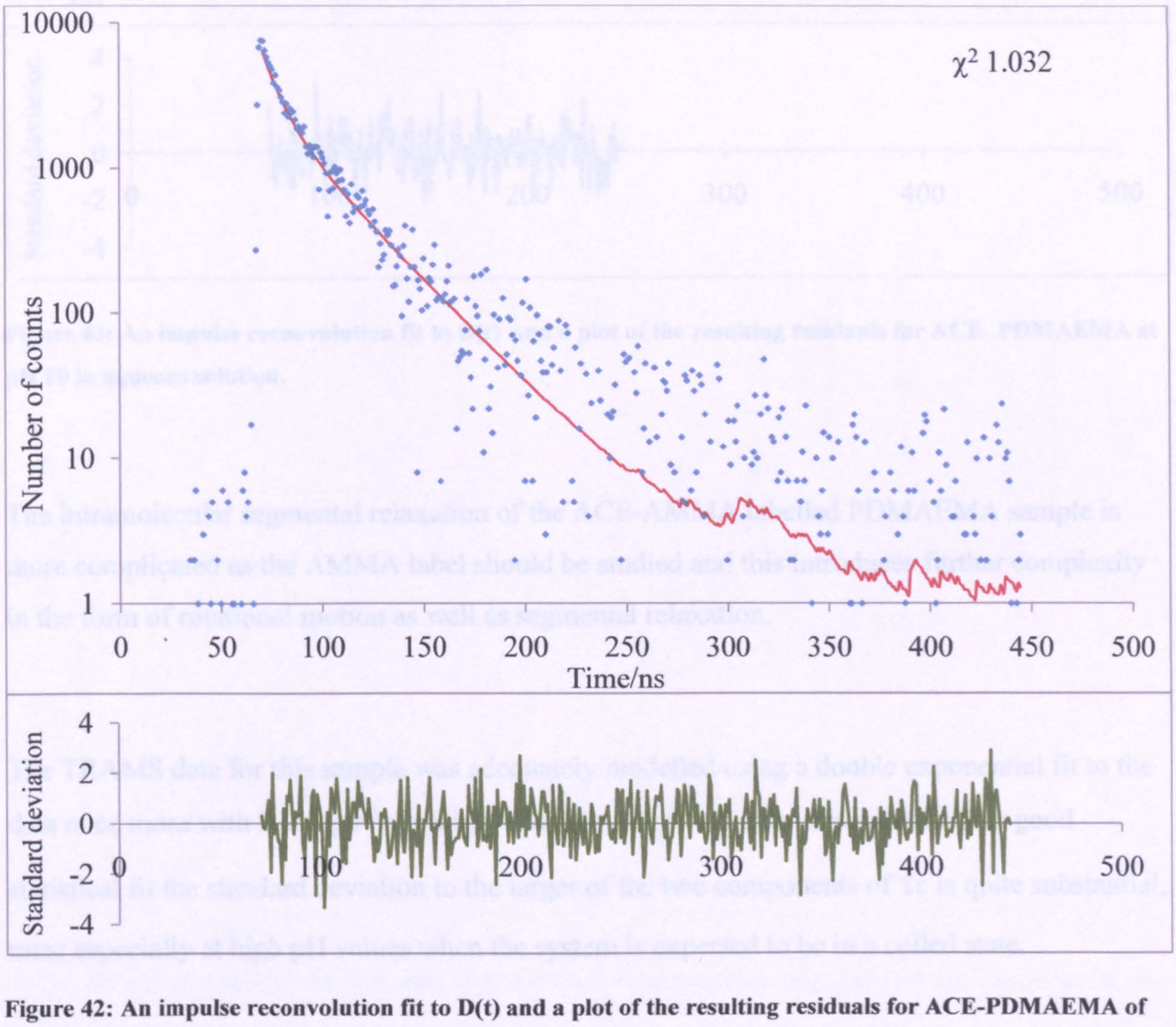

Figure 42: An impulse reconvolution fit to D(t) and a plot of the resulting residuals for ACE-PDMAEMA of pH 3 in aqueous solution.

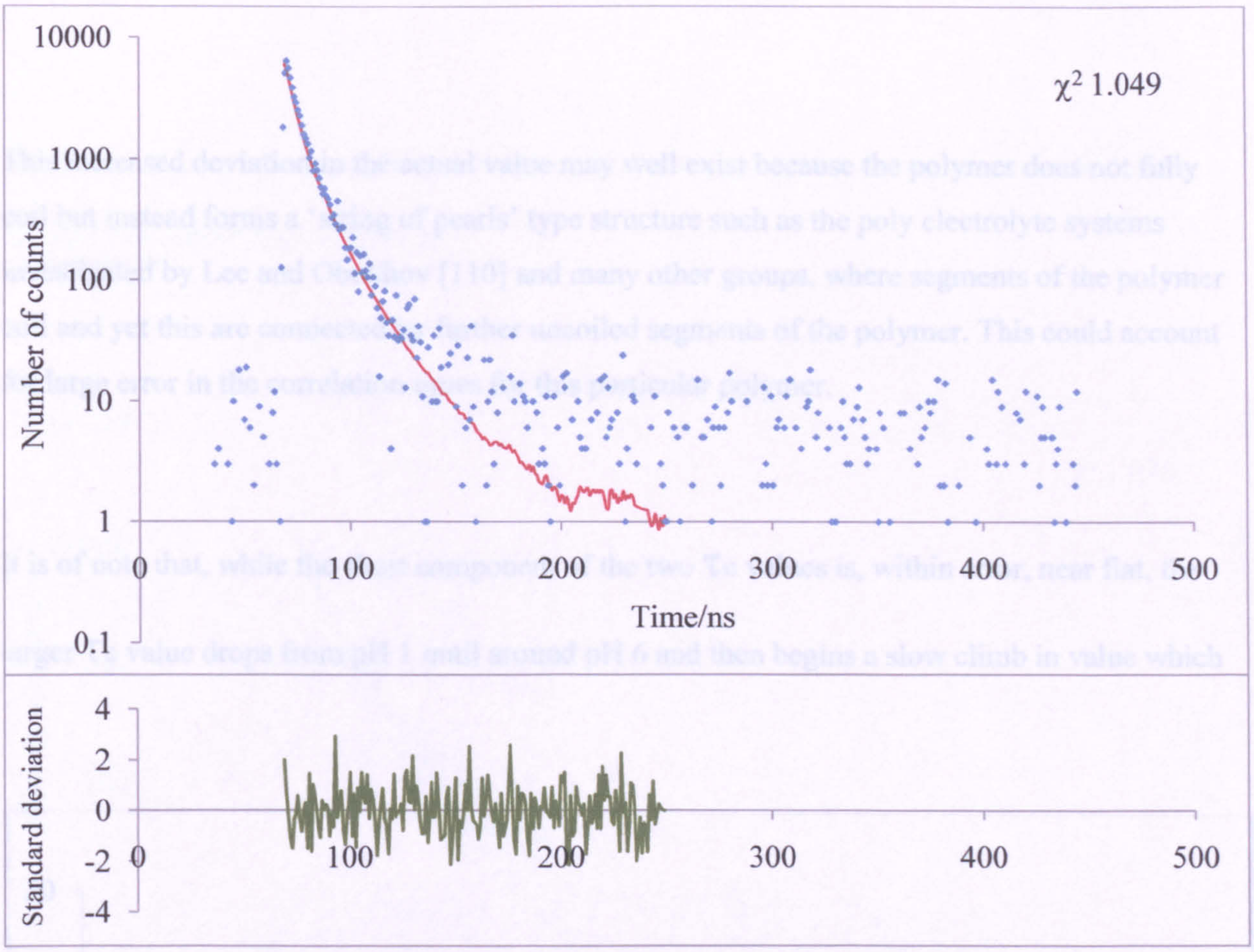

Figure 43: An impulse reconvolution fit to D(t) and a plot of the resulting residuals for ACE- PDMAEMA at pH 10 in aqueous solution.

The intramolecular segmental relaxation of the ACE-AMMA labelled PDMAEMA sample is more complicated as the AMMA label should be studied and this introduces further complexity in the form of rotational motion as well as segmental relaxation.

The TRAMS data for this sample was adequately modelled using a double exponential fit to the data once more with leaving r^{∞} varying. Although the χ^2 value for this data shows a good statistical fit the standard deviation to the larger of the two components of τc is quite substantial, most especially at high pH values when the system is expected to be in a coiled state.

This increased deviation in the actual value may well exist because the polymer does not fully coil but instead forms a 'string of pearls' type structure such as the poly electrolyte systems investigated by Lee and Obukhov [110] and many other groups, where segments of the polymer coil and yet this are connected by further uncoiled segments of the polymer. This could account for large error in the correlation times for this particular polymer.

It is of note that, while the short component of the two τc values is, within error, near flat, the larger τc value drops from pH 1 until around pH 6 and then begins a slow climb in value which

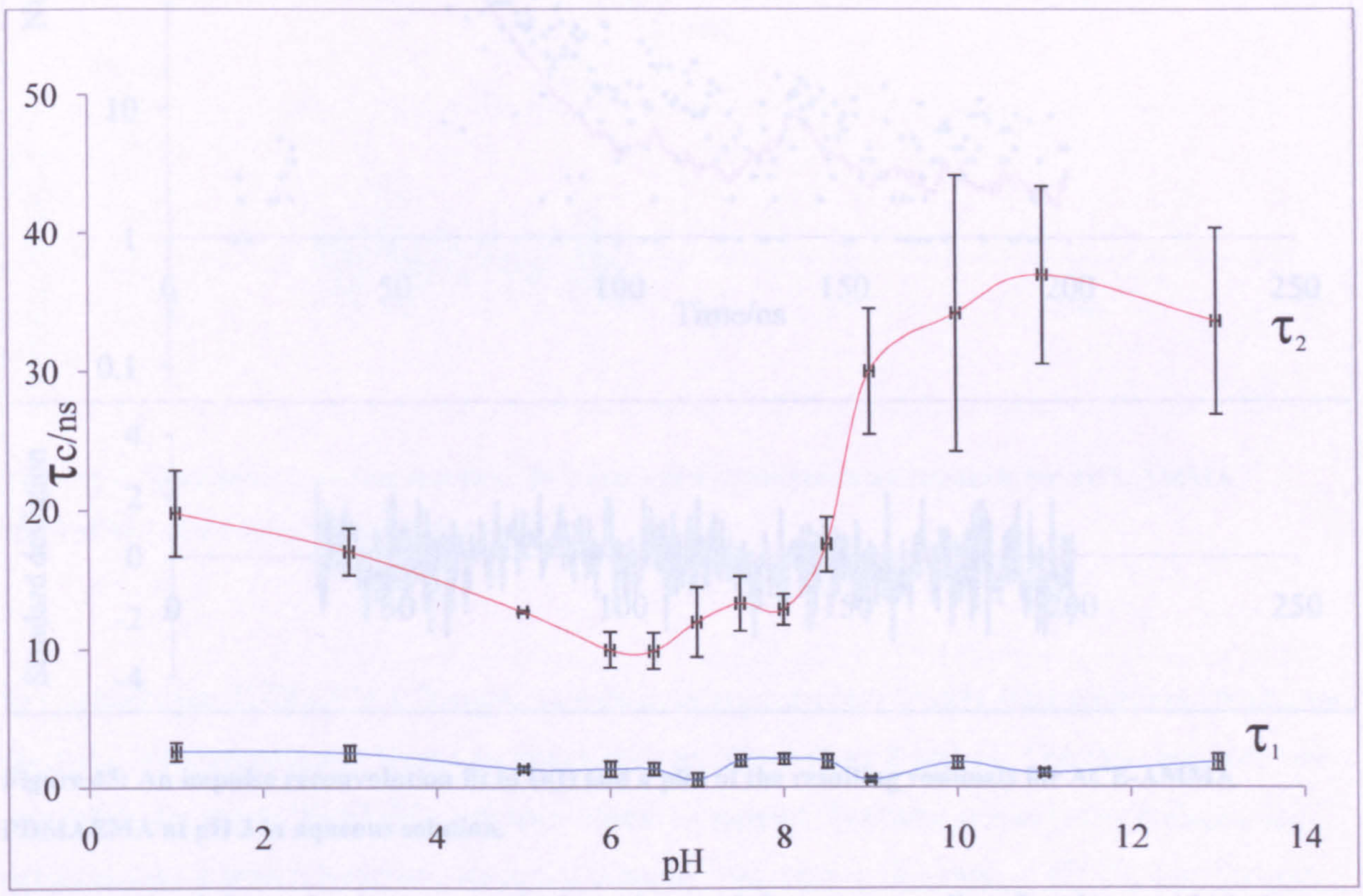

Figure 44: A plot of the τ_{c1} and τ_{c2} values obtained from Time Resolved Anisotropy Measurements on ACE-AMMA-PDMAEMA system in aqueous solution across a range of pH values.

accelerates from pH 8 up to pH 9 at which point the large standard deviations are seen and the τc could be considered to be steady.

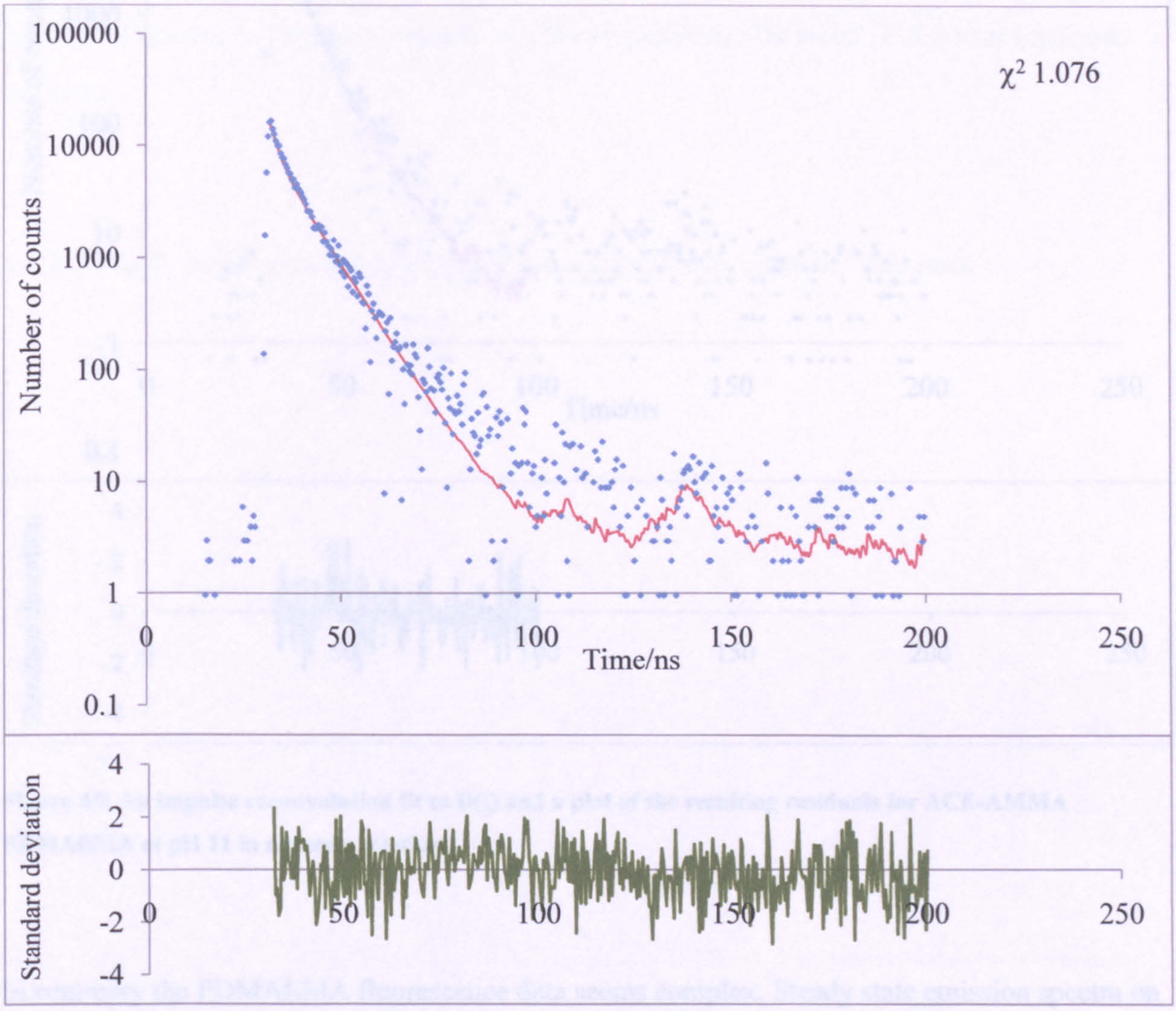

Figure 45: An impulse reconvolution fit to D(t) and a plot of the resulting residuals for ACE-AMMA PDMAEMA at pH 3 in aqueous solution.

Figures 45 and 46 again show example data plots and the corresponding fits along with their residuals, this time for the ACE-AMMA PDMAEMA system. The data at pH 11 has a much shorter decay than that at pH 3. This suggests that the anisotropy takes longer to decay at pH 11 and would be consistent with a collapsed conformation.

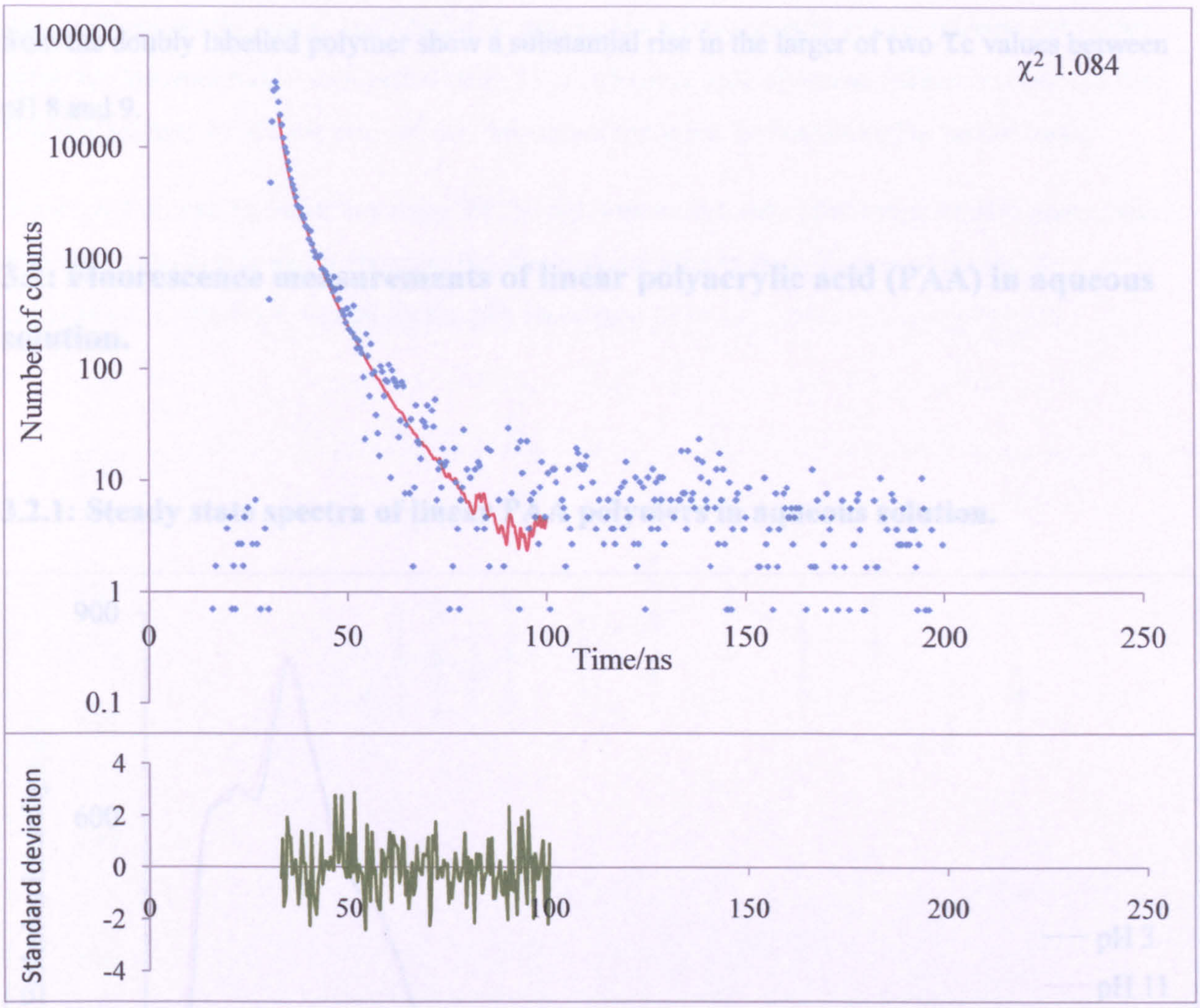

Figure 46: An impulse reconvolution fit to D(t) and a plot of the resulting residuals for ACE-AMMA PDMAEMA at pH 11 in aqueous solution.

In summary the PDMAEMA fluorescence data seems complex. Steady state emission spectra on the ACE labelled polymer shows an intensity drop between pH 8 and 11. The ratio between the two labels for the ACE-AMMA polymer seems to support that there is a polymer collapse and hence energy transfer, however, there is a dramatic decrease in this ratio at pH 10. The lifetime data for the two polymer systems also indicates a collapse of the polymer, although the lifetime data indicates a pH value between 7 and 8 is the point of collapse. The TRAMS data for the ACE label polymer shows a similar rapid drop, indicative of a more mobile phase in TRAMS readings, at pH 10 matching that of the double label steady state readings. The TRAMS data

from the doubly labelled polymer show a substantial rise in the larger of two τc values between pH 8 and 9.

3.2: Fluorescence measurements of linear polyacrylic acid (PAA) in aqueous solution.

3.2.1: Steady state spectra of linear PAA polymers in aqueous solution.

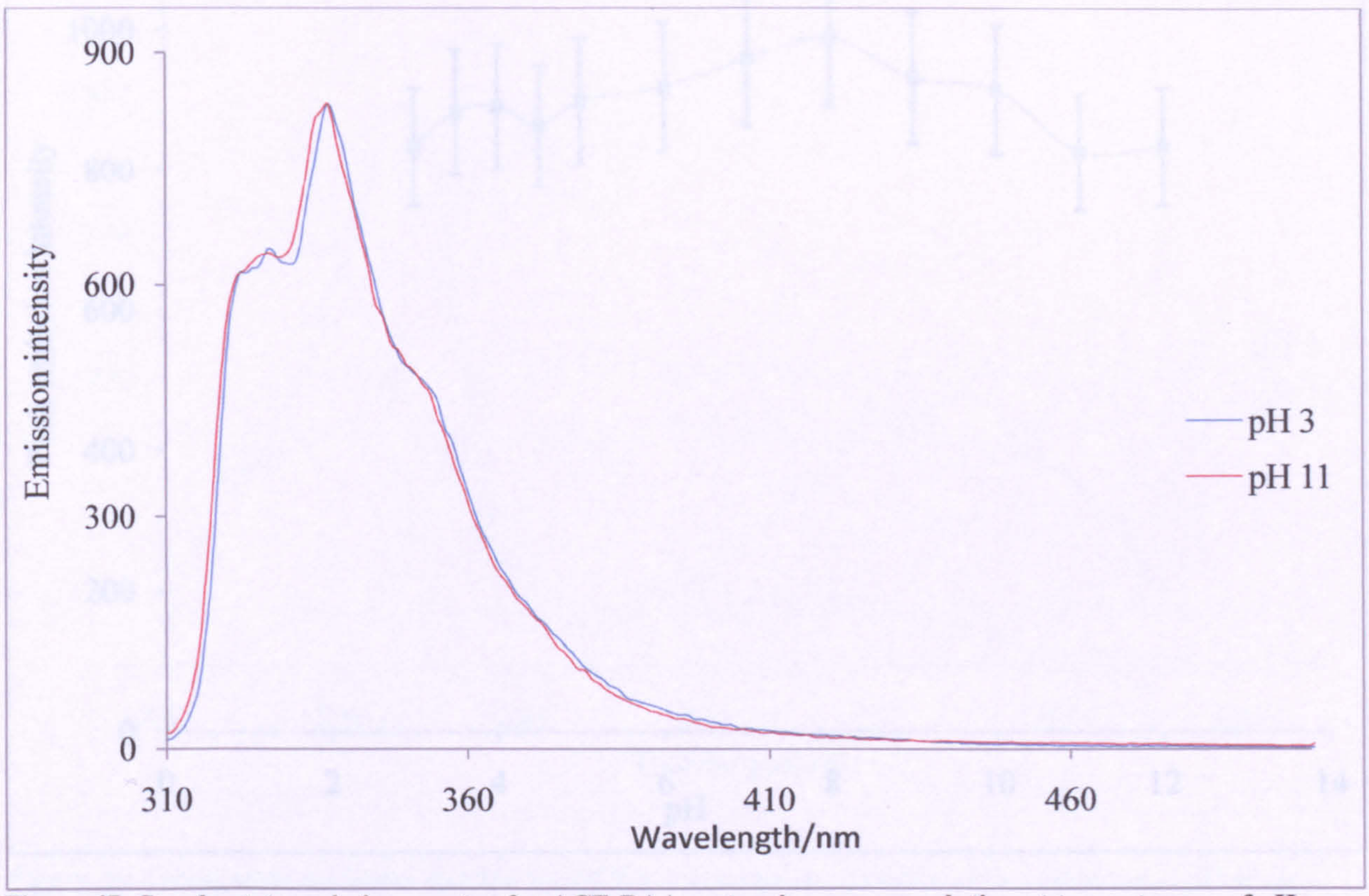

Figure 47: Steady state emission spectra for ACE-PAA system in aqueous solution at two extremes of pH when excited at 290 nm.

Figure 47 shows the steady state emission spectra for a PAA sample at two extreme pH values when the polymer has been labelled with ACE . There is little apparent difference between the two spectra and within the error of the instrument these can be considered to be the same.

A plot of the peak emission intensity for the polymer across the entire range of pH values (see figure 48) shows that this is the case and that nothing affects the emission of the ACE fluorophore in the PAA sample as the pH increases.

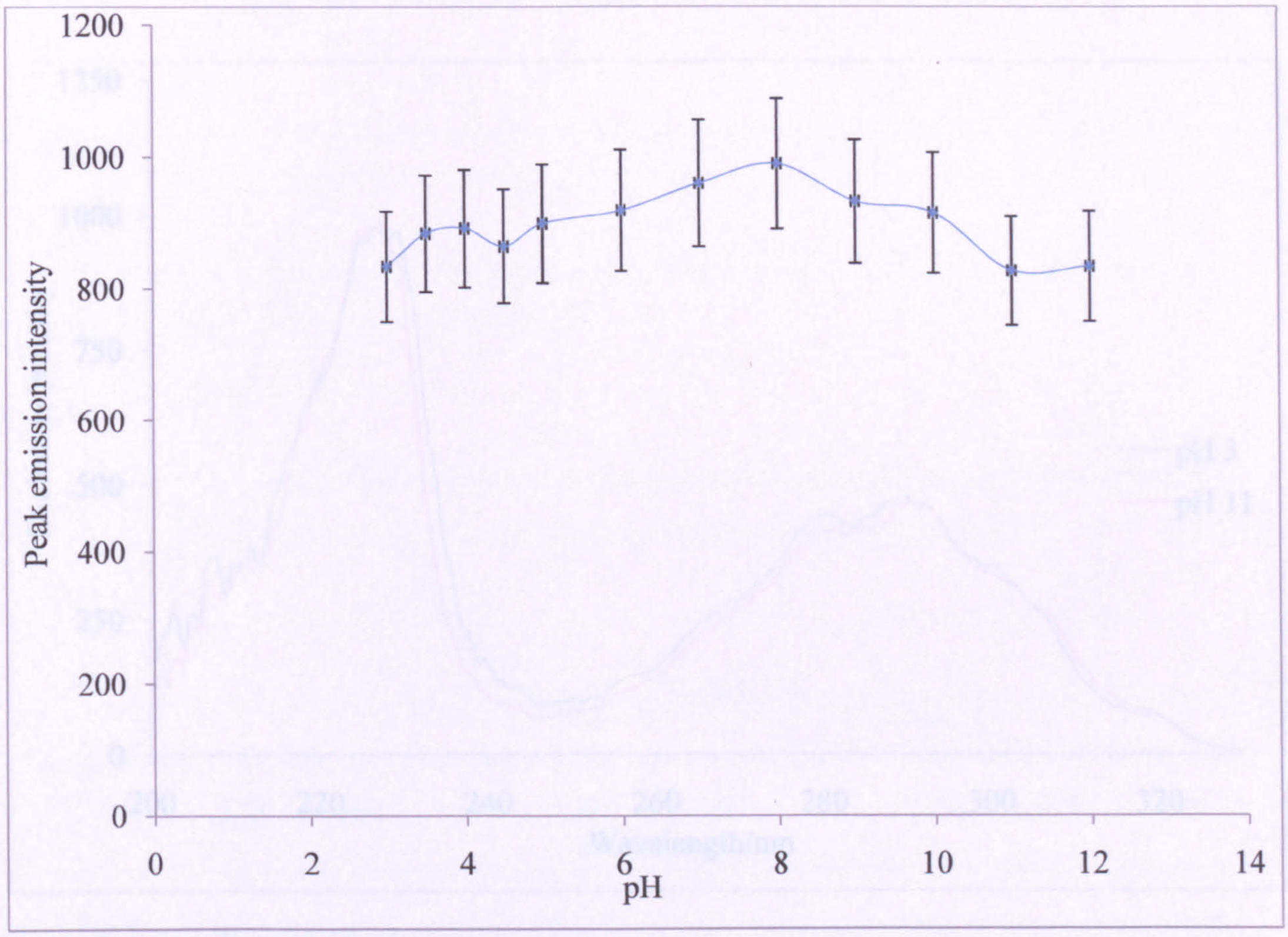

Figure 48: A plot of the peak emission intensity (observed at 337nm) from steady state emission spectra of ACE-PPA in aqueous solution across a range of pH values when excited at 290nm.

A plot of the corresponding excitation spectra for the polymer system (see figure 48) confirms that there appears to be no effect at all on the fluorescence of the system with increasing pH value.

This is to be expected as only minor changes in the intensity are seen potentially showing some exclusion of aqueous media from the fluorophore and no large changes in intensity are seen indicating a lack of any quenching internal to the polymer chain such as was seen with PDMAEMA.

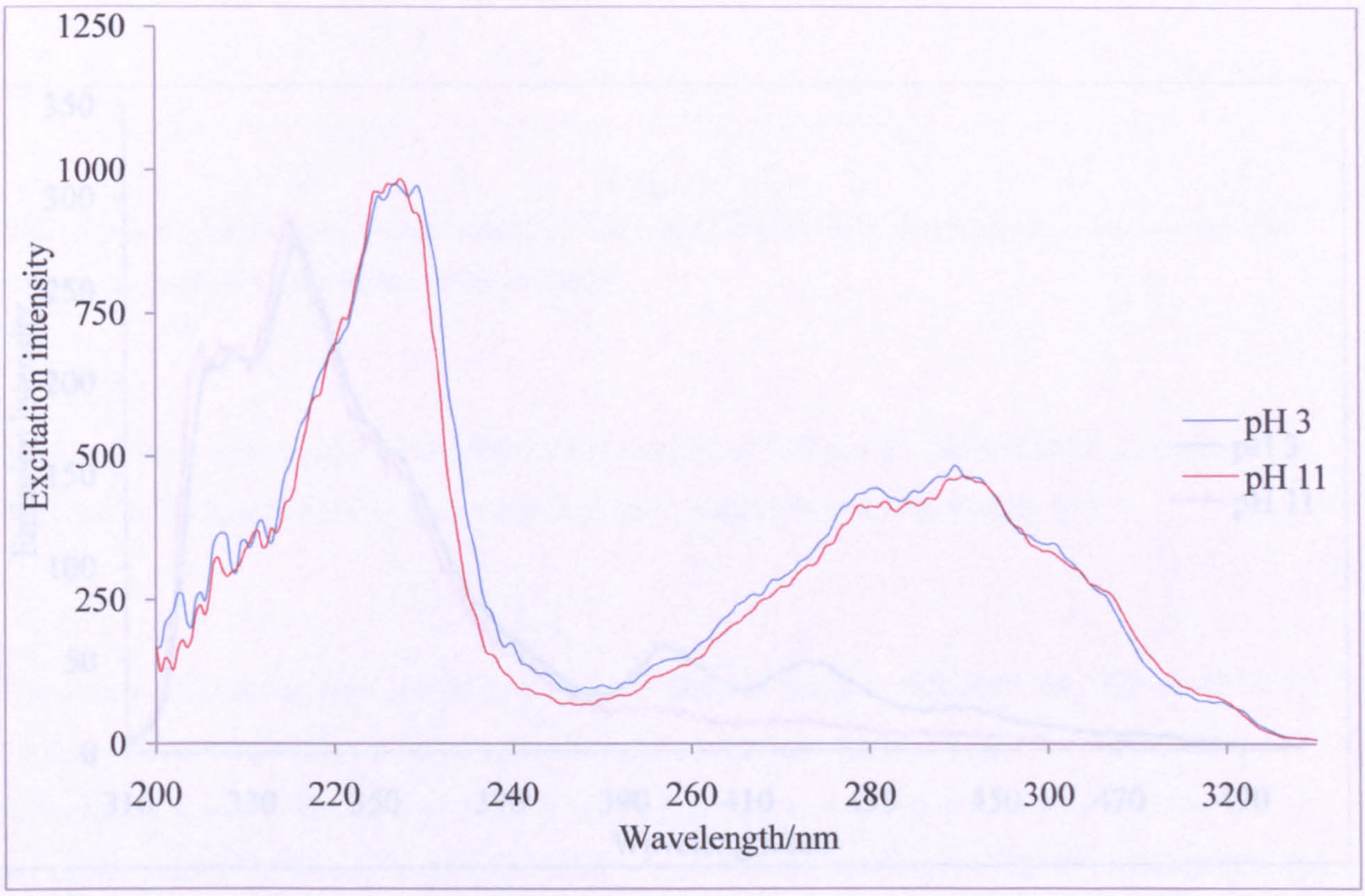

Figure 49: Steady state excitation spectra for ACE-PAA in aqueous solution at two extremes of pH when observed at 340nm.

Figure 50 shows a plot of the emission spectra of ACE-AMMA-PAA when an excitation wavelength of 290 nm is used. At pH 11 the emission is dominated by that from ACE. This indicates that the donor to acceptor distance is outside the critical transfer distance and so NRET

is minimal. This is consistent with the expanded conformation in the polysalt form. At pH 3 on the other hand, there is emission from both ACE and AMMA (at ca 420 nm). Under these conditions the polymer contracts due to formation of hydrophobic carboxylic acid units. This brings the donor and acceptor to within 10nm and allows NRET to take place.

A plot of the peak emission intensities across the entire pH range (See figure 50) confirms this and although within error the ACE emission could be considering to remain constant the emission of the AMMA label shows a clear drop in intensity between pH 4 and 7.

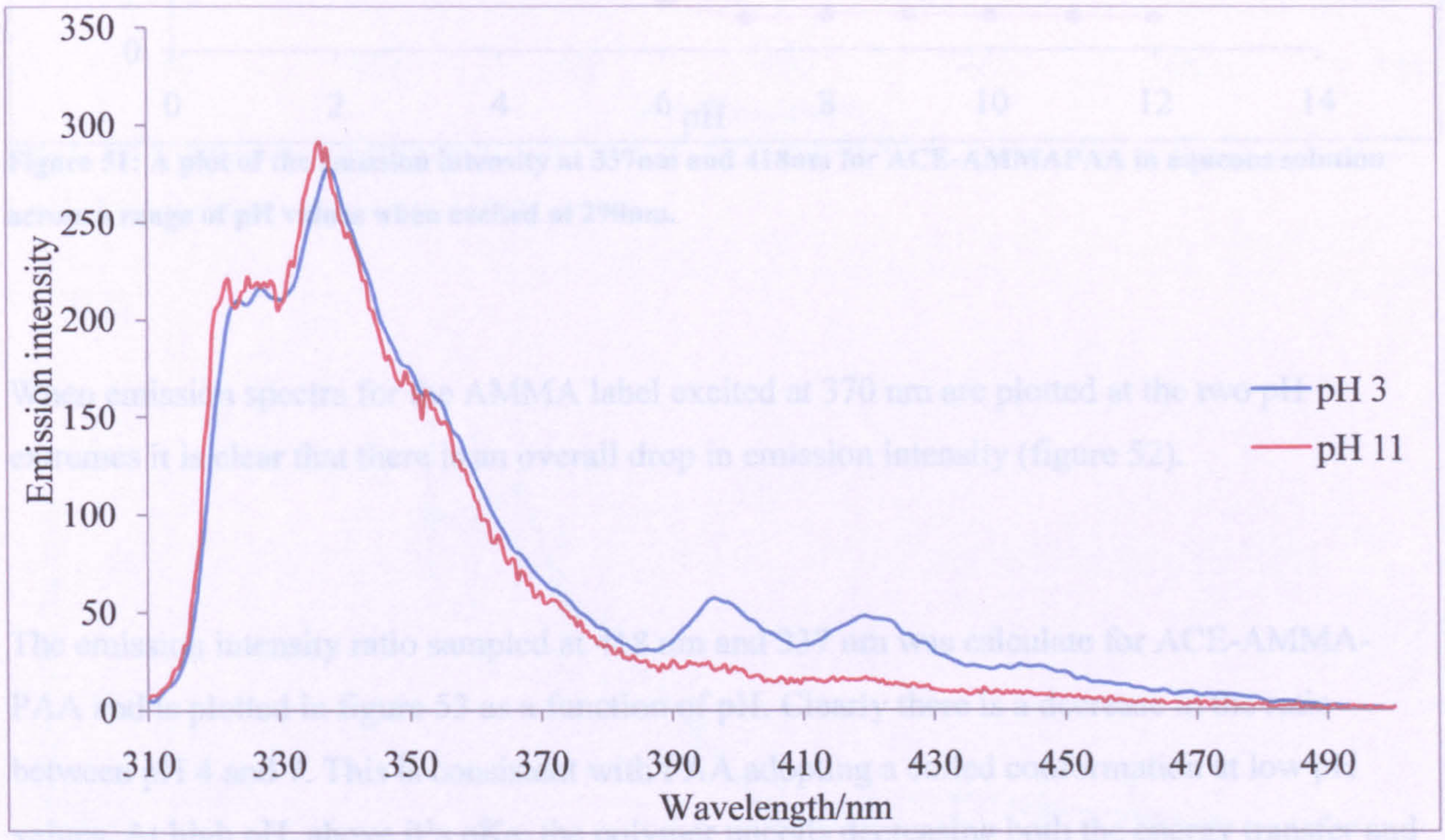

Figure 50: Steady state emission spectra for ACE-AMMA PAA in aqueous solution at two extremes of pH when excited at 290nm.

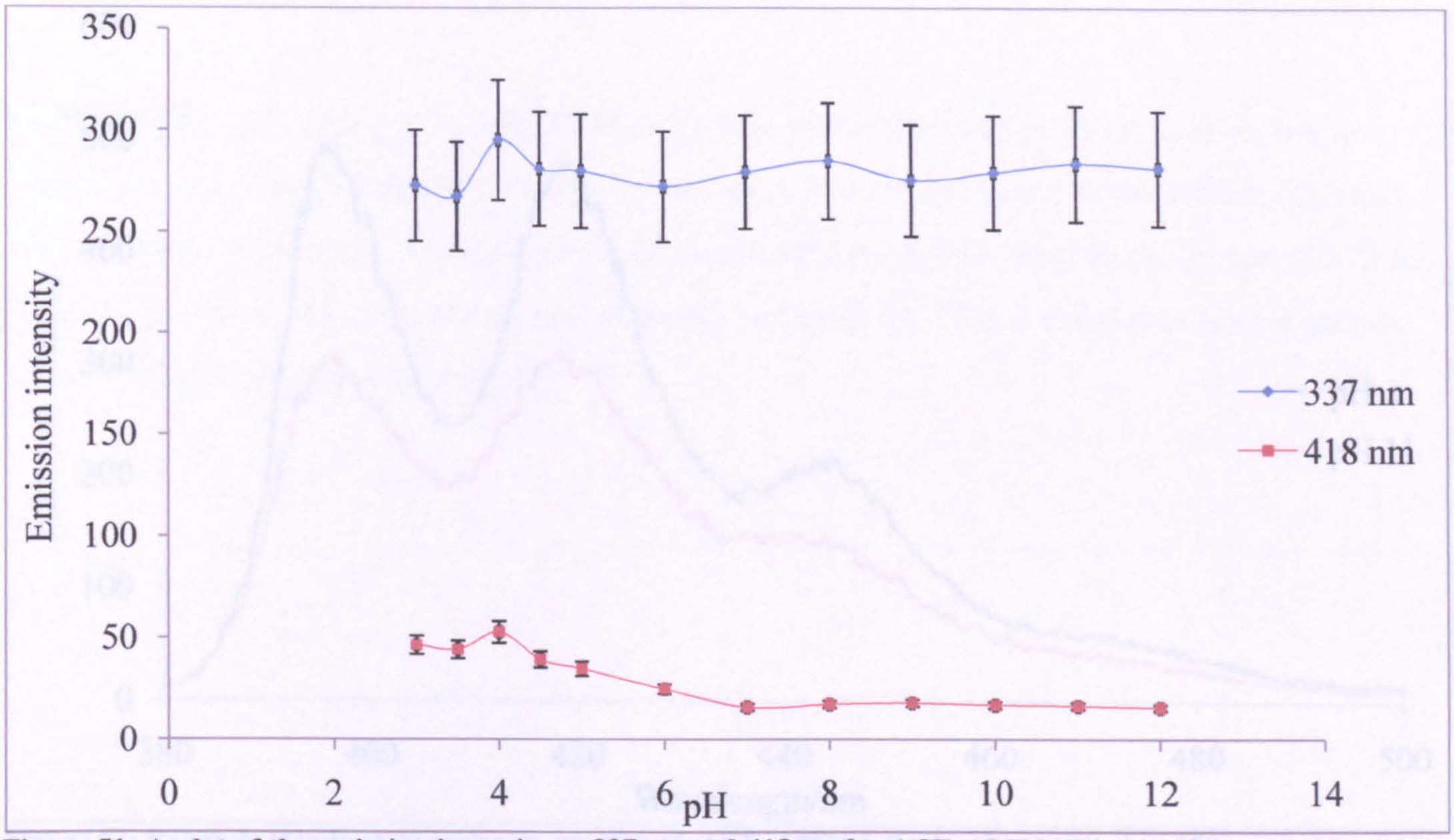

Figure 51: A plot of the emission intensity at 337nm and 418nm for ACE-AMMAPAA in aqueous solution across a range of pH values when excited at 290nm.

When emission spectra for the AMMA label excited at 370 nm are plotted at the two pH extremes it is clear that there is an overall drop in emission intensity (figure 52).

The emission intensity ratio sampled at 418 nm and 337 nm was calculate for ACE-AMMA-PAA and is plotted in figure 53 as a function of pH. Clearly there is a decrease in the ratio between pH 4 and 7. This is consistent with PAA adopting a coiled conformation at low pH values. At high pH, above it's pKa, the polymer uncoils decreasing both the energy transfer and the intensity ratio.

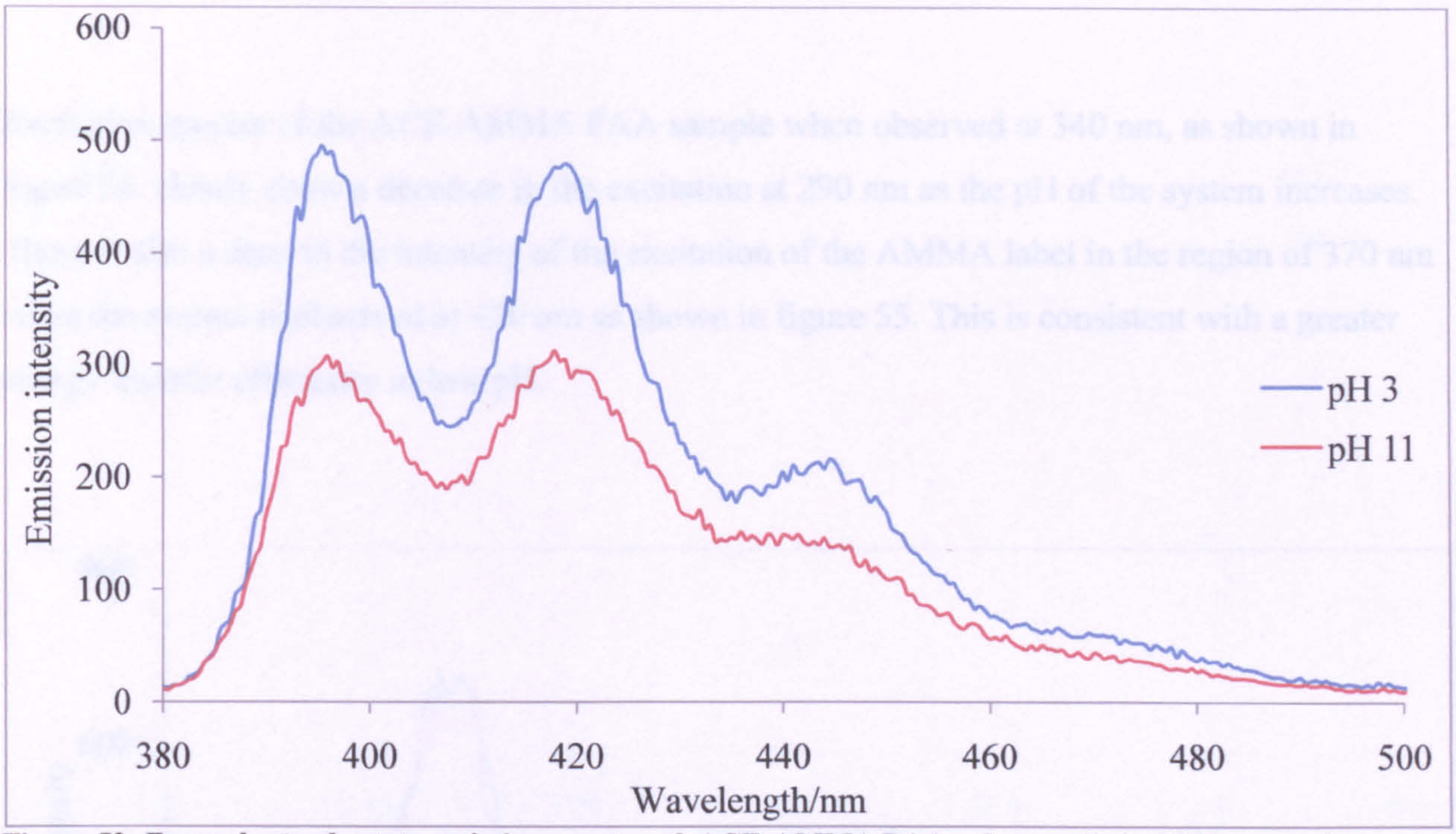

Figure 52: Example steady state emission spectra of ACE-AMMA PAA when excited at 370 nm to observe the AMMA emissions over a range of pH values.

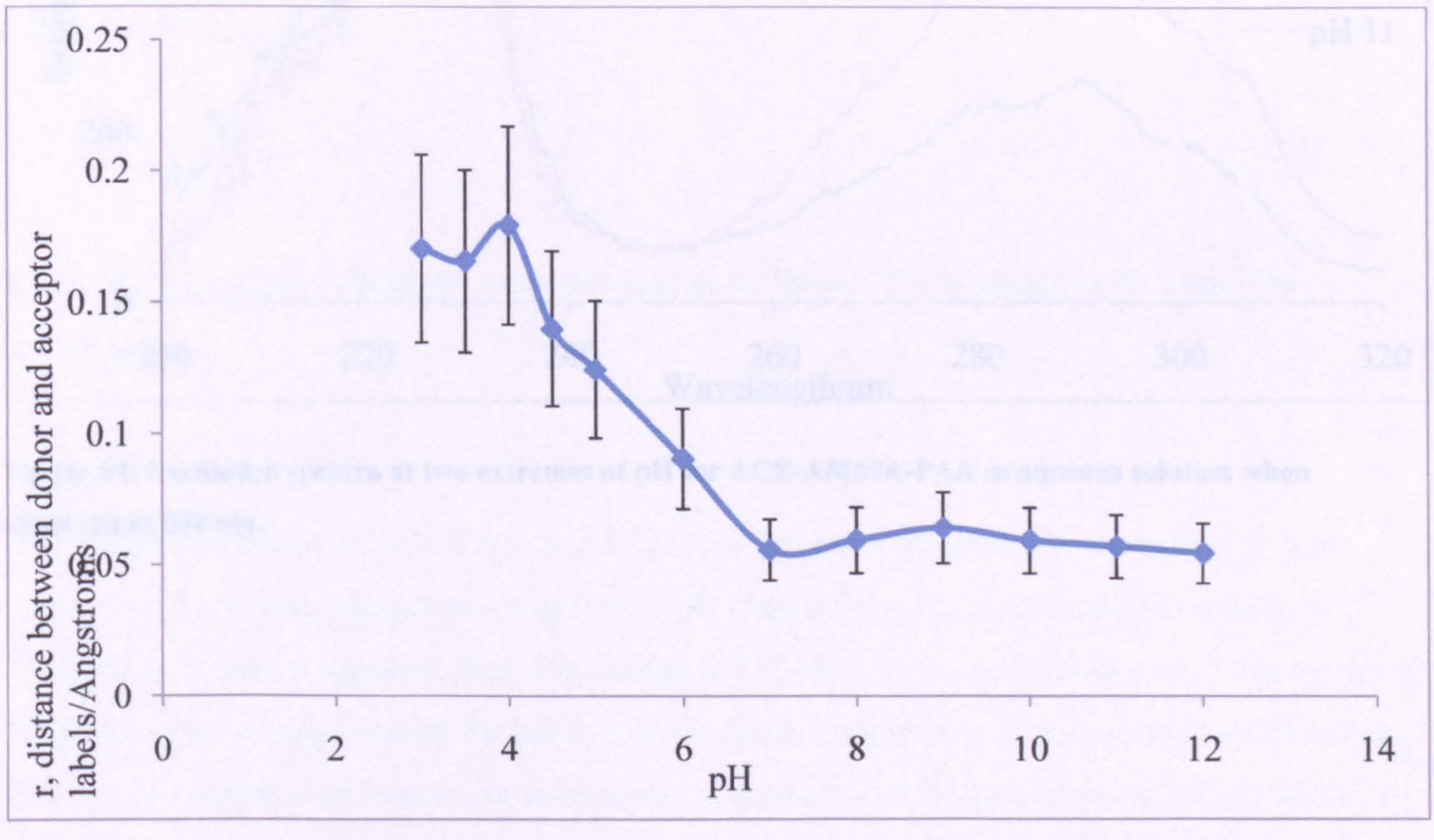

Figure 53: A plot of the emission intensity ratio between the AMMA emission at 418 nm and the ACE emission at 337 nm for ACE-AMMA-PAA in aqueous solution when excited at 290 nm across a range of pH values.

Excitation spectra of the ACE-AMMA PAA sample when observed at 340 nm, as shown in figure 54, clearly show a decrease in the excitation at 290 nm as the pH of the system increases. There is also a drop in the intensity of the excitation of the AMMA label in the region of 370 nm when the system is observed at 420 nm as shown in figure 55. This is consistent with a greater energy transfer efficiency at low pH.

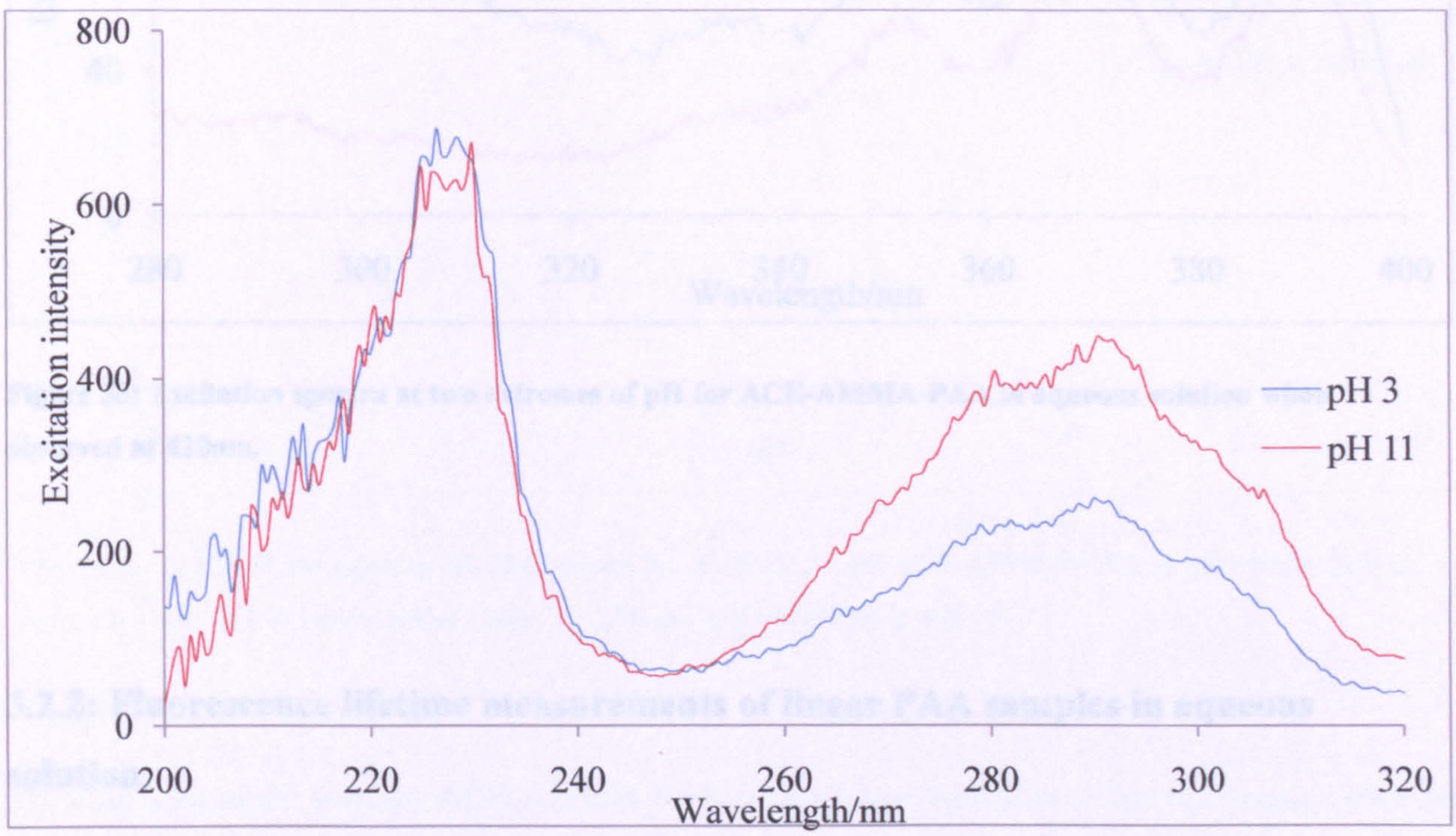

Figure 54: Excitation spectra at two extremes of pH for ACE-AMMA-PAA in aqueous solution when observed at 340 nm.

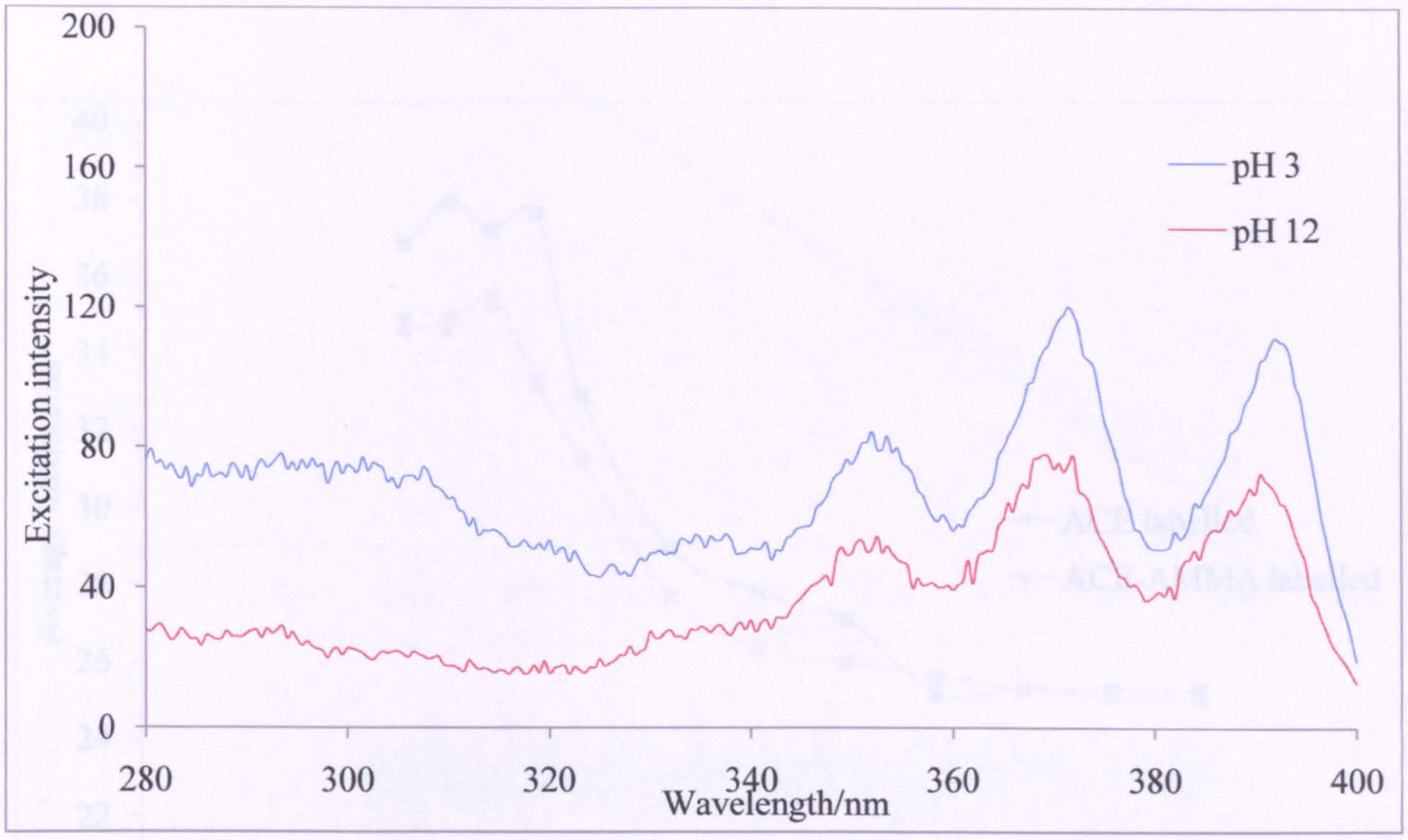

Figure 55: Excitation spectra at two extremes of pH for ACE-AMMA-PAA in aqueous solution when observed at 420nm.

3.2.2: Fluorescence lifetime measurements of linear PAA samples in aqueous solution.

The average lifetime for ACE-PAA and ACE-AMMA-PAA respectively were derived from equation 1.4 and then plotted as a function of pH (figure 56) The conformational transition of ACE-PAA is clearly apparent from the change in lifetime. At low pH values a partially collapsed structure exists which protects the label from the quenching effects of the aqueous phase hence the ACE emission lives longer. As ionisation commences and the pKa is exceeded a gradual decrease in lifetime is apparent as expansion of the PAA occurs in to the polysalt form. The excited state lifetime of ACE decreases due to a combination of quenching from the aqueous phase and carboxylate anions.

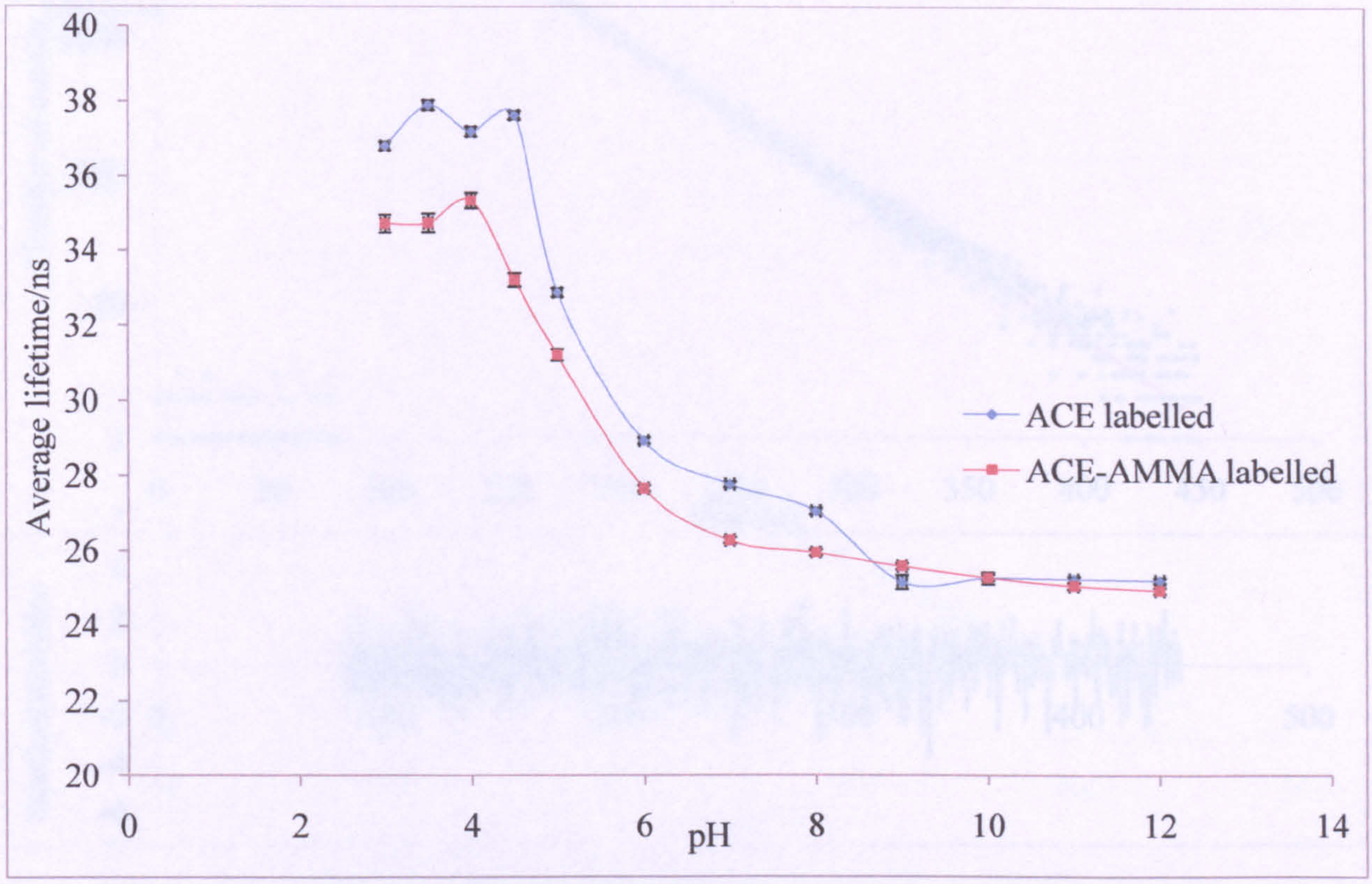

Figure 56: A plot of the average lifetime values for ACE-PAA and ACE-AMMA-PAA in aqueous solution across a range of pH values when excited at 290 nm and observed at 340 nm.

Examination of the data for ACE-AMMA PAA on the other hand shows that the average lifetime is always less than that of the singly labelled sample at pH values less than 7. This suggests that NRET occurs due to the labels being in close proximity in the collapsed form. At pH values in excess of 7 similar average lifetimes are obtained for both the singly and doubly labelled samples. This is consistent with formation of an expanded, water swollen coil, under these conditions. The donor and acceptor are now separated by more than the critical transfer distance and no NRET occurs.

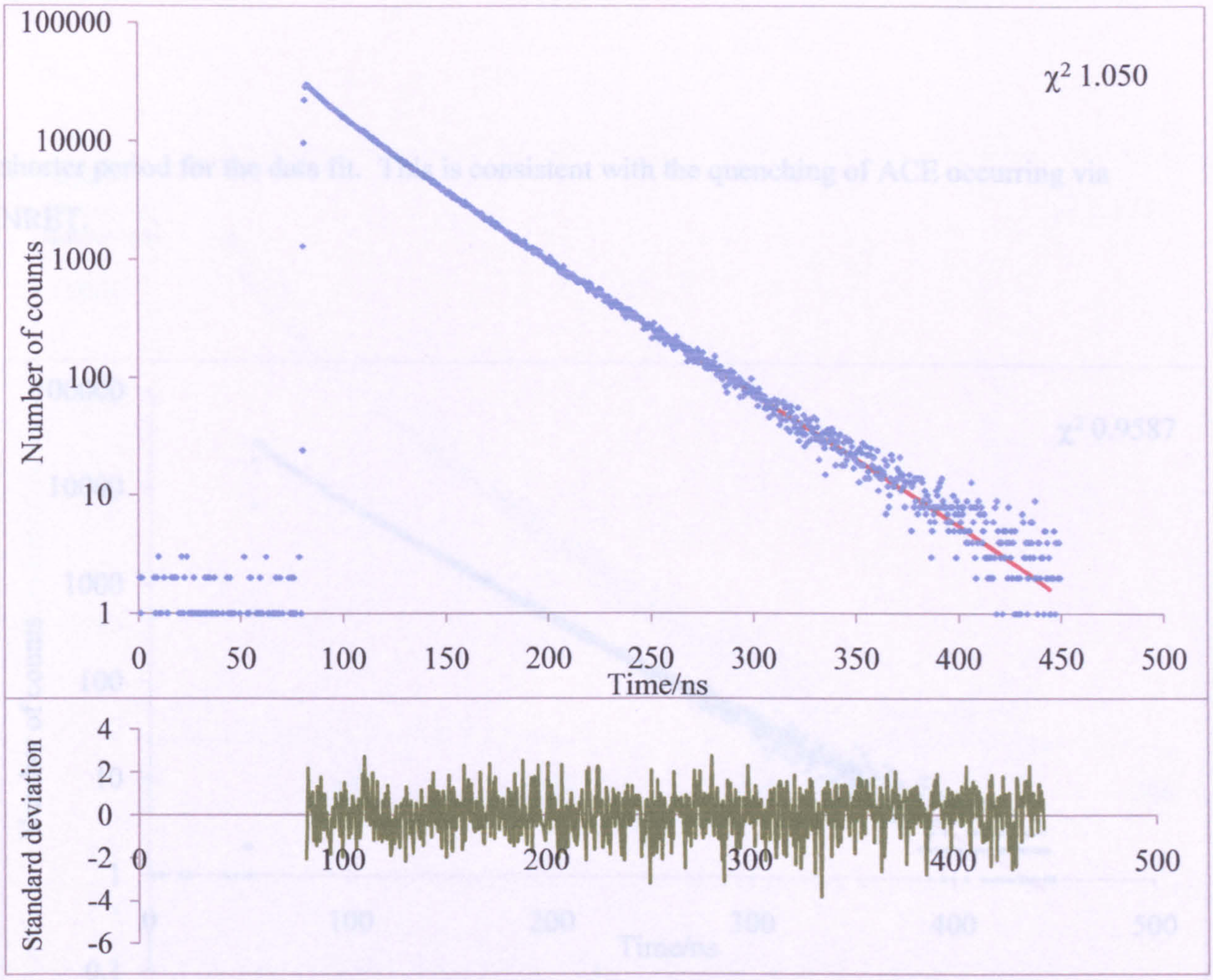

Figure 57: A fluorescence decay with corresponding mathematical fit (shown in red) and a plot of the resulting residuals for ACE-PAA at pH 3.

Like the PDMAEMA samples the data was again fitted using a triple exponential fit such as equation 1.3, this fit showed the best statistical fit according to both χ^2 and the standard deviations of the resulting lifetimes as well as exhibiting a relatively even distribution of residuals.

The residuals plots also show that the triple exponential fits to the lifetime values were statistically good. It is worth noting how the high pH double label sample shows a substantially

shorter period for the data fit. This is consistent with the quenching of ACE occurring via NRET.

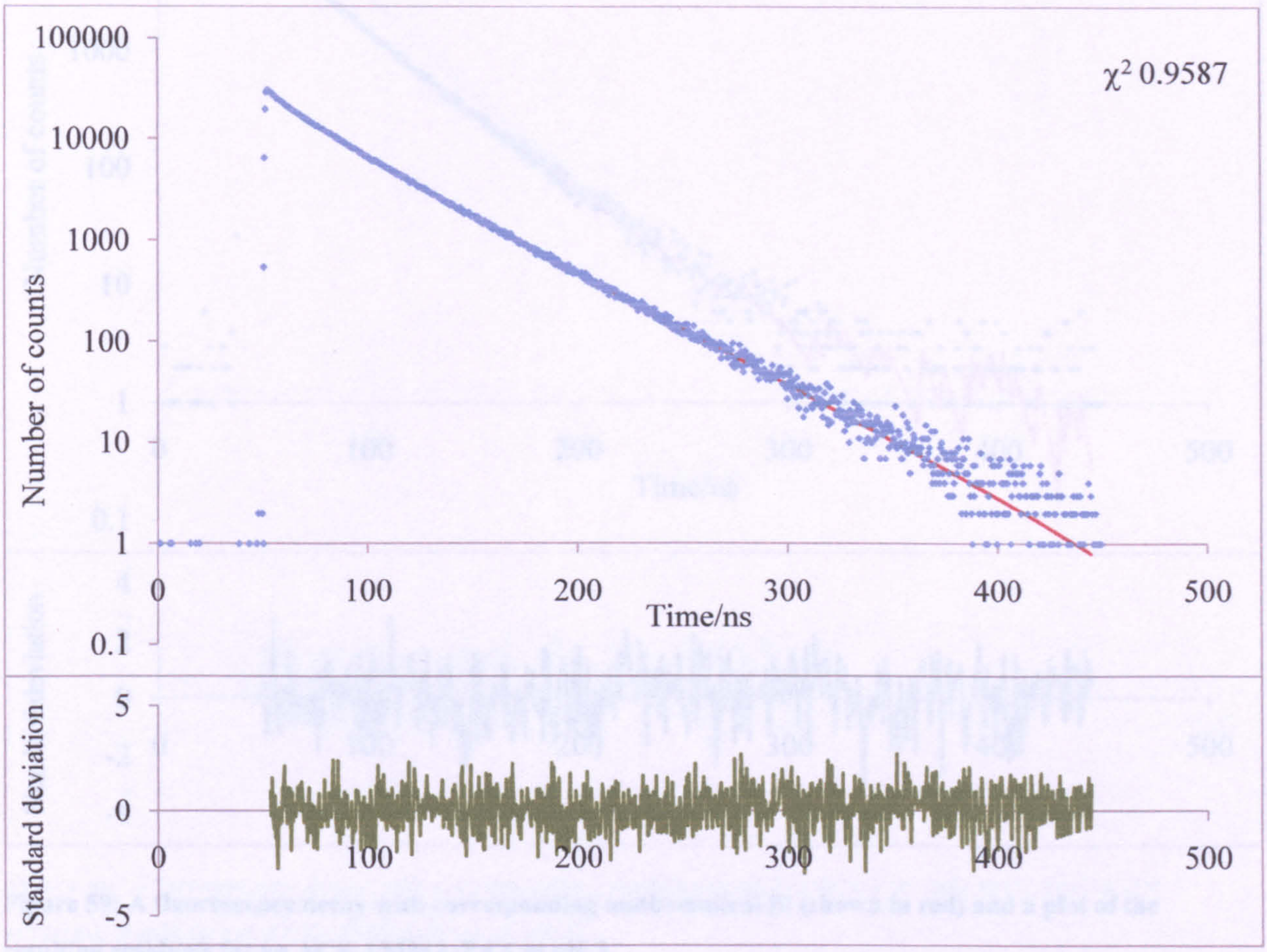

Figure 58: A fluorescence decay with corresponding mathematical fit (shown in red) and a plot of the resulting residuals for an ACE-PAA at pH 7

It is of note that the point at which this appears to be the case is of a higher pH value than the point at which the emission intensity ratio between the two labels plateaus as shown from the steady state spectra.

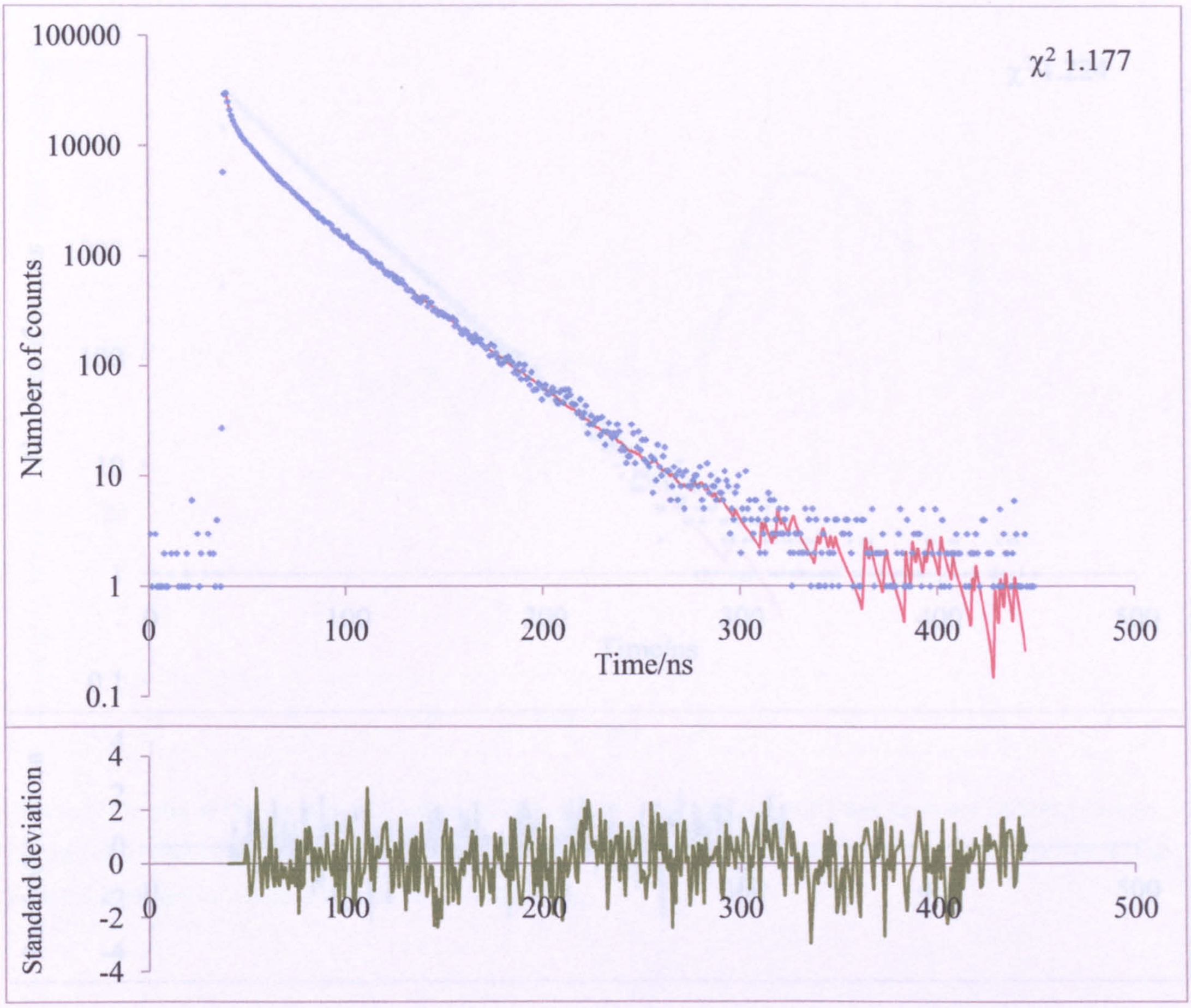

Figure 59: A fluorescence decay with corresponding mathematical fit (shown in red) and a plot of the resulting residuals for an ACE-AMMA-PAA at pH 3.

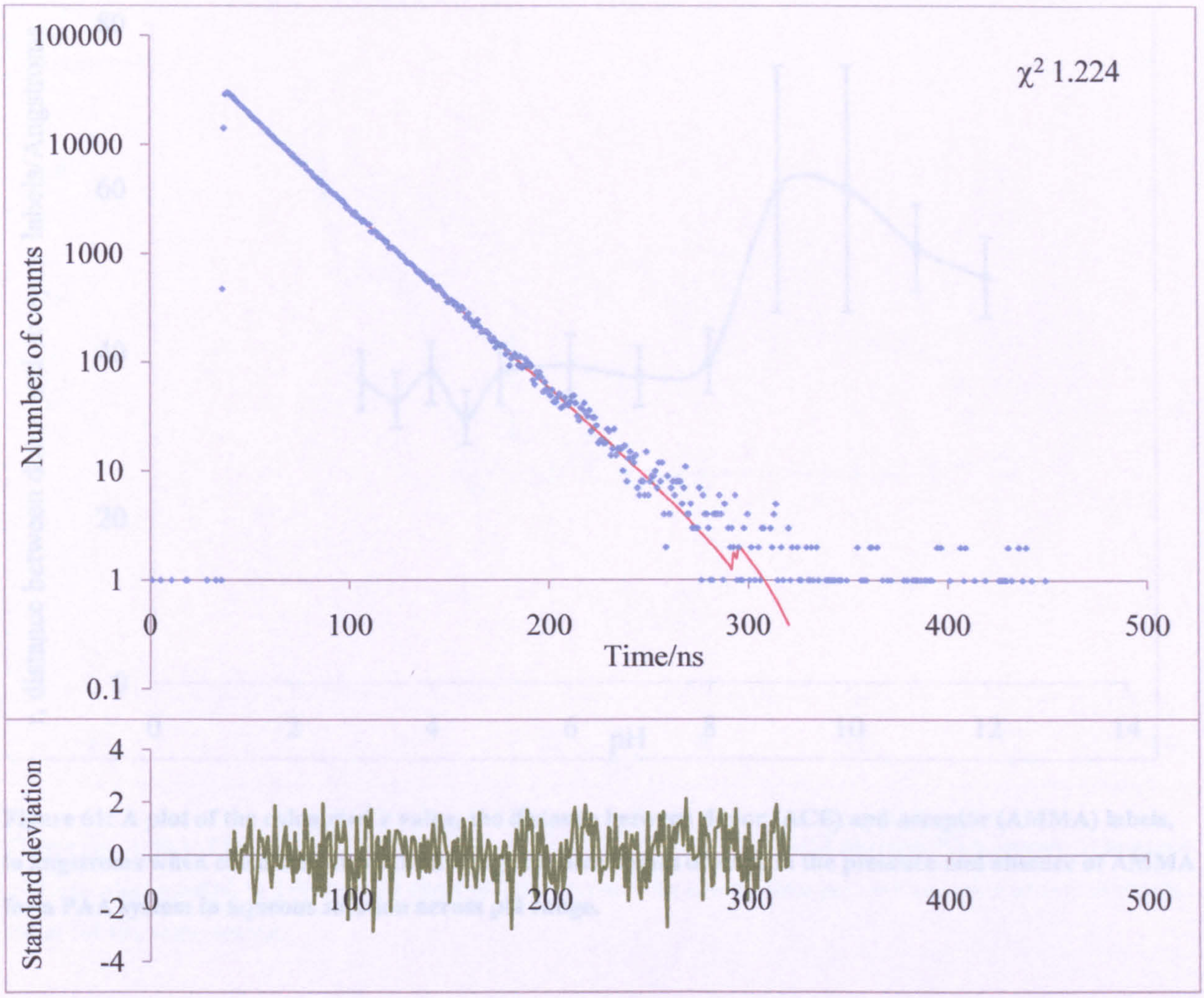

Figure 60: A fluorescence decay with corresponding mathematical fit (shown in red) and a plot of the resulting residuals for ACE-AMMA-PAA at pH 11.

The average separation distance, r, was subsequently calculated from equations 3.1 and 3.2. The resulting data is plotted as a function of pH for PAA in figure 61. The two large values of r in figure 61 at pH 9 and 10 are outside of the resolution of the experiment. Clearly up to around pH 7 the average separation distance between D and A in approximately 40 angstroms which is consistent with a collapsed coiled form. Above pH 7 PAA expands and the distance between the labels is greater than that over which NRET occurs.

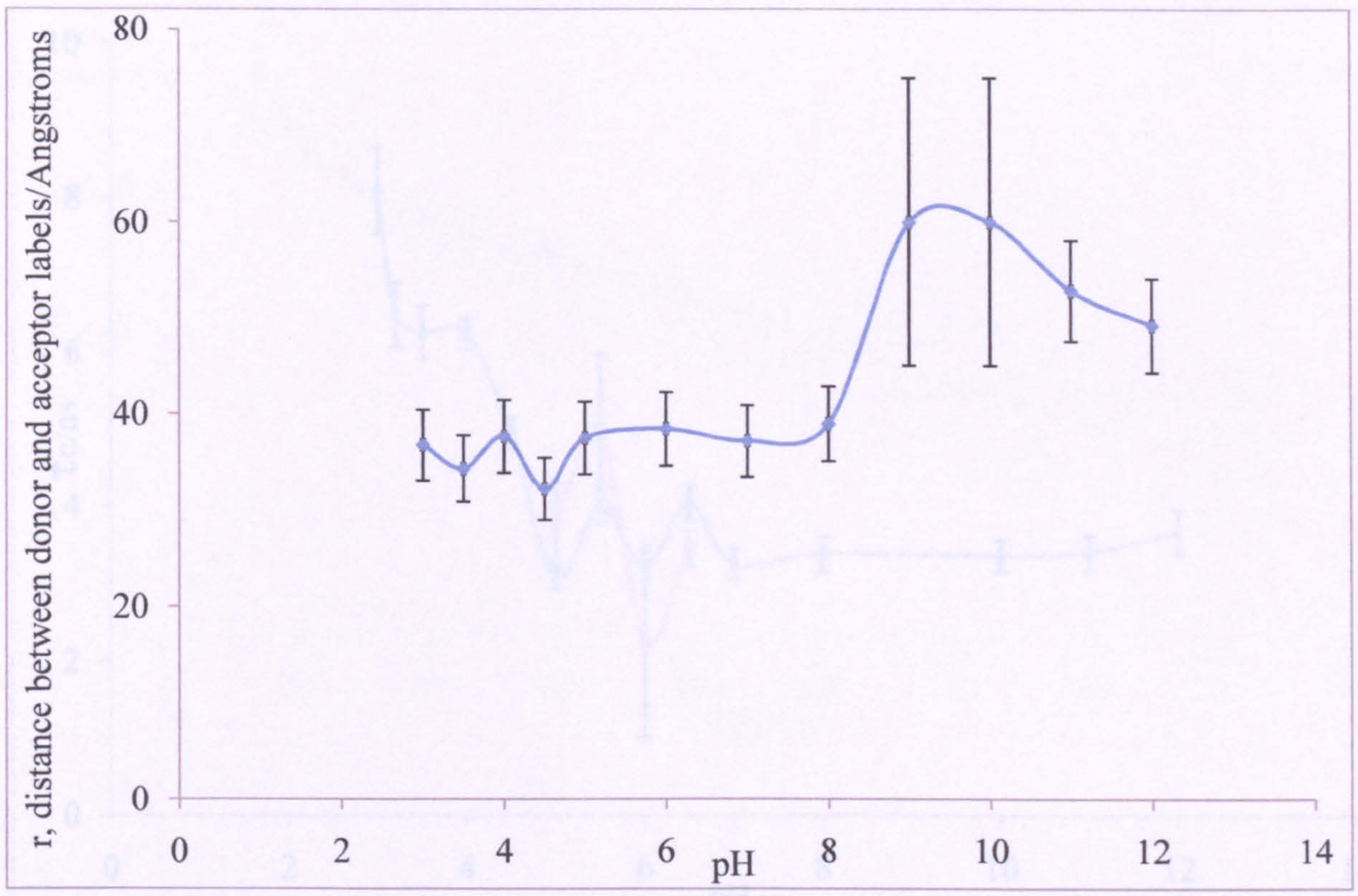

Figure 61: A plot of the calculated r value, the distance between donor (ACE) and acceptor (AMMA) labels, in angstroms when calculated from the average lifetime values of ACE in the presence and absence of AMMA for a PAA system in aqueous solution across pH range.

3.2.3: Time Resolved Anisotropy Measurements on linear PAA samples in aqueous solution.

TRAMS experiments run on ACE PAA samples across a range of pH values were best fitted to a single exponential mathematical model of the form for which a triple exponential is shown in equation 1.7. Double exponential fits had a number of marginally better χ^2 values, however, across the entire data range the statistical fit at low pH values was poor. The residuals for figures 63 and 64 show that the single exponential model fit well.

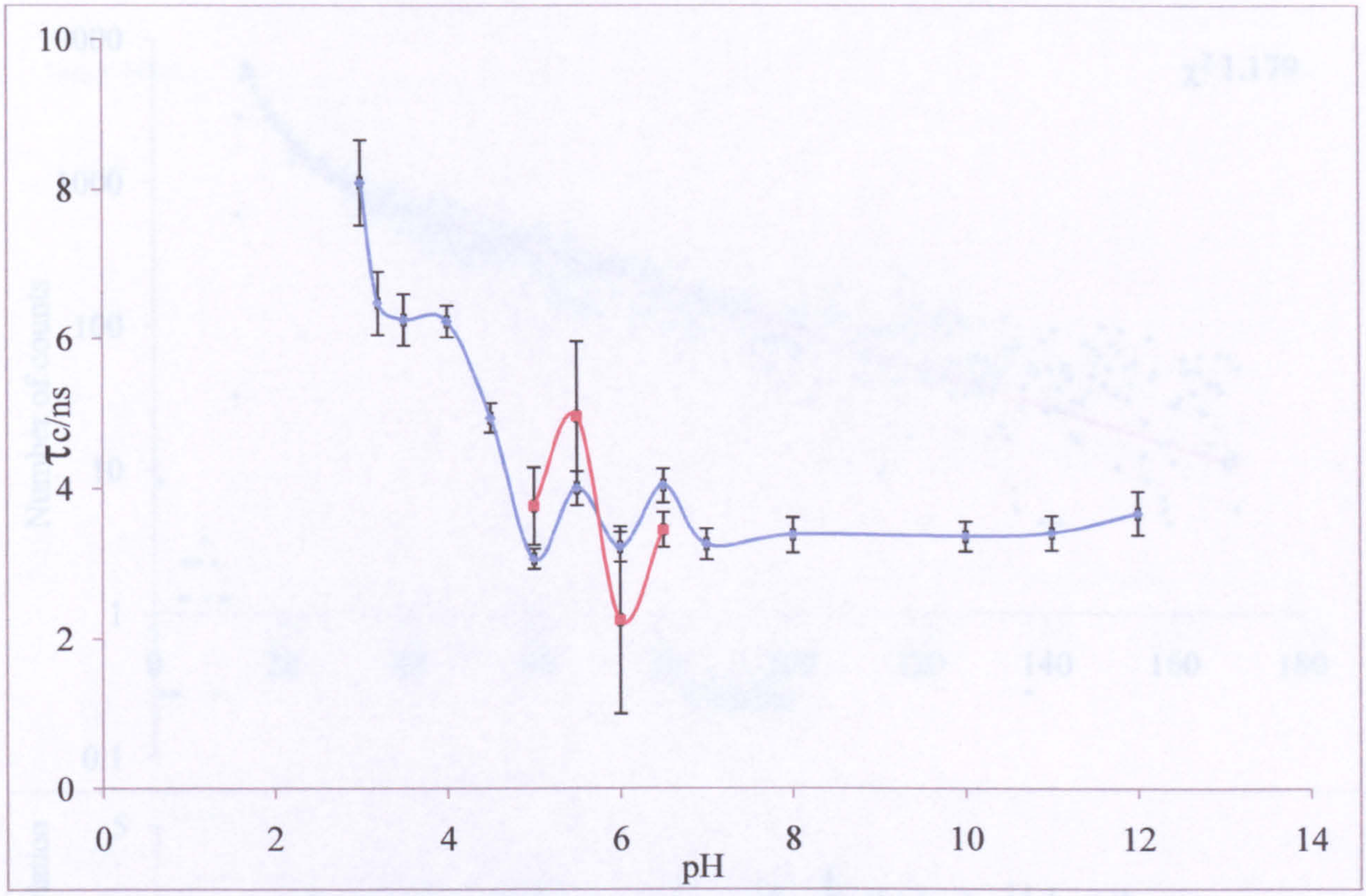

Figure 62: A plot of correlation time across a range of pH values for an ACE labelled PAA sample in aqueous solution when excited at 290 nm and observed at 340 nm. The second data plot is a selection of repeat values taken for the same system.

There is a general decrease in the τc value obtains from TRAMS experiments from pH 3 to pH 5 which suggests that the data becomes more complex. The second plot of data in figure 62 shows that although the transition point between pH 5 and 7 can be replicated the error within these values can be considered to mean that there is no actual variance within pH across this data range and that at pH values of 5 or greater the polymer system remains at a constant expanded conformation and the τc value remains unchanged.

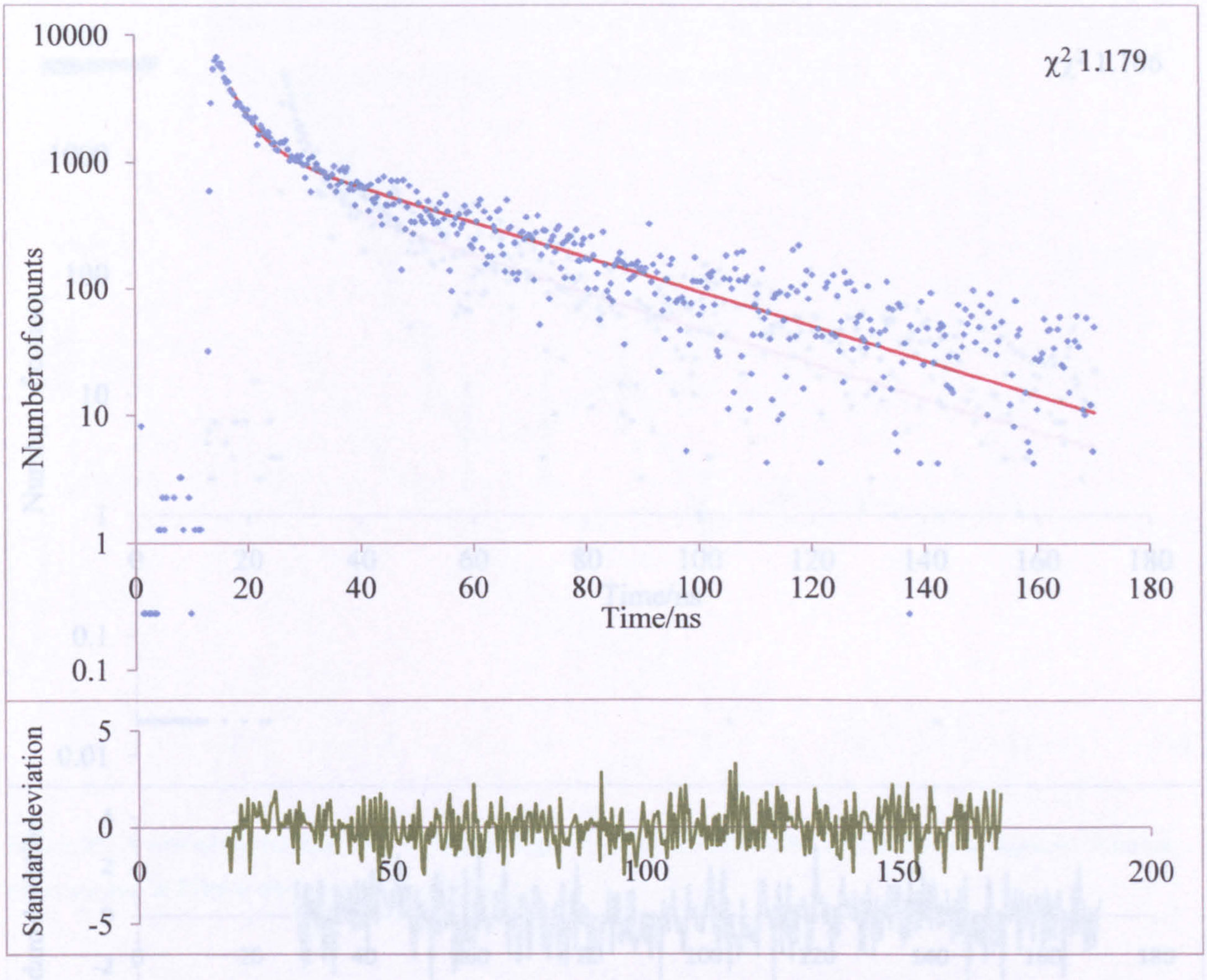

Figure 63: An impulse reconvolution fit to D(t) and a plot of the resulting residuals for ACE-PAA sample of pH 3 in aqueous solution.

However if this is the case then TRAMS data would indicate that the polymer conformation change is finished at a much earlier pH value (pH 5) than is indicated by either the steady state or lifetime results both of which indicate this happens at a higher pH value (pH 7 to 8).

The TRAMS data from the ACE-AMMA labelled PAA sample shows events in both of these pH regions (figure 65).

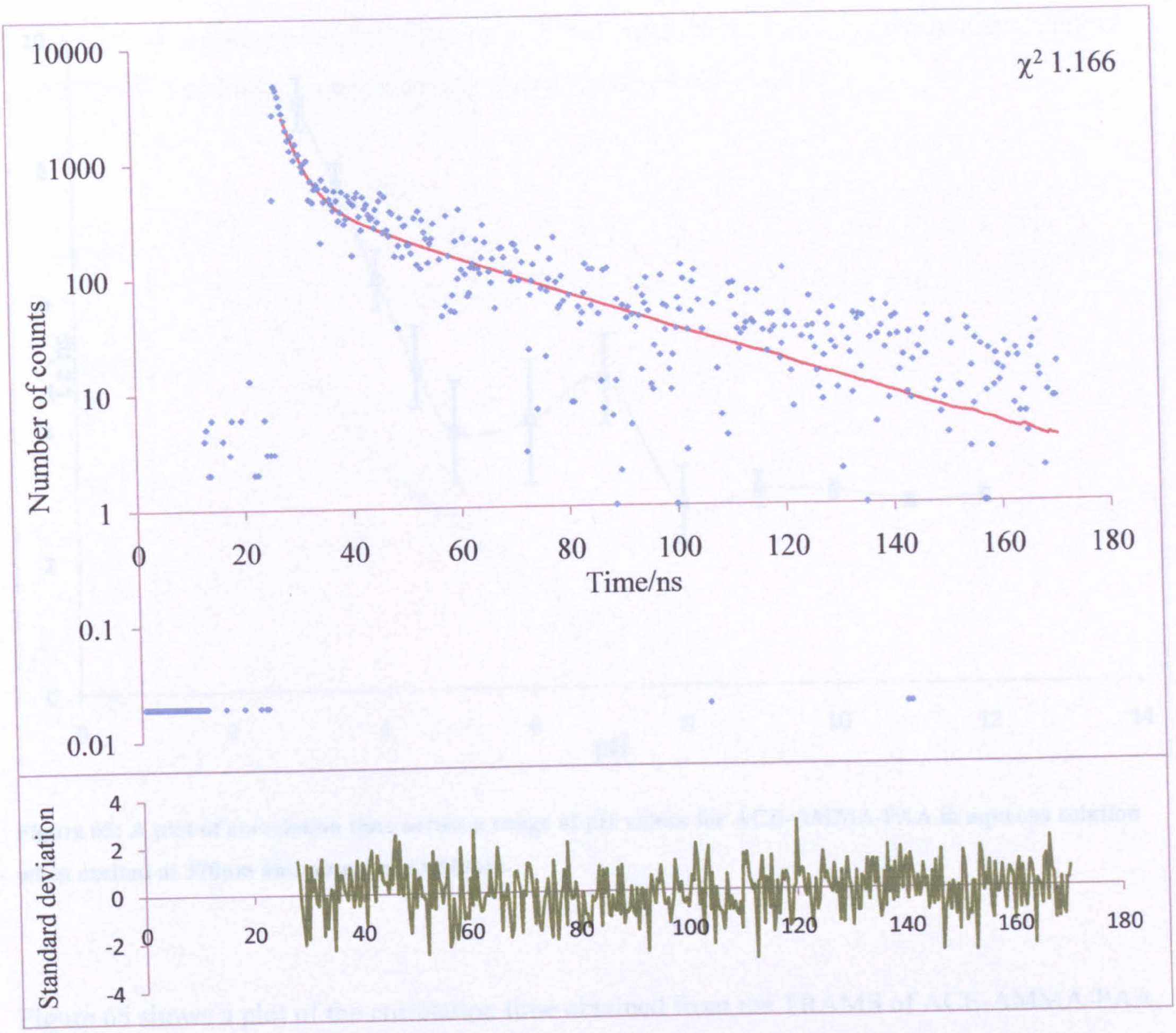

Figure 64: An impulse reconvolution fit to D(t) and a plot of the resulting residuals for ACE- PAA at pH 11 in aqueous solution.

The data is not quite fit from the peak of the information as to exclude the fast component observed from free rotation of the AMMA. This simplifies the resulting information and makes it easier to directly compare with. ACE-PAA. The best fit for this was again a triple exponential, providing an even distribution of residuals along with good statistical fits based on standard deviations of the correlation times and a χ^2 close to unity.

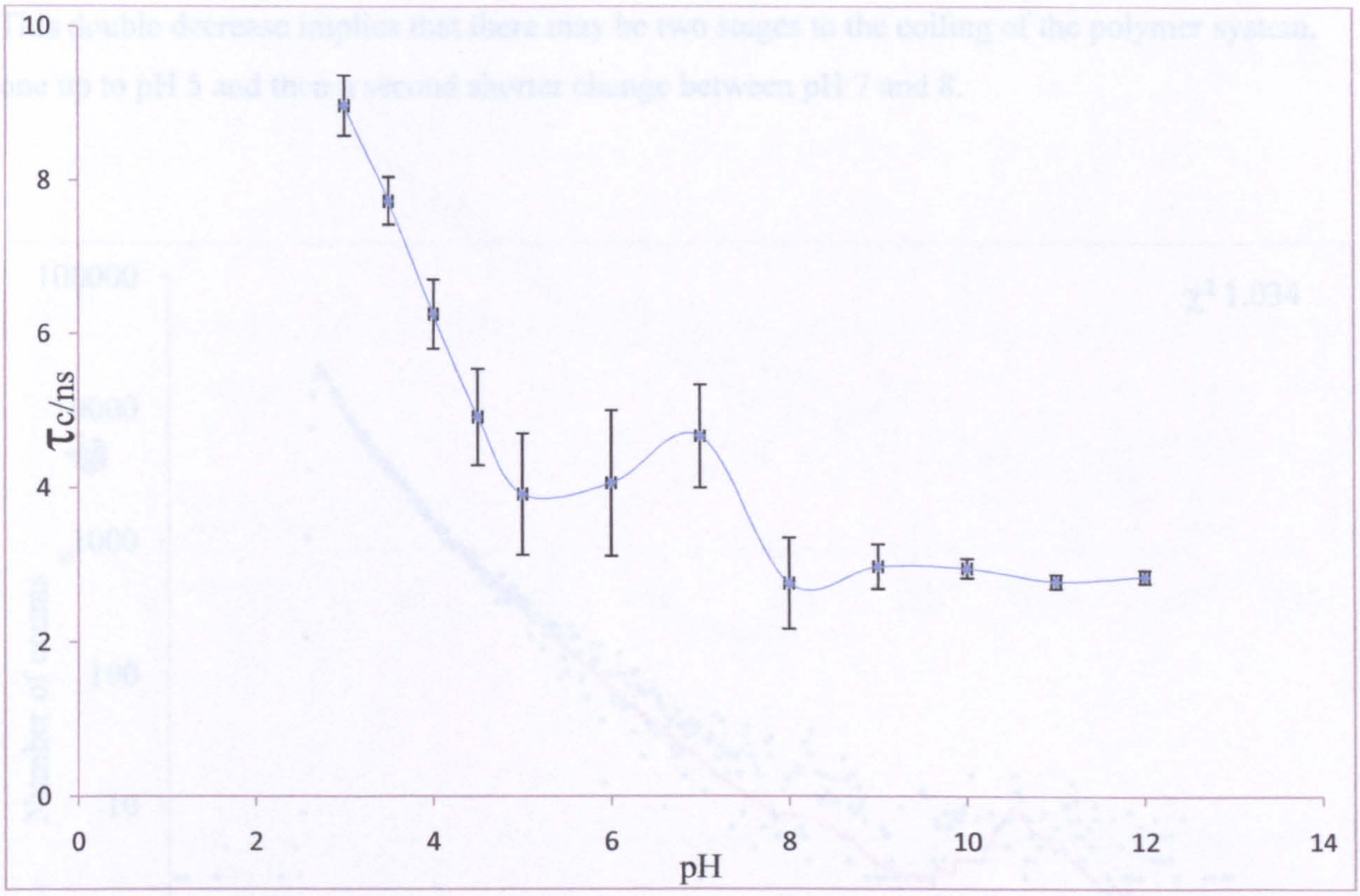

Figure 65: A plot of correlation time across a range of pH values for ACE-AMMA-PAA in aqueous solution when excited at 370nm and observed at 340nm.

Figure 65 shows a plot of the correlation time obtained from the TRAMS of ACE-AMMA-PAA, it suggests that the PAA sample appears to be only partially coiled, indicated by the fact that τc values never exceed 10 ns.

There is a consistent decrease in τc value from pH 3 until pH 5 at which point, when standard deviation is taken in to account, the value reaches a plateau until between pH 7 and 8 the τc value again drops and remains consistent upon further increasing the pH value.

This double decrease implies that there may be two stages to the coiling of the polymer system, one up to pH 5 and then a second shorter change between pH 7 and 8.

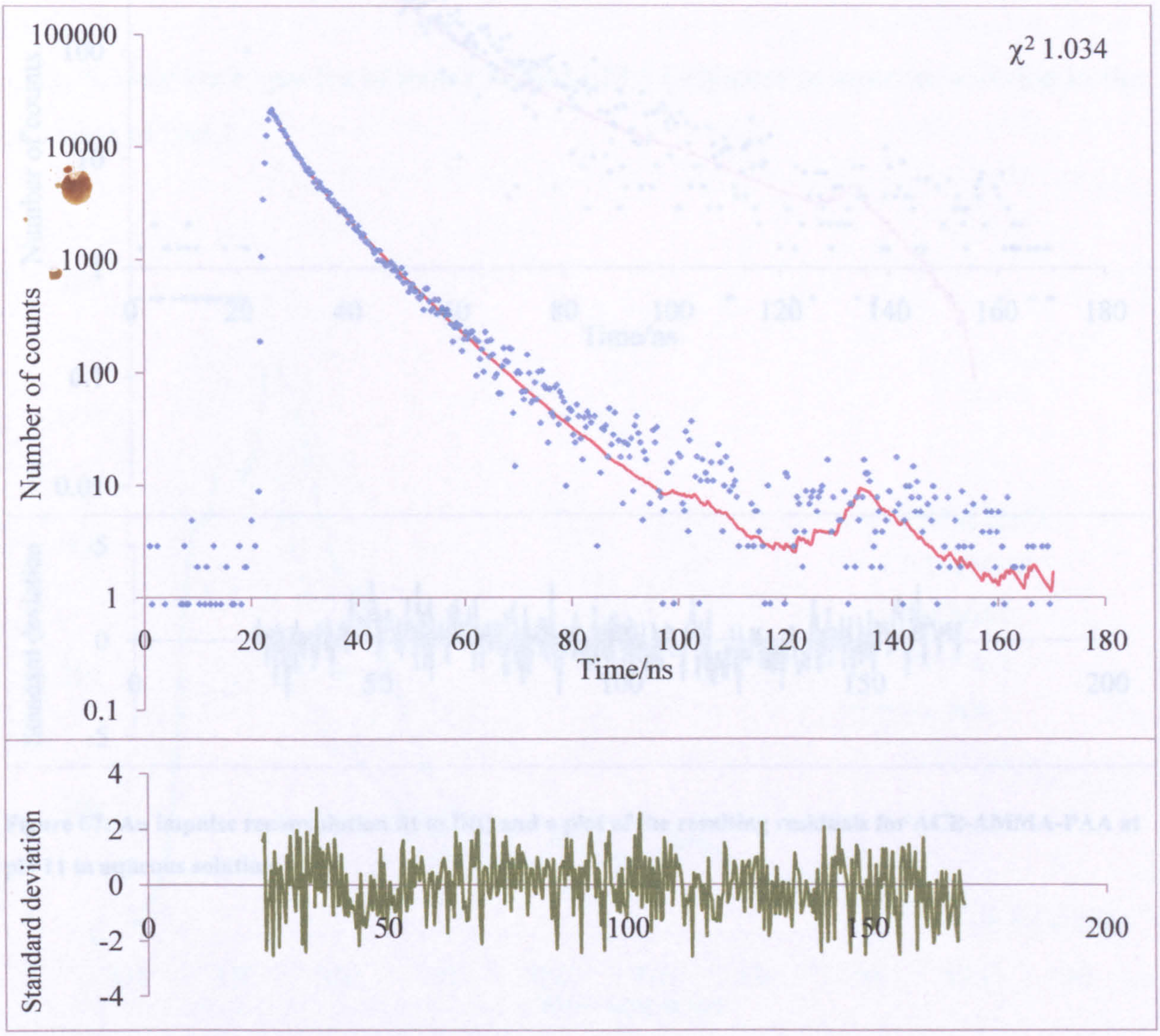

Figure 66: An impulse reconvolution fit to D(t) and a plot of the resulting residuals for ACE-AMMA-PAA at pH 3 in aqueous solution.

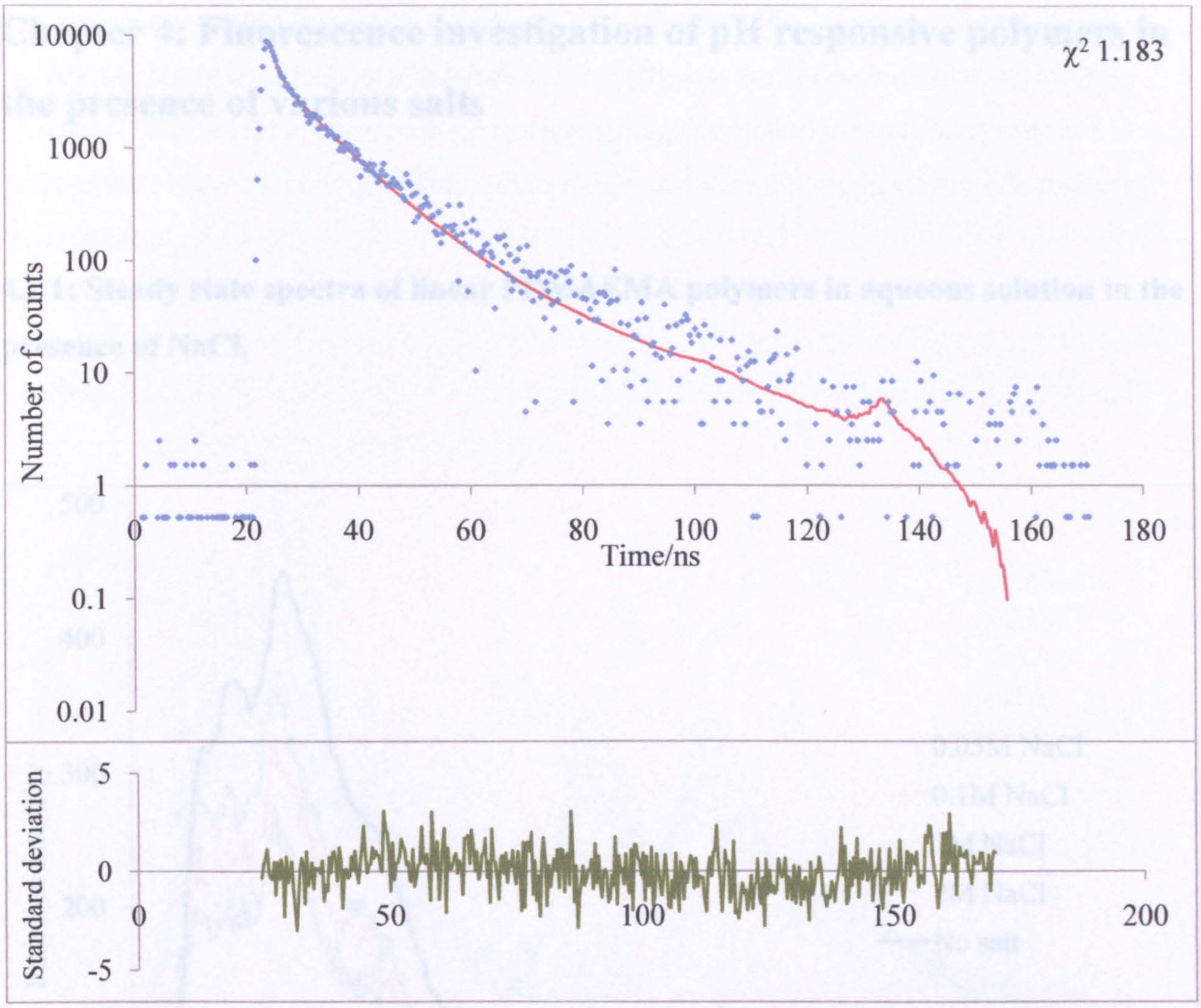

Figure 67: An impulse reconvolution fit to D(t) and a plot of the resulting residuals for ACE-AMMA-PAA at pH 11 in aqueous solution

Chapter 4: Fluorescence investigation of pH responsive polymers in the presence of various salts

4.1.1: Steady state spectra of linear PDMAEMA polymers in aqueous solution in the presence of NaCl.

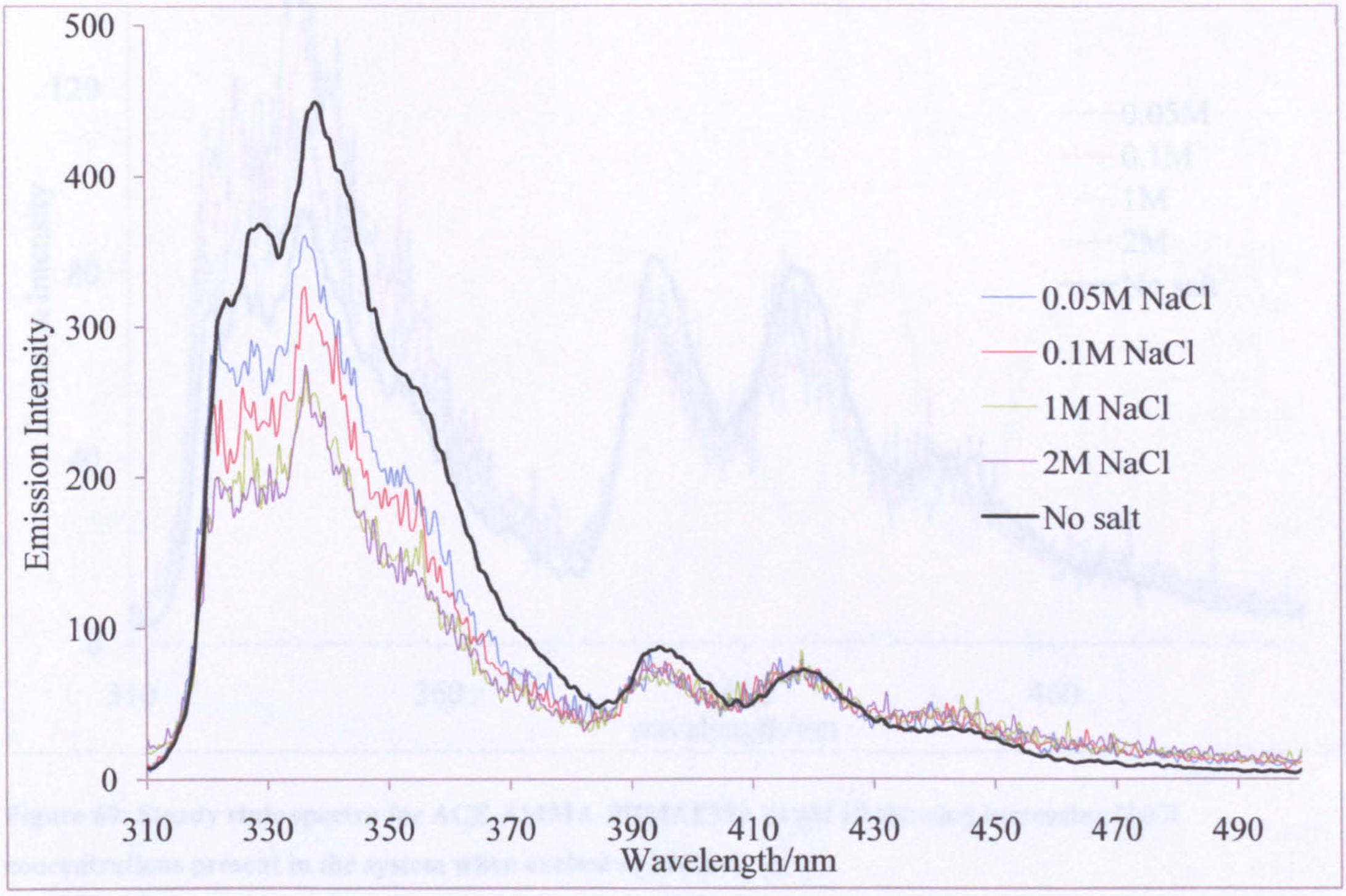

Figure 68: Steady state spectra for ACE-AMMA-PDMAEMA in aqueous solution at pH 3 showing increasing concentrations of NaCl present in the system when excited at 290 nm.

Of immediate notice on addition of NaCl to the polymer systems is that clearly defined steady state spectra became harder to achieve and are generally substantially noisier than those in the absence of salt. At pH 3, shown in figure 68, there is little appreciable change in the emission

intensity of the AMMA label seen at around 420 nm, however there is a consistent decrease in the emission intensity of the ACE label shown at 340 nm as the concentration of the NaCl is increased. This would seem to indicate that quenching within the system is increasing and perhaps the polymer is coiling slightly, given further quenching from the amine side chains of the polymer.

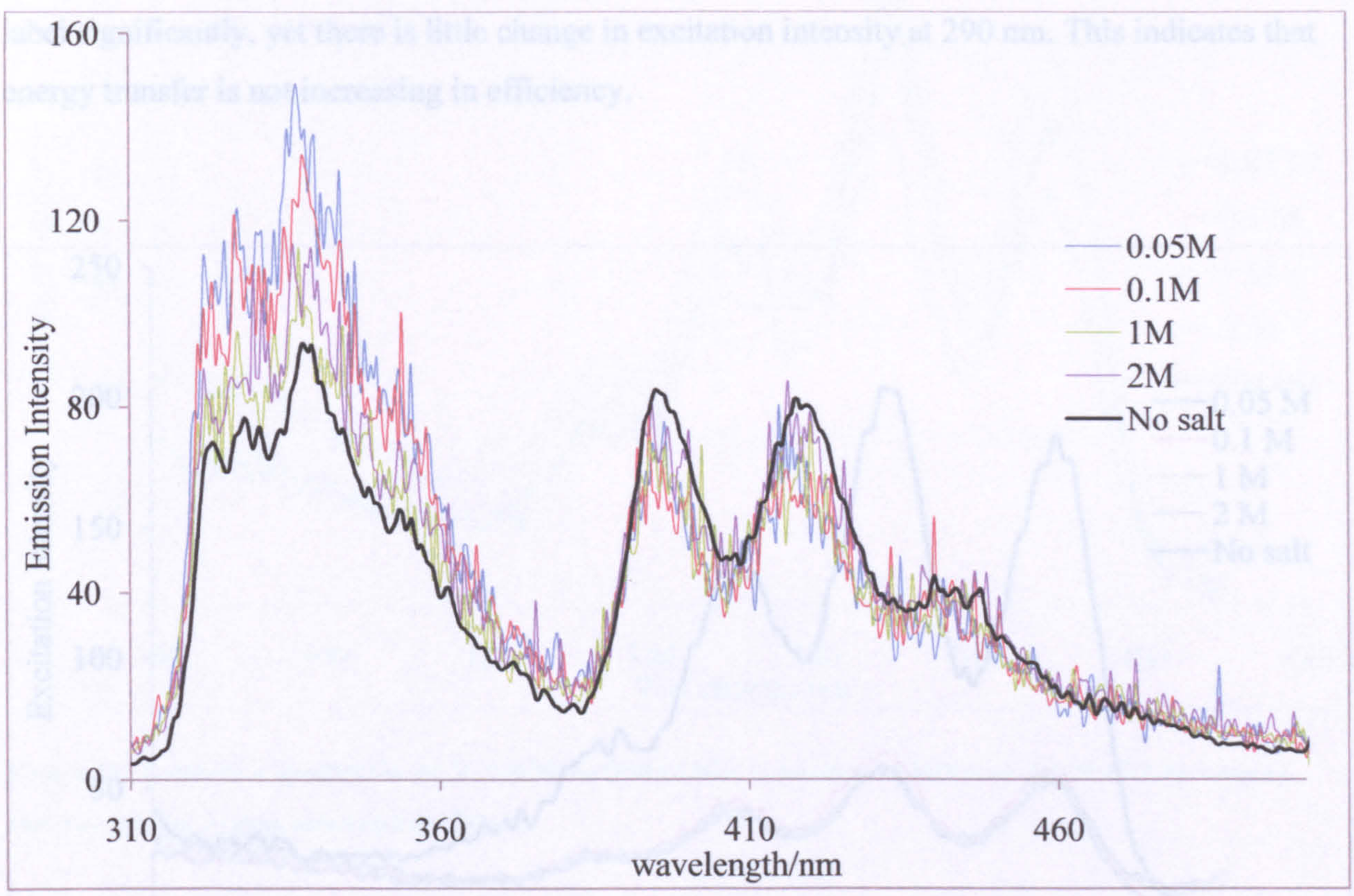

Figure 69: Steady state spectra for ACE-AMMA-PDMAEMA at pH 10 showing increasing NaCl concentrations present in the system when excited at 290 nm.

At pH 10 the noise of the spectra is progressively worse than at pH 3 because of the significantly reduced emission intensity under these conditions. (see figure 69) While it can be seen that the emission intensity for the ACE label shows a slight increase between salt concentrations of 0.05 M and 2 M they all show a slight increase in the emission intensity relative to that of the polymer system in the absence of any salt. Conversely the emission intensity of the AMMA label is

greatest for the polymer system in the absence of salt and the greatest emission intensity for the label in the presence of salt occurs with 2 M of salt.

Examination of the excitation spectra at the same pH values and NaCl concentrations (see figure 70) there is little change in the excitation intensity with increasing salt concentration at pH 3. However even a small concentration of salt clearly reduces the excitation intensity of the AMMA label significantly, yet there is little change in excitation intensity at 290 nm. This indicates that energy transfer is not increasing in efficiency.

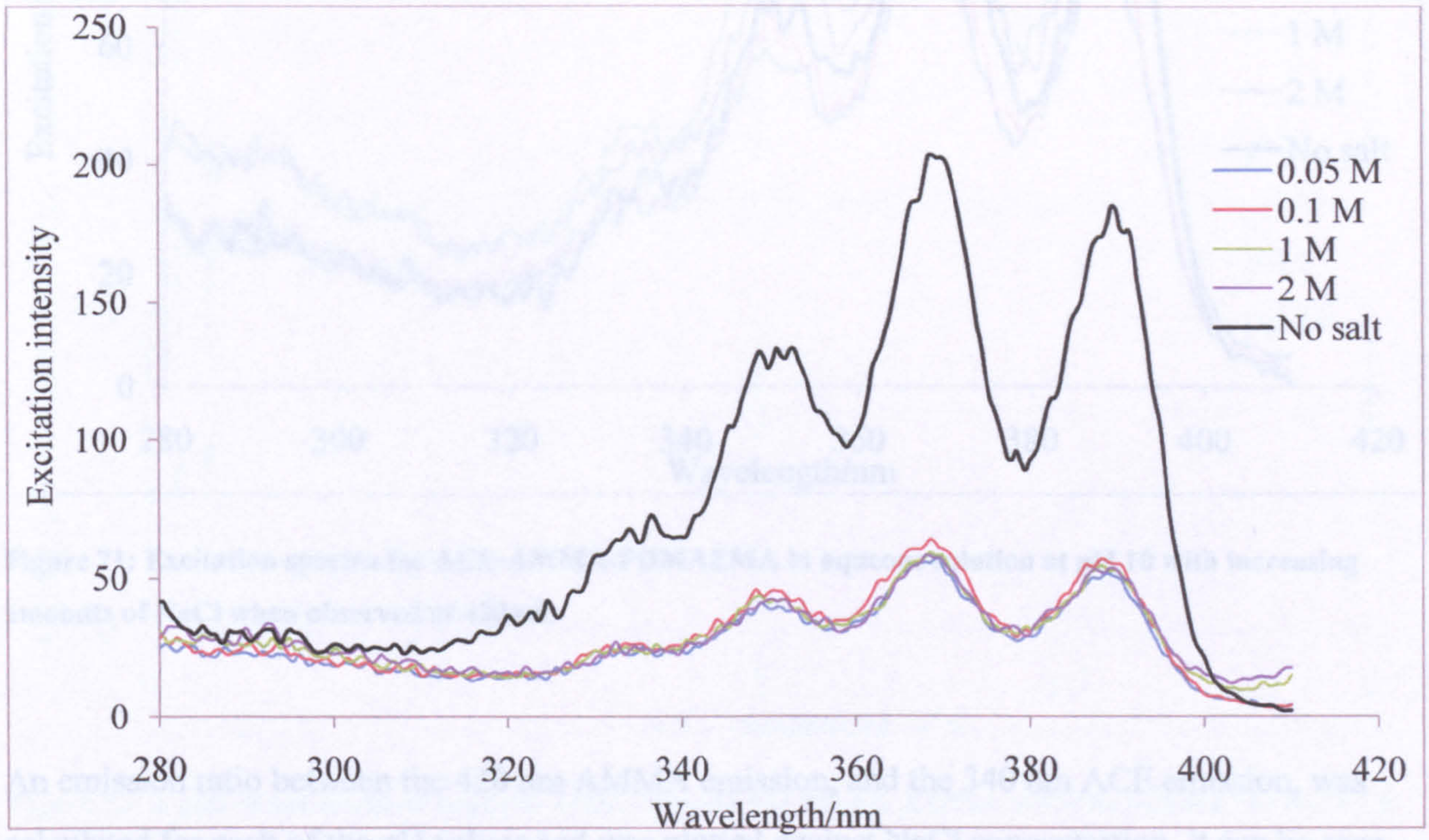

Figure 70: Steady state excitation spectra of ACE-AMMA-PDMAEMA in aqueous solution at pH 3 with increasing amounts of NaCl when observed at 420nm.

At pH 10 the situation is quite different (see figure 71). Addition of small concentrations of NaCl slightly decreases the excitation intensity of AMMA compared to the system in the absence of salt. However at concentrations of 1 M and 2 M of NaCl the excitation intensity of AMMA

increases across the entire wavelength range, indicating greater direct excitation of AMMA, as well as an increase in the energy transfer from the ACE label to the AMMA.

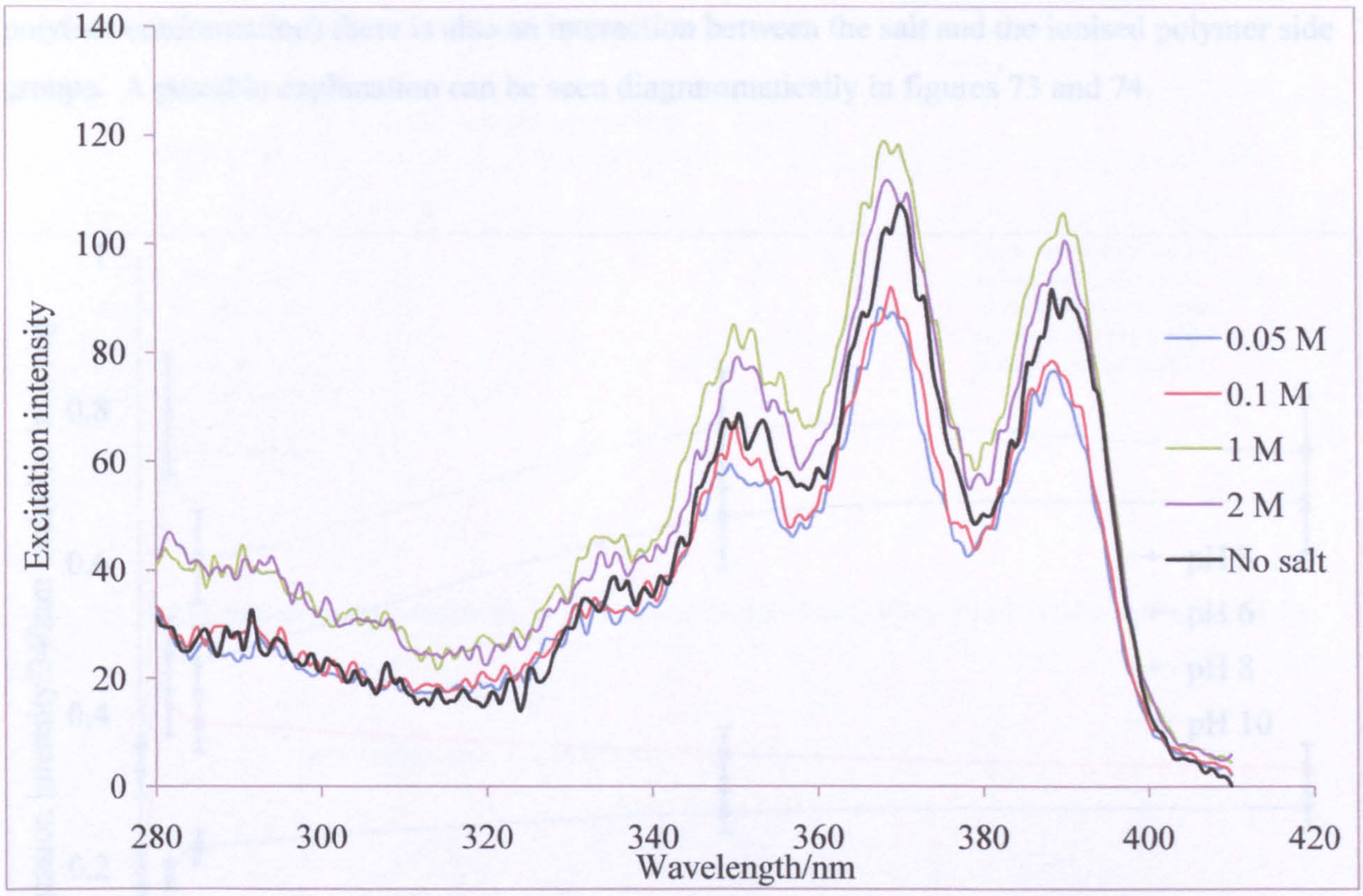

Figure 71: Excitation spectra for ACE-AMMA-PDMAEMA in aqueous solution at pH 10 with increasing amounts of NaCl when observed at 420nm.

An emission ratio between the 420 nm AMMA emission, and the 340 nm ACE emission, was calculated for each of the pH values and was plotted against NaCl concentration. It can be seen that the ratio changes are complicated (see figure 72).

Compared to the emission ratio of the system in the absence of NaCl the polymer shows an increase in the ratio across the entire pH range, indicating an increase in the energy transfer between the ACE and AMMA labels.

Many of the pH values also show a drop in the ratio between salt concentrations of 0.05 M and 0.1 M indicating that there are presumably two effects on the polymer system from the presence of salt, however within the error margin for the ratio this is only significant for a pH value of 8 in which it can be assumed that as well as whatever general effect the salt has on the system (ie polymer conformation) there is also an interaction between the salt and the ionised polymer side groups. A possible explanation can be seen diagrammatically in figures 73 and 74.

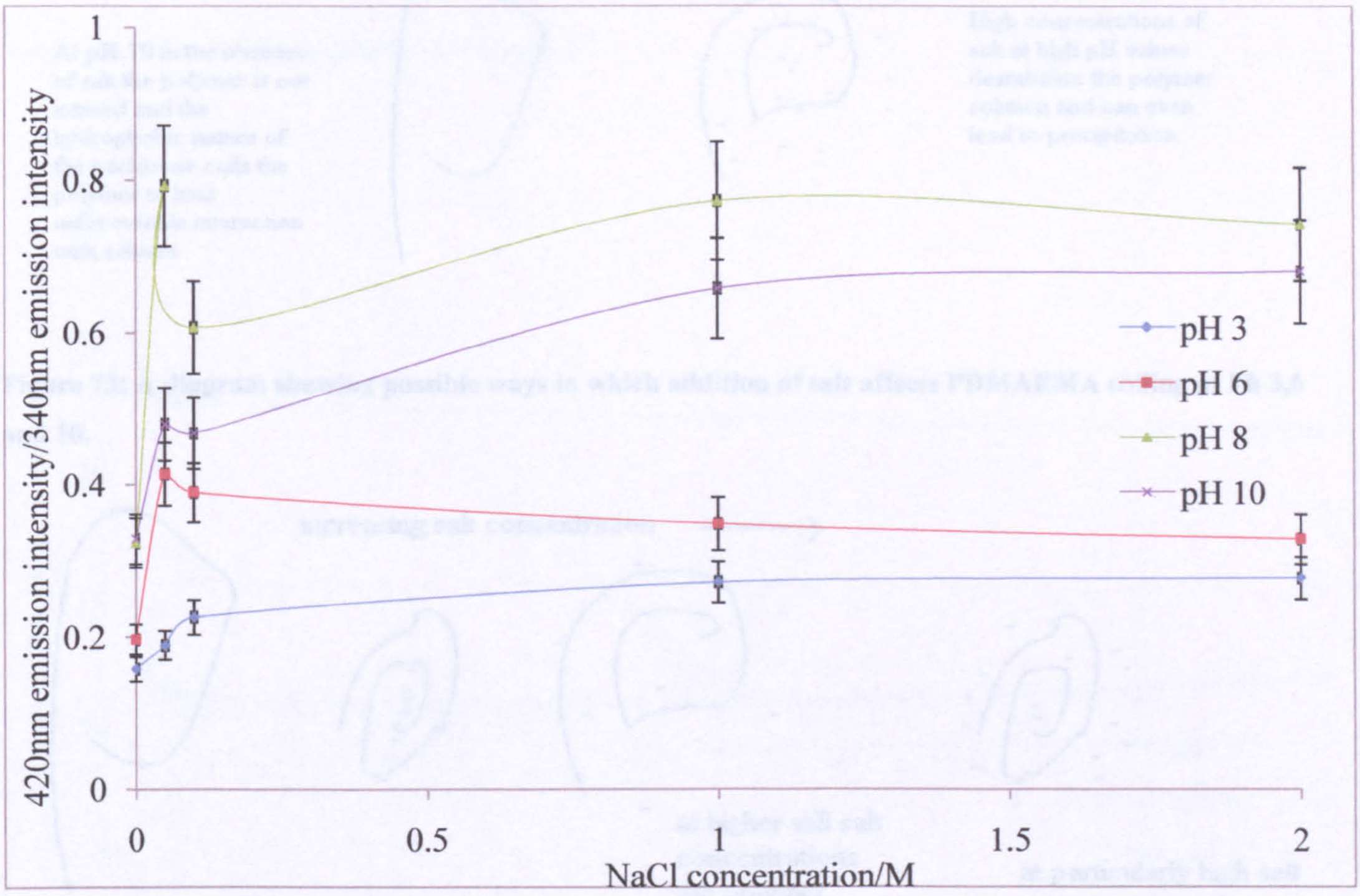

Figure 72: A plot of the emission intensity ratios between the 420 nm AMMA emission and the 340 nm ACE emission for ACE-AMMA-PDMAEMA in aqueous solution with increasing NaCl concentrations for 4 different pH values.

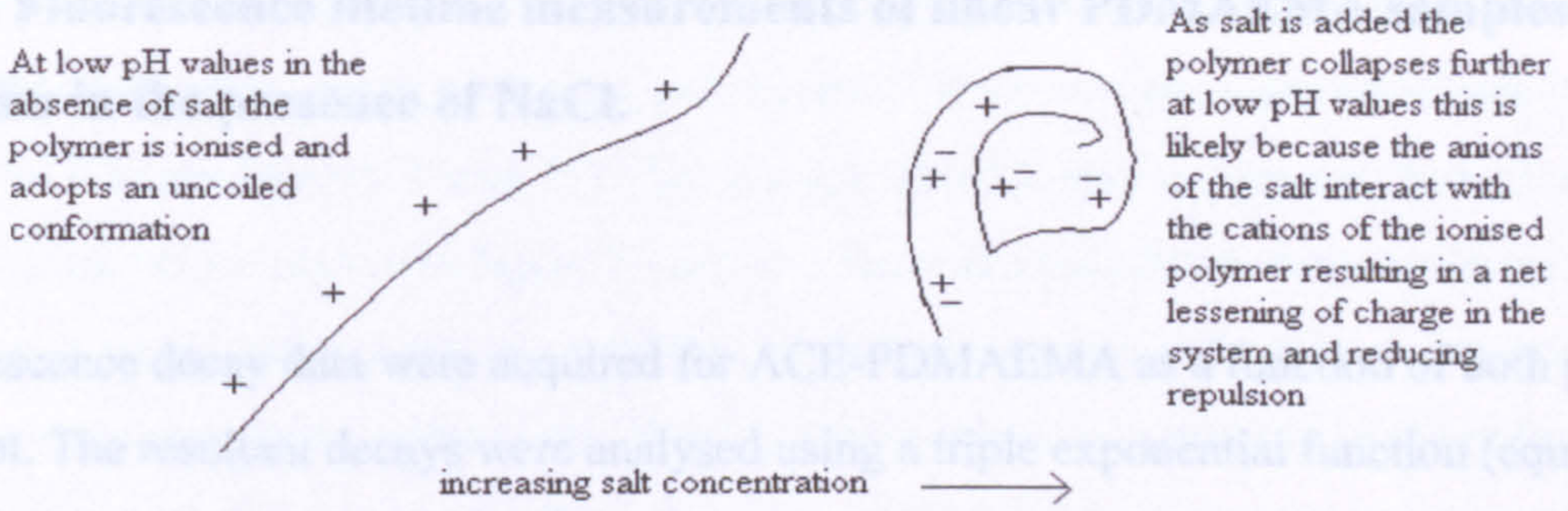

Figure 73: A diagram showing possible ways in which addition of salt affects PDMAEMA coiling at Ph 3,6 and 10.

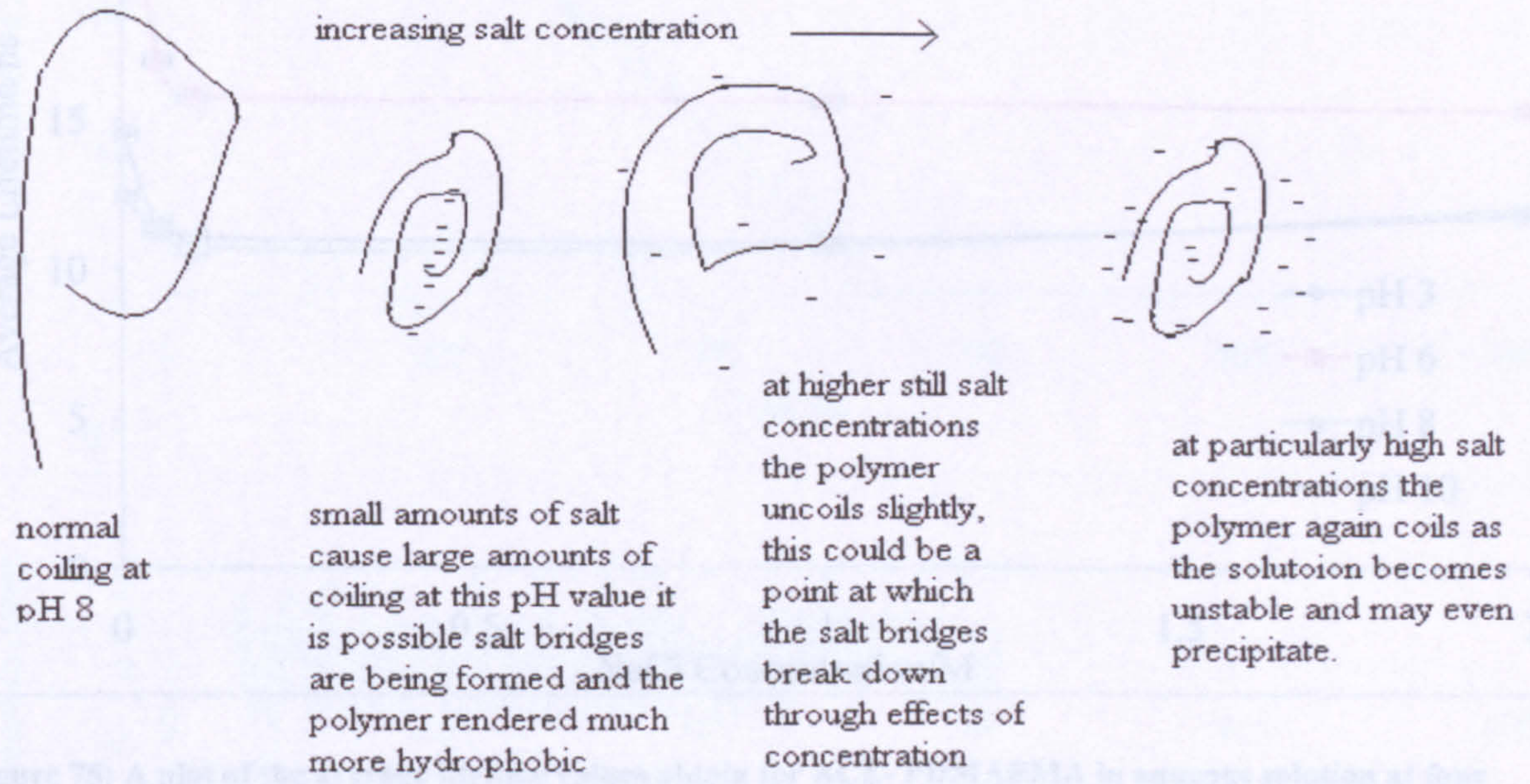

Figure 74: A diagram showing a possible explanation for the complex coiling and uncoiling of PDMAEMA at pH 8 on addition of increasing salt concentrations.

4.1.2: Fluorescence lifetime measurements of linear PDMAEMA samples in aqueous solution in the presence of NaCl.

Fluorescence decay data were acquired for ACE-PDMAEMA as a function of both pH and salt content. The resultant decays were analysed using a triple exponential function (equation 1.3) as a model. And the subsequent lifetime values were treated using equation 1.4 to provide an average value. This then allows a relative comparison between different solution conditions. The average lifetime data is plotted in figure 75.

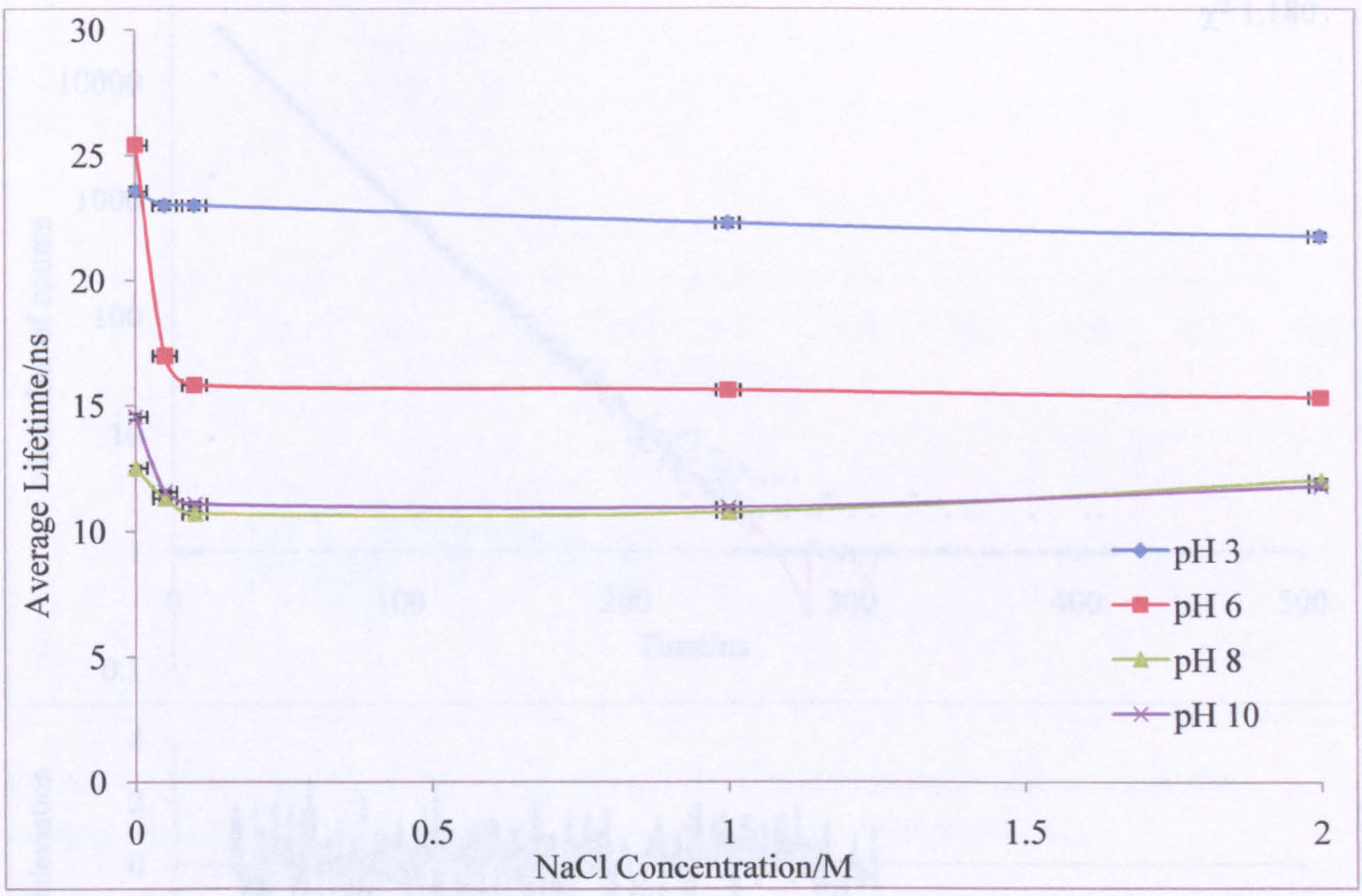

Figure 75: A plot of the average lifetime values obtain for ACE- PDMAEMA in aqueous solution at four different pH values with increasing NaCl concentration when excited at 290 nm and observed at 340 nm.

The fluorescence decays from ACE-PDMAEMA at the four pH values at which NaCl concentrations were increased show good statistical fits to a triple exponential analysis using equation 1.3 (see figures 76 and 77). The average lifetime values obtained from these triple exponential fits are shown in figure 75 above. There is a significant decrease in the average lifetime at all pH values upon the addition of salt to the system indicating an increase in fluorescence quenching of the label. The most likely cause is a collapse of the polymer chain with a corresponding increase in the quenching of the label by the polymer amine groups. This decrease is most significant at pH 6. Presumably charge screening by the counter-ions induces a

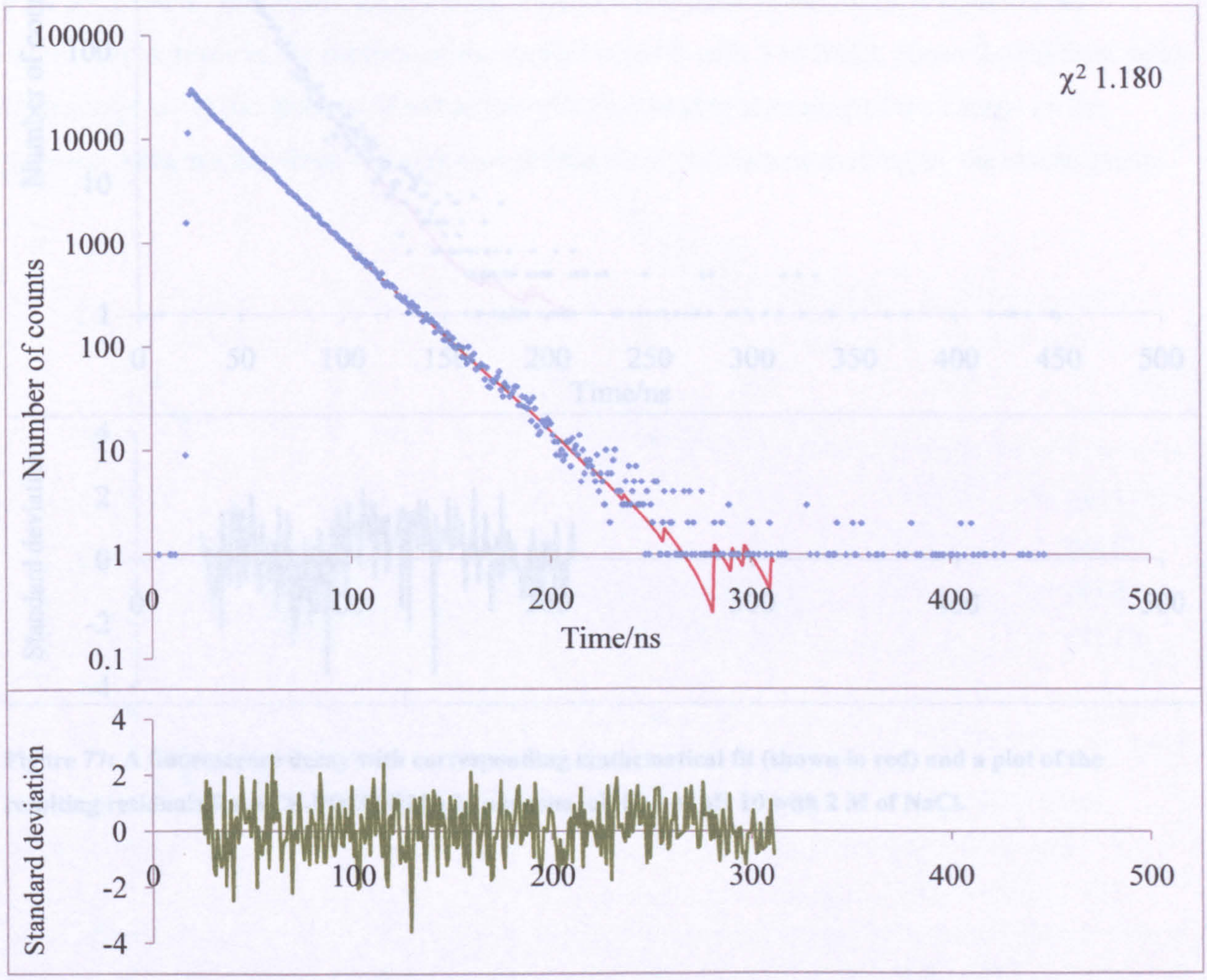

Figure 76: A fluorescence decay with corresponding mathematical fit (shown in red) and a plot of the resulting residuals for ACE-PDMAEMA in aqueous solution of pH 3 with 0.05M of NaCl.

collapse in the polymer chain, increasing the contact between the label and the polymer.

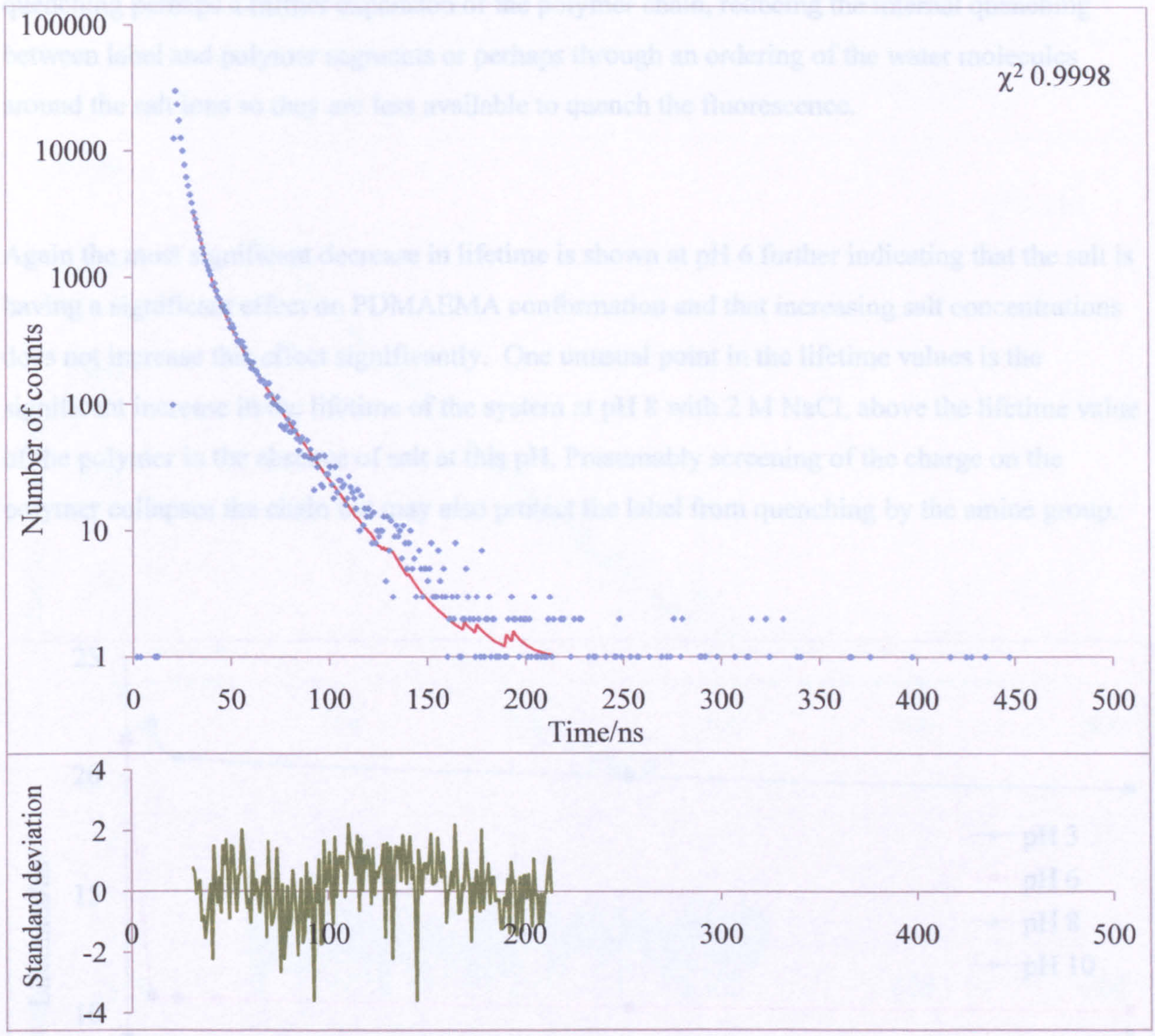

Figure 77: A fluorescence decay with corresponding mathematical fit (shown in red) and a plot of the resulting residuals for ACE-PDMAEMA in aqueous solution of pH 10 with 2 M of NaCl.

On consideration of the lifetime data for ACE-AMMA-PDMAEMA various pH values and NaCl concentrations (see figure 78) it can be observed that there is a significant drop in τ compared to

those obtained for the polymer system in the absence of salt. This is true for all pH values except 3 for which there is shown to be an initial small increase in τ. This indicates a reduction of quenching perhaps a further expansion of the polymer chain, reducing the internal quenching between label and polymer segments or perhaps through an ordering of the water molecules around the salt ions so they are less available to quench the fluorescence.

Again the most significant decrease in lifetime is shown at pH 6 further indicating that the salt is having a significant effect on PDMAEMA conformation and that increasing salt concentrations does not increase this effect significantly. One unusual point in the lifetime values is the significant increase in the lifetime of the system at pH 8 with 2 M NaCl, above the lifetime value of the polymer in the absence of salt at this pH. Presumably screening of the charge on the polymer collapses the chain but may also protect the label from quenching by the amine group.

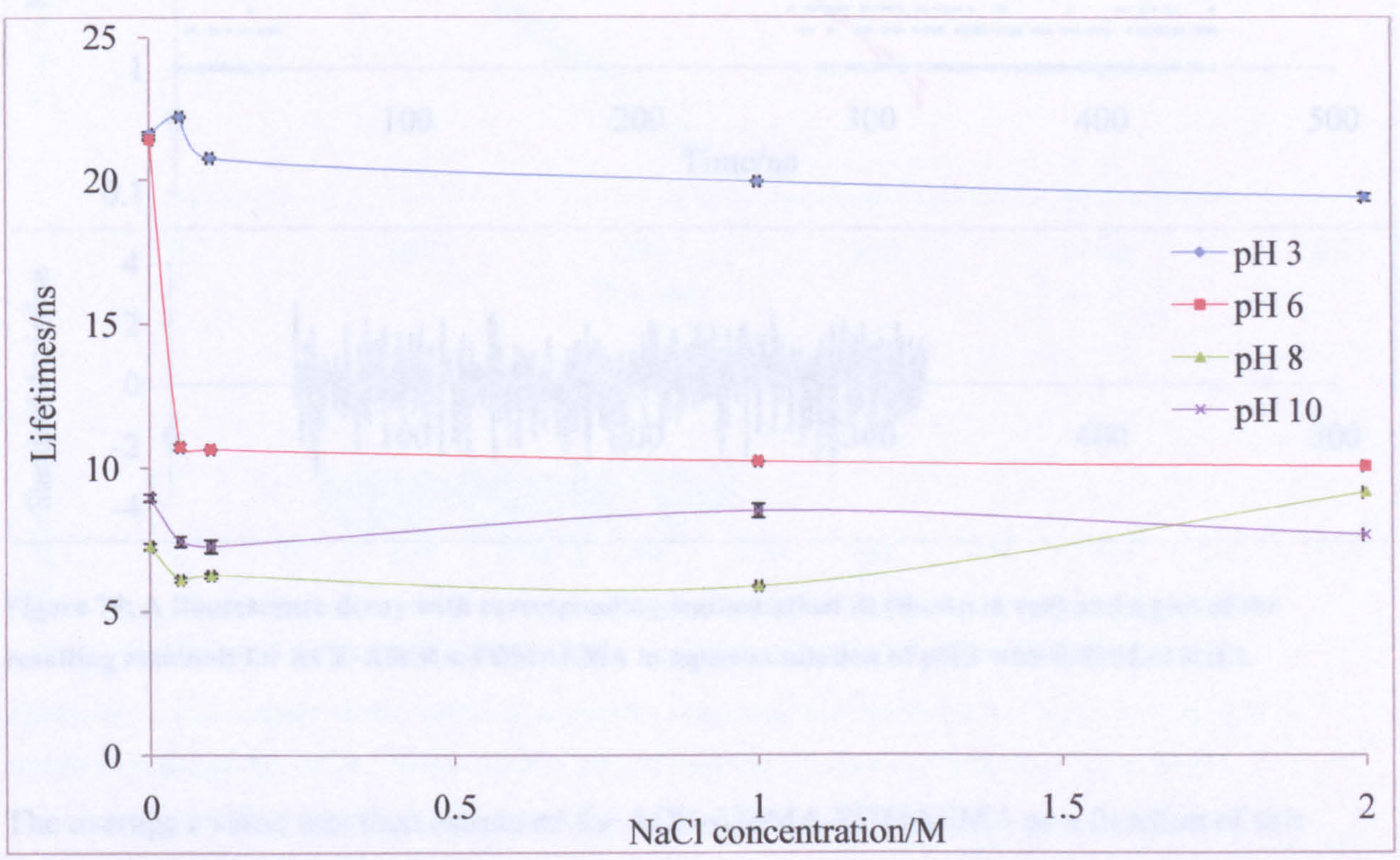

Figure 78: A plot of the average lifetime values obtain for ACE-AMMA-PDMAEMA in aqueous solution at four different pH values with increase NaCl concentration when excited at 290 nm and observed at 340 nm.

As shown below the fluorescence decay curves were again fitted to a triple exponential as in equation 1.3, the average lifetime value from these were used in the above plot (figure 78)

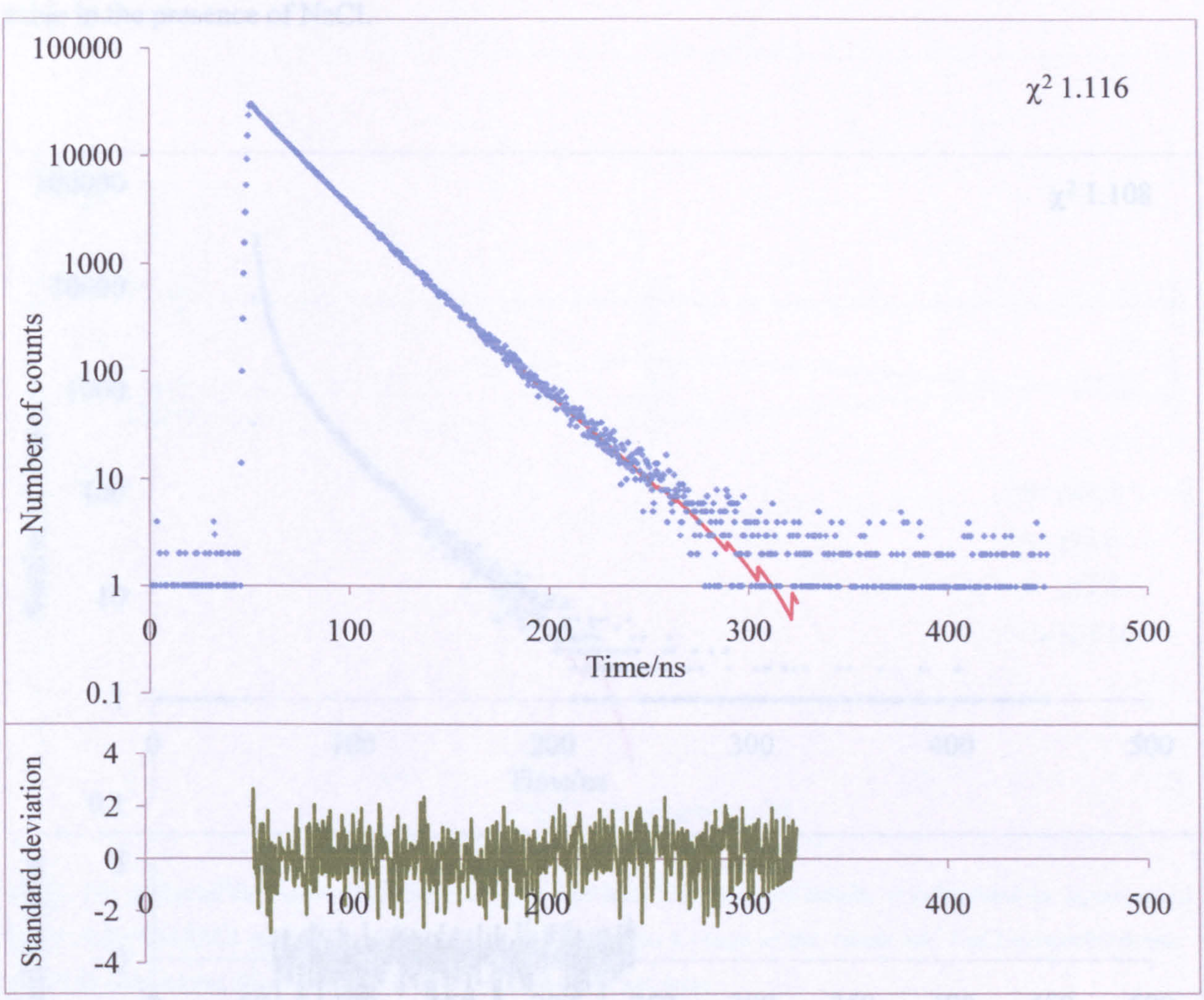

Figure 79: A fluorescence decay with corresponding mathematical fit (shown in red) and a plot of the resulting residuals for ACE-AMMA-PDMAEMA in aqueous solution of pH 3 with 0.05 M of NaCl.

The average r value was then estimated for ACE-AMMA-PDMAEMA as a function of salt concentration and pH via equation 1.3 and 1.4 respectively. Figure 81 shows the calculated r values for the distance between the ACE and AMMA labels in the double label polymer system

at varying pH values and salt concentrations. The label distance at pH 3 shows an initial increase with the addition of small amounts of NaCl consistent with the small lifetime increase observed in the double label system. The distance between the labels at this pH then reduces to be of a similar distance to that of the system in the absence of salt. The distance between labels shows a significant decrease at pH6 as might be expected given that the polymer collapses at a lower pH value in the presence of NaCl.

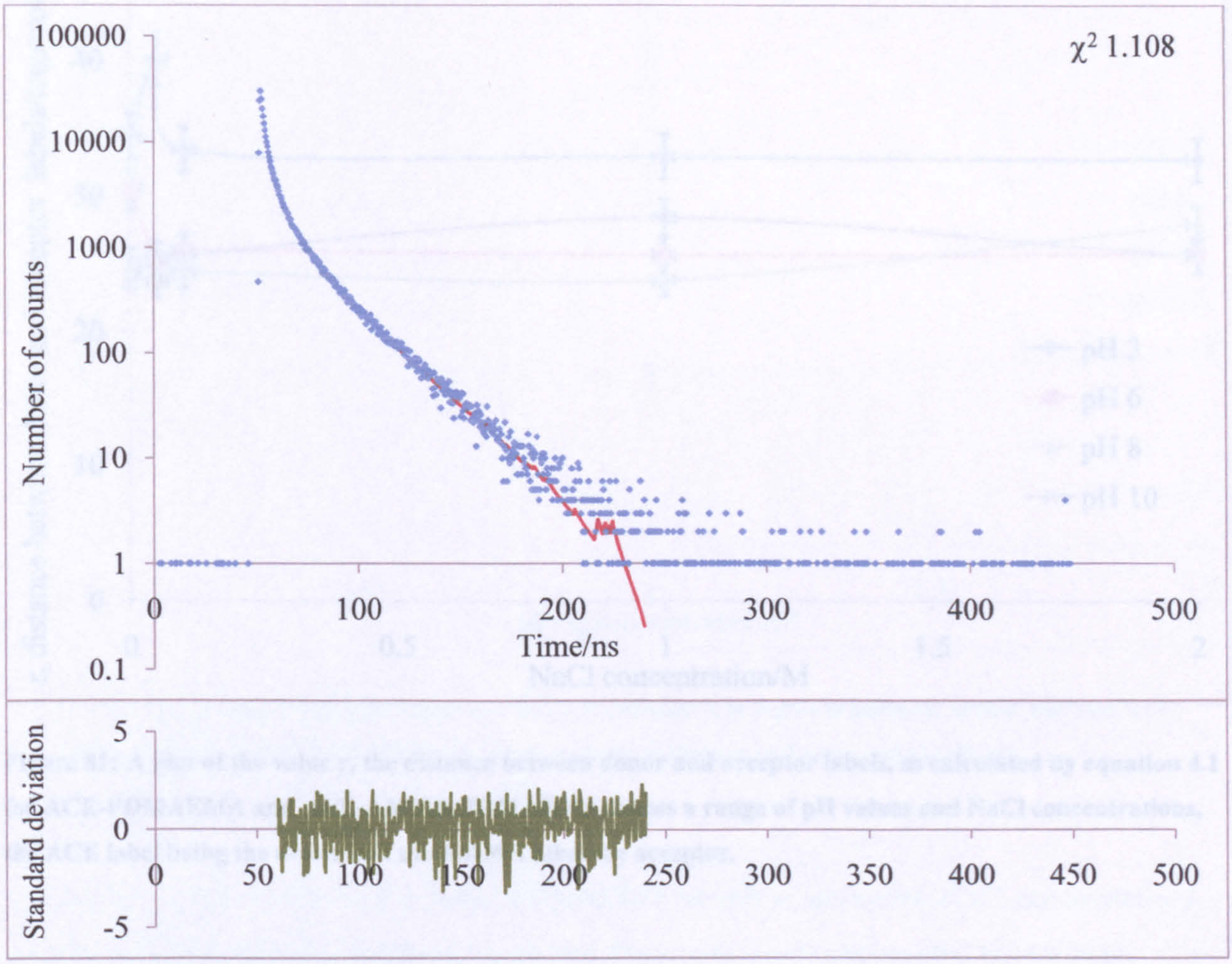

Figure 80: A fluorescence decay with corresponding mathematical fit (shown in red) and a plot of the resulting residuals for ACE-AMMA-PDMAEMA in aqueous solution of pH 10 with 2M of NaCl.

The only other significant change in the distance between labels is the increase in the label distance at 2 M NaCl concentration at pH 8, this is an effect of the increased lifetime of the double label system shown at this same value.

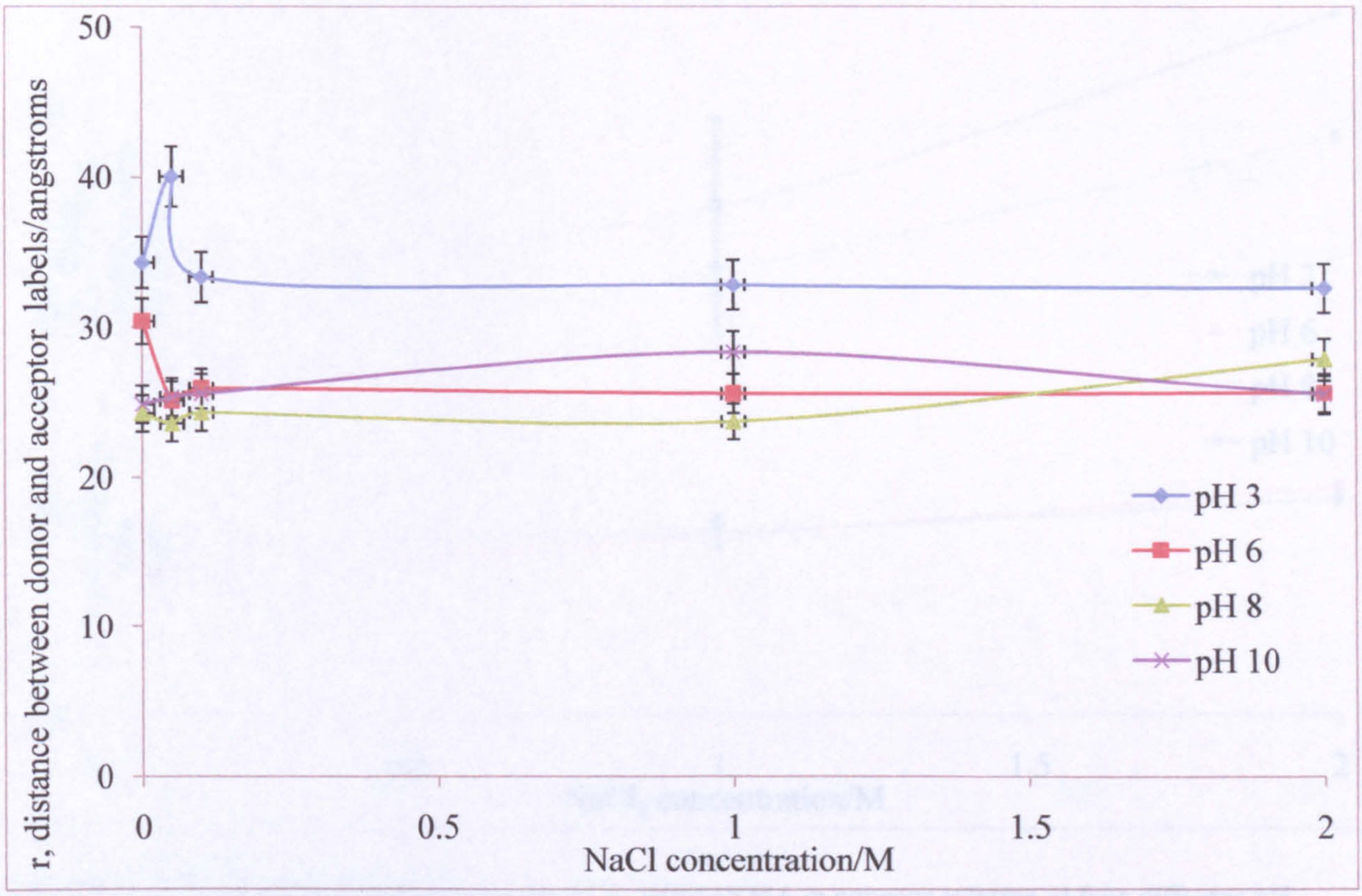

Figure 81: A plot of the value r, the distance between donor and acceptor labels, as calculated by equation 4.1 for ACE-PDMAEMA and ACE-AMMA-PDMAEMA across a range of pH values and NaCl concentrations, the ACE label being the donor and the AMMA label the acceptor.

4.1.3: Time Resolved Anisotropy Measurements on linear PDMAEMA samples in aqueous solution in the presence of NaCl.

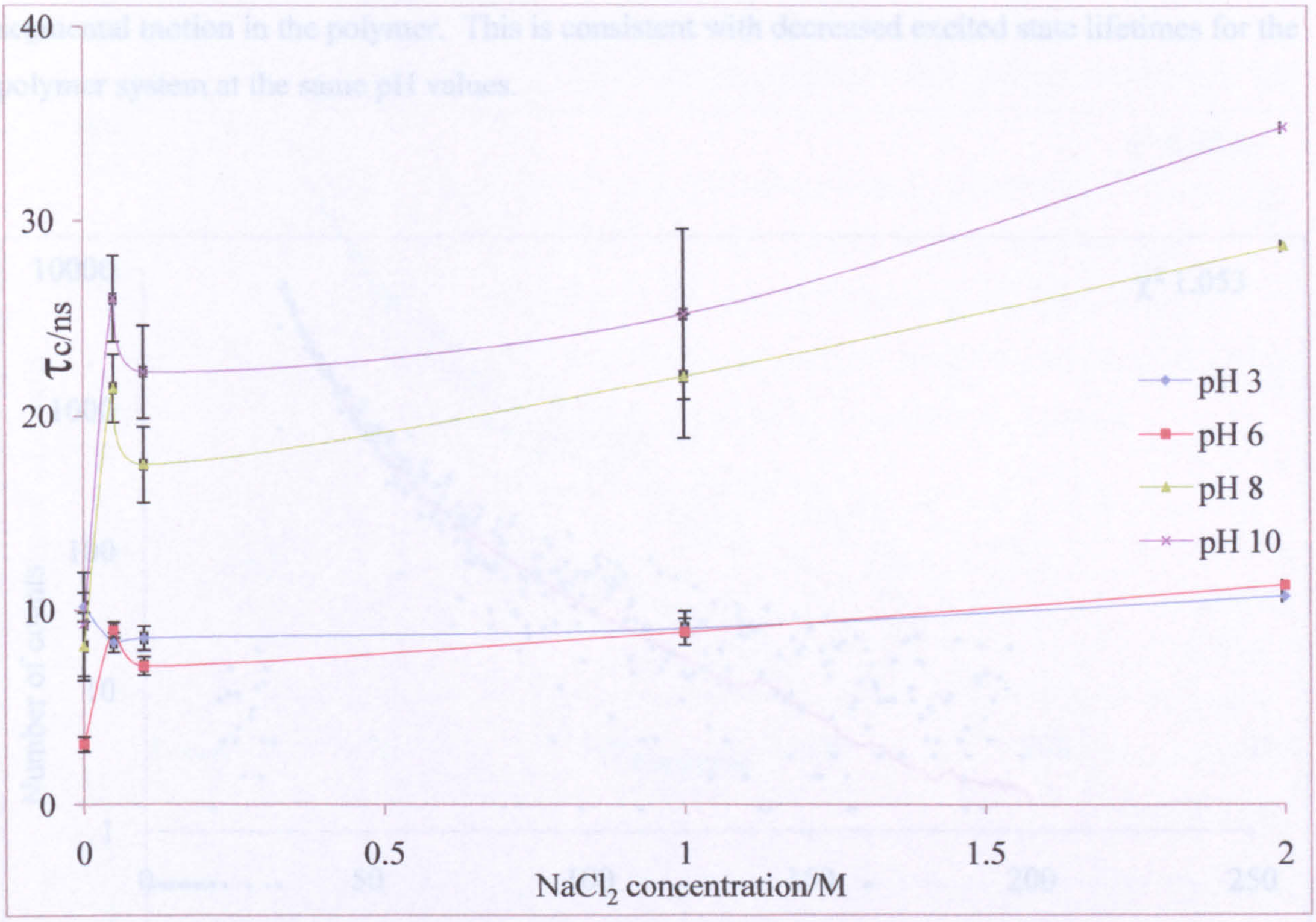

Figure 82: A plot of the correlation times for ACE- PDMAEMA in aqueous solution at four different pH values with increasing NaCl concentration when excited at 290 nm and observed at 340 nm.

The TRAMS data for the ACE labelled PDMAEMA sample at increasing NaCl concentrations across a selection of pH values were again best fitted with single exponential fits using an impulse reconvolution method and leaving r^{∞} to vary. This gave the best statistical fit both according to χ^2 values and the residuals seen for each fit when compared to the data.

There is an increase in the τc value for pH values of 6 and above upon the addition of NaCl to the system. This indicates that the segmental motion of the polymer is significantly decreased, given that increased τc indicates a longer time before anisotropy is lost and thus slower segmental motion in the polymer. This is consistent with decreased excited state lifetimes for the polymer system at the same pH values.

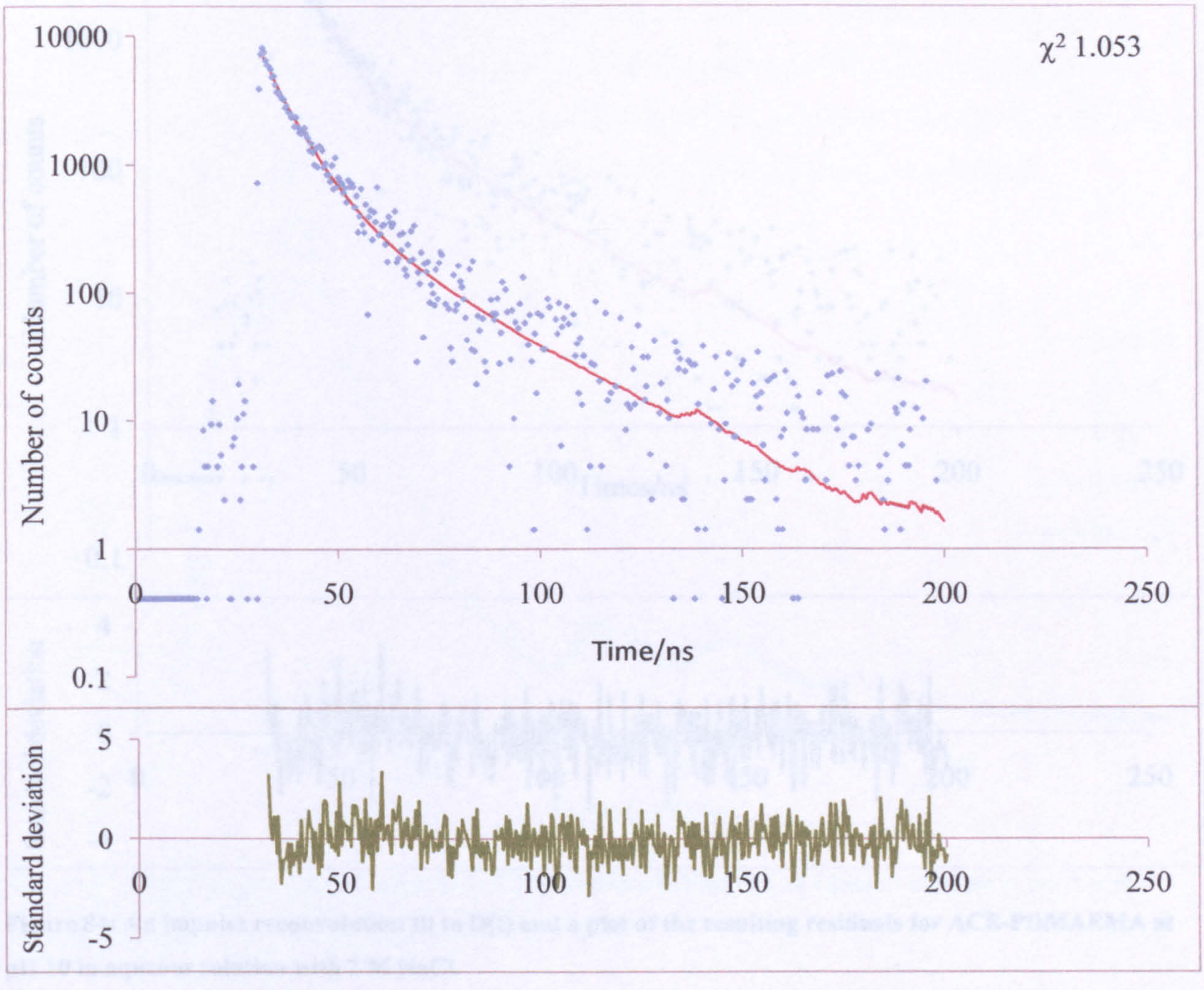

Figure 83: An impulse reconvolution fit to D(t) and a plot of the resulting residuals for ACE-PDMAEMA at pH 3 in aqueous solution with 0.05M NaCl.

The τc values for pH 8 and 10 show the most significant increase upon addition of NaCl to the system, pH 10 apparently no longer exhibiting the decrease in τ_c previously shown in the absence of any salt.

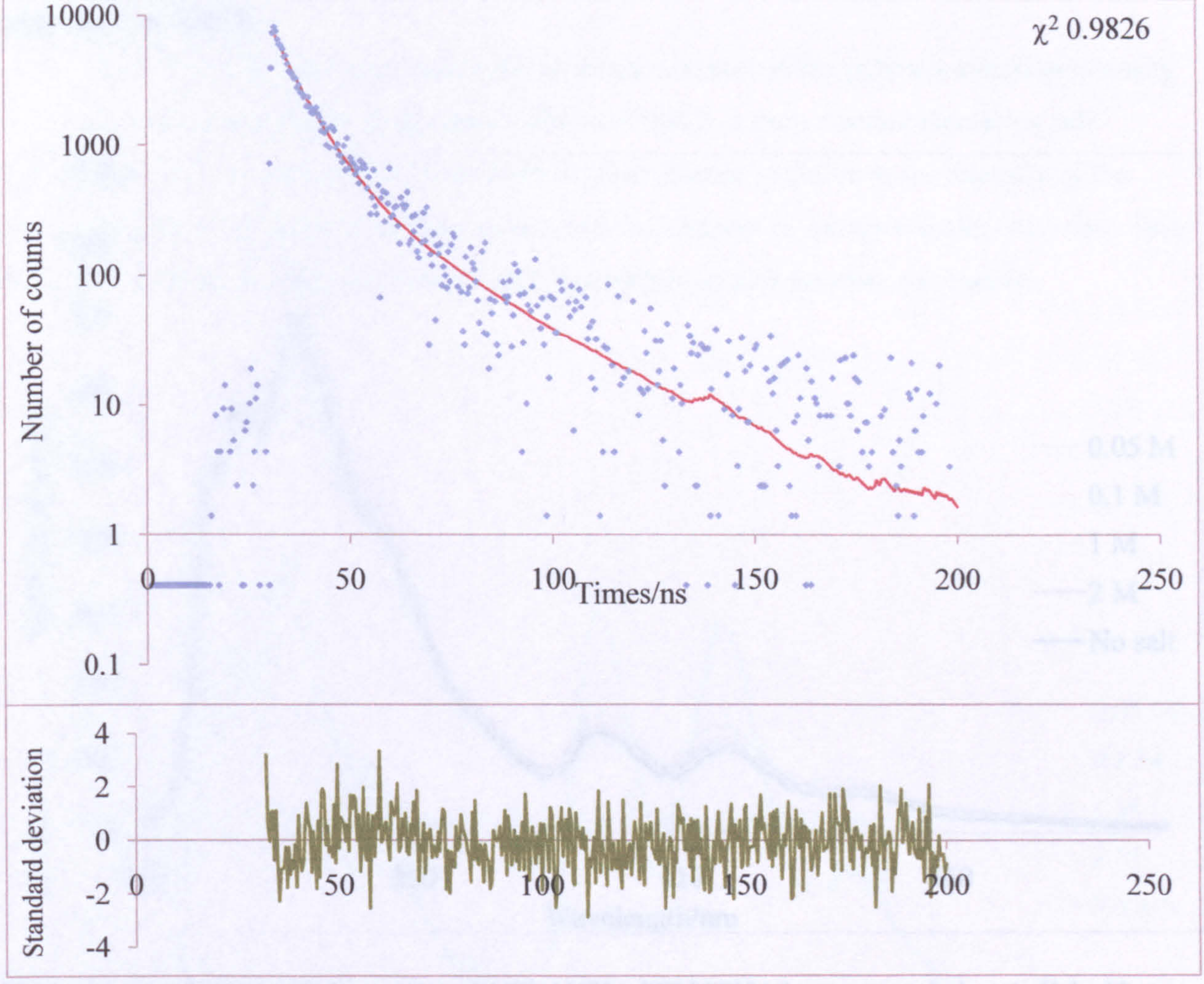

Figure 84: An impulse reconvolution fit to D(t) and a plot of the resulting residuals for ACE-PDMAEMA at pH 10 in aqueous solution with 2 M NaCl.

Unlike with the lifetime values, the correlation times at pH 8 and 10 continue to increase as the salt concentration increases. This indicates that the segmental motion is reducing even further yet

there was no corresponding increase in the previous lifetime data. This could indicate that the aqueous system around the polymer is being ordered by the large amounts of salt and this is reducing the segmental motion of the polymer without further coiling the polymer.

4.1.4: Steady state spectra of linear PDMAEMA polymers in aqueous solution in the presence of $CaCl_2$.

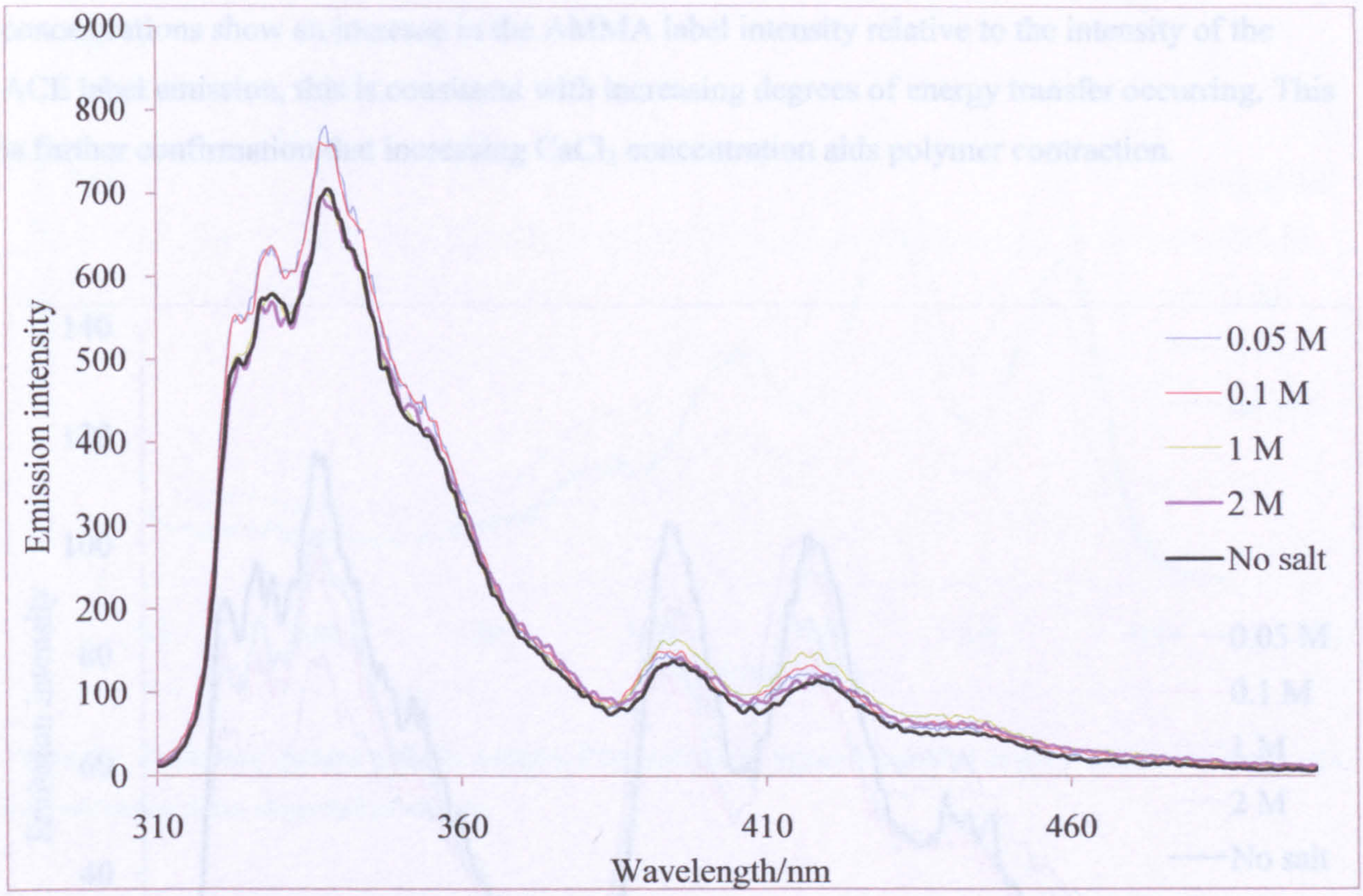

Figure 85: Steady state emission spectra of ACE-AMMA-PDMAEMA in aqueous solution at pH 3 with increasing concentration of $CaCl_2$ when excited at 290 nm.

The addition of $CaCl_2$ to a sample of ACE-AMMA PDMAEMA in aqueous solution at pH 3 shows an initial increase in the emission intensity of the steady state spectra of the polymer (figure 85). At higher salt concentrations, the emission intensity of the ACE label then decreases

with a corresponding minor increase in the emission intensity of the AMMA label. This indicates that, while at low salt concentrations shielding of the polymer from external quenching occurs, at higher salt concentrations the salt induces polymer coiling. The emission intensity changes upon addition of $CaCl_2$ to ACE-AMMA-PDMAEMA are much smaller than the changes seen upon addition of NaCl to the same polymer as was seen in figure 68.

At pH 10 on the other hand, (see figure 86) an initial decrease in the polymer emission intensity across the entire wavelength range upon addition of $CaCl_2$ occurs. Further increasing salt concentrations show an increase in the AMMA label intensity relative to the intensity of the ACE label emission, this is consistent with increasing degrees of energy transfer occurring. This is further confirmation that increasing $CaCl_2$ concentration aids polymer contraction.

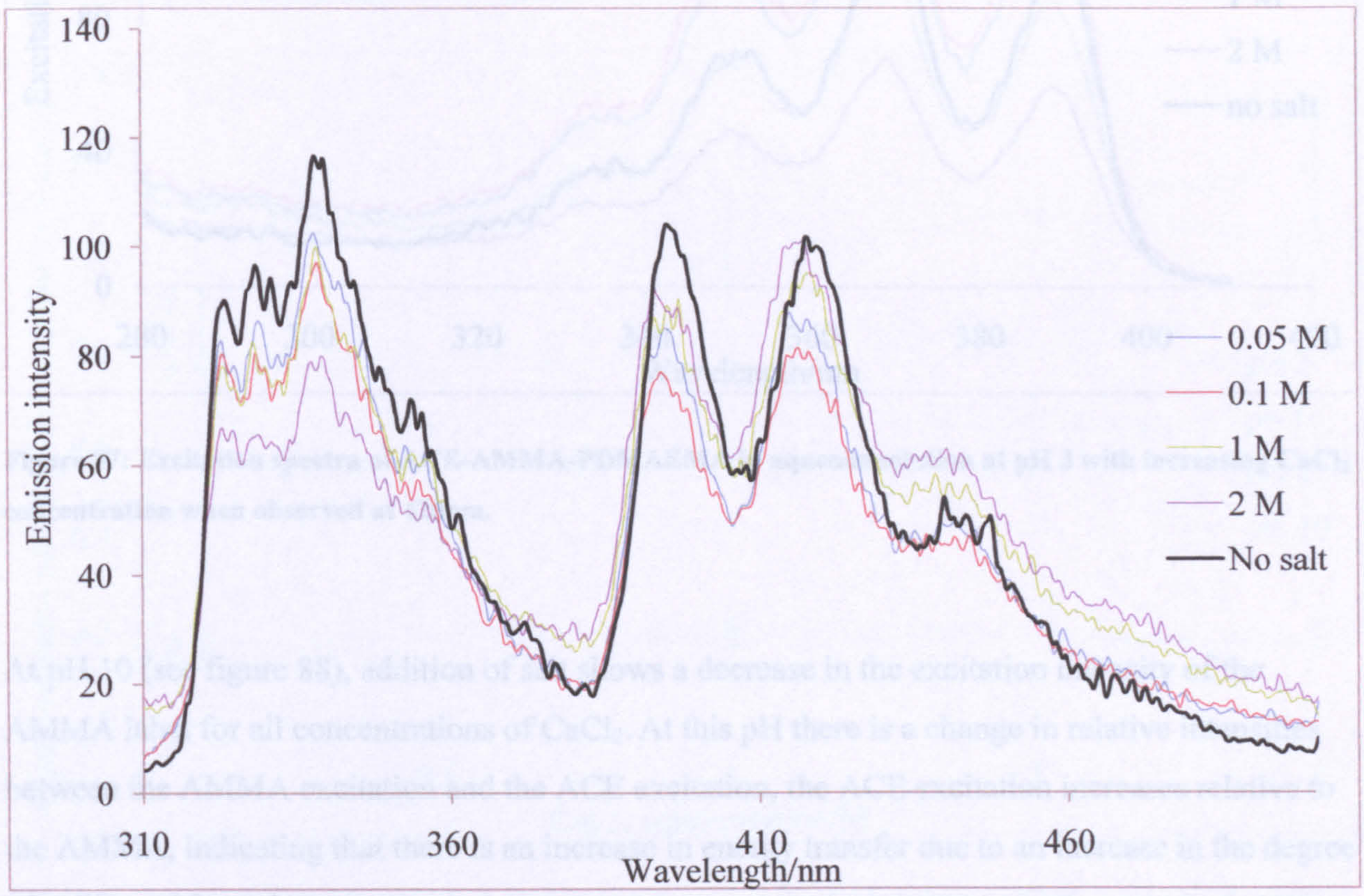

Figure 86: Steady state emission spectra of ACE-AMMA-PDMAEMA in aqueous solution at pH 10 with increasing $CaCl_2$ concentration when excited at 290 nm.

Figure 87 shows that upon addition of small amounts of $CaCl_2$ there is an overall increase in the excitation intensity of the polymer system. This would again indicate that small amounts of salt in some way shield ACE-AMMA-PDMAEMA from quenching by the aqueous media. At higher $CaCl_2$ concentrations, the relative intensity of the AMMA excitation to the ACE excitation decreases indicating a possible collapse of the polymer backbone.

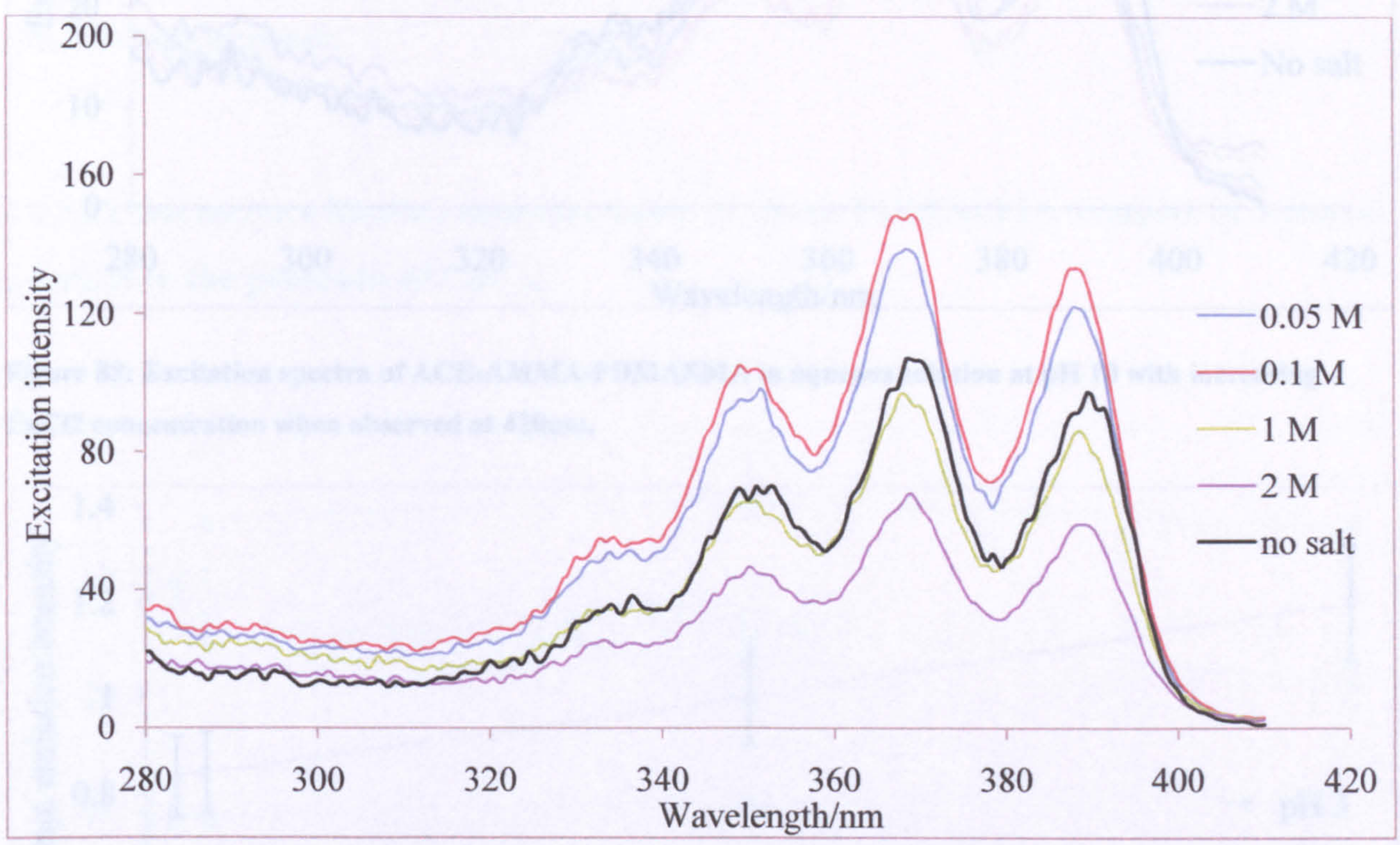

Figure 87: Excitation spectra of ACE-AMMA-PDMAEMA in aqueous solution at pH 3 with increasing $CaCl_2$ concentration when observed at 420nm.

At pH 10 (see figure 88), addition of salt shows a decrease in the excitation intensity of the AMMA label for all concentrations of $CaCl_2$. At this pH there is a change in relative intensities between the AMMA excitation and the ACE excitation, the ACE excitation increases relative to the AMMA, indicating that there is an increase in energy transfer due to an increase in the degree of coiling of the polymer system.

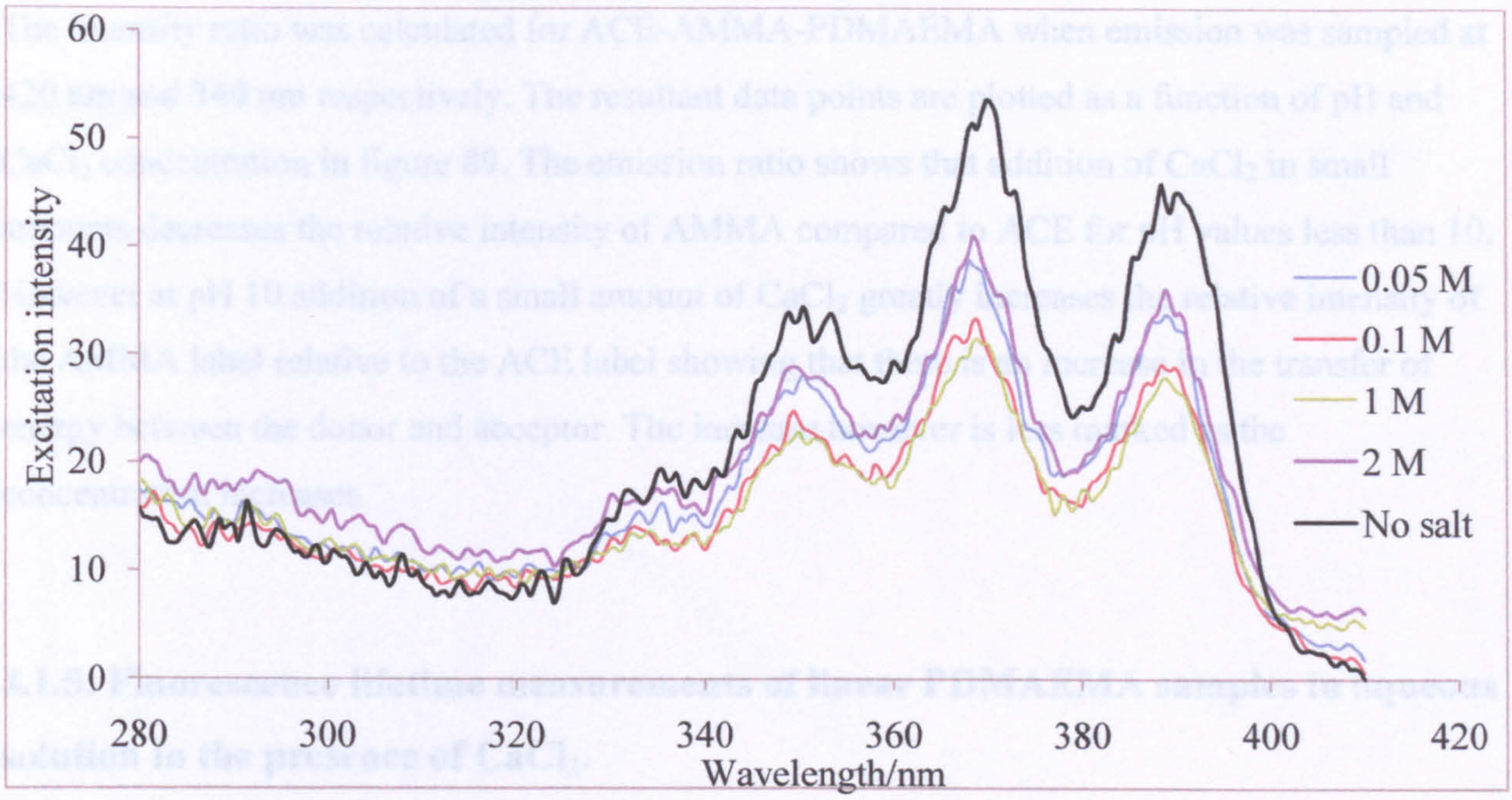

Figure 88: Excitation spectra of ACE-AMMA-PDMAEMA in aqueous solution at pH 10 with increasing CaCl2 concentration when observed at 420nm.

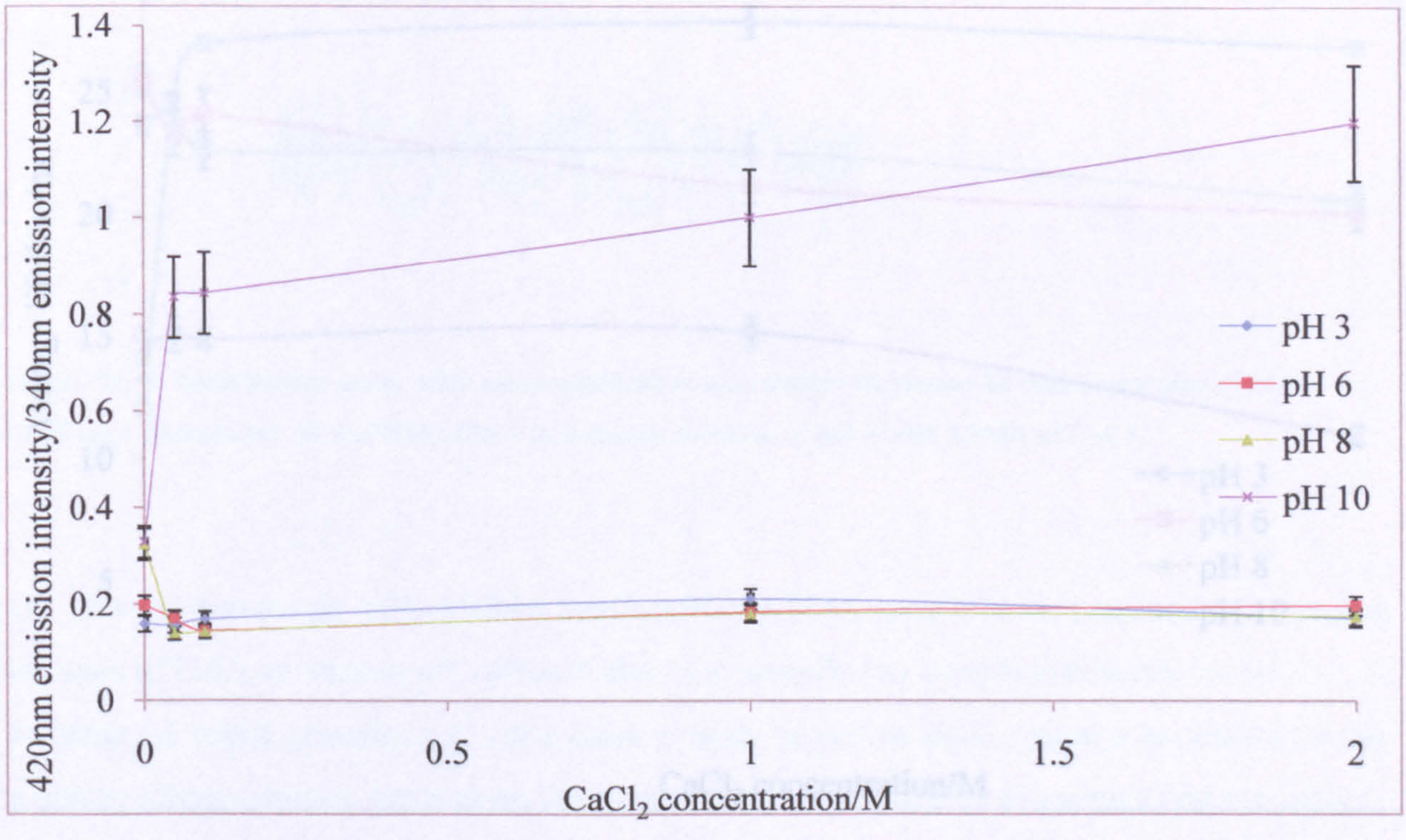

Figure 89: Ratio between the AMMA emission of 420 nm and the ACE emission of 340 nm for ACE-AMMA –PDMAEMA in aqueous solution at four different pH values with increasing concentrations of $CaCl_2$ when excited at 290 nm.

The intensity ratio was calculated for ACE-AMMA-PDMAEMA when emission was sampled at 420 nm and 340 nm respectively. The resultant data points are plotted as a function of pH and $CaCl_2$ concentration in figure 89. The emission ratio shows that addition of $CaCl_2$ in small amounts decreases the relative intensity of AMMA compared to ACE for pH values less than 10. However at pH 10 addition of a small amount of $CaCl_2$ greatly increases the relative intensity of the AMMA label relative to the ACE label showing that there is an increase in the transfer of energy between the donor and acceptor. The increase however is less marked as the concentration increases.

4.1.5: Fluorescence lifetime measurements of linear PDMAEMA samples in aqueous solution in the presence of $CaCl_2$.

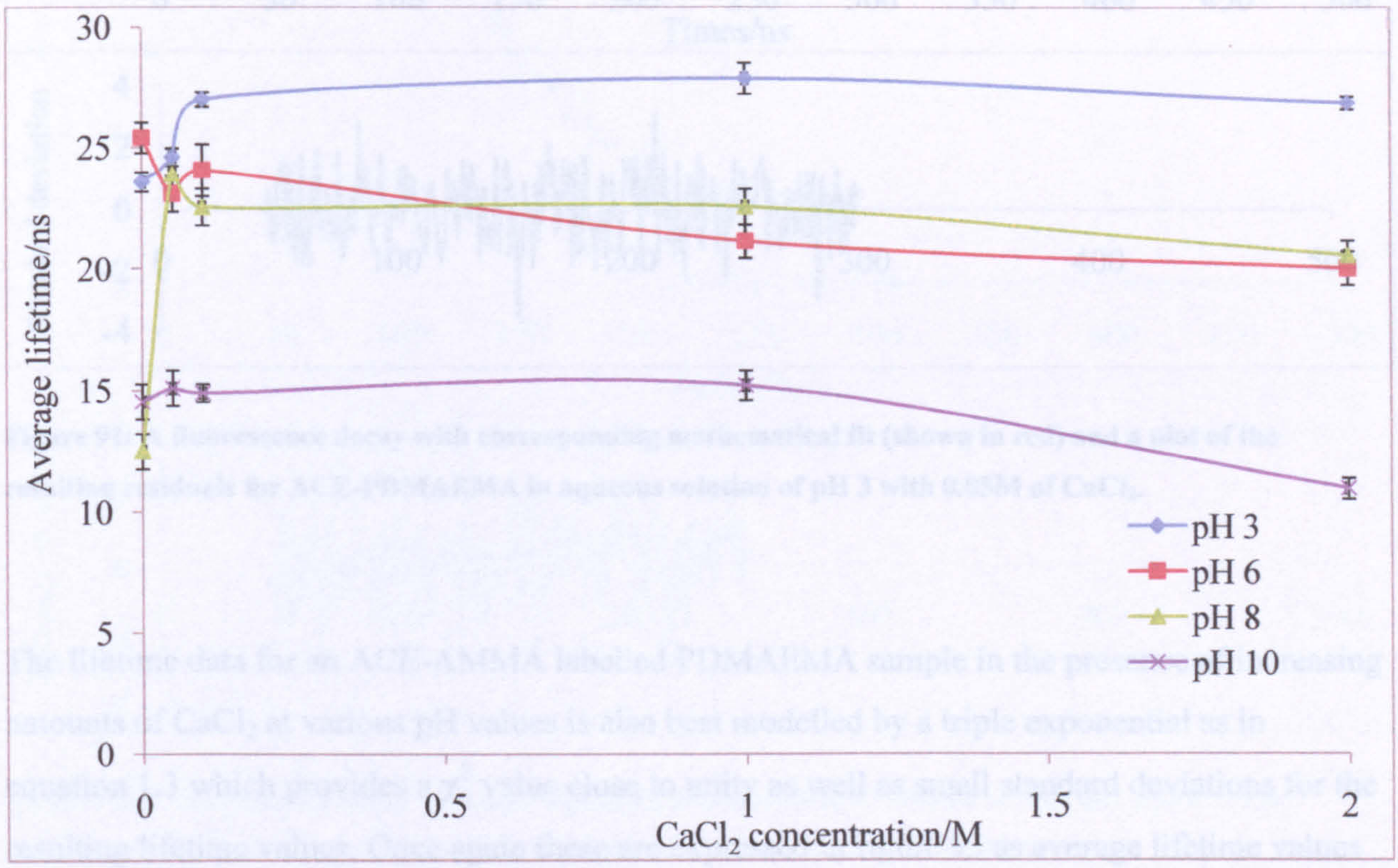

Figure 90: Average fluorescence lifetime values for ACE-PDMAEMA in aqueous solution at four different pH values with increasing $CaCl_2$ concentration when excited at 290 nm and observed at 340 nm.

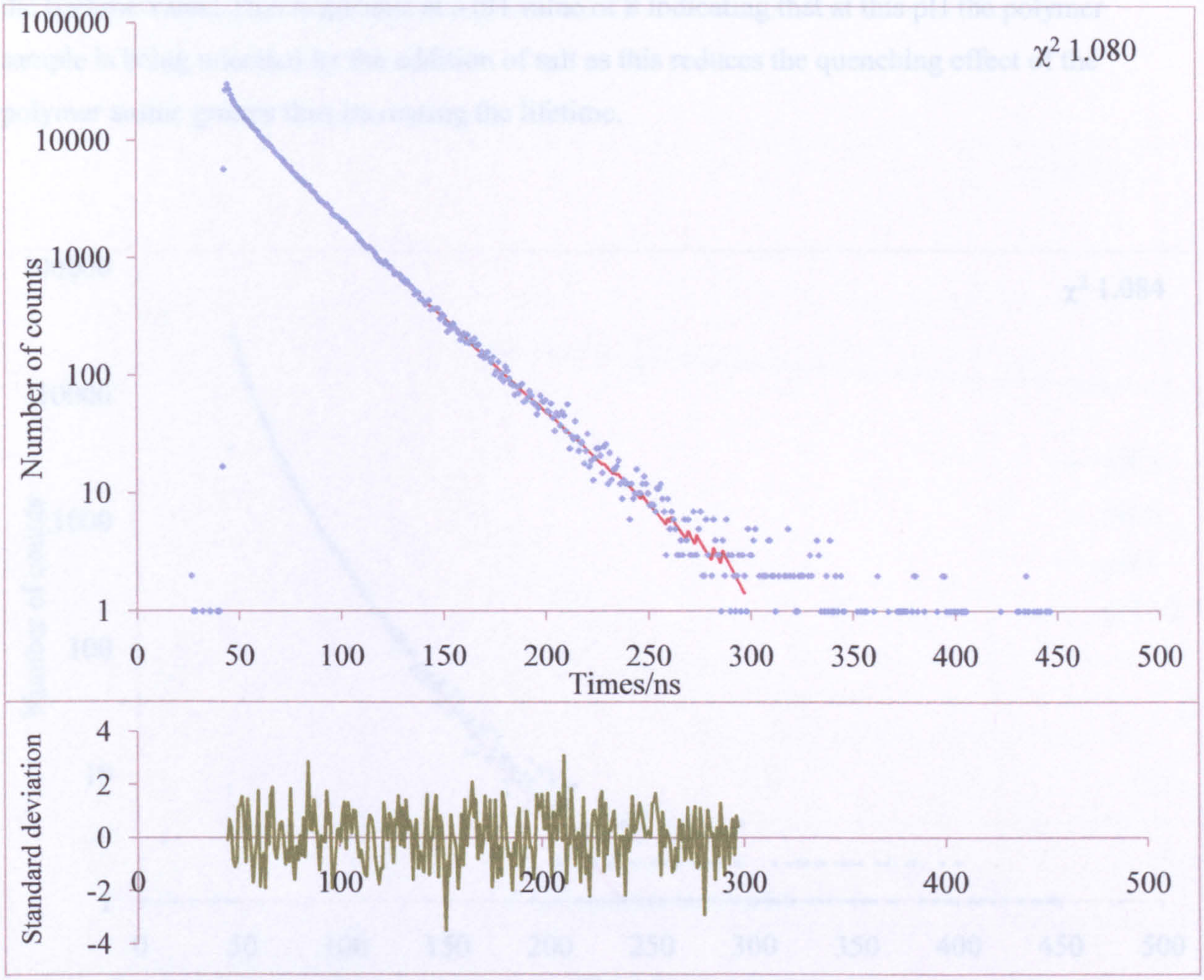

Figure 91: A fluorescence decay with corresponding mathematical fit (shown in red) and a plot of the resulting residuals for ACE-PDMAEMA in aqueous solution of pH 3 with 0.05M of $CaCl_2$.

The lifetime data for an ACE-AMMA labelled PDMAEMA sample in the presence of increasing amounts of $CaCl_2$ at various pH values is also best modelled by a triple exponential as in equation 1.3 which provides a χ^2 value close to unity as well as small standard deviations for the resulting lifetime values. Once again these are expressed in figure 93 as average lifetime values for ease of comparison.

Addition of even small amounts of $CaCl_2$ to PDMAEMA samples generally shows an increase in the lifetime value. This is greatest at a pH value of 8 indicating that at this pH the polymer sample is being uncoiled by the addition of salt as this reduces the quenching effect of the polymer amine groups thus increasing the lifetime.

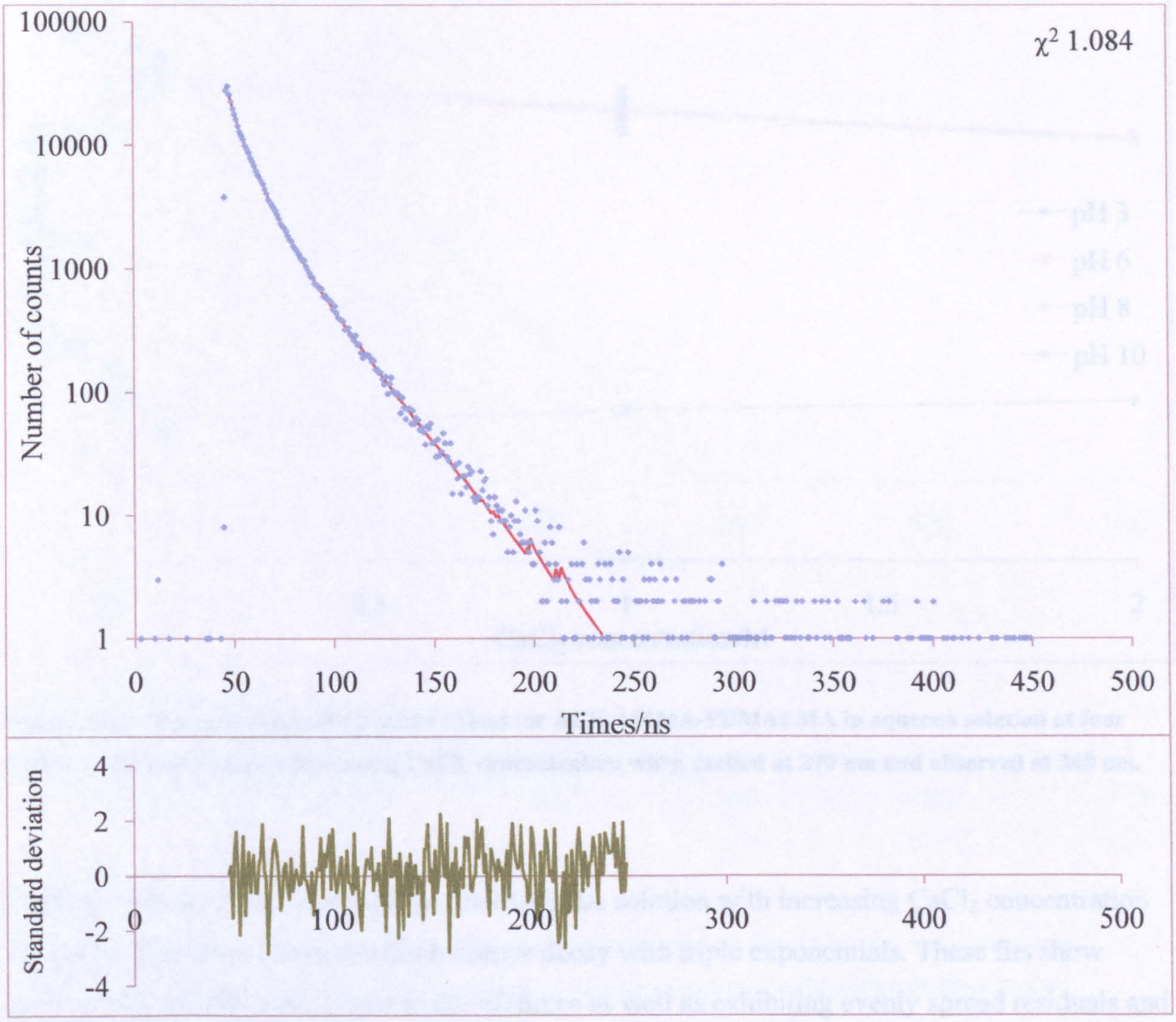

Figure 92: A fluorescence decay with corresponding mathematical fit (shown in red) and a plot of the resulting residuals for ACE-PDMAEMA in aqueous solution of pH 10 with 2 M $CaCl_2$.

The general effect with further increases in salt concentration is a slight decrease in the lifetime indicating a collapse of the polymer chain as the $CaCl_2$ concentration increases further.

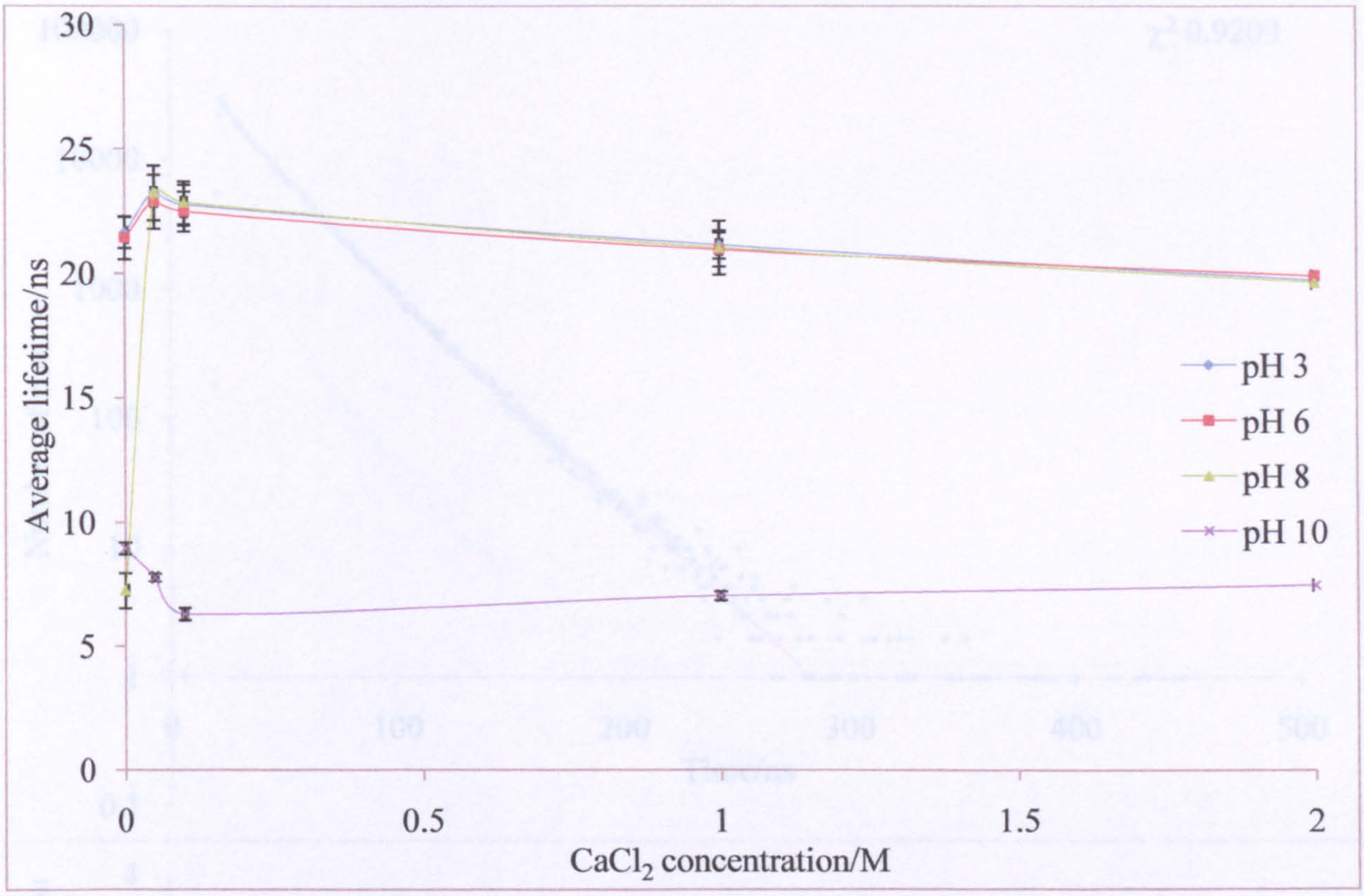

Figure 93: Average fluorescence lifetime values for ACE-AMMA-PDMAEMA in aqueous solution at four different pH values across increasing $CaCl_2$ concentration when excited at 290 nm and observed at 340 nm.

Lifetime values for an ACE-AMMA PDMAEMA solution with increasing $CaCl_2$ concentration are best achieved by fitting the fluorescence decay with triple exponentials. These fits show good, small, standard deviations to the lifetimes as well as exhibiting evenly spread residuals and χ^2 values close to unity.

The lifetime values of a double labelled PDMAEMA system upon addition of a small amount of $CaCl_2$ show increases in lifetime value for pH values of 3, 6 and 8. The greatest increase in this

lifetime, and thus uncoiling of the PDMAEMA system, is at pH 8. As further salt is added the lifetime value slowly decreases indicating an eventual collapse of the polymer.

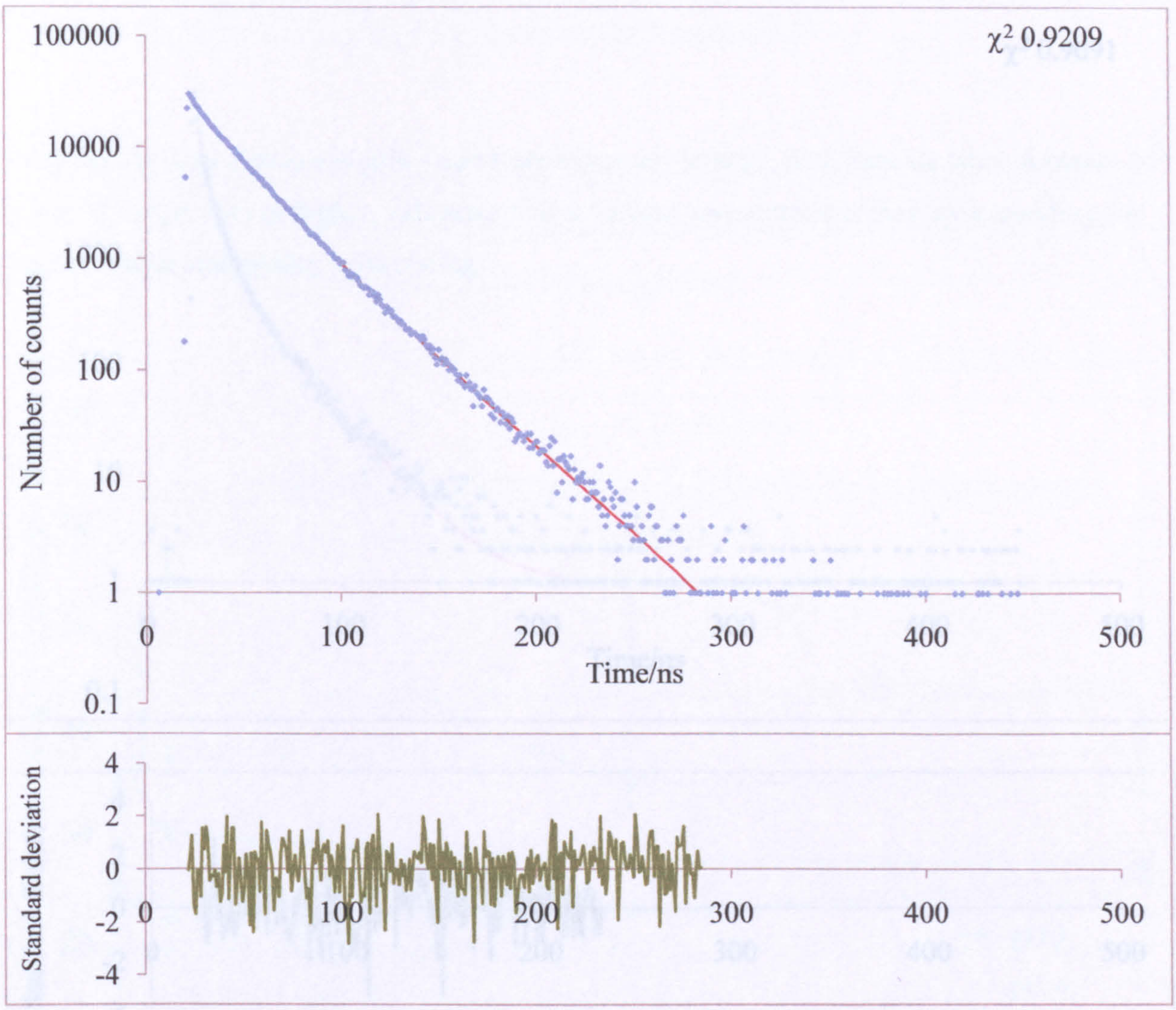

Figure 94: A fluorescence decay with corresponding mathematical fit (shown in red) and a plot of the resulting residuals for ACE-AMMA-PDMAEMA in aqueous solution of pH 3 with 0.05 M of $CaCl_2$.

At pH 10 addition of a small amount of $CaCl_2$ instead seems to decrease the lifetime, presumably coiling the polymer and increasing quenching, further addition of $CaCl_2$ at this concentration seems to increase the lifetime slightly. A consideration here however is at $CaCl_2$ concentrations

of 1 M or higher the pH 10 solution does exhibit small amounts of precipitation, indicating a further collapse of the polymer, a situation not supported by the increase in lifetime.

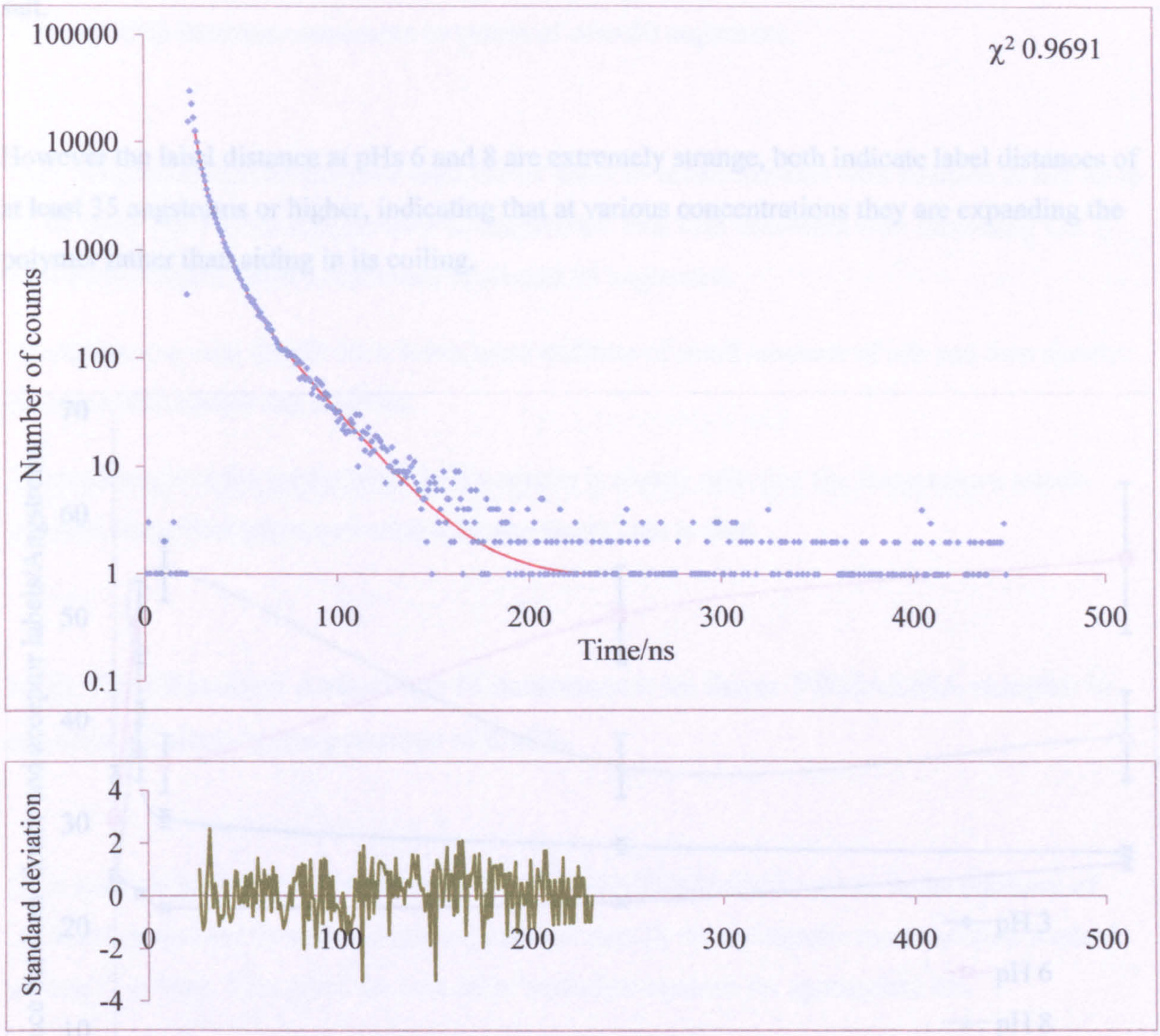

Figure 95: A fluorescence decay with corresponding mathematical fit (shown in red) and a plot of the resulting residuals for ACE-AMMA-PDMAEMA in aqueous solution of pH 10 with 2M of $CaCl_2$.

The distance between the labels, r, when calculated using equation 3.1 as seen before further complicates matters.

The distance between the labels at pH 3 drops from around 35 angstroms, similar to the polymer in the absence of any salt, at 0.05 M $CaCl_2$ to around 30 angstroms at higher concentrations of salt.

However the label distance at pHs 6 and 8 are extremely strange, both indicate label distances of at least 35 angstroms or higher, indicating that at various concentrations they are expanding the polymer rather than aiding in its coiling.

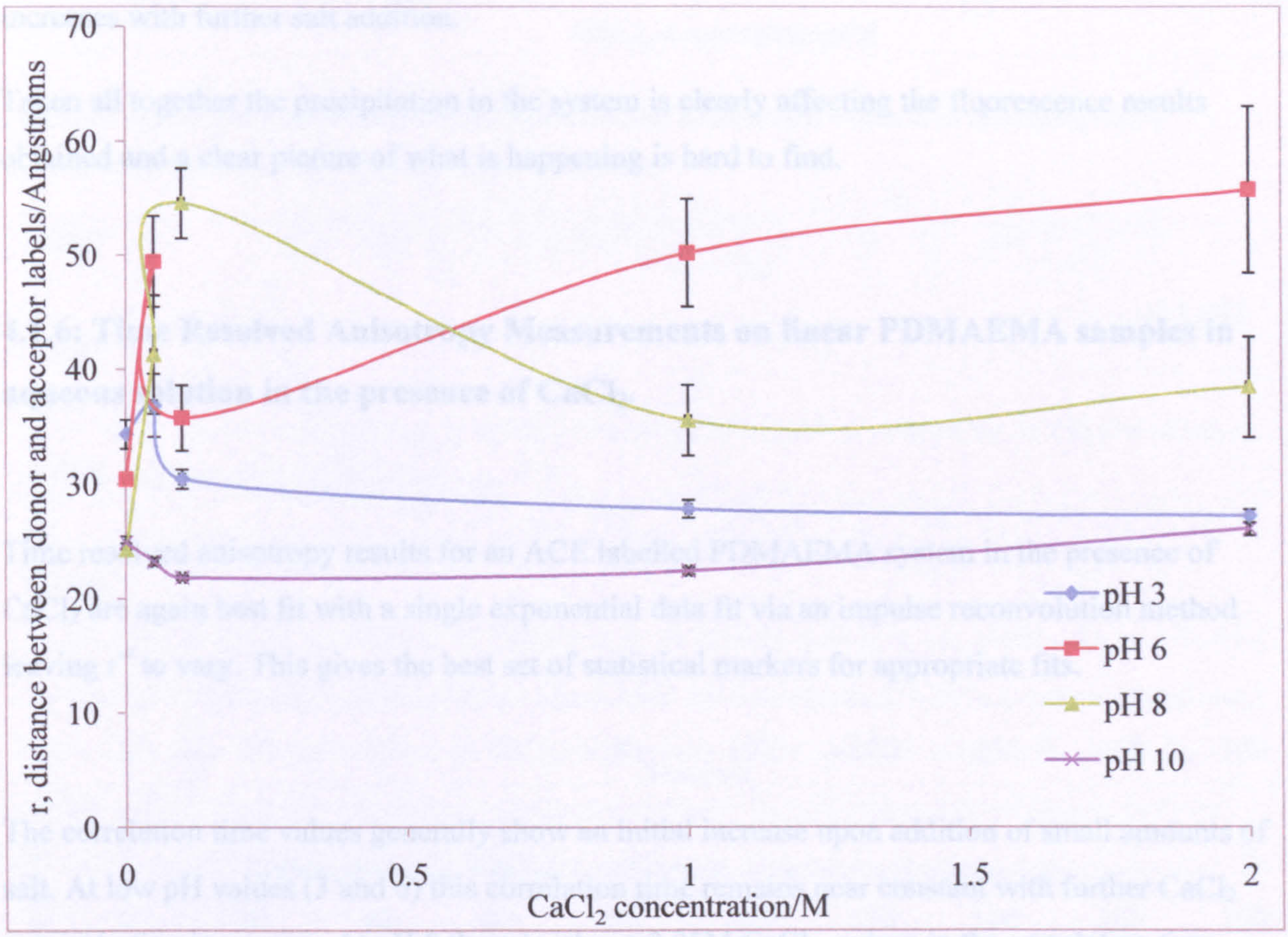

Figure 96: A plot of the value r, the distance between donor and acceptor labels, as calculated by equation 4.1 for ACE-PDMAEMA and ACE-AMMA-PDMAEMA across a range of pH values and $CaCl_2$ concentrations.

However they are also very strange in another way. At pH 6 there is an initial increase in the label distance upon addition of small amounts of salts followed by a substantial decease at 0.1 M in label distance from about 50 angstroms, significantly higher than in the absence of salt. to around 35 angstroms, similar to the initial label distance at pH 3. At salt concentrations above 0.1M this then increases once more to values of over 50 angstroms.

The r values obtained for the pH 8 data follow show an initial increase with addition of salt up to 0.1 M where the r value reaches over 50 angstroms. This then decreases with increasing $CaCl_2$ concentration back down to distances of around 35 angstroms.

The distance, r, seen for pH 10 is lower upon addition of small amounts of salt and then slowly increases with further salt addition.

Taken all together the precipitation in the system is clearly affecting the fluorescence results obtained and a clear picture of what is happening is hard to find.

4.1.6: Time Resolved Anisotropy Measurements on linear PDMAEMA samples in aqueous solution in the presence of $CaCl_2$.

Time resolved anisotropy results for an ACE labelled PDMAEMA system in the presence of $CaCl_2$ are again best fit with a single exponential data fit via an impulse reconvolution method leaving r^{∞} to vary. This gives the best set of statistical markers for appropriate fits.

The correlation time values generally show an initial increase upon addition of small amounts of salt. At low pH values (3 and 6) this correlation time remains near constant with further $CaCl_2$ concentration increases. At pH 8 there is, above 0.05M $CaCl_2$, a drop in the correlation time indicating an opening of the polymer system, this then increases slightly again at particularly high salt concentrations.

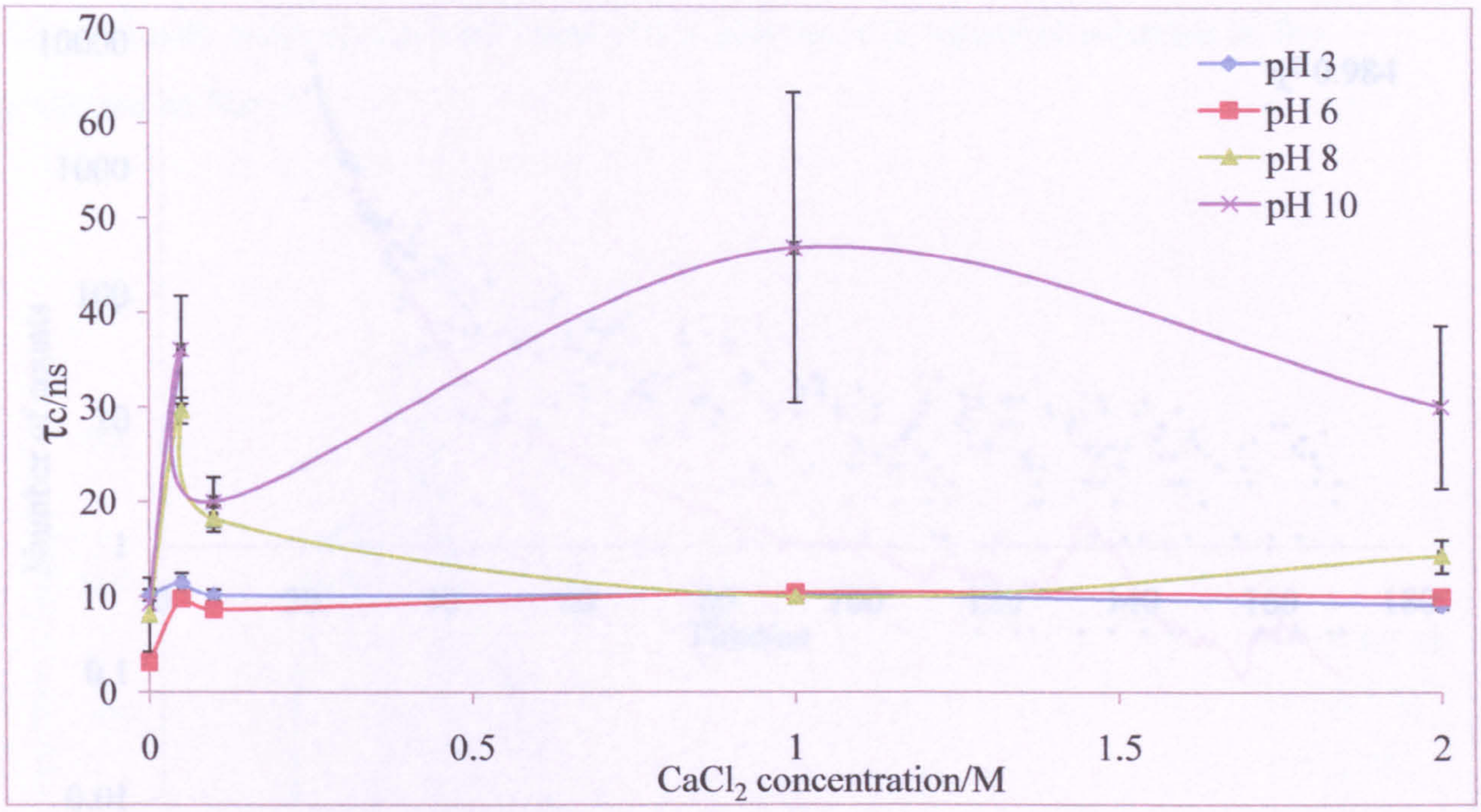

Figure 97: A plot of the correlation times obtained at four different pH values with increasing $CaCl_2$ concentration for ACE-PDMAEMA in aqueous solution.

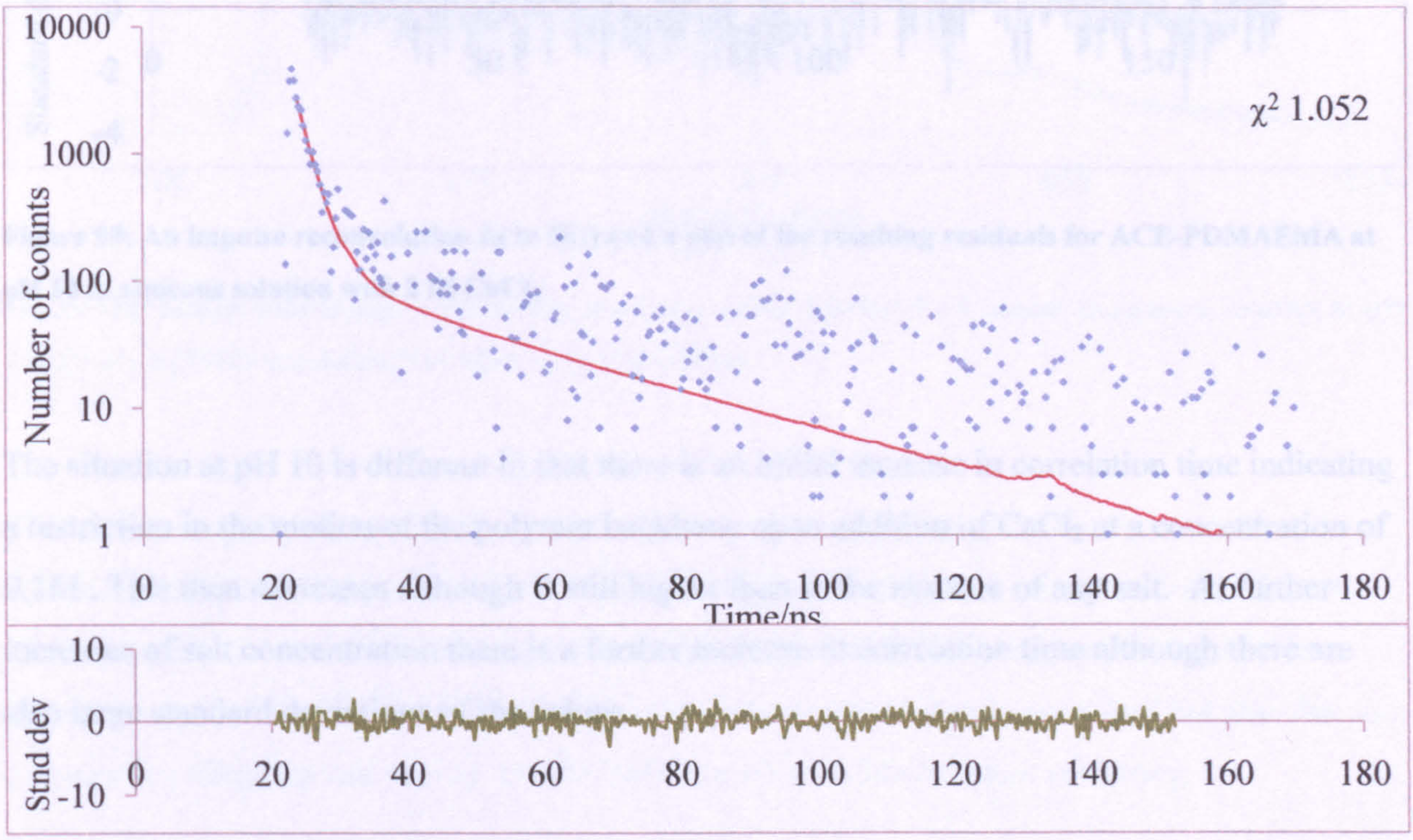

Figure 98: An impulse reconvolution fit to D(t) and a plot of the resulting residuals for ACE- PDMAEMA at pH 3 in aqueous solution with 0.05M $CaCl_2$.

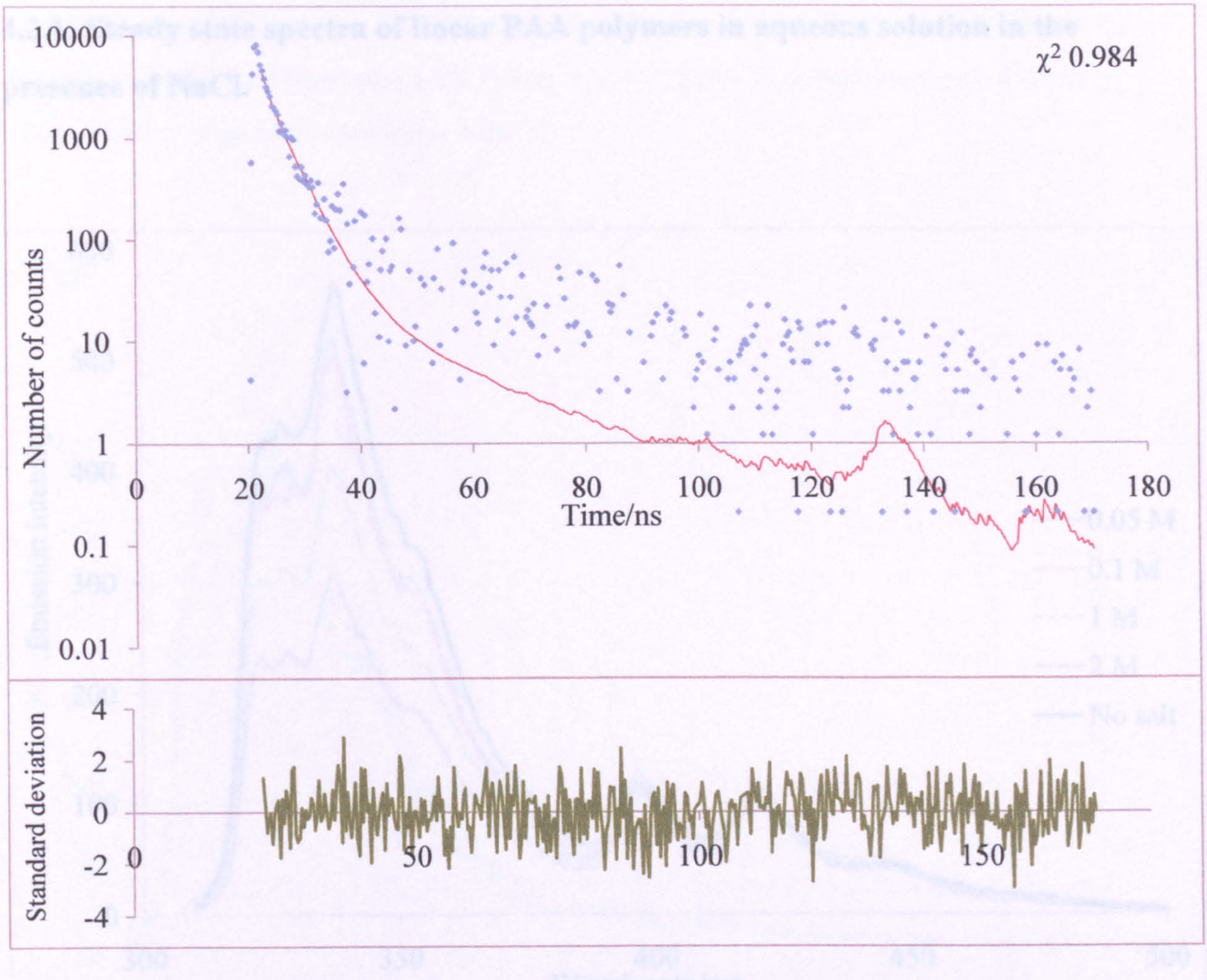

Figure 99: An impulse reconvolution fit to D(t) and a plot of the resulting residuals for ACE-PDMAEMA at pH 10 in aqueous solution with 2 M $CaCl_2$.

The situation at pH 10 is different in that there is an initial increase in correlation time indicating a restriction in the motion of the polymer backbone upon addition of $CaCl_2$ at a concentration of 0.1M . This then decreases although is still higher than in the absence of any salt. At further increases of salt concentration there is a further increase in correlation time although there are also large standard deviations of the values.

4.2.1: Steady state spectra of linear PAA polymers in aqueous solution in the presence of NaCl.

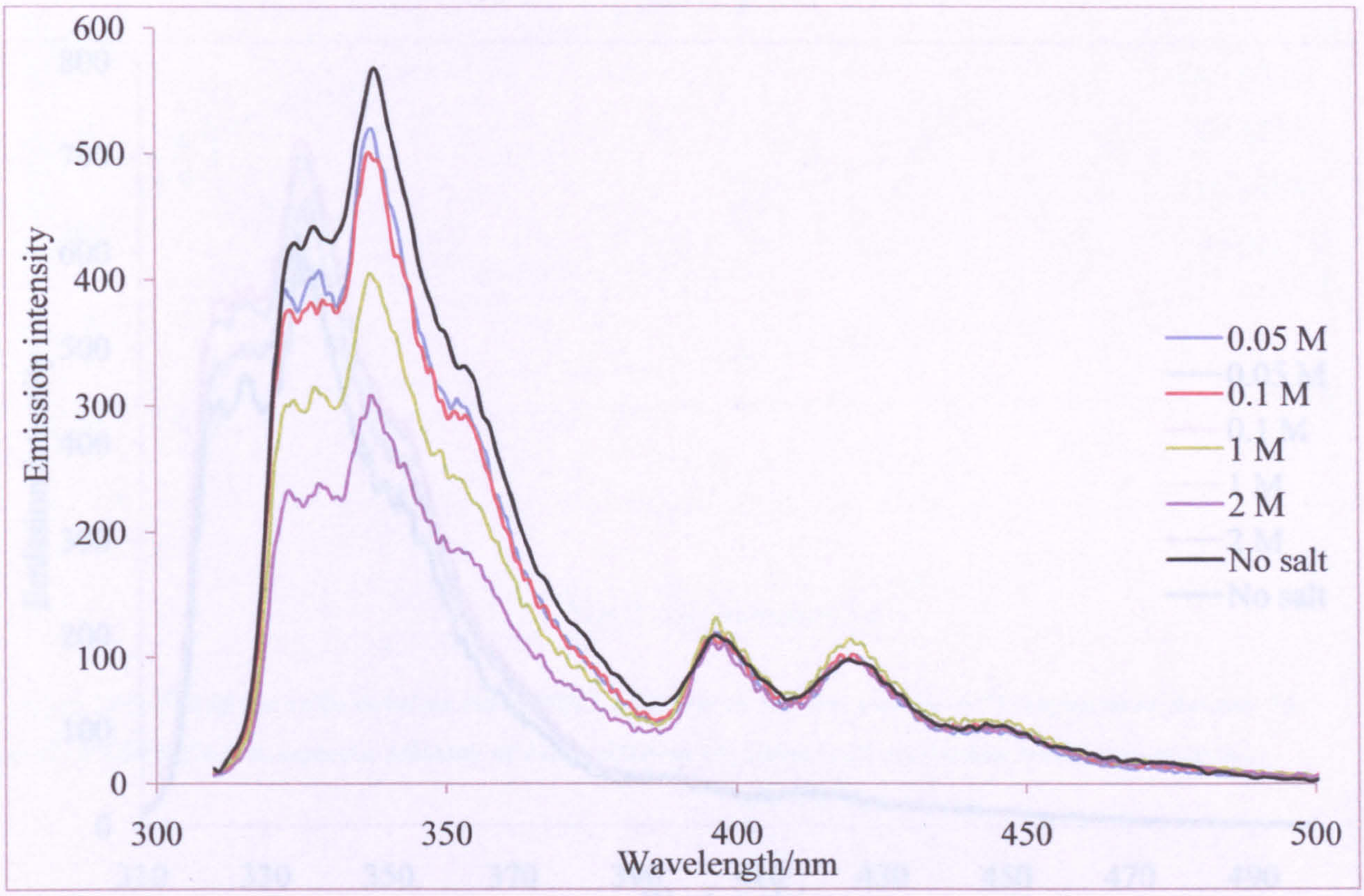

Figure 100: Steady state emission spectra for an ACE-AMMA labelled PAA sample in aqueous solution at pH 3 and varying NaCl concentrations when excited at 290nm.

The emission spectra for an ACE-AMMA labelled PAA sample at pH3 (see figure 100) show a decrease in emission intensity of the ACE label with increasing NaCl concentrations. There is little change in the emission intensity of the AMMA label indicating that something is either selectively quenching ACE emission or that the entire system is being quenched but also that the polymer is collapsing and energy transfer between the two labels is also occurring.

At pH 10 however (see figure 101) there is an initial increase in the emission intensity of the ACE label, which then decreases with further increasing NaCl concentration and there is no considerable change to the AMMA emission.

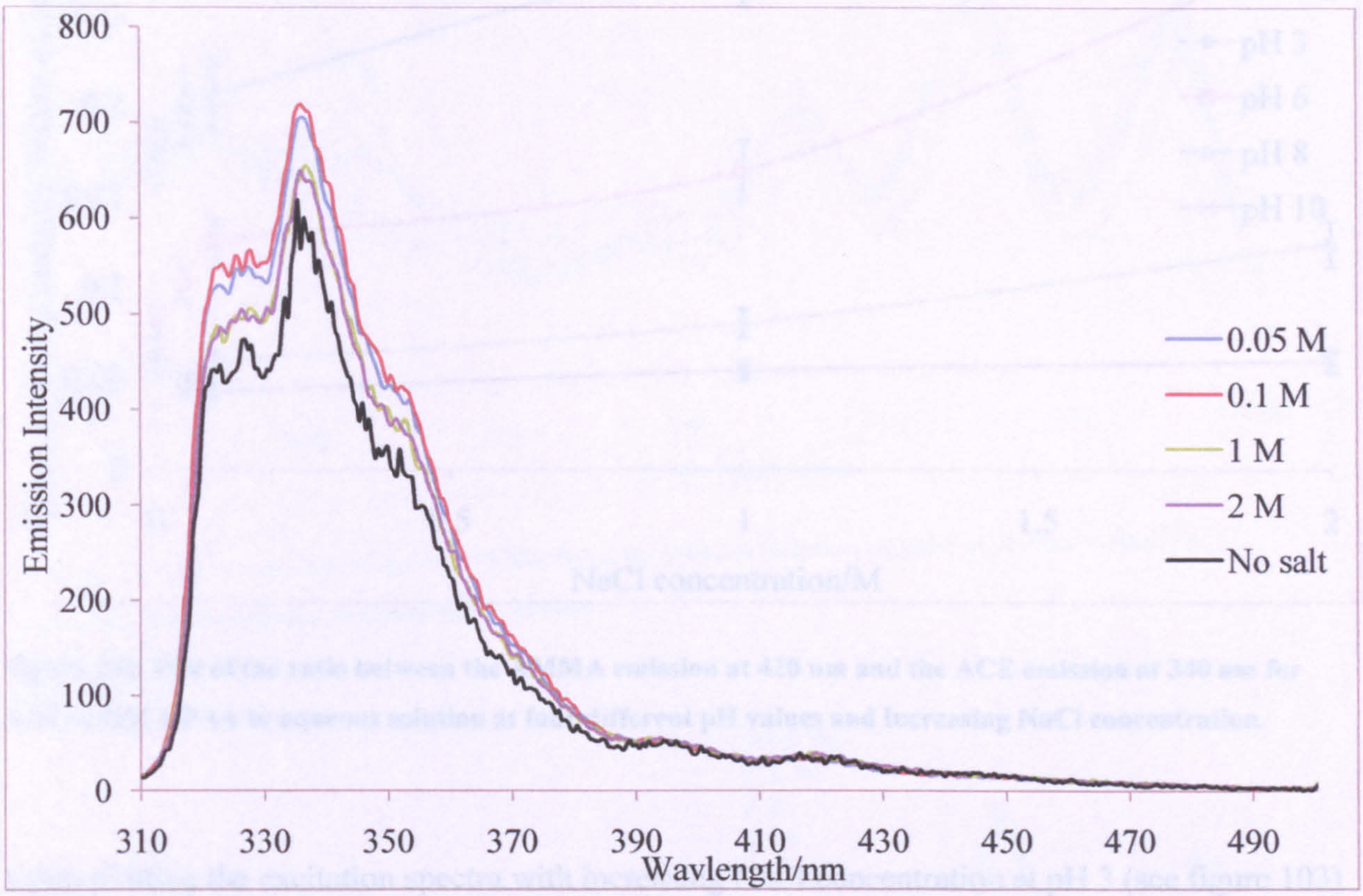

Figure 101: Steady state emission spectra for an ACE-AMMA PAA sample in aqueous solution at pH 10 and varying NaCl concentration when excited at 290 nm.

The ratio between the ACE and the AMMA emission at the four different pH values with increasing NaCl concentration is shown in figure 100. At pH values of 6 or less there is a general increase in the ratio between the labels as NaCl concentration increases, this indicates an increase in the energy transfer between the donor and acceptor. At pH values over 6 small amounts of NaCl decrease the emission ratio indicating n increased distance between the donor and acceptor and an uncoiling of the polymer.

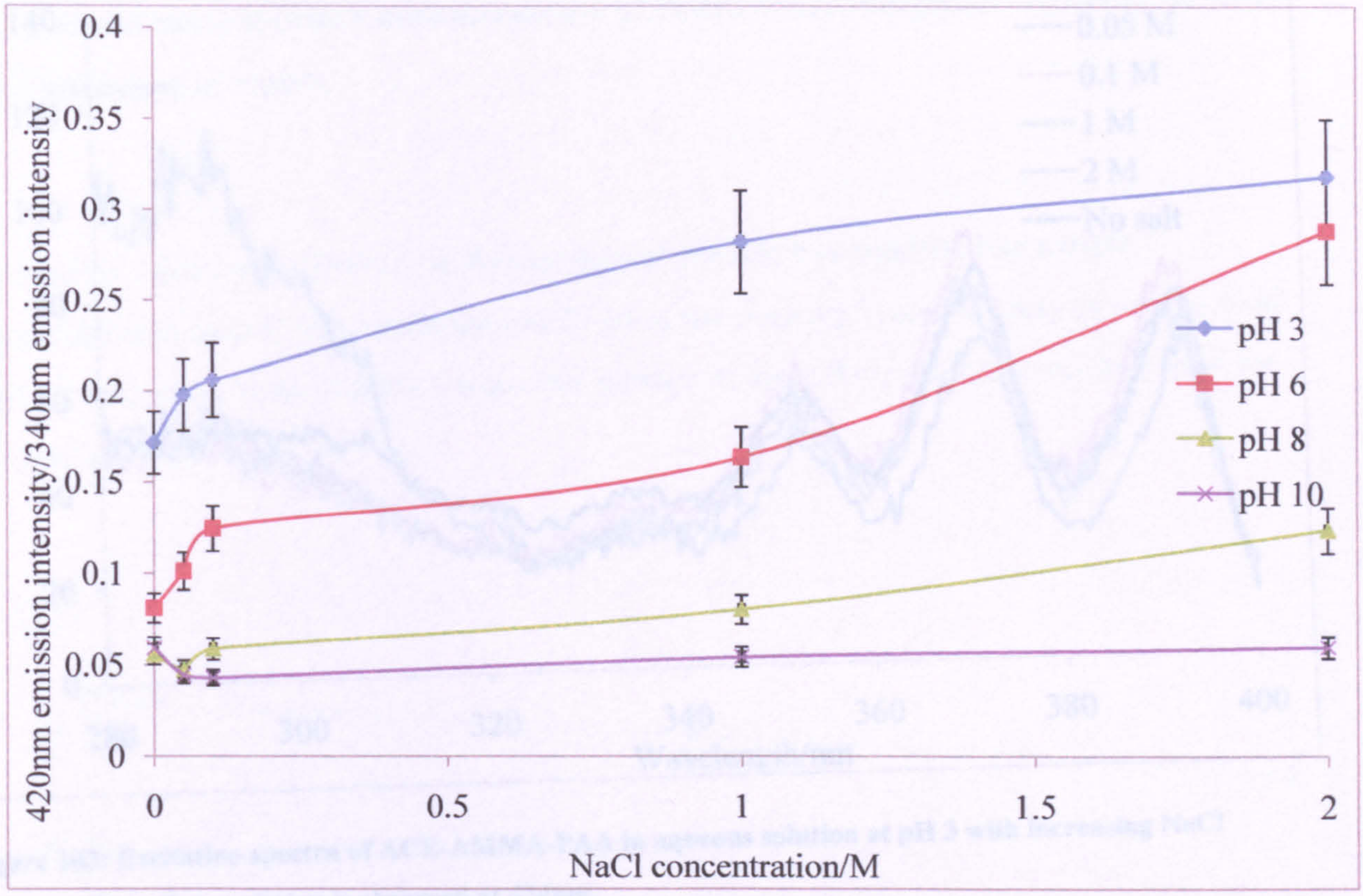

Figure 102: Plot of the ratio between the AMMA emission at 420 nm and the ACE emission at 340 nm for ACE-AMMA-PAA in aqueous solution at four different pH values and increasing NaCl concentration.

Upon plotting the excitation spectra with increasing NaCl concentration at pH 3 (see figure 103) it can be seen the ratio between the ACE and the AMMA excitation regions when observing the AMMA emission show an initial large increase in the excitation at 290 nm indicating an initial collapse of the polymer compared to that in the absence of salt. This ratio then drops at the salt concentration increases further.

At pH 10 there is an increase in the excitation at 290nm for all increasing amounts of NaCl indicating a collapse of the polymer system.

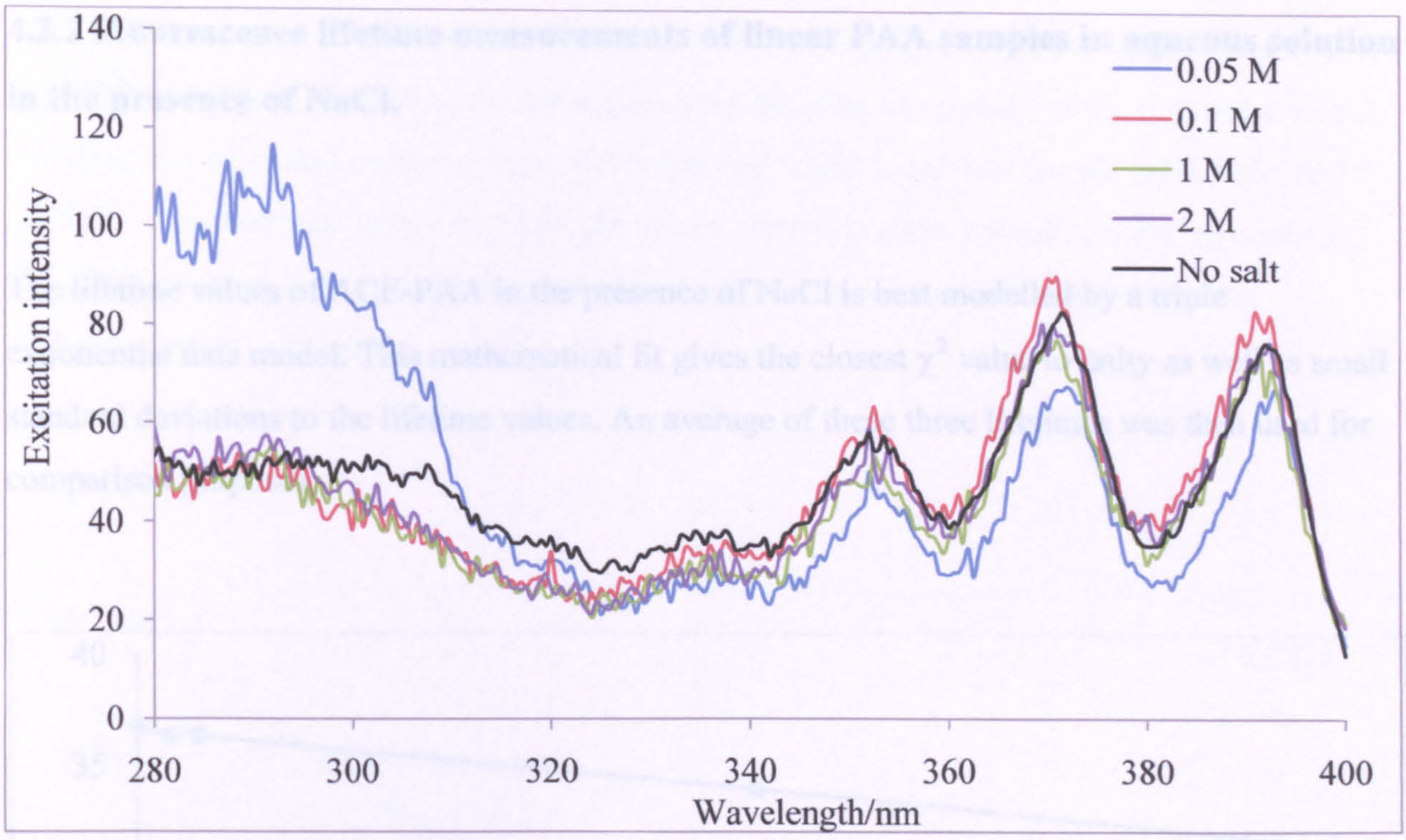

Figure 103: Excitation spectra of ACE-AMMA-PAA in aqueous solution at pH 3 with increasing NaCl concentration when emission is observed at 420nm.

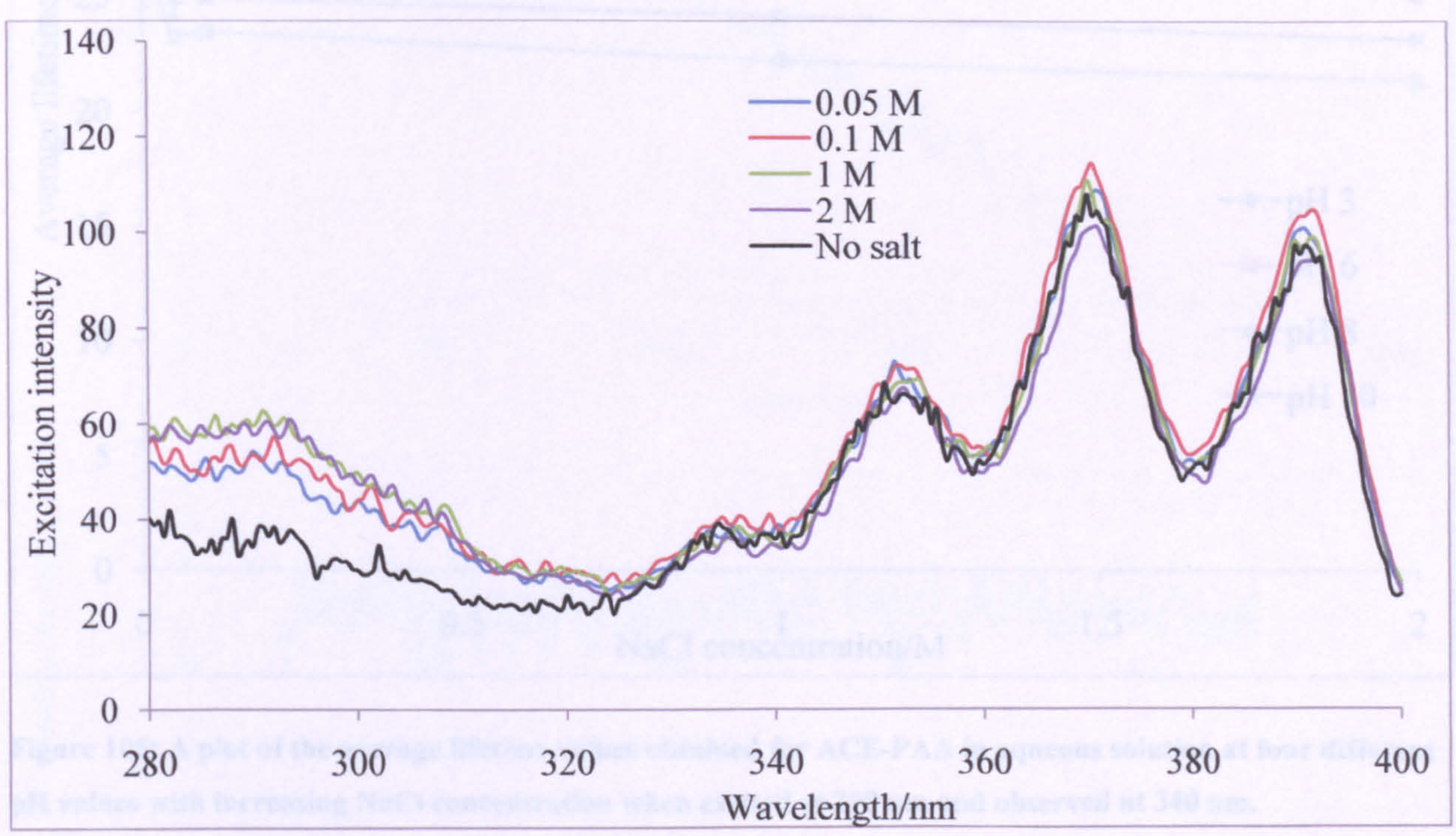

Figure 104: Excitation spectra of ACE-AMMA-PAA in aqueous solution at pH 10 with increasing NaCl concentration when emission is observed at 420nm.

4.2.2 Fluorescence lifetime measurements of linear PAA samples in aqueous solution in the presence of NaCl.

The lifetime values of ACE-PAA in the presence of NaCl is best modelled by a triple exponential data model. This mathematical fit gives the closest χ^2 value to unity as well as small standard deviations to the lifetime values. An average of these three lifetimes was then used for comparison purposes.

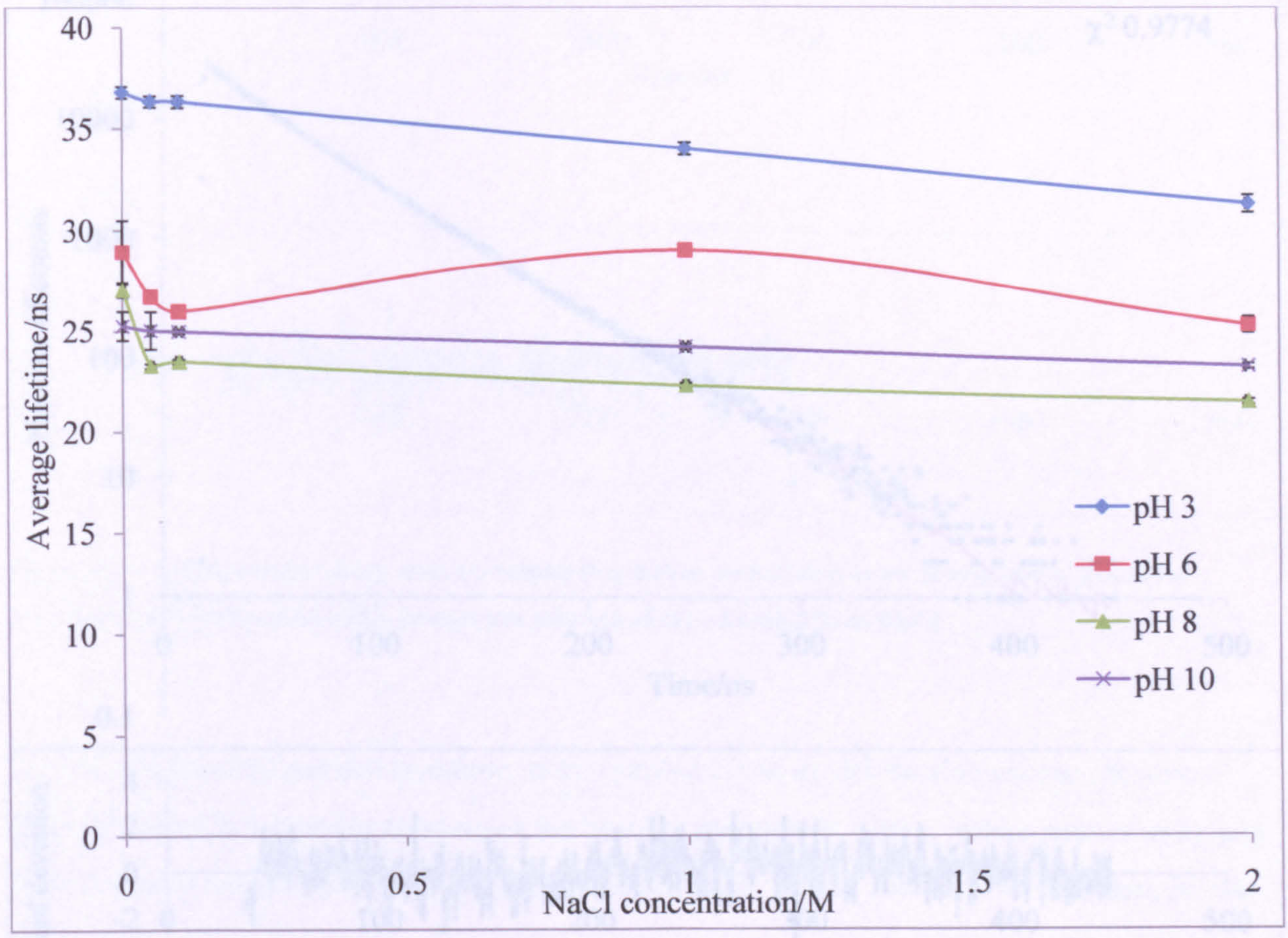

Figure 105: A plot of the average lifetime values obtained for ACE-PAA in aqueous solution at four different pH values with increasing NaCl concentration when excited at 290 nm and observed at 340 nm.

The initial inclusion of small concentrations of NaCl to the polymer system causes a decrease in the lifetime value of the polymer system, perhaps indicating an opening of the lose polymer coil enabling increased quenching by aqueous media, this effect is greatest for pH values of 6 and 8. At NaCl concentrations above 0.1M all pH values generally show a small, further, decrease in the lifetime value. At pH 6 however there is a strange increase in the lifetime value at a concentration of 1 M NaCl.

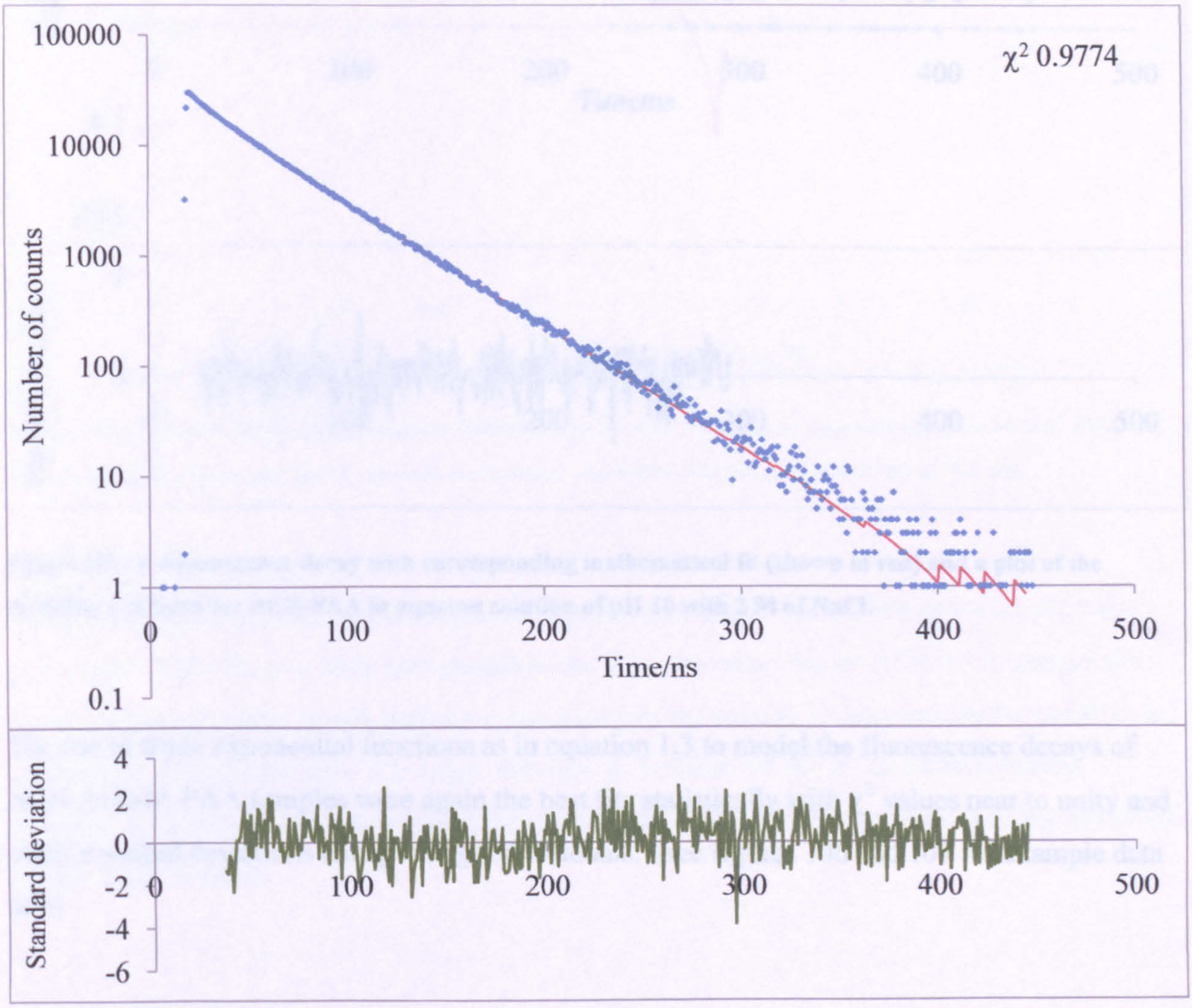

Figure 106: A fluorescence decay with corresponding mathematical fit (shown in red) and a plot of the resulting residuals for ACE-PAA in aqueous solution of pH 3 with 0.05M of NaCl.

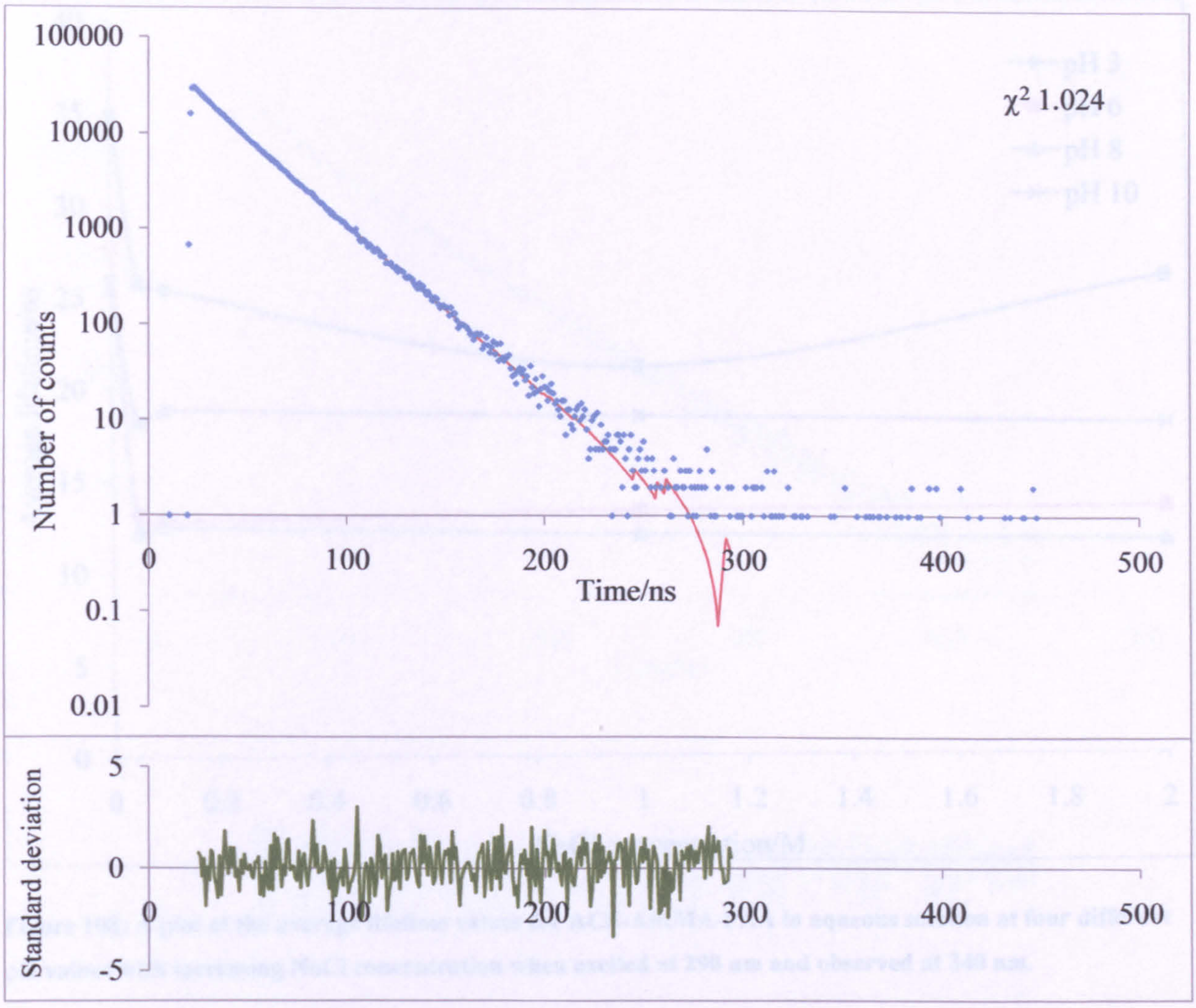

Figure 107: A fluorescence decay with corresponding mathematical fit (shown in red) and a plot of the resulting residuals for ACE-PAA in aqueous solution of pH 10 with 2 M of NaCl.

.

The use of triple exponential functions as in equation 1.3 to model the fluorescence decays of ACE-AMMA PAA samples were again the best fits statistically with χ^2 values near to unity and small standard deviations along with good residuals. (see figures 106 and 107 for example data sets)

Again average lifetime values were used for the purposes of comparison to give an overall picture. These average lifetimes were calculated using equation 1.4 as before.

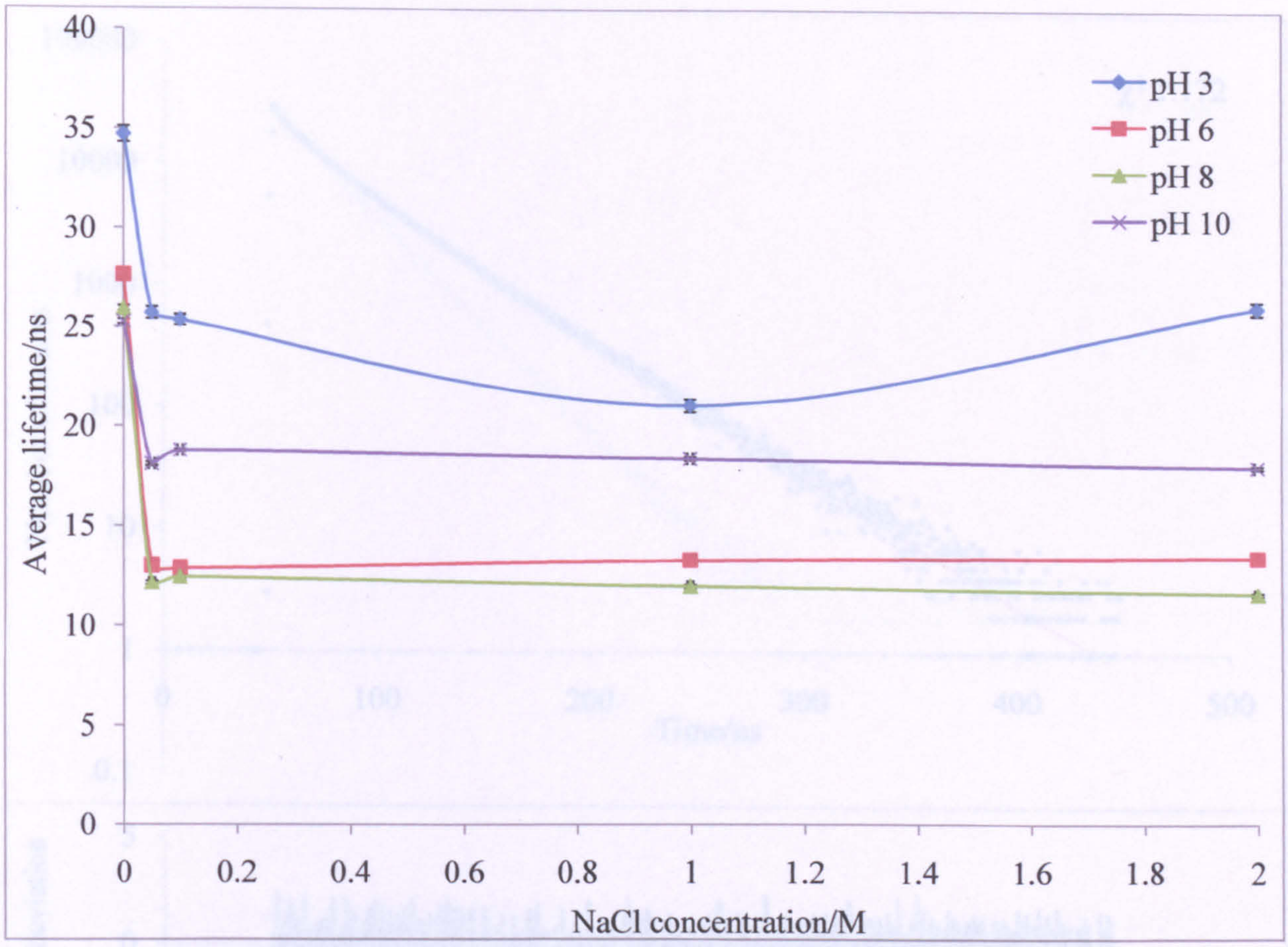

Figure 108: A plot of the average lifetime values for ACE-AMMA-PAA in aqueous solution at four different pH values with increasing NaCl concentration when excited at 290 nm and observed at 340 nm.

Addition of NaCl in small amounts give a substantial decrease in the lifetime for all pH values. (see figure 108) This is a little unexpected as the lifetime values for an ACE-PAA sample also show a decrease which would indicate a quenching of the system by aqueous media and thus an opening of the polymer coil. The larger decrease in lifetime for the ACE-AMMA system however indicates that the system is coiling further and the ACE fluorescence is being quenched by the AMMA label.

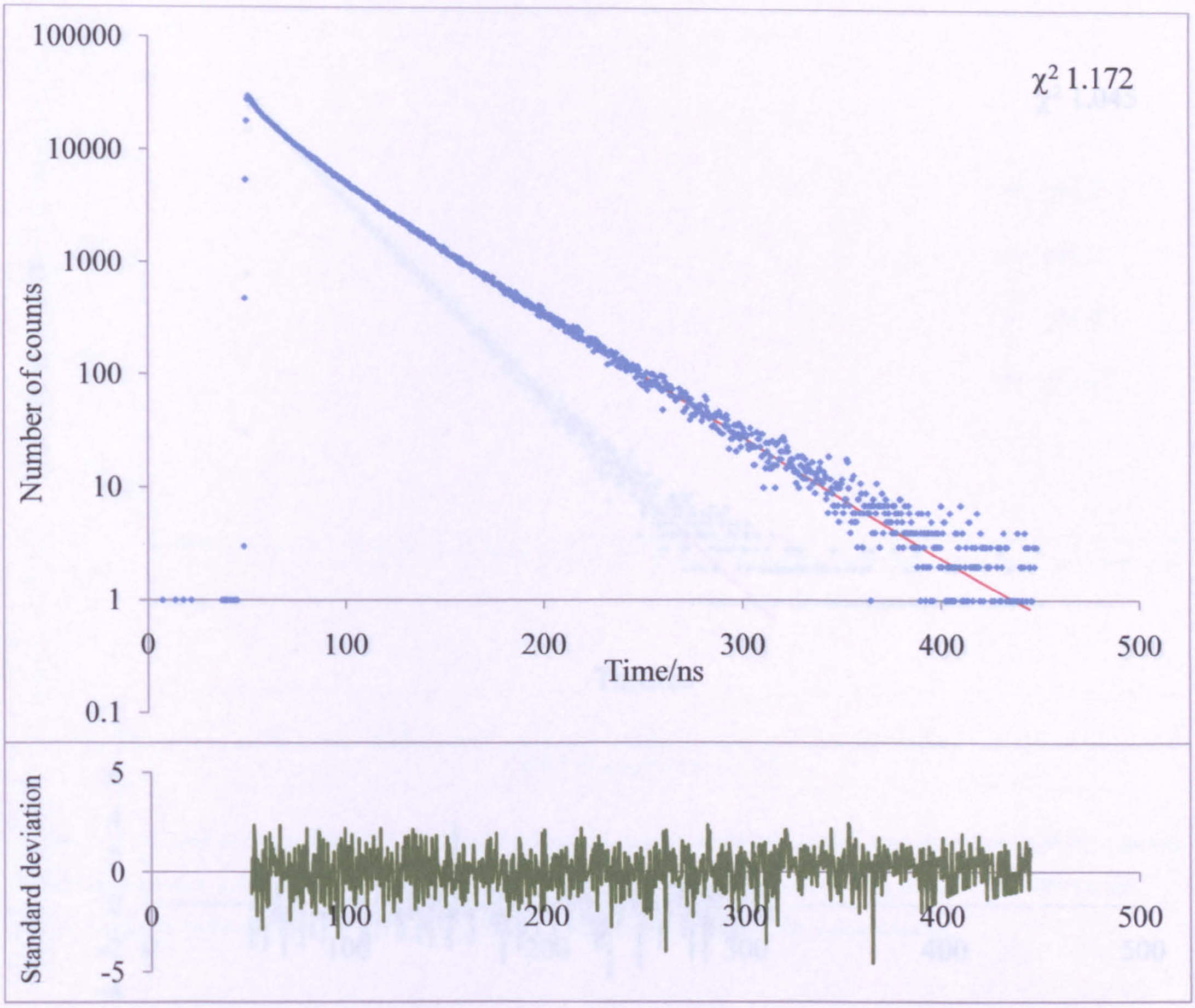

Figure 109: A fluorescence decay with corresponding mathematical fit (shown in red) and a plot of the resulting residuals for ACE-AMMA-PAA in aqueous solution of pH 3 with 0.05 M of NaCl.

Again the distance value, r, was calculated from the lifetime values of ACE both in the presence and absence of the AMMA label using equation 3.1.

Figure 111 shows these r distances in angstroms for the PAA systems in the presence of NaCl of increasing amounts

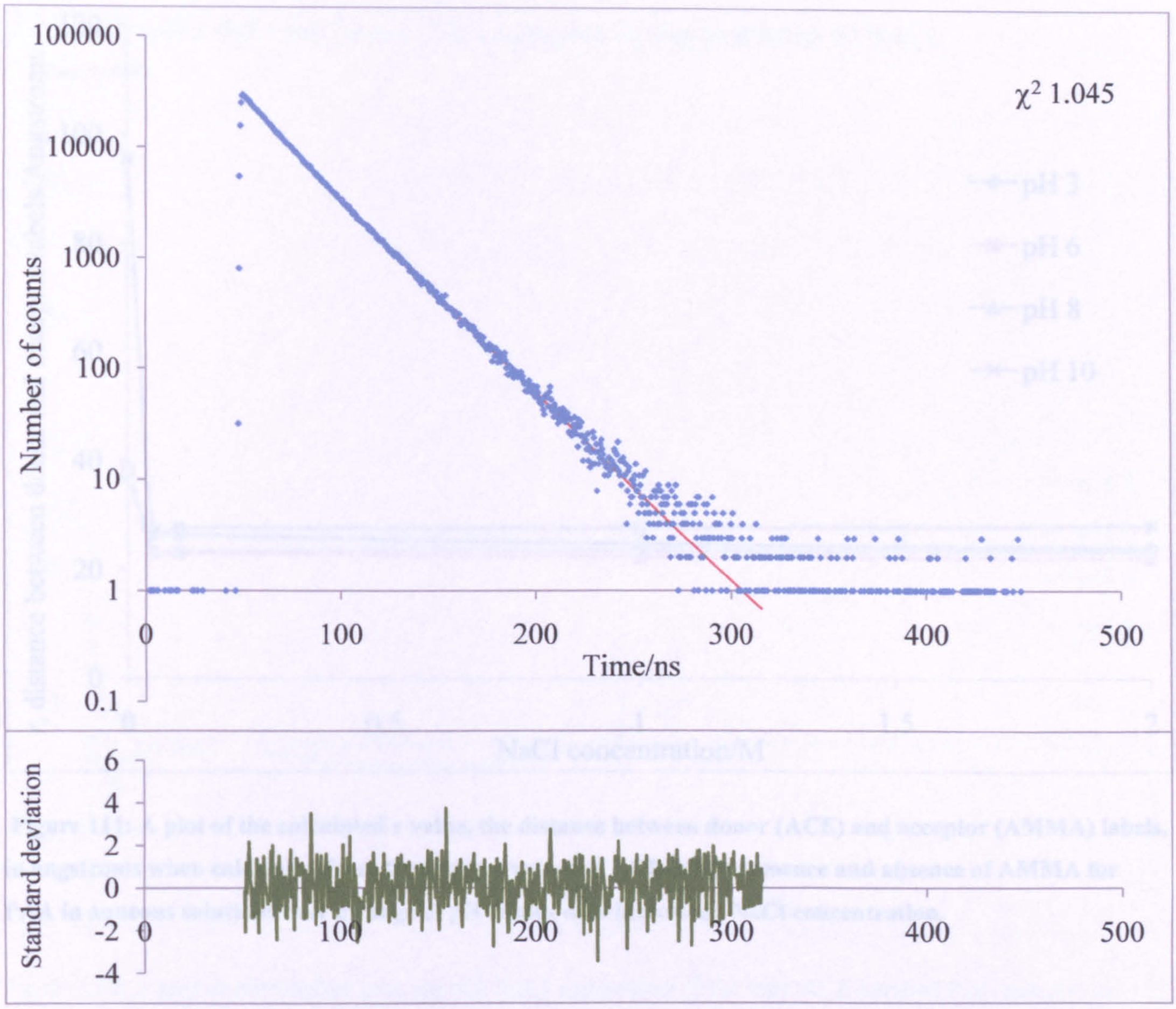

Figure 110: A fluorescence decay with corresponding mathematical fit (shown in red) and a plot of the resulting residuals for ACE-AMMA-PAA in aqueous solution of pH 10 with 2 M of NaCl.

With error taken in to account there is a substantial decrease in the distance between the ACE and AMMA labels upon initial addition of NaCl but then no further change in the label distance as the salt concentration increases further.

This indicates that the polymer contracts upon addition of a small amount of NaCl and to a similar degree no matter the pH value as all the label distances after addition of salt are similar.

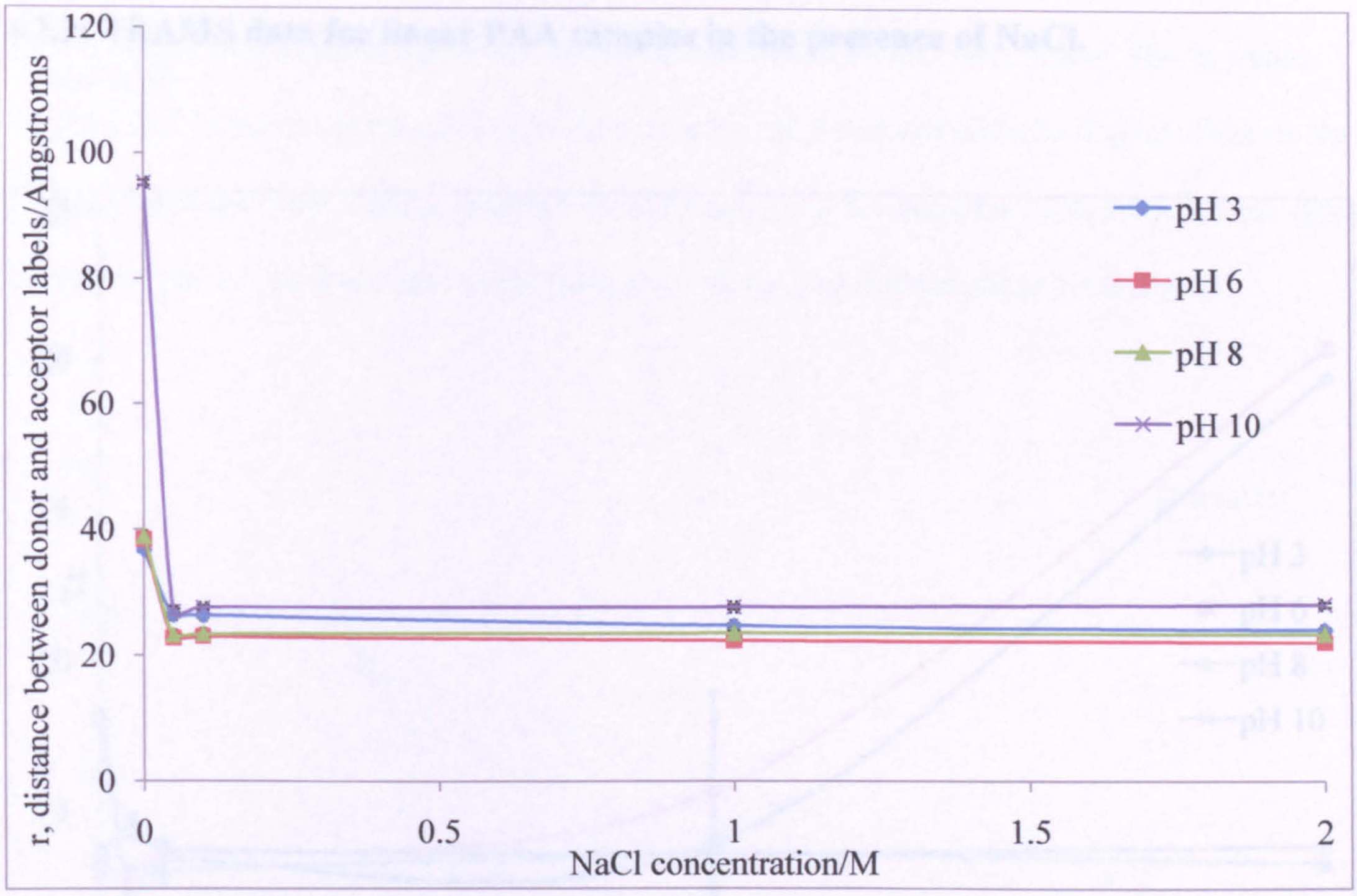

Figure 111: A plot of the calculated r value, the distance between donor (ACE) and acceptor (AMMA) labels, in angstroms when calculated from the lifetime values of ACE in the presence and absence of AMMA for PAA in aqueous solutions over a range of pH values with increasing NaCl concentration.

4.2.3: TRAMS data for linear PAA samples in the presence of NaCl.

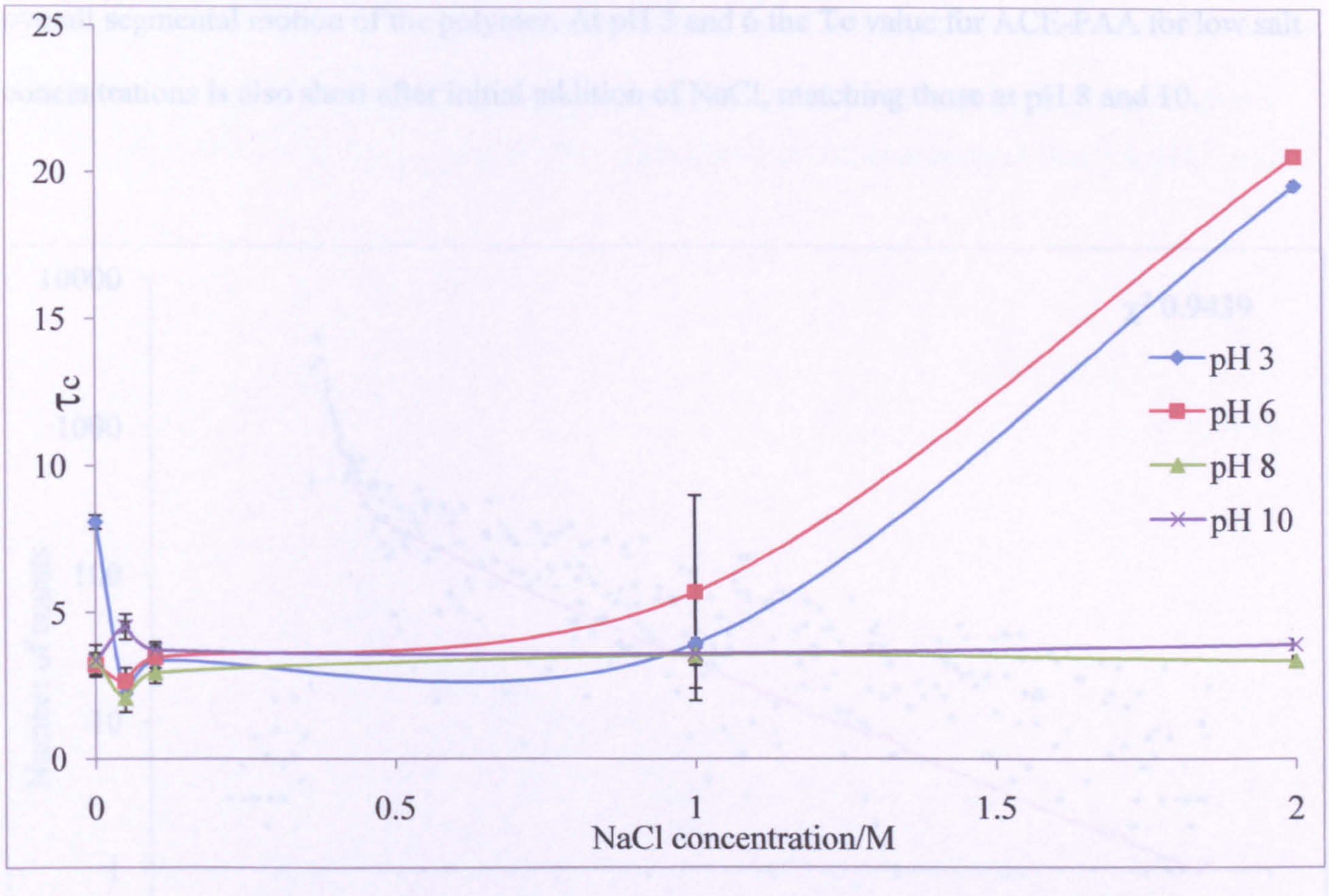

Figure 112: A plot of correlation time against NaCl concentration for four ACE labelled PAA samples in aqueous solution at four different pH values when excited at 290nm and observed at 340nm.

The TRAMS data for the ACE label PAA system across a range of pH values and NaCl concentrations were best fitted using a single exponential model via impulse reconvolution with r^{∞} left to vary. This provided the best fit with regards to small standard deviations relative to the τc value as well as χ^2 values closest to unity and random residuals as shown in figures 113 and 114.

The τc data were plotted in figure 112 as a function of both pH and salt content. The τc values for pH 8 and 10 appear to be constant with increasing NaCl concentration having no effect on the overall segmental motion of the polymer. At pH 3 and 6 the τc value for ACE-PAA for low salt concentrations is also short after initial addition of NaCl, matching those at pH 8 and 10.

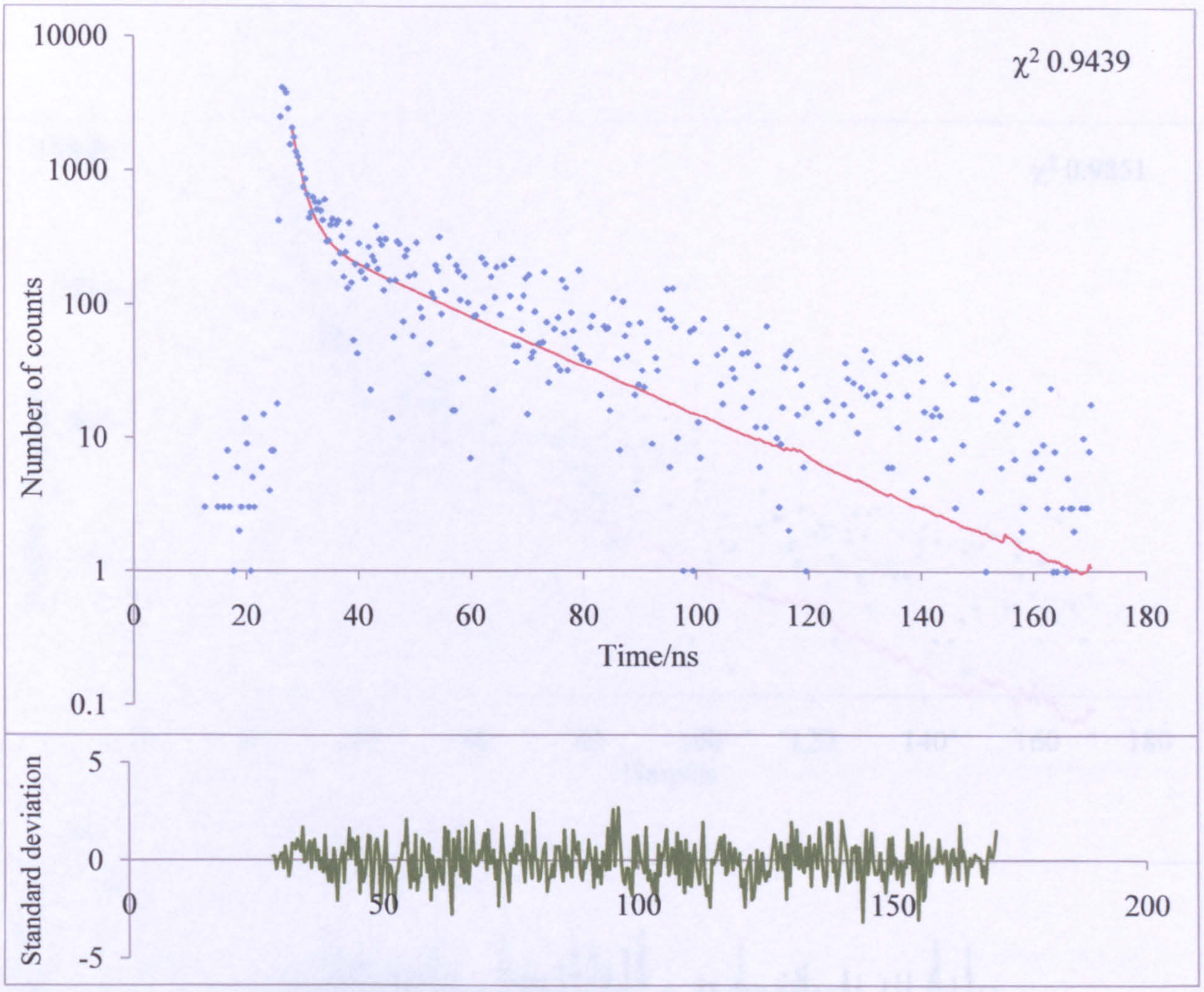

Figure 113: An impulse reconvolution fit to D(t) and a plot of the resulting residuals for ACE-PAA at pH 3 in aqueous solution with 0.05M NaCl.

Once the NaCl concentration of the PAA-ACE solution reaches a concentration of 1 M at pH 3 and 6 the τc value increases dramatically until a 2 M concentration of NaCl is reached. At all salt concentrations, the τc values for pH 6 are slightly greater than the τc values for pH 3 unlike for the polymer system in the absence of any salt. This indicates that the polymer undergoes a conformational collapse upon addition of a relatively large concentration of NaCl at pH 3 and 6.

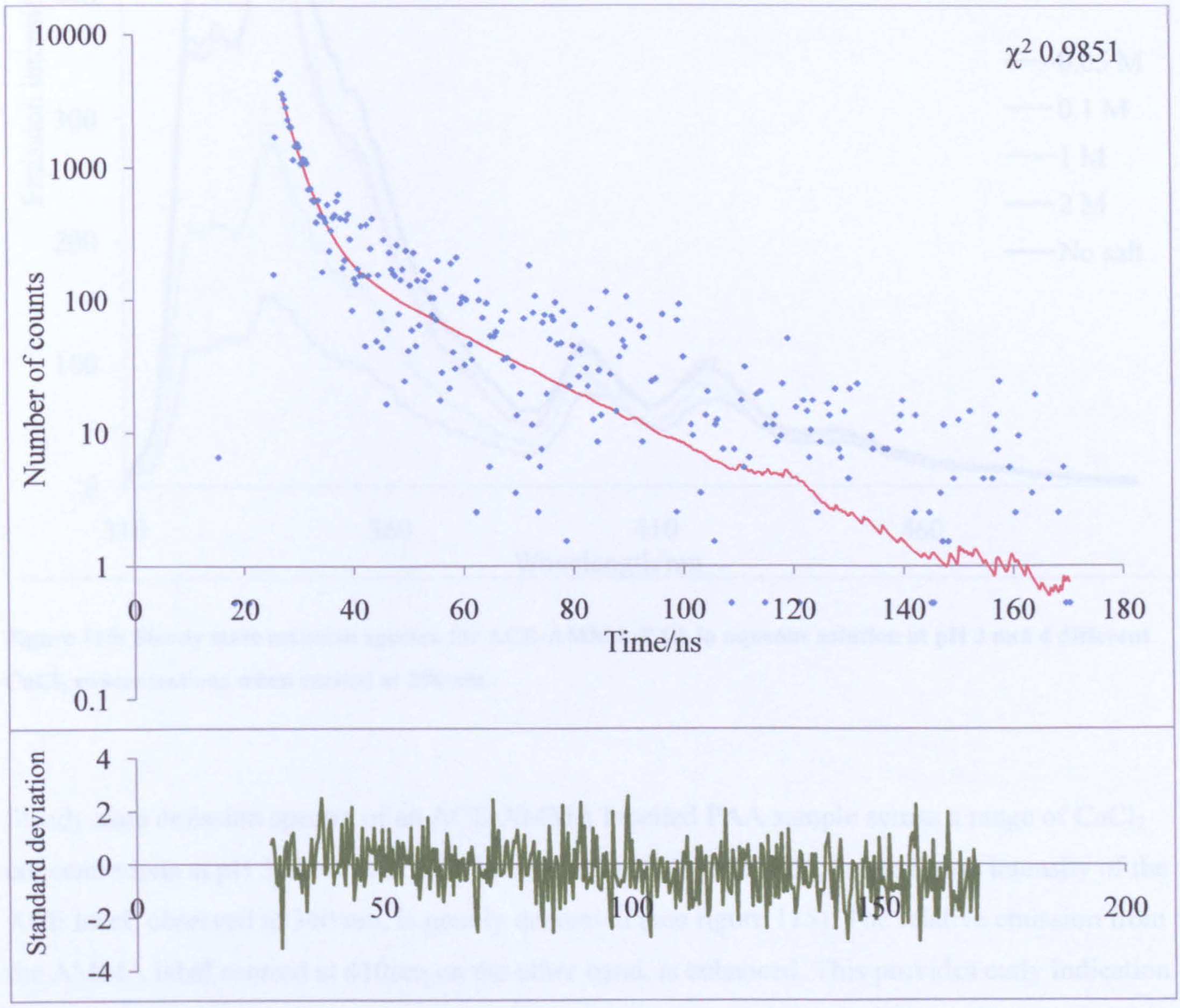

Figure 114: An impulse reconvolution fit to D(t) and a plot of the resulting residuals for ACE-PAA at pH 10 in aqueous solution with 2 M NaCl.

4.2.4: Steady state spectra of linear PAA in aqueous solution in the presence of $CaCl_2$.

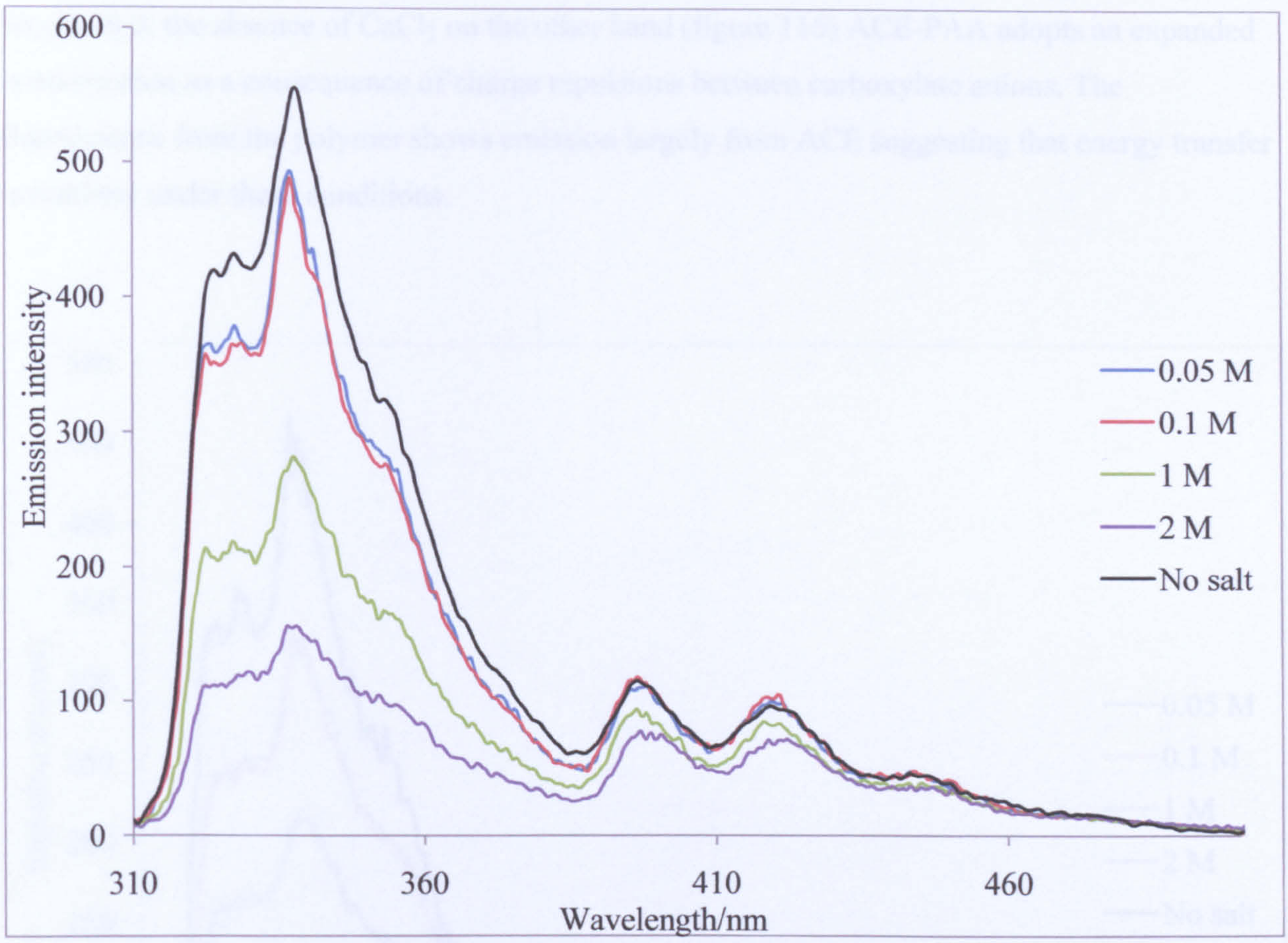

Figure 115: Steady state emission spectra for ACE-AMMA-PAA in aqueous solution at pH 3 and 4 different $CaCl_2$ concentrations when excited at 290 nm.

Steady state emission spectra of an ACE-AMMA labelled PAA sample across a range of $CaCl_2$ concentrations at pH 3 show that, with increasing salt concentration, the emission intensity of the ACE label, observed at 340 nm, is greatly decreased (see figure 115). The relative emission from the AMMA label centred at 410nm on the other hand, is enhanced. This provides early indication of the existence of energy transfer from ACE to AMMA under these conditions. Even in the

absence of $CaCl_2$ a degree of energy transfer is apparent which is consistent with a partially collapsed polymer conformation at low pH.

At pH 10 in the absence of $CaCl_2$ on the other hand (figure 116) ACE-PAA adopts an expanded conformation as a consequence of charge repulsions between carboxylate anions. The fluorescence from the polymer shows emission largely from ACE suggesting that energy transfer is minimal under these conditions.

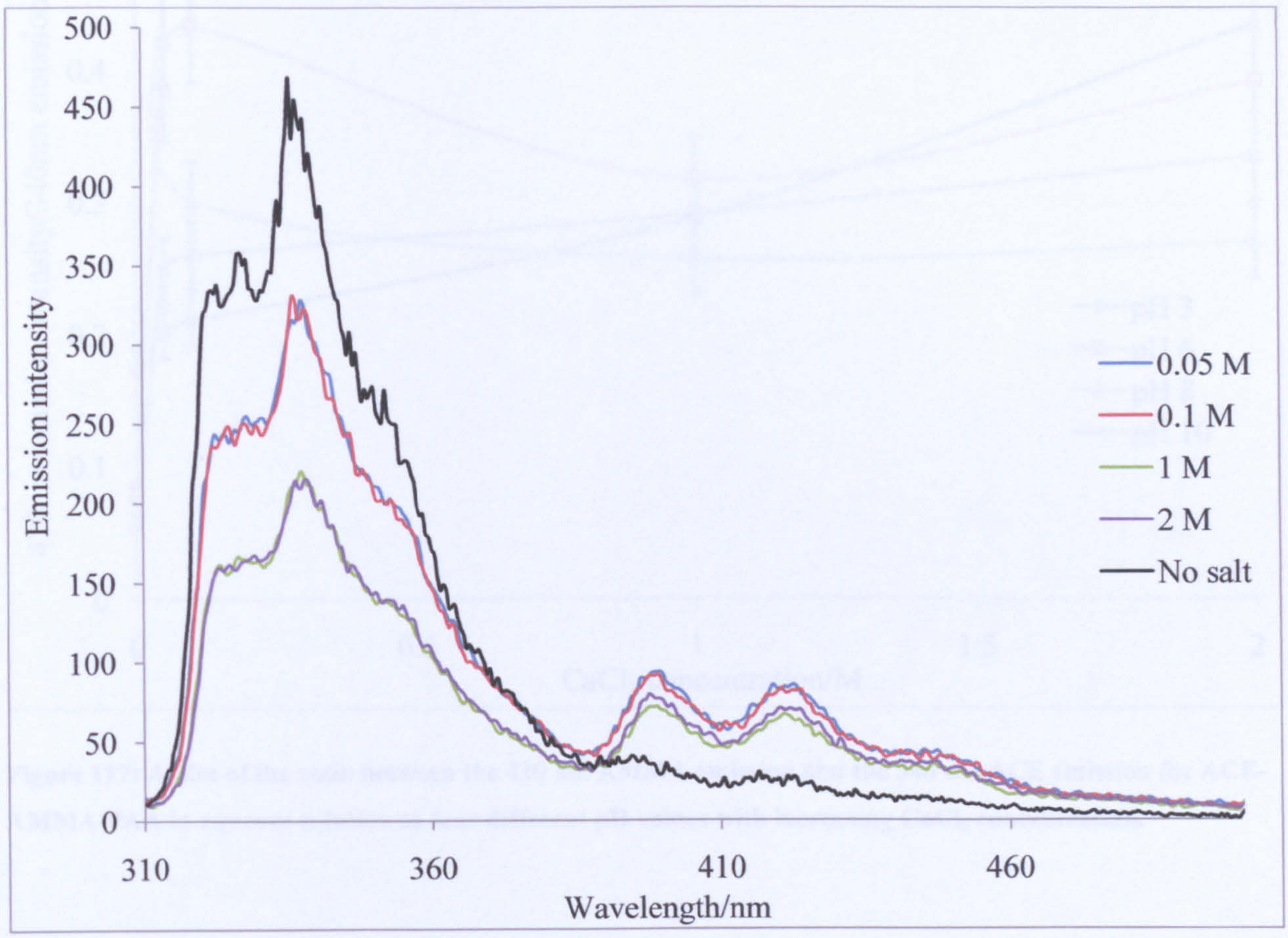

Figure 116: Steady state emission spectra on ACE-AMMA-PAA in aqueous solution at pH 10 with increasing $CaCl_2$ concentration when excited at 290 nm.

Addition of increasing concentrations of $CaCl_2$ serves to reduce the naphthyl emission with a corresponding increase in anthryl fluorescence presumably the Ca^{2+} ions complex to the carboxylate anions, collapsing the polymer chain and increasing the degree of energy transfer in the process.

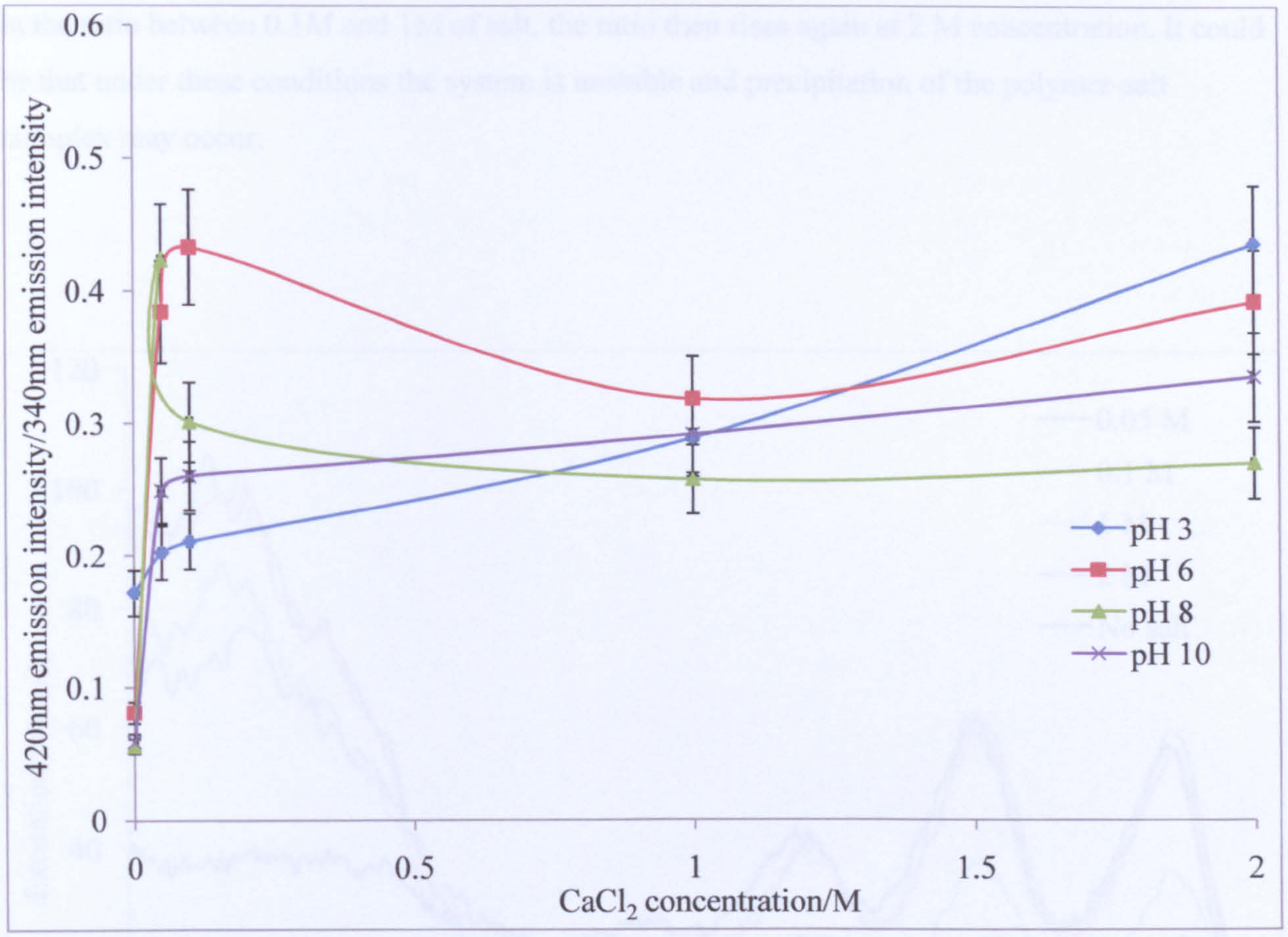

Figure 117: A plot of the ratio between the 420 nm AMMA emission and the 340 nm ACE emission for ACE-AMMA-PAA in aqueous solution at four different pH values with increasing $CaCl_2$ concentration.

The ratio between the emission intensities of the AMMA label (at 420 nm) and ACE label (at 340 nm) were calculated in the presence of $CaCl_2$. The resultant data was plotted as a function of $CaCl_2$ concentration in figure 117. There is a general increase in the ratio irrespective of pH

with increasing concentrations of Ca^{2+}. This is consistent with formation of a collapse PAA conformation.

For pH values of 3 and 10 respectively there is a further increase in the ratio and the degree of coiling, with increasing salt concentration. For pH values of 6 and 8 however there is a decrease in the ratio between 0.1M and 1M of salt, the ratio then rises again at 2 M concentration. It could be that under these conditions the system is unstable and precipitation of the polymer-salt complex may occur.

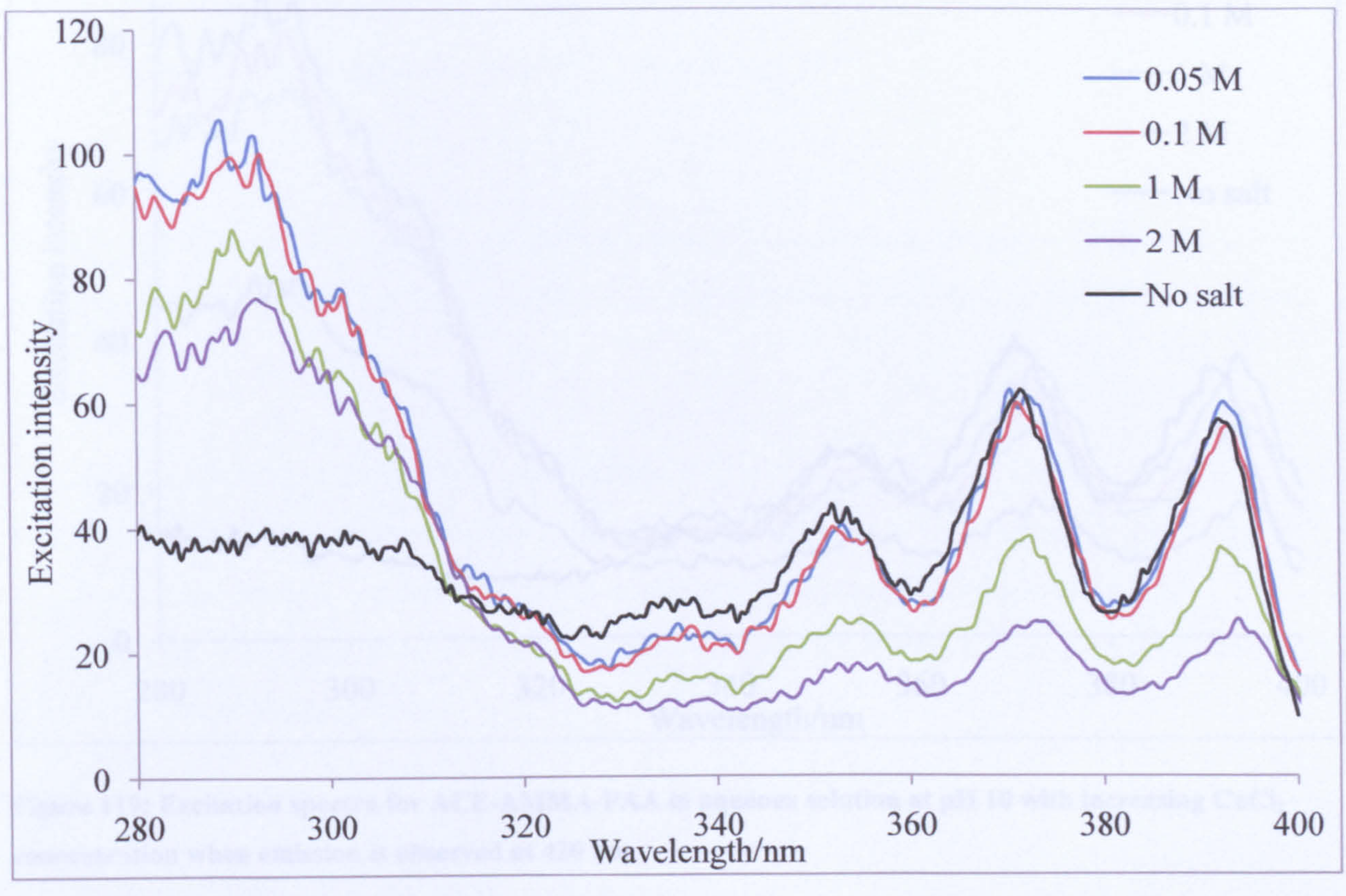

Figure 118: Excitation spectra of ACE-AMMA-PAA in aqueous solution at pH 3 with increasing $CaCl_2$ concentration when observed at 420 nm.

The excitation spectrum for ACE-AMMA-PAA at pH 3, shown in figure 98, provides further evidence for the existence of energy transfer. When the emission is analysed at 420nm in the absence of salt the excitation spectrum is characteristic of that of AMMA with little or no contribution from ACE. Increasing the $CaCl_2$ concentration results in a significant intensity centred at 290 nm which reflects energy transfer from ACE to AMMA. Clearly under these conditions the donor and acceptor are within the critical transfer distance and the ACE consequently makes an appreciable contribution to the emission samples in the anthryl region of the spectrum.

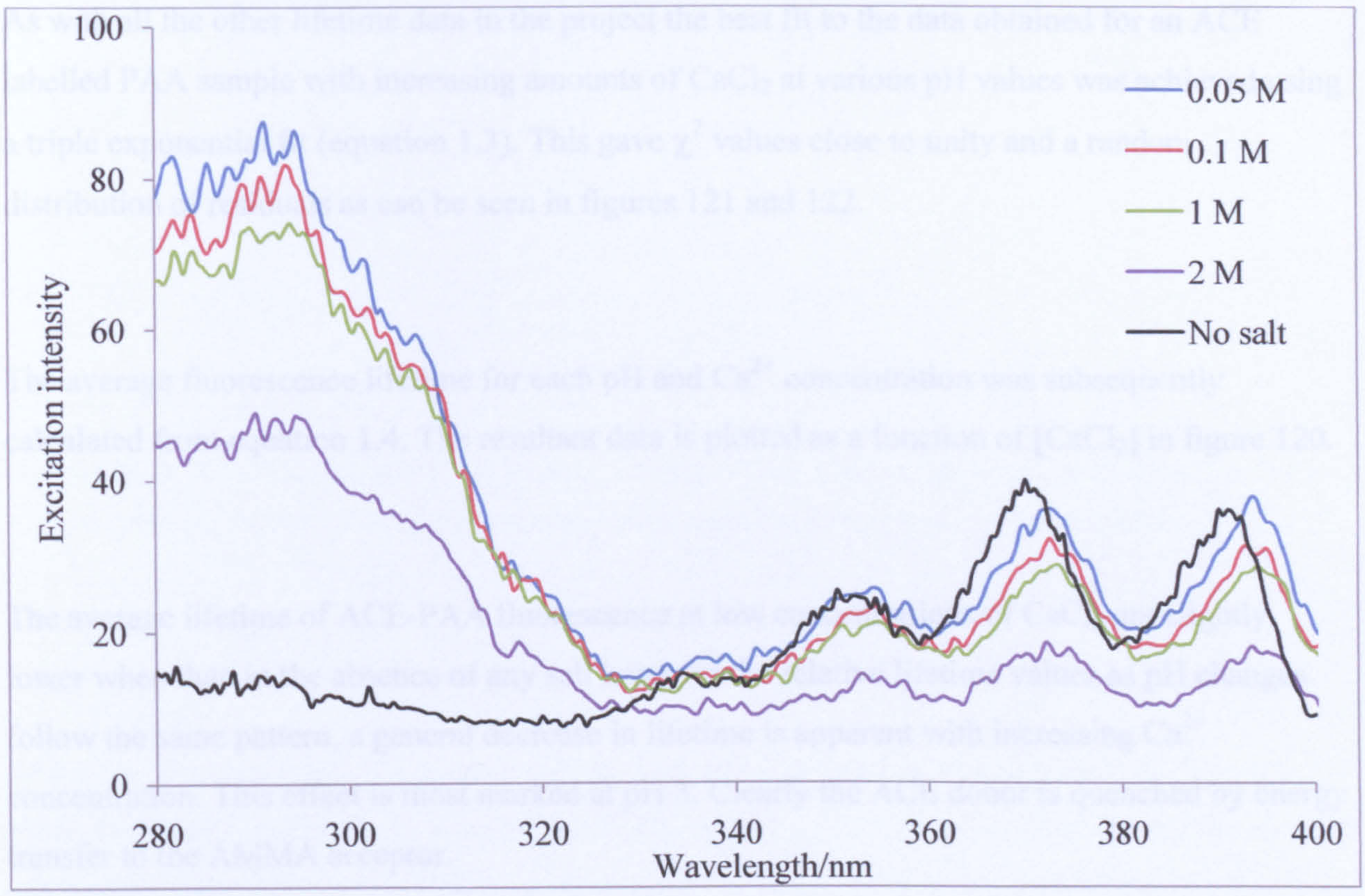

Figure 119: Excitation spectra for ACE-AMMA-PAA in aqueous solution at pH 10 with increasing $CaCl_2$ concentration when emission is observed at 420 nm.

At pH 10 (figure 119) this effect is slightly more pronounced, increasing the Ca^{2+} concentration results in significant ACE contribution at 290nm to the emission samples at 420 nm. Clearly

energy transfer is more efficient at high pH which is consistent with collapse of the negatively charged polymer in the presence of a positive cation.

4.2.5: Fluorescence lifetime measurements of linear PAA in aqueous solution in the presence of $CaCl_2$.

As with all the other lifetime data in the project the best fit to the data obtained for an ACE labelled PAA sample with increasing amounts of $CaCl_2$ at various pH values was achieved using a triple exponential fit (equation 1.3). This gave χ^2 values close to unity and a random distribution of residuals as can be seen in figures 121 and 122.

The average fluorescence lifetime for each pH and Ca^{2+} concentration was subsequently calculated from equation 1.4. The resultant data is plotted as a function of [$CaCl_2$] in figure 120.

The average lifetime of ACE-PAA fluorescence at low concentrations of $CaCl_2$ are slightly lower when than in the absence of any salt however the relative lifetime values as pH changes follow the same pattern, a general decrease in lifetime is apparent with increasing Ca^{2+} concentration. This effect is most marked at pH 3. Clearly the ACE donor is quenched by energy transfer to the AMMA acceptor.

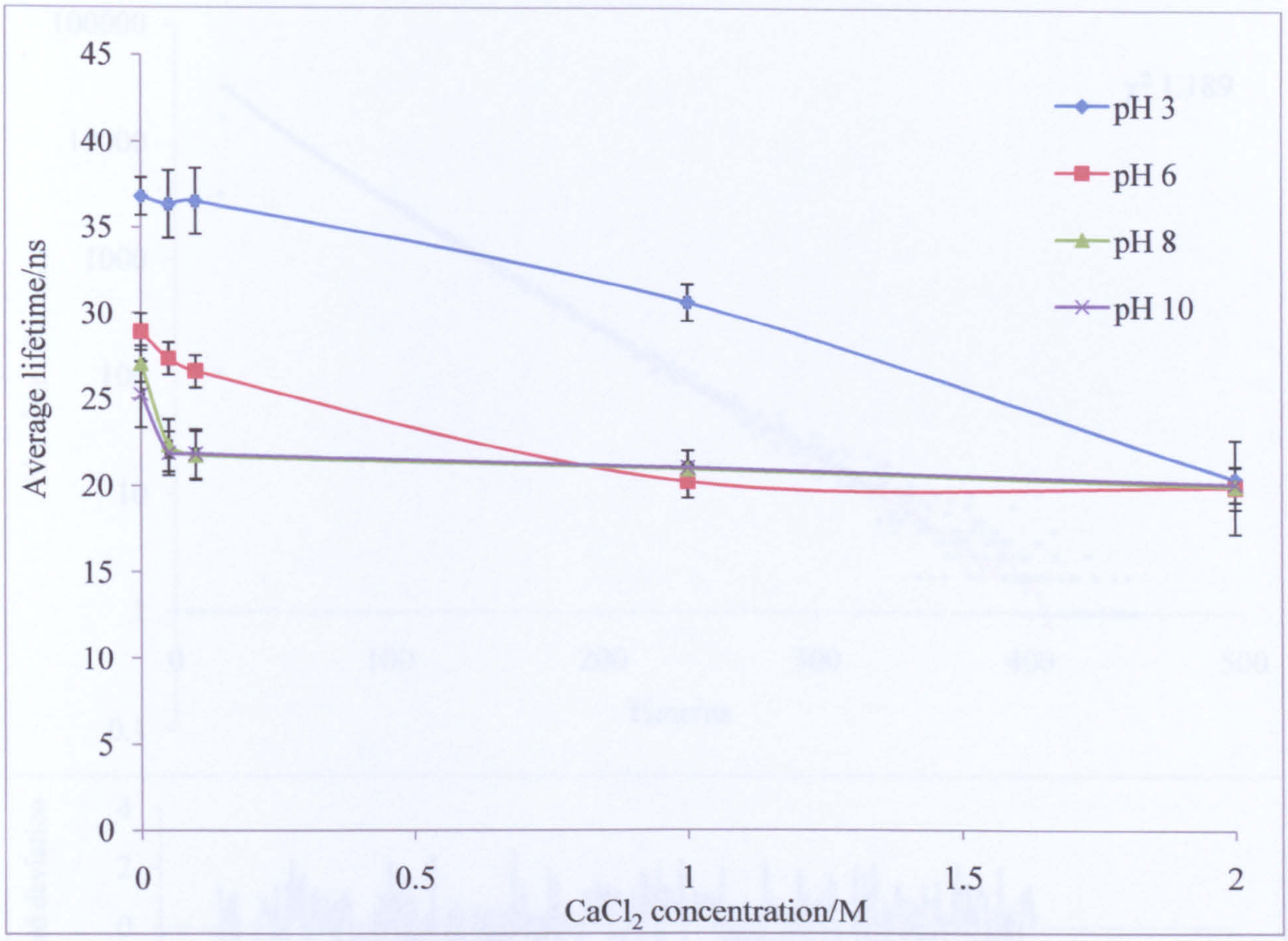

Figure 120: A plot of the average lifetime values obtained at four different pH values with increasing $CaCl_2$ concentration for ACE-PAA in aqueous solution when excited at 290nm and observed at 340nm.

At $CaCl_2$ concentrations of 1 M and a pH of 6 the lifetime value is similar to that of the open PAA coil as see at pH $\geq$ 8. At even higher $CaCl_2$ concentration, (ie 2 M), the lifetime observed at pH 3 reaches the same value. This is a clear indication that addition of $CaCl_2$ to the PAA-ACE system increases the quenching of the label thus decreasing the lifetime as a collapsed conformation is adopted.

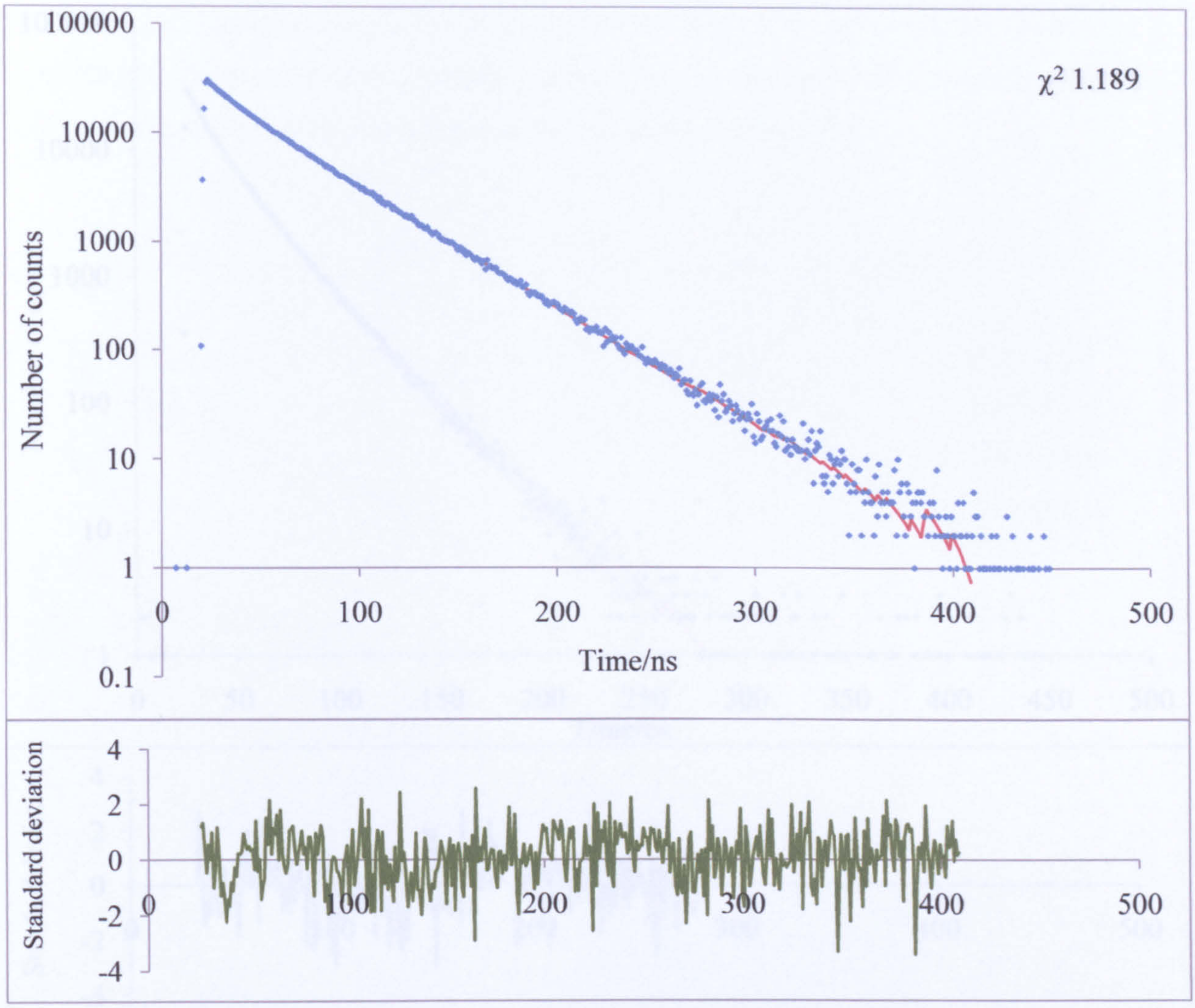

Figure 121: A fluorescence decay with corresponding mathematical fit (shown in red) and a plot of the resulting residuals for ACE-PAA in aqueous solution of pH 3 with 0.05M of $CaCl_2$.

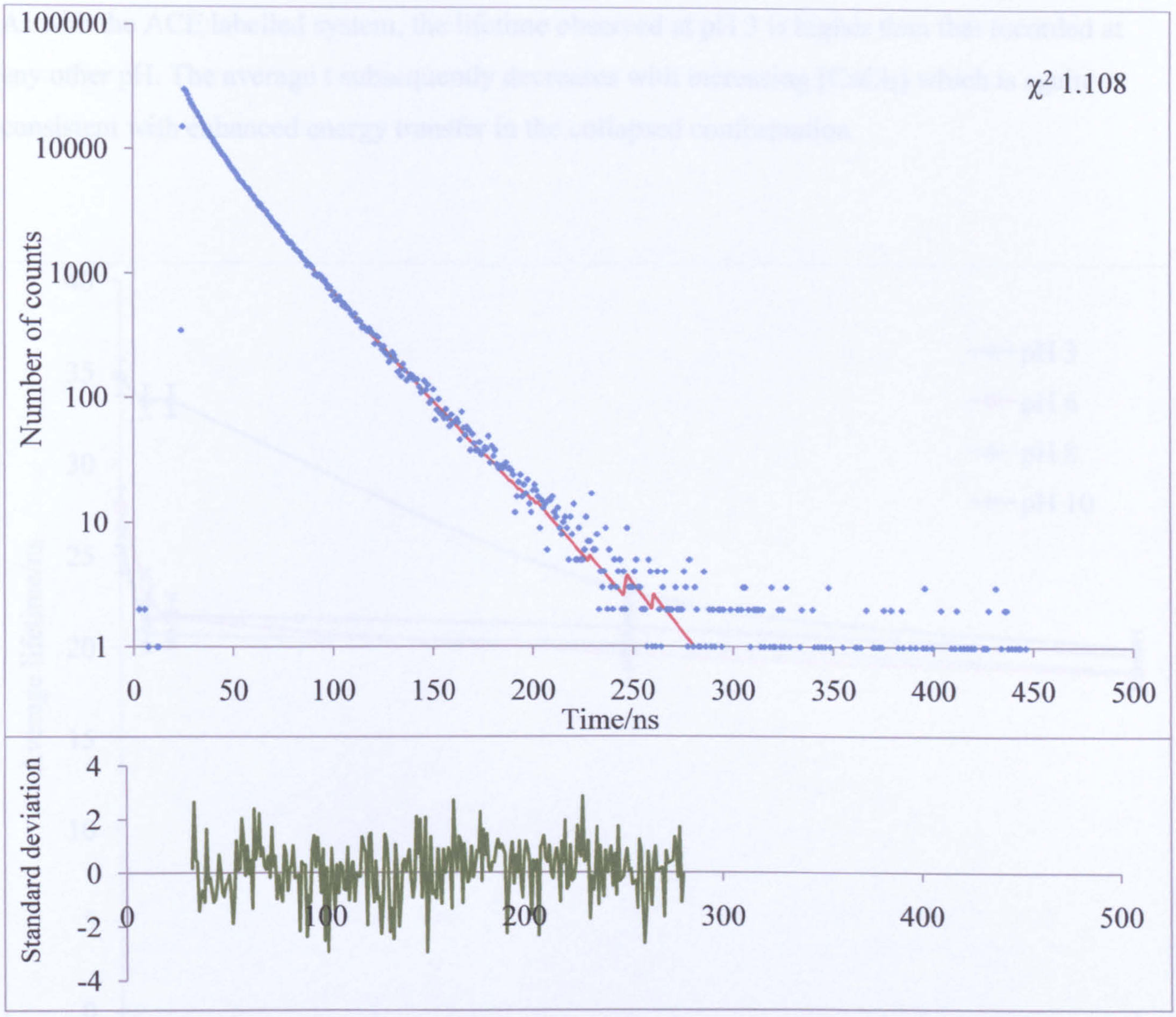

Figure 122: A fluorescence decay with corresponding mathematical fit (shown in red) and a plot of the resulting residuals for ACE-PDMAEMA in aqueous solution at pH 10 with 2 M of $CaCl_2$.

The lifetime of the ACE label in PAA-ACE-AMMA in the presence of $CaCl_2$ is different to that of the PAA-ACE system. Notably the lifetime at low $CaCl_2$ concentrations at pH 6 is similar to that at pH 8 and 10 respectively. As before a general decrease in lifetime is apparent, which is consistent with increased quenching as the collapsed conformation is adopted.

As with the ACE labelled system, the lifetime observed at pH 3 is higher than that recorded at any other pH. The average t subsequently decreases with increasing [$CaCl_2$] which is again consistent with enhanced energy transfer in the collapsed conformation

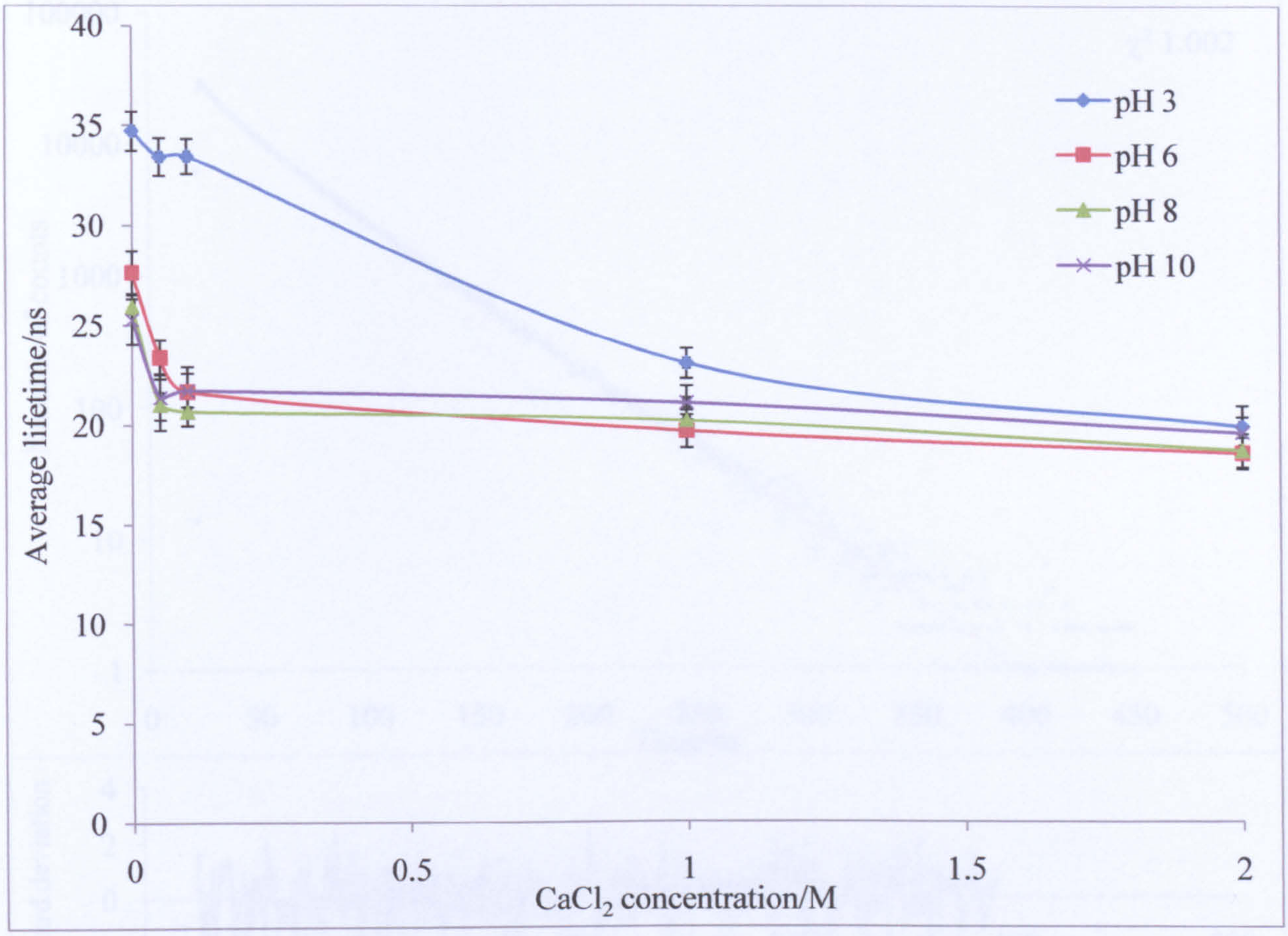

Figure 123: A plot of the average lifetimes values obtained for ACE-AMMA-PAA in aqueous solution at four different pH values with increasing $CaCl_2$ concentration when excited at 290 nm and observed at 340 nm.

The average separation distance, r, between D and A was calculated using equation 1.4 from the lifetime data shown in figures 119 and 122 are rather complex, this data is shown in figure 125.

At high and low concentrations of $CaCl_2$ the inter label distance seems to be similar at all pH values with that of pH 10 being generally the higher of the four. All pH values show an initial decrease in the distance between labels.

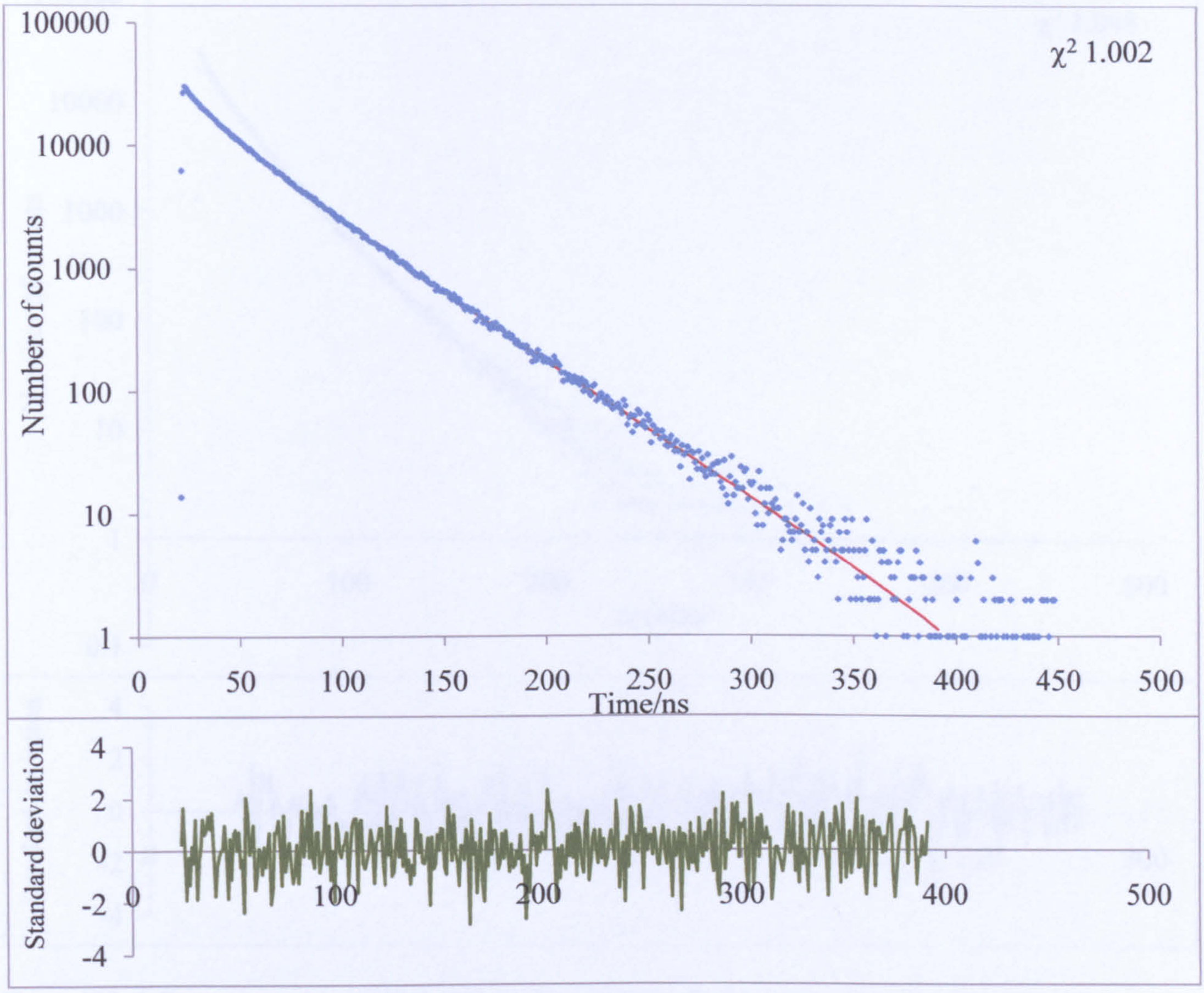

Figure 123: A fluorescence decay with corresponding mathematical fit (shown in red) and a plot of the resulting residuals for ACE-AMMA-PAA in aqueous solution of pH 3 with 0.05M of $CaCl_2$.

At the intermediate pH values of 6 and 8 there is little change in the distance between the donor and acceptor across the entire concentration range of $CaCl_2$. However the data collected at pH 6

does show a further increase in distance between labels; which is consistent with a slight expansion of the polymer chain.

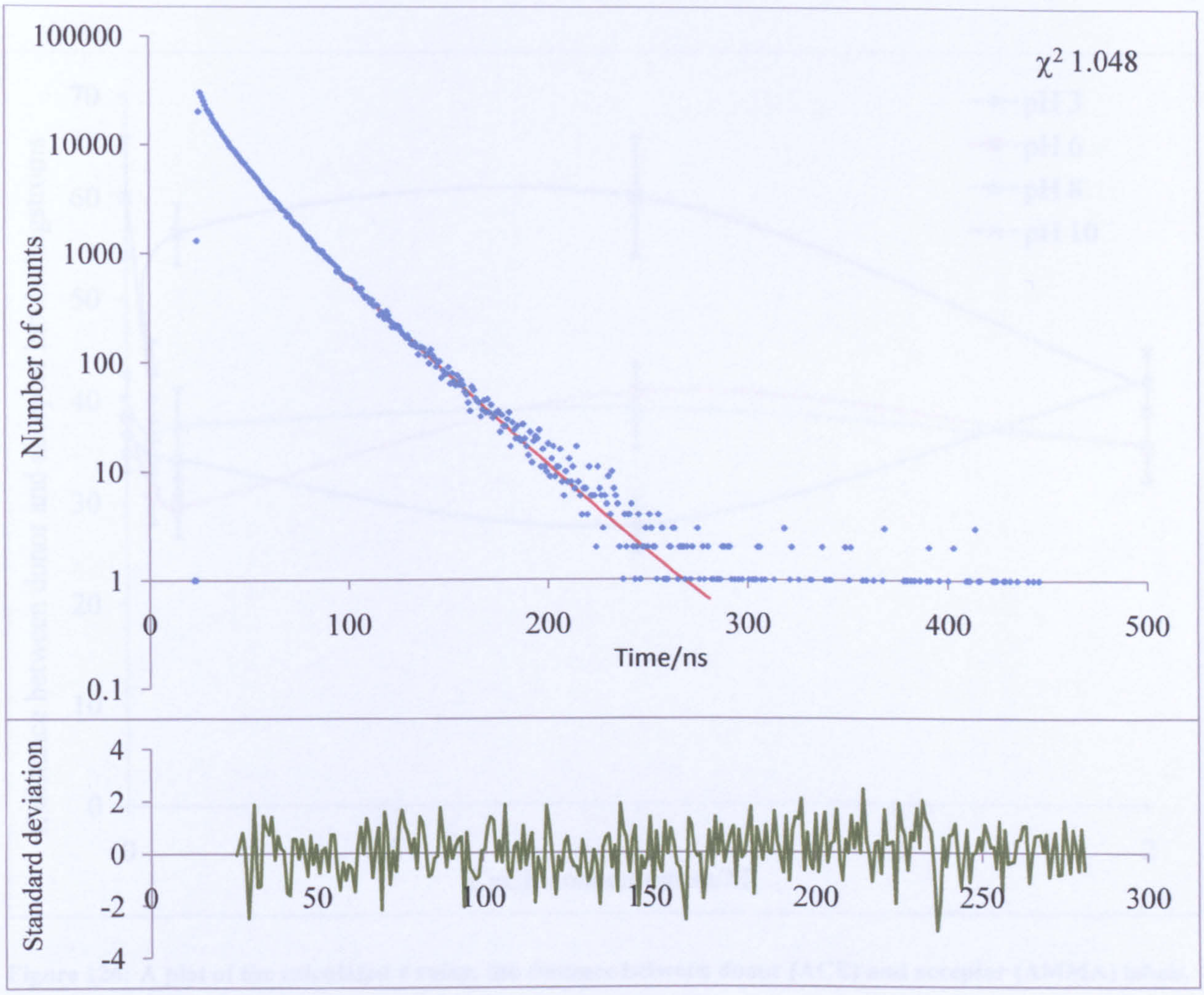

Figure 125: A fluorescence decay with corresponding mathematical fit (shown in red) and a plot of the resulting residuals for ACE-AMMA-PAA in aqueous solution of pH 10 with 2 M of $CaCl_2$.

The distance, r, at pH 3 however shows a decrease between 0.1 M and 1 M concentrations indicating a collapse in the system, the distance then rises once more as the concentration increases to 2 M.

The distance between the ACE and the AMMA labels at pH 10 shows a marked increase with rising $CaCl_2$ concentrations up to 1 M after the initial decrease and then a significant decrease in

the inter label distance can be seen as the concentration increases further to 2 M. Clearly collapse of the chain has occurred under these conditions as the carboxylate anion charge is screen by the Ca^{2+} cation indicating collapse as a consequence of increased degree of hydrophobic attraction.

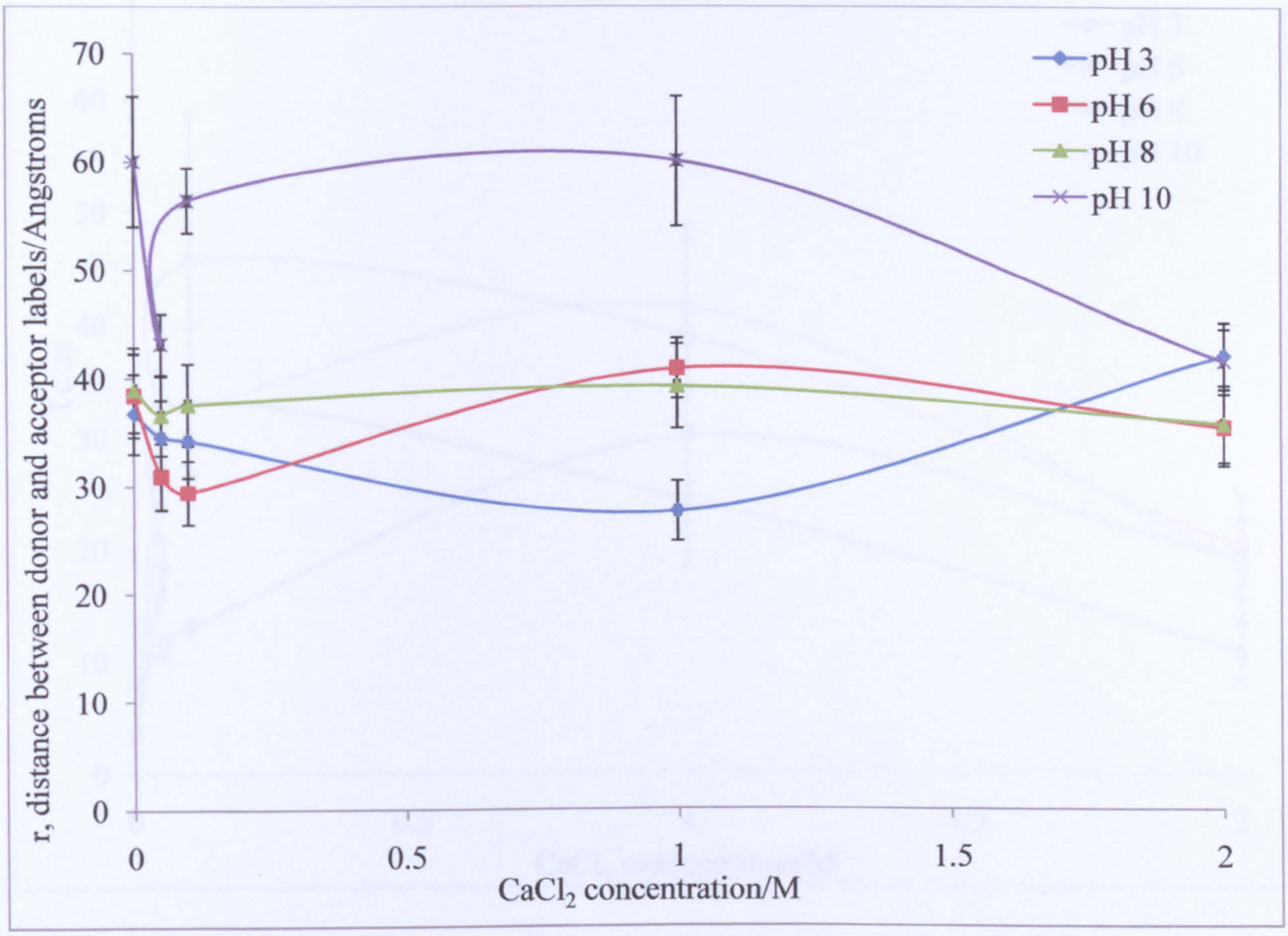

Figure 126: A plot of the calculated r value, the distance between donor (ACE) and acceptor (AMMA) labels, in angstroms when calculated from the lifetime values of ACE in the presence and absence of AMMA for PAA systems in aqueous solutions across range of $CaCl_2$ concentrations at four difference pH values.

4.2.6: Time Resolved Anisotropy Measurements on linear PAA in aqueous solution in the presence of $CaCl_2$.

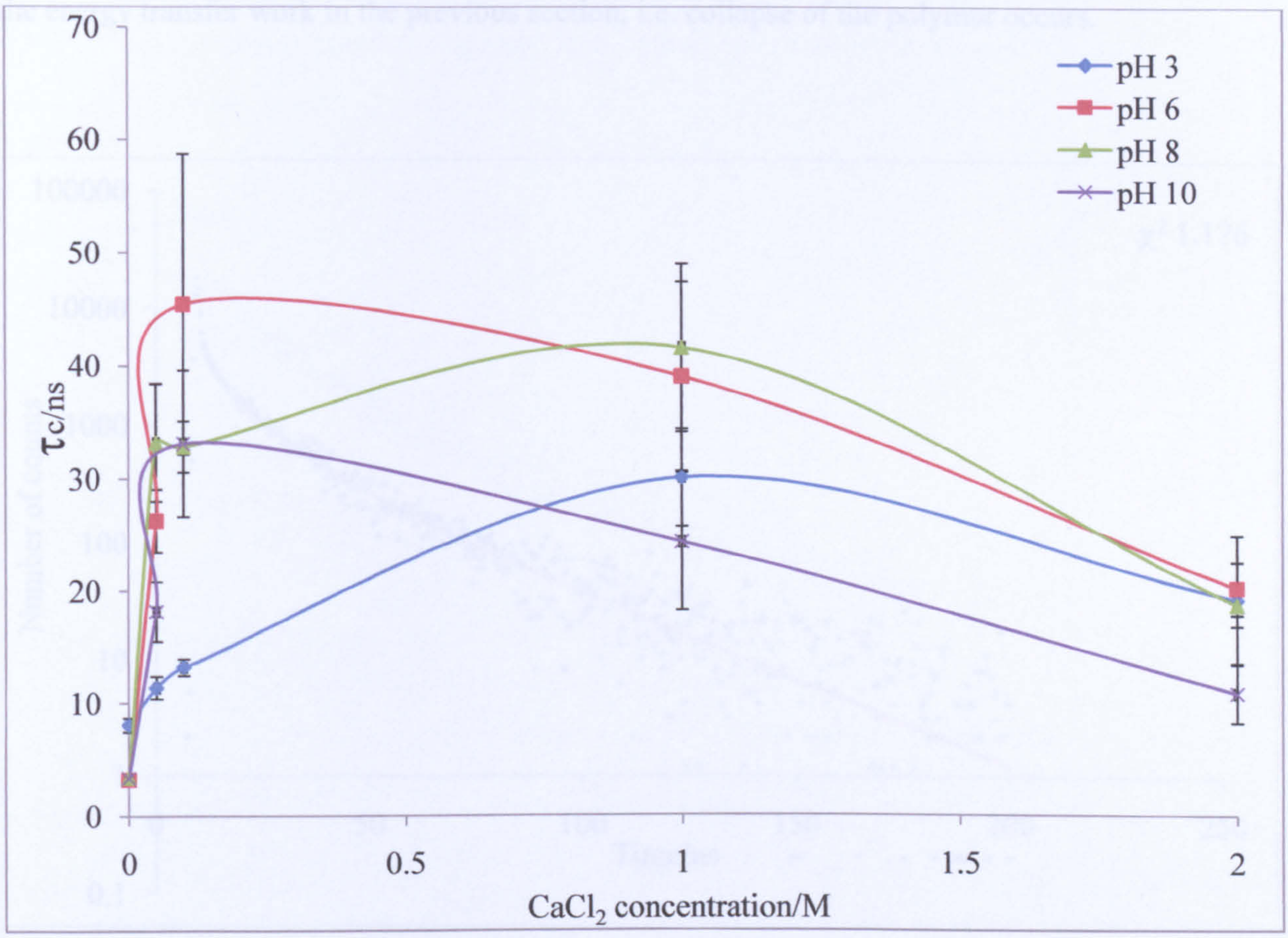

Figure 127: A plot of the τc values obtained for ACE-PAA in aqueous solution over a range of $CaCl_2$ concentrations at four different pH values.

TRAMS were conducted on ACE-PAA with increasing [$CaCl_2$] at various pH values in order to study the polymer dynamics. The best statistical fits to TRAMS data for ACE- PAA irrespective of solution condition was achieved using a single exponential fit via impulse reconvolution methods Figures 128 and 129 show example data sets: Clearly the residuals are randomly distributed around zero with a χ^2 close unity which provides statistical confidence in the quality of the fit.

The resultant τc data are plotted as a function of [$CaCl_2$] at several pH values in figure 107. In general there is an initial increase in τc upon addition of low concentrations of $CaCl_2$ (<0.5 M). This suggests that mobility of the label is reduced which is consistent with the findings of the of the energy transfer work in the previous section, i.e. collapse of the polymer occurs.

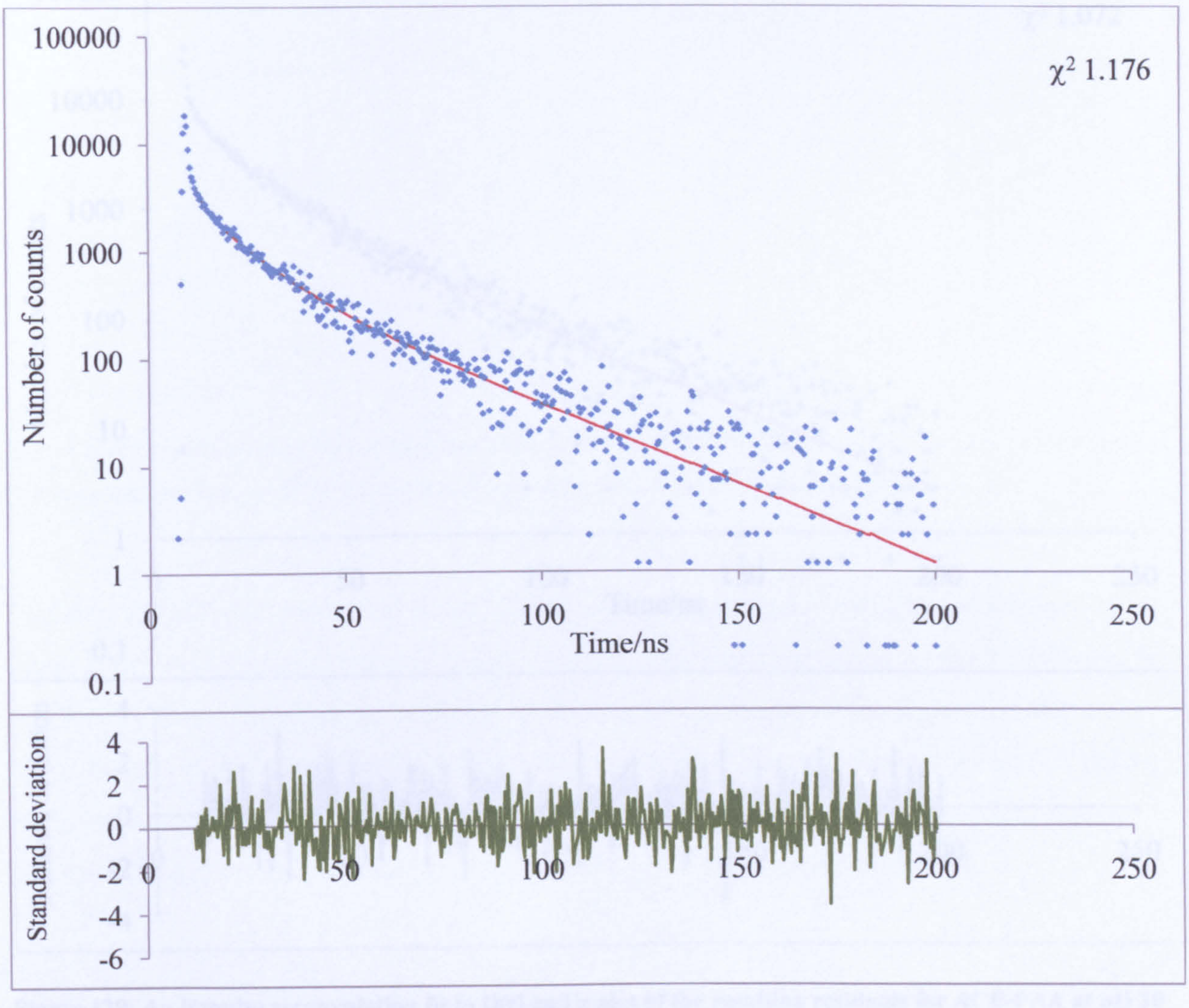

Figure 128: An impulse reconvolution fit to D(t) and a plot of the resulting residuals for ACE-PAA at pH 3 in aqueous solution with 0.05M $CaCl_2$.

The effect is more marked at higher pH values which suggests that complexation between the Ca^{2+} and carboxylate anions is more efficient. Upon further addition of Ca2+ (>1 M) there is a general decrease in τc irrespective of pH. This may indicate instability of the system and is in agreement with the observations from energy transfer: it could be that precipitation of the ACE-PAA/Ca^{2+} dispersion occurs leaving only 'free' uncomplexed polymer in solution.

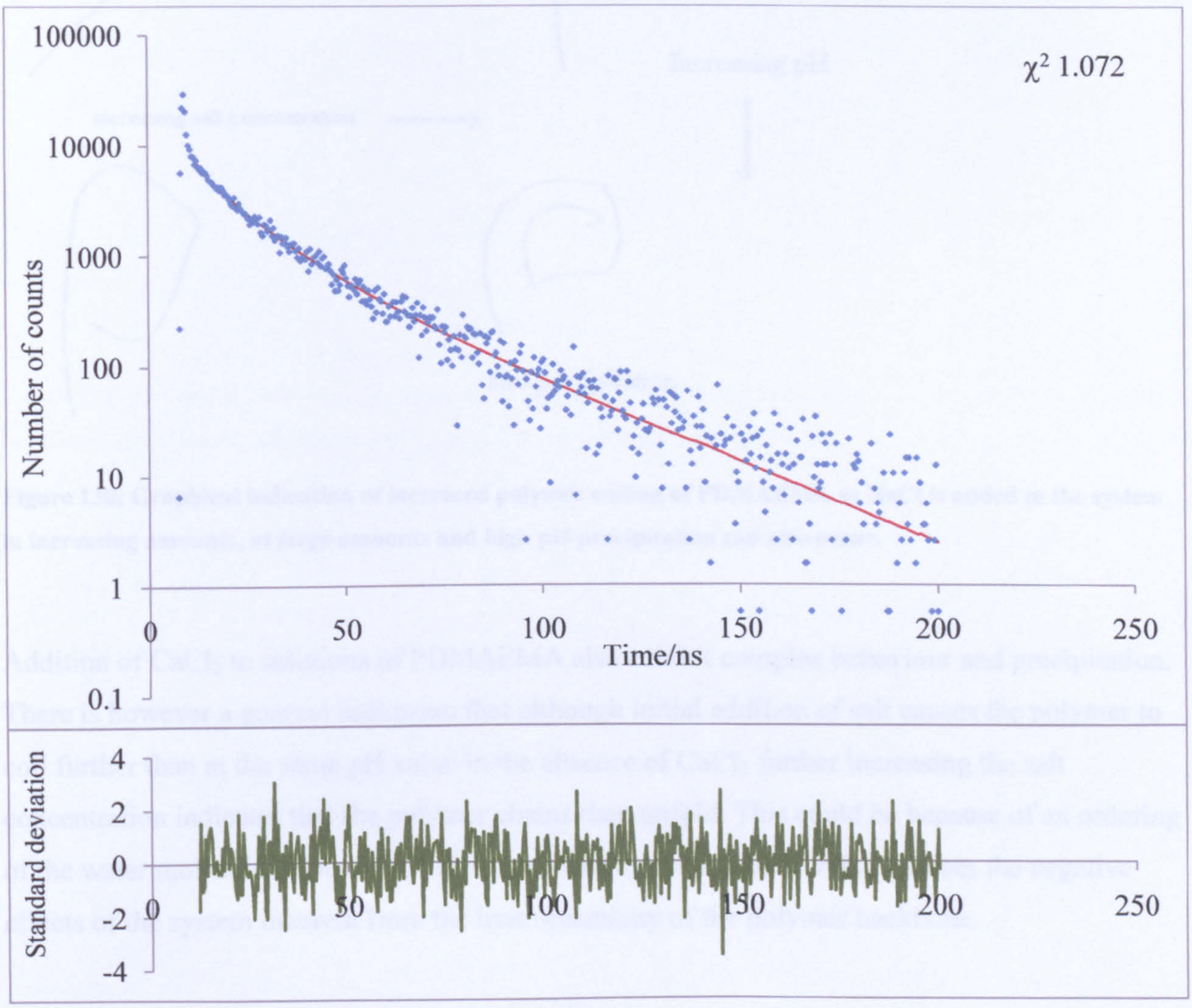

Figure 129: An impulse reconvolution fit to D(t) and a plot of the resulting residuals for ACE-PAA at pH 10 in aqueous solution with 2 M $CaCl_2$.

In summary; Addition of NaCl to solutions of PDMAEMA causes complex behaviour of the polymer systems with a general trend such that increasing salt concentrations causes the polymer

to collapse no matter the pH value of the system. At particularly high NaCl concentrations, and most especially at high pH values the polymer solution is unstable and precipitation can occur.

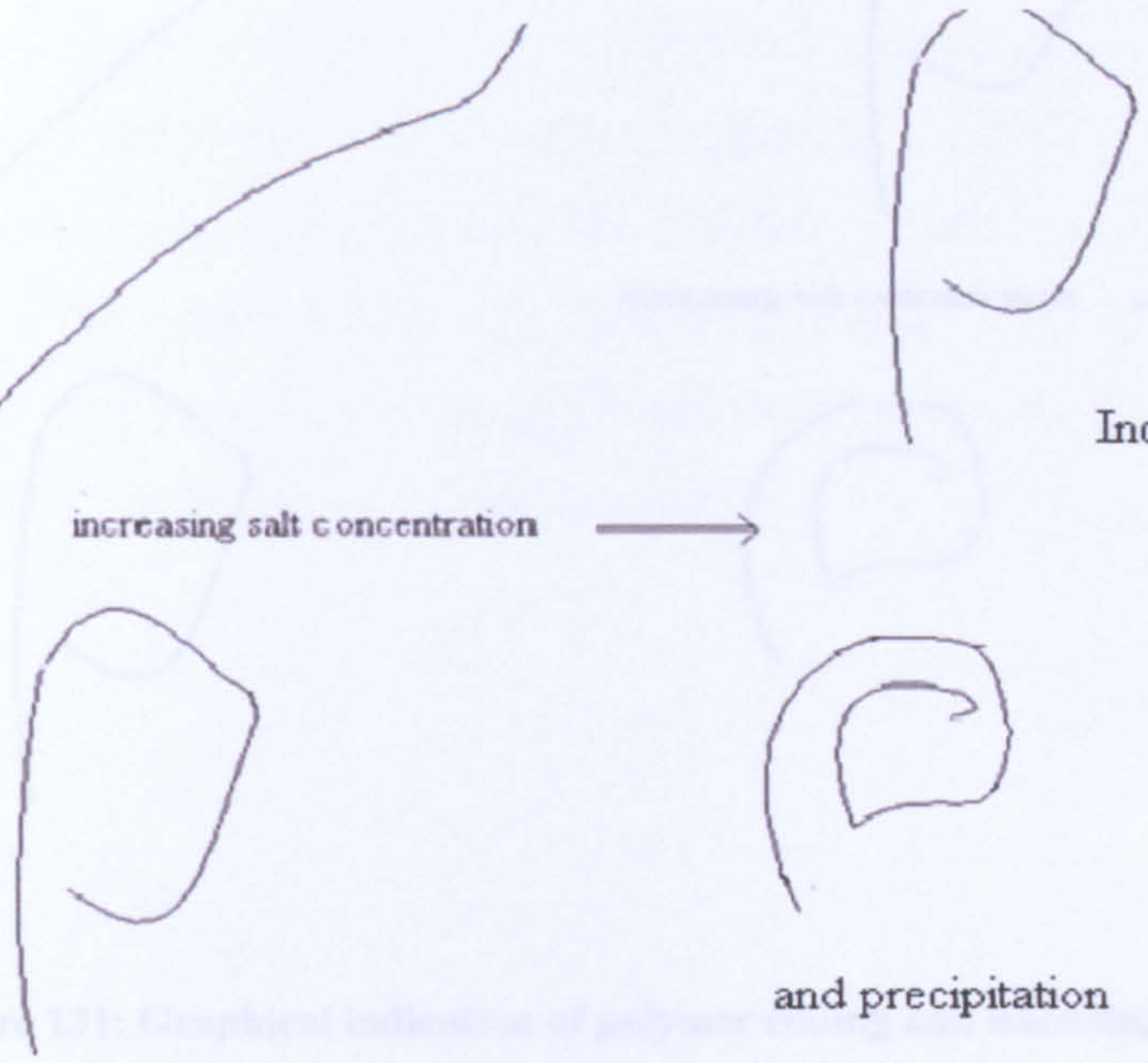

Figure 130: Graphical indication of increased polymer coiling of PDMAEMA as NaCl is added to the system in increasing amounts, at large amounts and high pH precipitation can also occur.

Addition of $CaCl_2$ to solutions of PDMAEMA also exhibit complex behaviour and precipitation. There is however a general indication that although initial addition of salt causes the polymer to coil further than at the same pH value in the absence of $CaCl_2$ further increasing the salt concentration indicates that the polymer chains then unfold. This could be because of an ordering of the water molecules around the polymer chains by the salt ions which reduces the negative effects of the system inherent from the hydrophobicity of the polymer backbone.

Addition of NaCl to solutions of PAA indicates that addition of salt causes the polymer chains to collapse at all pH values. At particularly low pH values and high salt concentrations the situation appears complex as the polymer solution can become unstable and precipitation can occur.

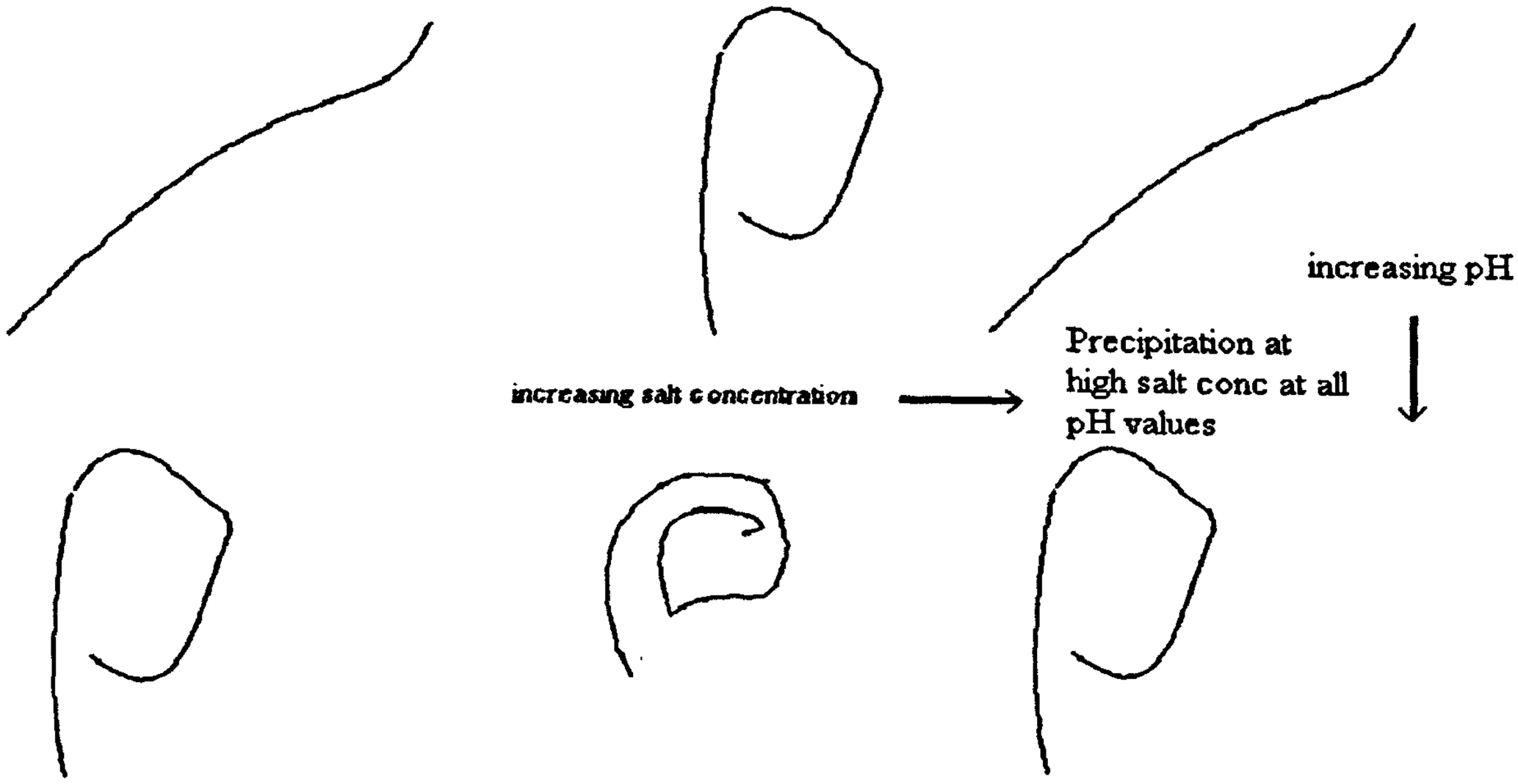

Figure 131: Graphical indication of polymer coiling and uncoiling as $CaCl_2$ is added to PDMAEMA solutions in increasing amounts, at large amounts of CaCl2 precipitation can also occur.

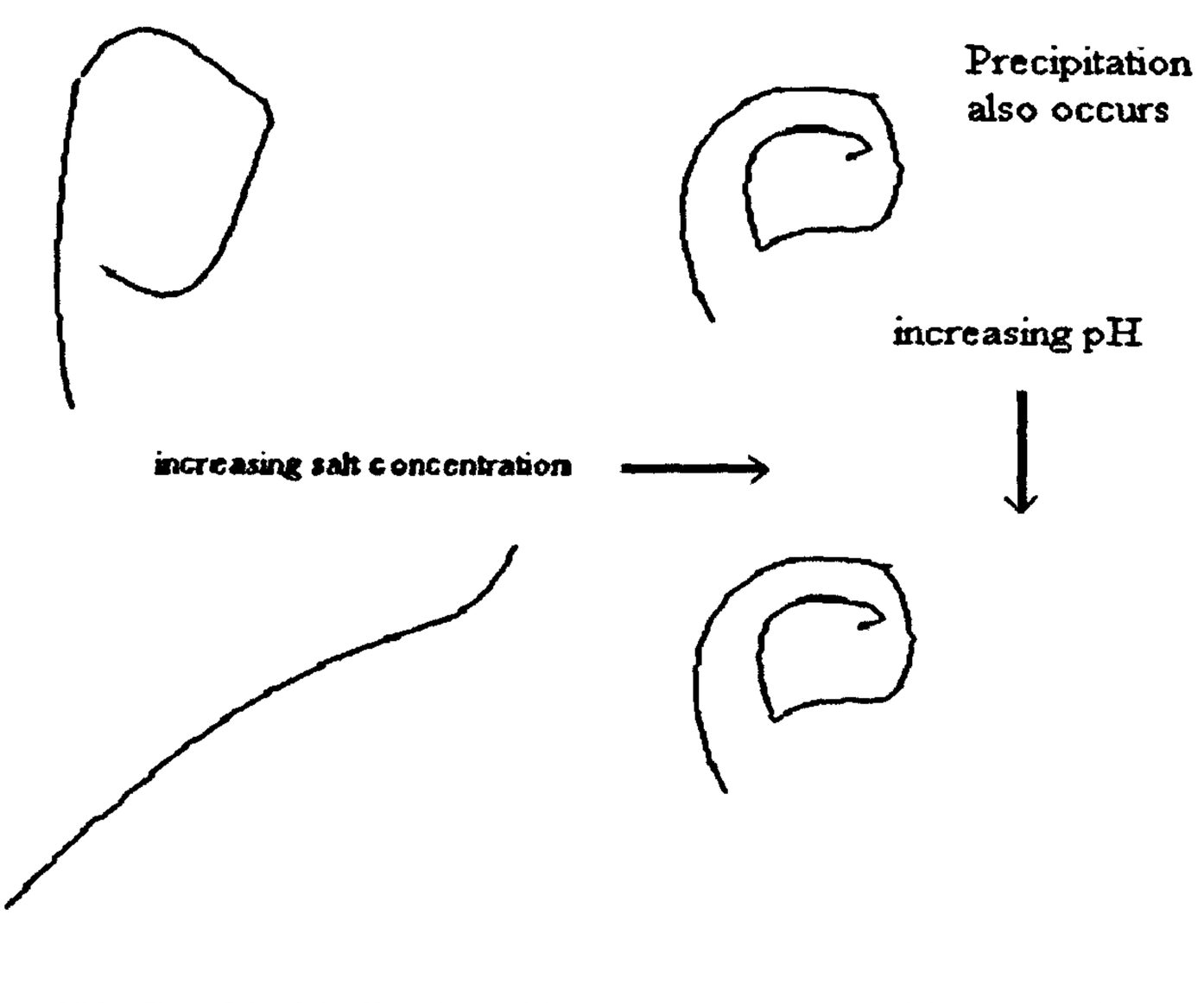

Figure 132: Graphical indication of increased polymer coiling of PAA as NaCl is added to the system in increasing amounts, at large concentrations of salt and low pH precipitation can also occur.

Addition of $CaCl_2$ to solutions of PAA shows the most complex behaviour of all, TRAMS results do not appear to follow a clear pattern and precipitation may cause problems with those readings however the steady state experiments indicate a collapse of the polymer system on addition of the salt as might be expected. The lifetimes values however seem to contradict this as quenching within the system seems to be increasing, usually indicative of an opening of the polymer coil when the polymer contains no groups which may quench itself. Thus the behaviour of PAA with $CaCl_2$ is not here easily demonstrated.

Chapter 5: Fluorescence investigation of complexation between polydimethylaminoethyl methacrylate and polyacrylic acid in aqueous solutions.

In this chapter fluorescence spectroscopic techniques, primarily TRAMS and energy transfer, will be used to gain information at the molecular level concerning complexation between a polyacid and a polybase. The complexation process between synthetic polyelectrolytes is of interest since it can be viewed as a model for more biological, complex, biopolymers: biopolymer complexation or aggregation forms the basis of many common diseases such as Parkinson's and Alzheimer's. As far as the current work is concerned the effects of varying the amount of polyacid or polybase on complex formation will be monitored via fluorescence spectroscopy. The pH of the solution will also be varied in order to gauge the effect upon complex stability. PAA is the polyacid while PDMAEMA is the polybase that will be studied in the current work.

5.1: Fluorescence Energy Transfer Measurements

5.1.1: Steady state spectra of an aqueous solution of unlabelled PDMAEMA and ACE-AMMA labelled PAA at various pH values.

The effect of complex formation with PDMAEMA on the conformation of PAA was investigated through intramolecular energy transfer. In order to achieve this ACE-AMMA labelled PAA sample at 10^{-2} wt% with concentrations of unlabelled PDMAEMA varying from 10^{-4} wt % to 10^{-1} wt %. This amounts to PDMAEMA to PAA stoichiometric ratios of 0.01: 1, 0.1:1, 1:1 and 10:1. The solutions were investigated at four different pH values (3, 6, 8 and 10).

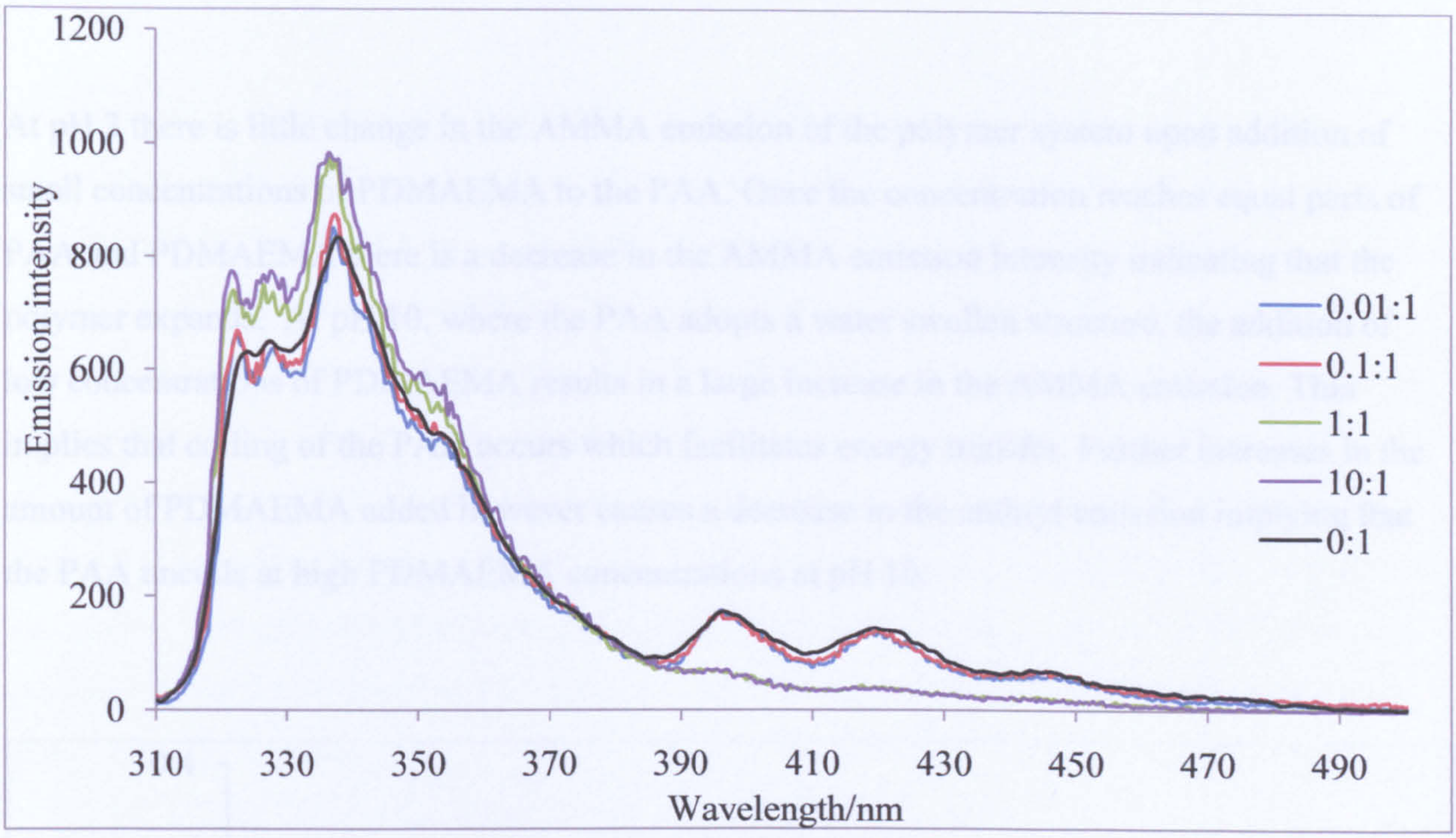

Figure 133: Emission spectra for an aqueous solution of unlabelled PDMAEMA and ACE-AMMA-PAA where the PDMAEMA concentration is varying, at pH 3 when excited at 290nm.

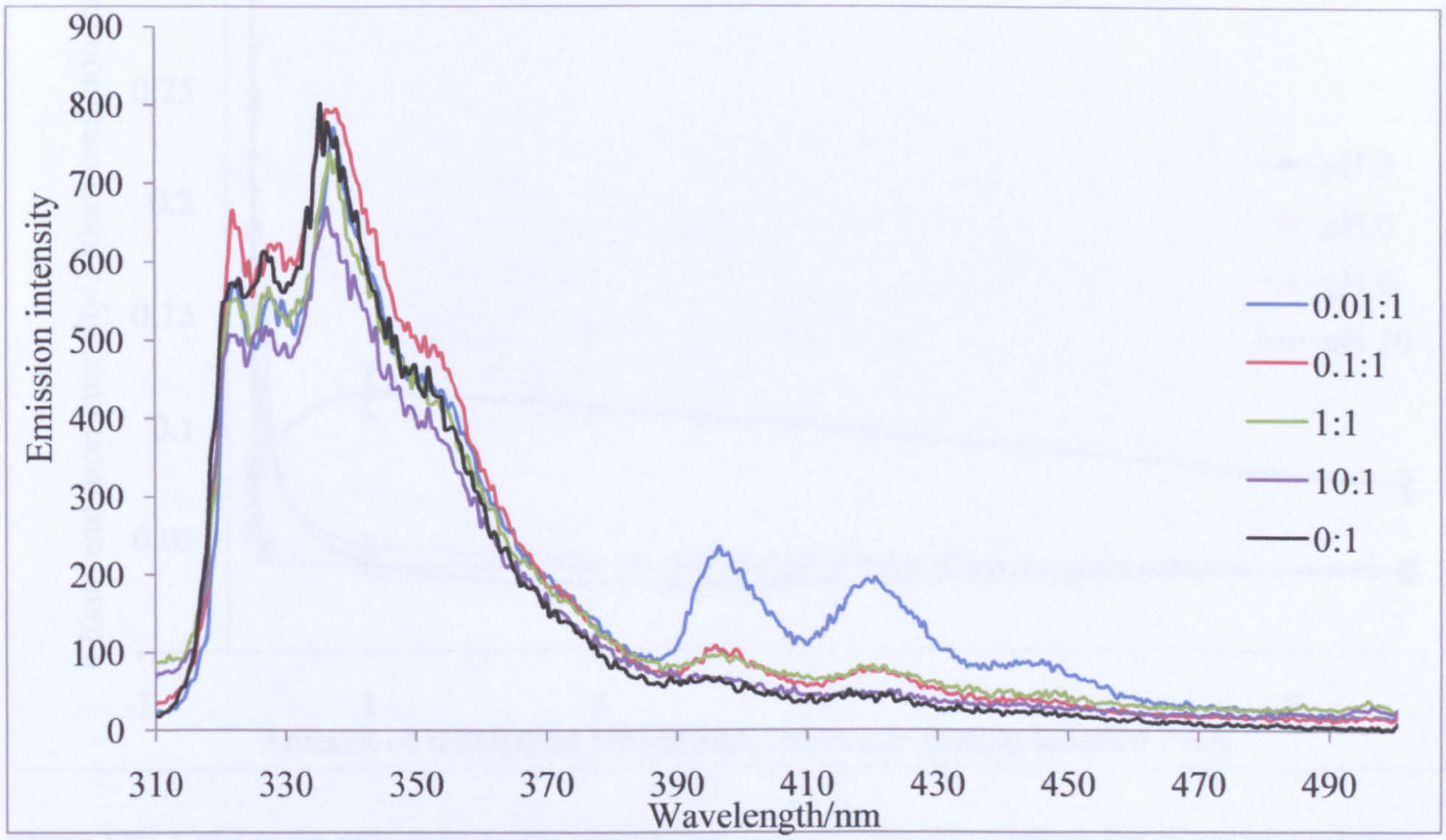

Figure 134: Emission spectra for an aqueous solution of unlabelled PDMAEMA and ACE-AMMA-PAA where the PDMAEMA concentration is varying at pH 10 when excited at 290nm.

At pH 3 there is little change in the AMMA emission of the polymer system upon addition of small concentrations of PDMAEMA to the PAA. Once the concentration reaches equal parts of PAA and PDMAEMA there is a decrease in the AMMA emission intensity indicating that the polymer expands. At pH 10, where the PAA adopts a water swollen structure, the addition of low concentrations of PDMAEMA results in a large increase in the AMMA emission. This implies that coiling of the PAA occurs which facilitates energy transfer. Further increases in the amount of PDMAEMA added however causes a decrease in the anthryl emission implying that the PAA uncoils at high PDMAEMA concentrations at pH 10.

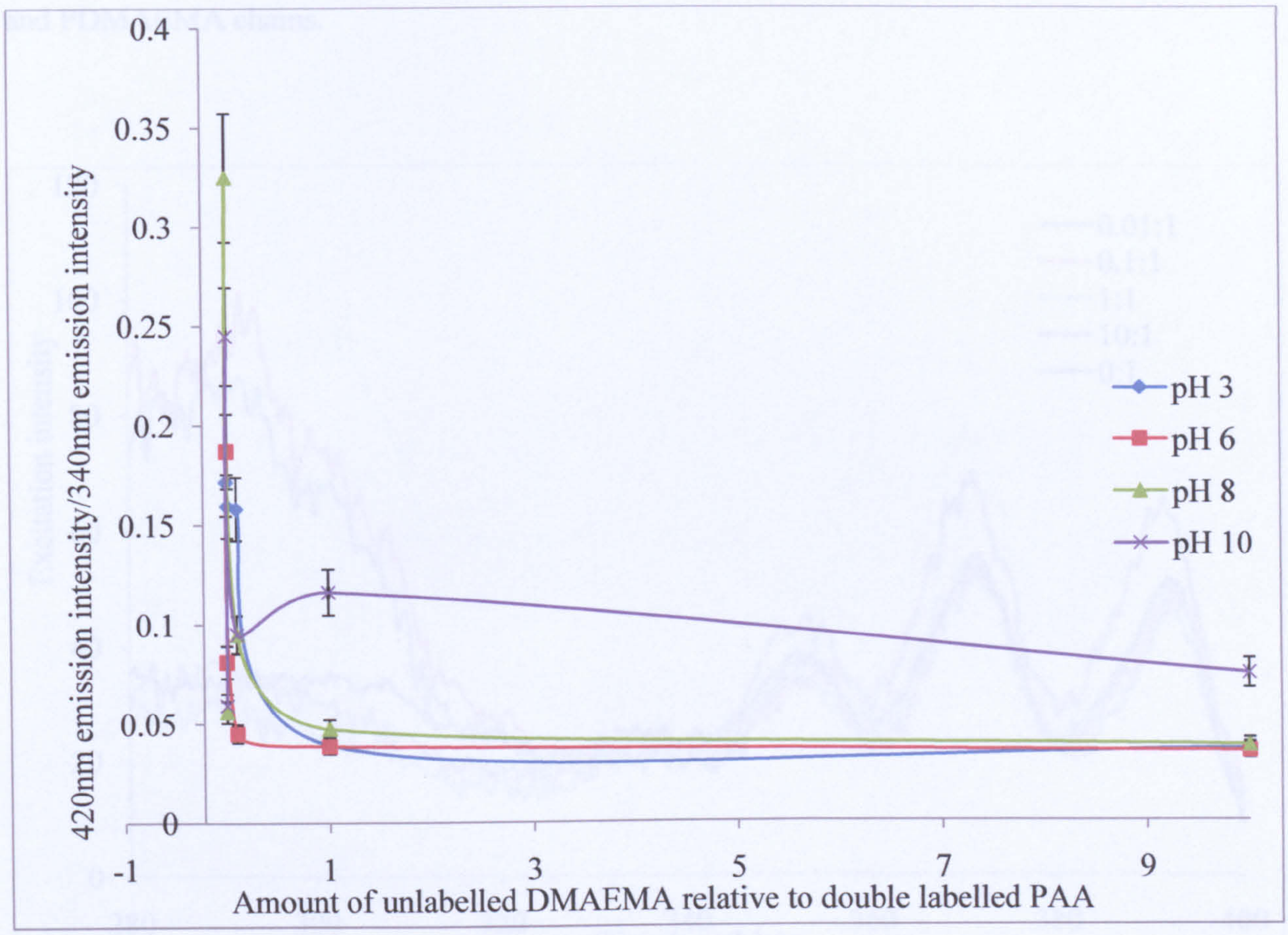

Figure 135: A plot of the ratio between the emission intensity at 420 nm and 340 nm for an aqueous solution of unlabelled PDMAEMA and ACE-AMMA-PAA at four different pH values where the PDMAEMA concentration is varying, when excited at 290 nm.

The ratio of the emission for the AMMA and ACE labels, sampled at 420 nm and 340 nm respectively, with increasing PDMAEMA concentration vary substantially upon initial addition of PDMAEMA for all pH values. The ratio for pH 3 and 6 decrease substantially while the ratios for pH 8 and 10 increase substantially. This indicates that at pH 3 and 6 the donor and acceptor are outside the distance for energy transfer when PDMAEMA is added to the system pH values >6 however a high ratio indicates a substantial degree of energy transfer. At [PDMAEMA] ≥ PAA the ratio is small at all pH values indicating an open conformation for PAA. Clearly the complex topography changes with increasing PDMAEMA content such that at high content the topography is largely independent of pH and given the lack of energy transfer in the PAA-ACE-AMMA system the structure at this stage may well be a ladder like complex between the PAA and PDMAEMA chains.

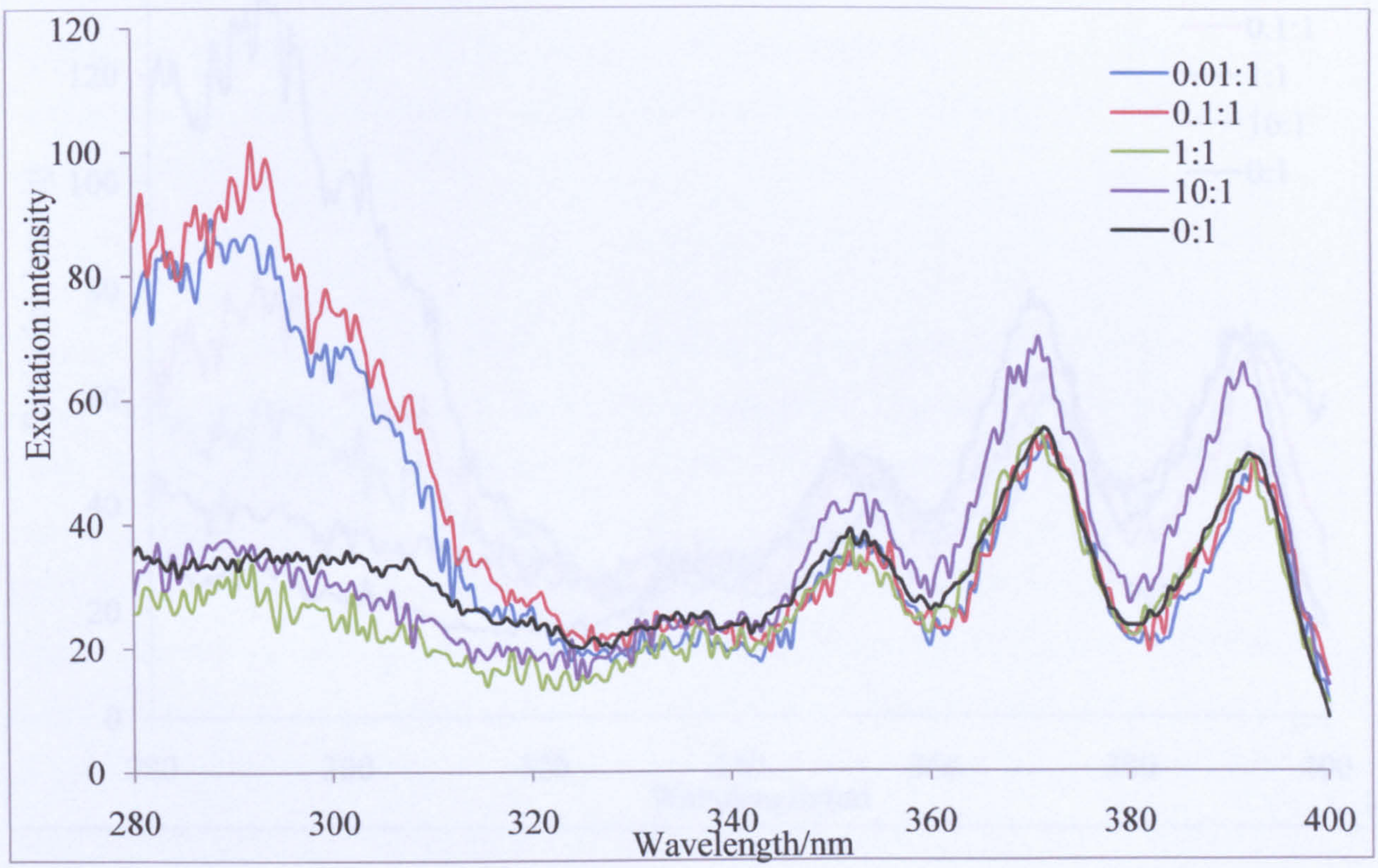

Figure 136: Excitation spectra for an aqueous solution of unlabelled PDMAEMA and ACE-AMMA-PAA where the PDMAEMA concentration is varying at pH 3 when observed at 340 nm.

Examination of the fluorescence excitation spectra of the complex at pH 3 (see figure 136) reveals that initial coiling of the doubly labelled PAA occurs upon addition of small amounts of PDMAEMA compared to the polyacid alone in solution. This is due to an increase in the excitation intensity at 290 nm when sampled at 420 nm. At higher concentrations, this increased excitation at 290nm is reduced once more. This data suggests that the excitation at 290 nm (from ACE label) makes a larger contribution to the AMMA emission samples at 420 nm when low content of polybase was added. This suggests a greater degree of energy transfer occurs which is consistent with a coiled PAA conformation.

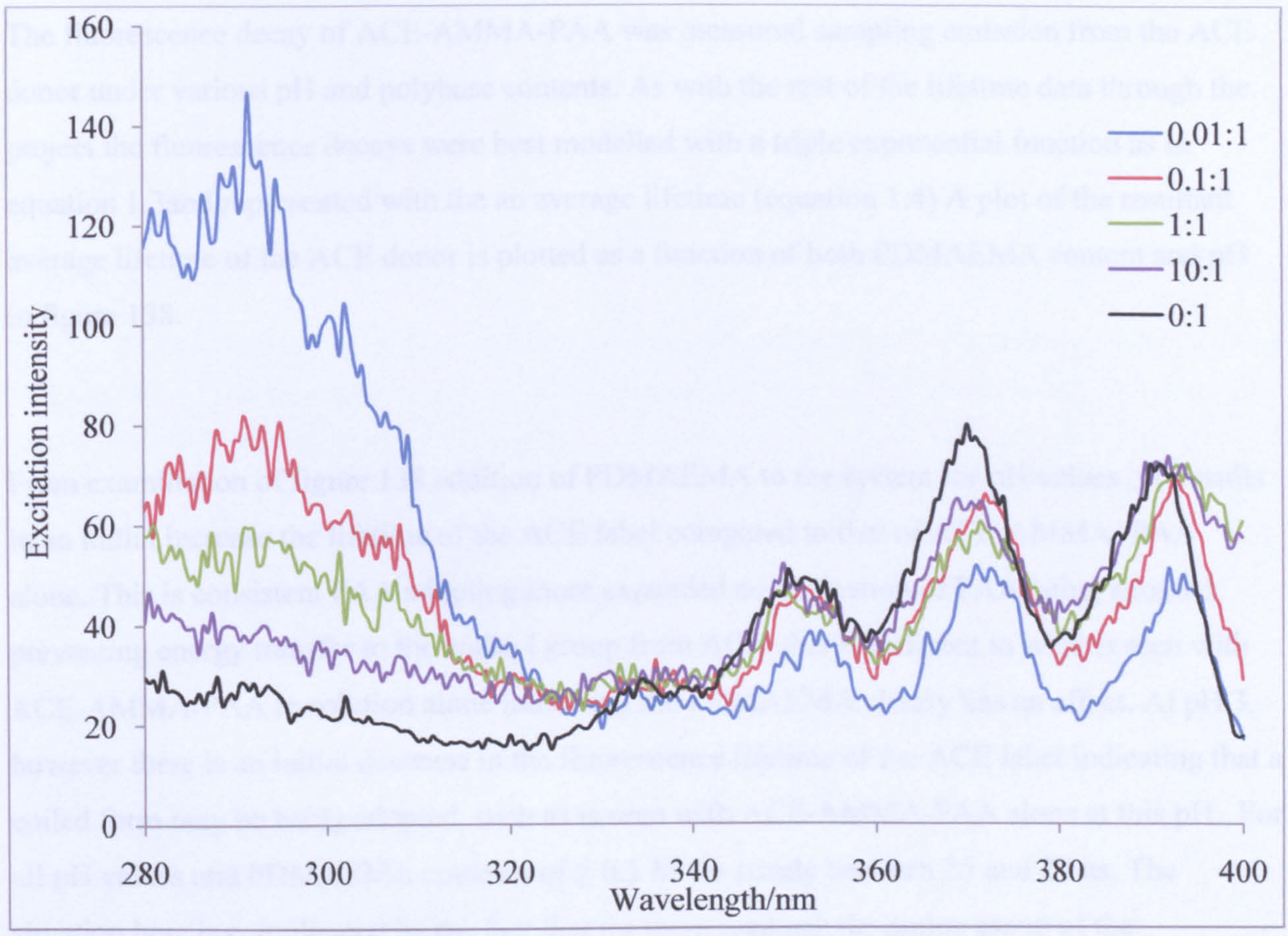

Figure 137: Excitation spectra for an aqueous solution of unlabelled PDMAEMA and ACE-AMMA-PAA where the PDMAEMA concentration is varying at pH 10 when observed at 340 nm.

The excitation spectra for the same system at pH 10 shows an initial large increase in the excitation intensity at 290 nm that then decreases with further addition of PDMAEMA. This would indicate that although small amounts of PDMAEMA promote coiling of PAA larger amounts have further effect (see figure 137).

5.1.2: Fluorescence lifetime measurements of an aqueous solution of ACE-AMMA-PAA and unlabelled PDMAEMA at various pH values.

The fluorescence decay of ACE-AMMA-PAA was measured sampling emission from the ACE donor under various pH and polybase contents. As with the rest of the lifetime data through the project the fluorescence decays were best modelled with a triple exponential function as in equation 1.3and represented with the an average lifetime (equation 1.4) A plot of the resultant average lifetime of the ACE donor is plotted as a function of both PDMAEMA content and pH in figure 138.

From examination of figure 138 addition of PDMAEMA to the system for pH values ≥ 6 results in an initial increase the lifetime of the ACE label compared to that of ACE-AMMA- PAA alone. This is consistent PAA adopting more expanded conformation of PAA being adopted preventing energy transfer to the anthryl group from ACE, this is different to what is seen with ACE-AMMA-PAA in solution alone indicating the PDMAEMA clearly has an effect. At pH 3 however there is an initial decrease in the fluorescence lifetime of the ACE label indicating that a coiled form may be being adopted, such as is seen with ACE-AMMA-PAA alone at this pH. For all pH values and PDMAEMA contents of ≥ 0.1 M t is steady between 25 and 27 ns. The situation here is complicated by the fact that for these readings the amine group of the PDMAEMA may be quenching the ACE fluorescence if a ladder like structure is being observed or energy transfer between the ACE and AMMA labels is taking place and the PAA is coiled under these conditions also.

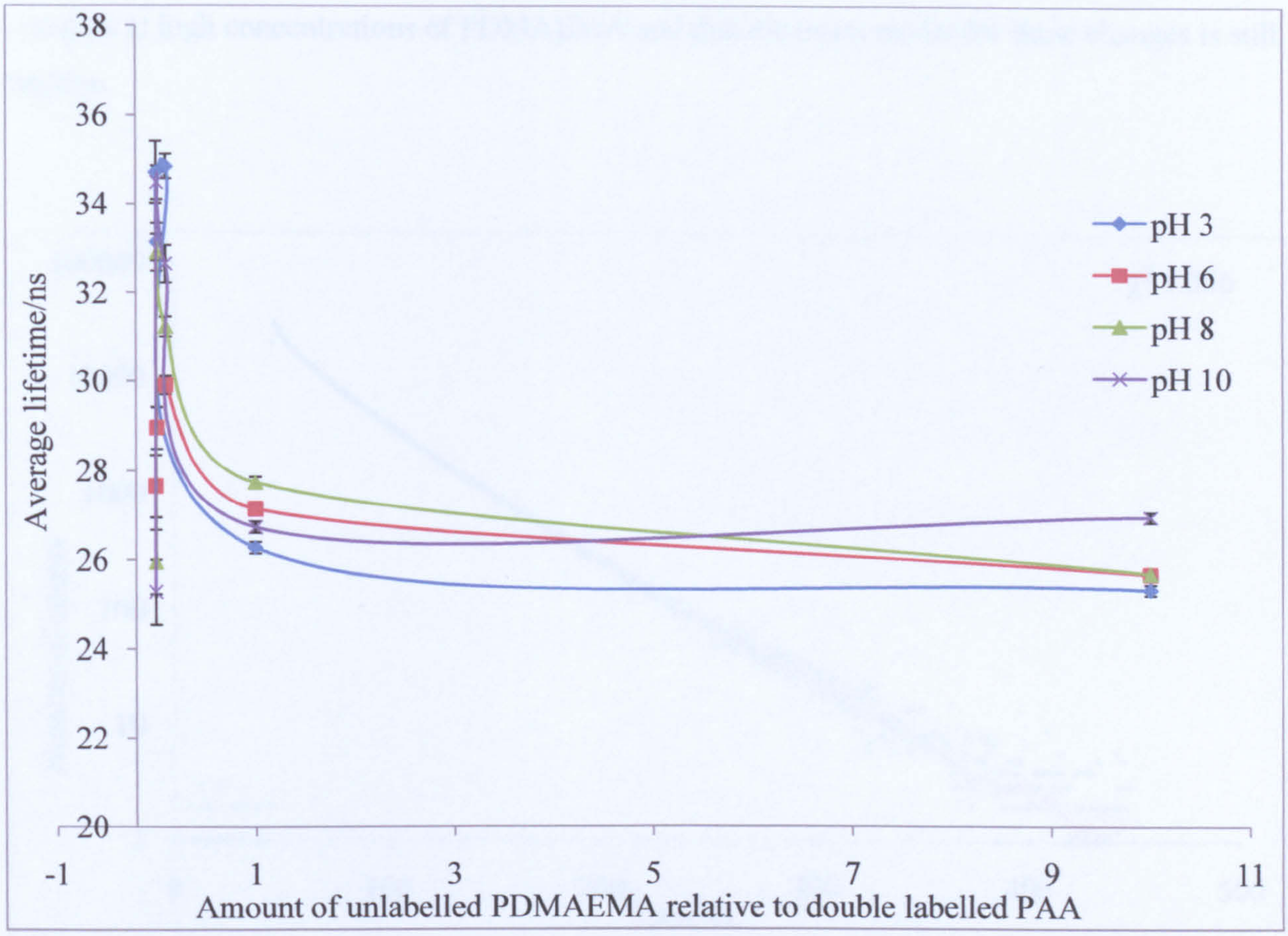

Figure 138: A plot of the average ACE label lifetime for an aqueous solution of unlabelled DMAEMA and ACE-AMMA-PAA at four different pH values where the concentration of DMAEMA is varying. The sample was excited at 290 nm and observed at 340 nm.

Both of these possibilities however are counter to the information observer using steady state experiments. The steady state measurements observed a decrease in the ratio between the AMMA and ACE emission at higher concentrations of PDMAEMA indicating an open structure such as a ladder like complex between PAA and PDMAEMA however no indication of quenching of fluorescence by the amine groups on the PDMAEMA was found. It could be that the steady state data has been in some way contaminated by radiative energy transfer and is unreliable in this case. (effects such as these have been observed before [23]) It is likely however that both fluorescence decay and steady state data reflect changes in the topography of the

complex at high concentrations of PDMAEMA and that the exact model for these changes is still unclear.

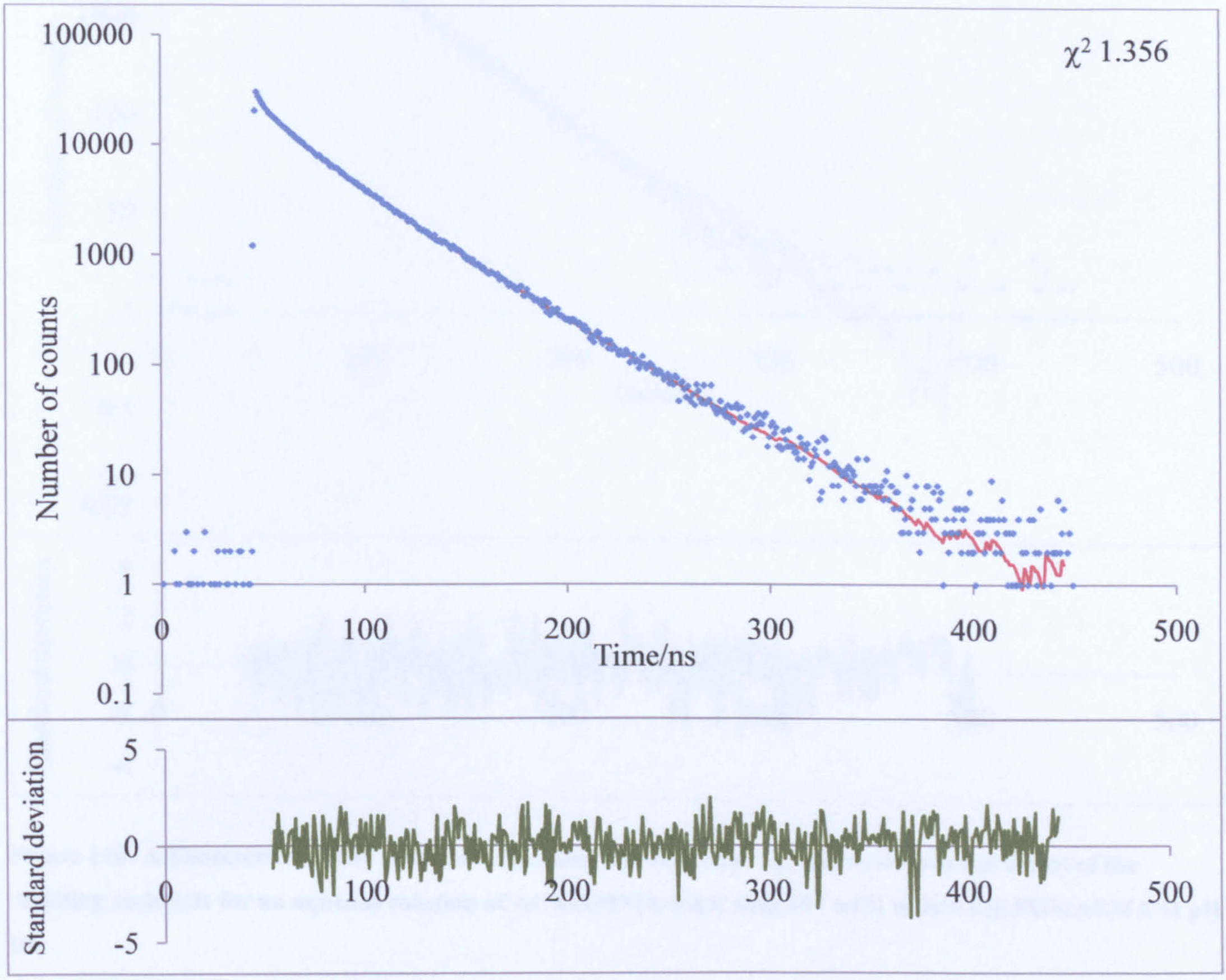

Figure 139: A fluorescence decay with corresponding mathematical fit (shown in red) and a plot of the residuals for an aqueous solution of ACE-AMMA-PAA with 10^{-4} wt% unlabelled PDMAEMA at pH 3.

As before the fluorescence decays were best fit to a triple exponential model as in equation 1.3. This gave a random distribution of residuals and χ^2 values close to unity. An average lifetime value was then obtained from equation 1.4 and it is these values that are shown in figure 138.

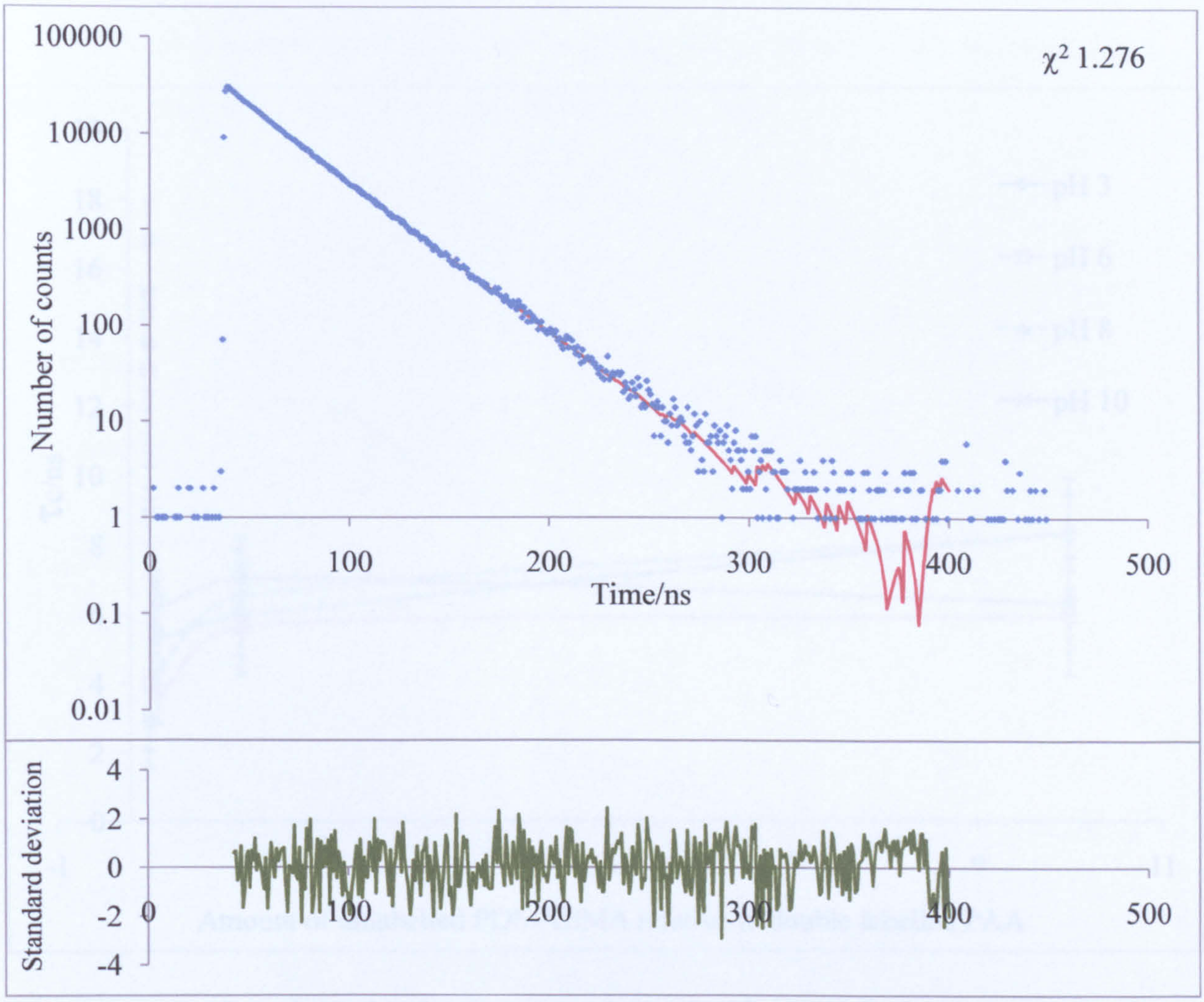

Figure 140: A fluorescence decay with corresponding mathematical fit (shown in red) and a plot of the resulting residuals for an aqueous solution of ACE-AMMA-PAA with 10^{-1} wt% unlabelled PDMAEMA at pH 10.

5.1.3: Time Resolved Anisotropy Measurements on an aqueous solution of unlabelled PDMAEMA with ACE-AMMA labelled PAA at various pH values.

The decay of fluorescence anisotropy of the AMMA label (excited at 370 nm and analysed at 420 nm) in ACE-AMMA-PAA was use as an additional tool to probe the mobility of the complex formed with PDAMEMA under various aqueous solution conditions.

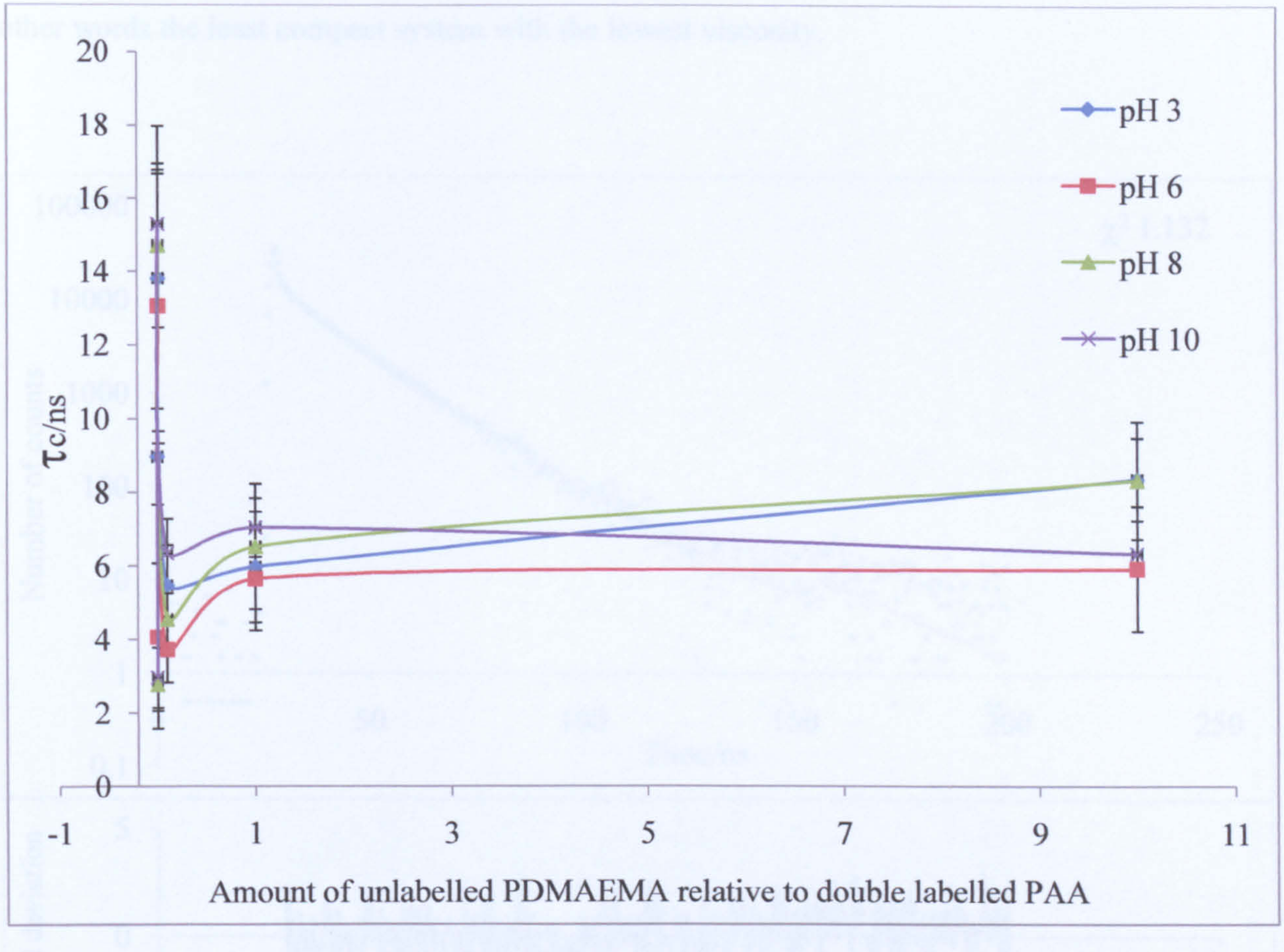

Figure 141: A plot of correlation time for an aqueous solution of ACE-AMMA-PAA with varying concentrations of unlabelled PDMAEMA at four different pH values.

The TRAMS data for complexes between ACE-AMMA-PAA and unlabelled PDMAEMA was analysed using a single exponential fit via impulse reconvolution methods. The data was analysed beyond the peak of the decay due to segmental backbone motion and free rotation of the ester being present in analysis of the AMMA label.[23] This complicates data analysis so in order to allow a comparison between the solution conditions here and in other experiments the data was treated like this to eliminate the rotational contribution from the label and so τ_c should reflect the backbone motion of the PAA. Within the error given by the standard deviations the

pattern of τ_c is consistent across all pH values, generally pH 6 seems to show the lowest τ_c, in other words the least compact system with the lowest viscosity.

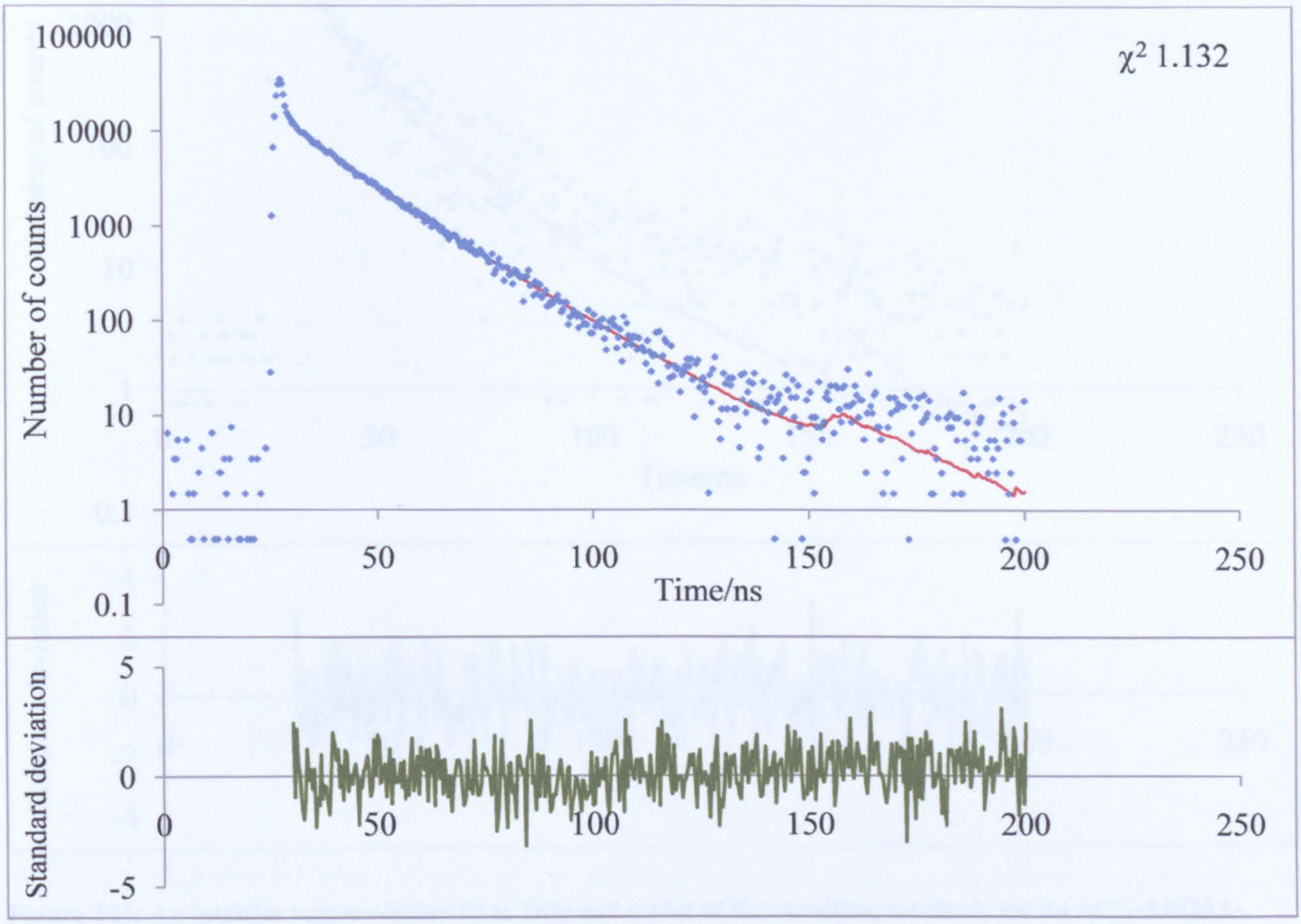

Figure 142: An impulse reconvolution fit to D(t) and a plot of the residuals for ACE-AMMA-PAA at pH 3 in aqueous solution with 10^{-4}wt% unlabelled PDMAEMA when excited at 370 nm and analysed at 420 nm.

Initial addition of PDMAEMA in small amounts shows a large decrease in the correlation time for all pH values indicating an increase in the polymer segmental motion is a decrease in the microviscosity of the complex. With increasing concentrations of PDMAEMA the correlation time then increases, perhaps indicating that the nature of the complex formed changes; i.e. the microviscosity within the complex changes which could indicate a change in topography

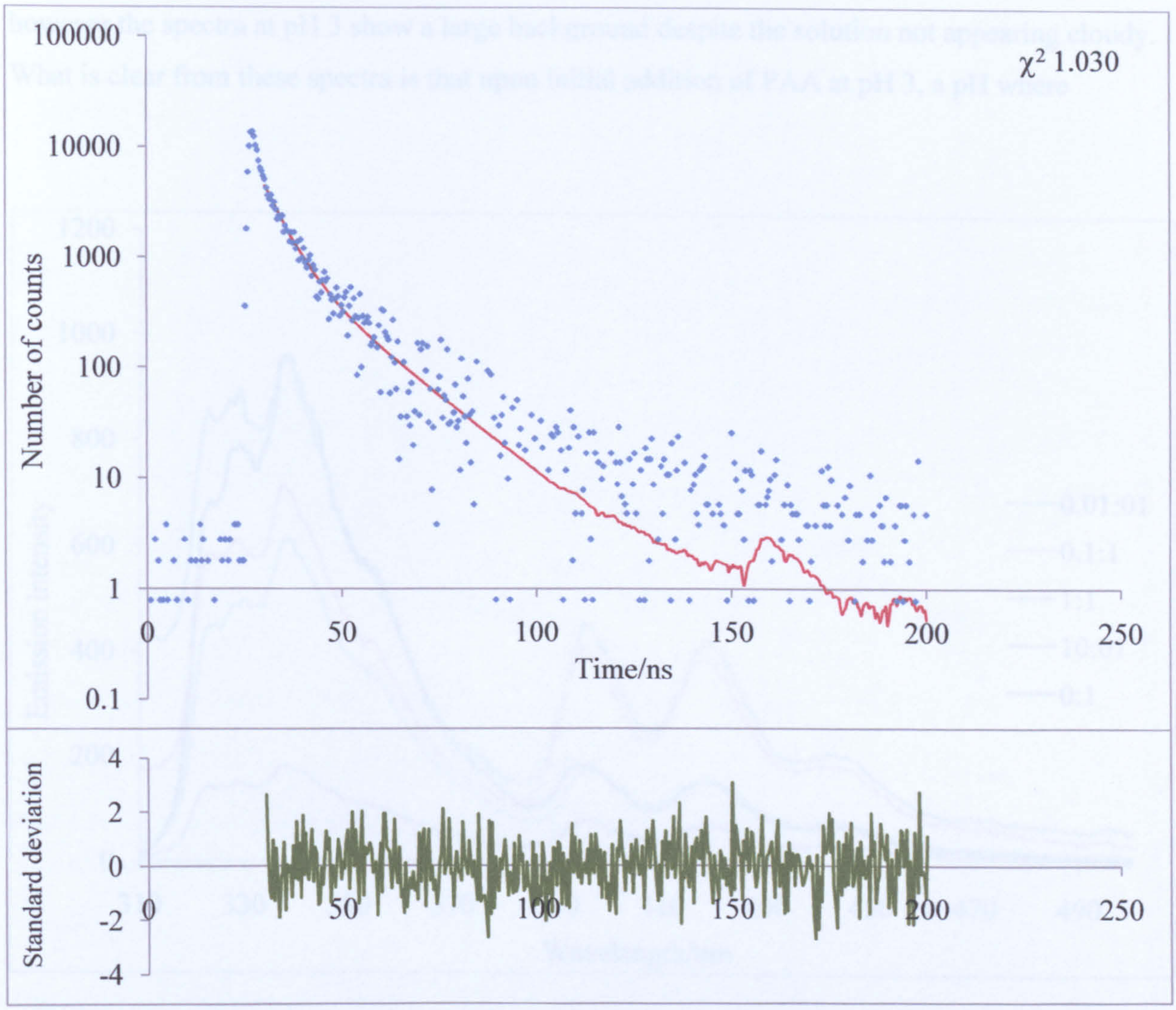

Figure 143: An impulse reconvolution fit to D(t) and a plot of the resulting residuals for an ACE-AMMA-PAA sample of pH 10 in aqueous solution with 10^{-1} wt% unlabelled PDMAEMA when excited at 370 nm and analysed at 420 nm.

5.2.1: Steady state spectra of an aqueous solution of unlabelled PAA and ACE-AMMA labelled PDMAEMA at various pH values.

The steady state emission spectra for solutions of 10^{-2} wt% ACE-AMMA labelled PDMEAEMA with varying pH values and concentrations of unlabelled PAA were recorded (see figure 144)

however the spectra at pH 3 show a large background despite the solution not appearing cloudy. What is clear from these spectra is that upon initial addition of PAA at pH 3, a pH where

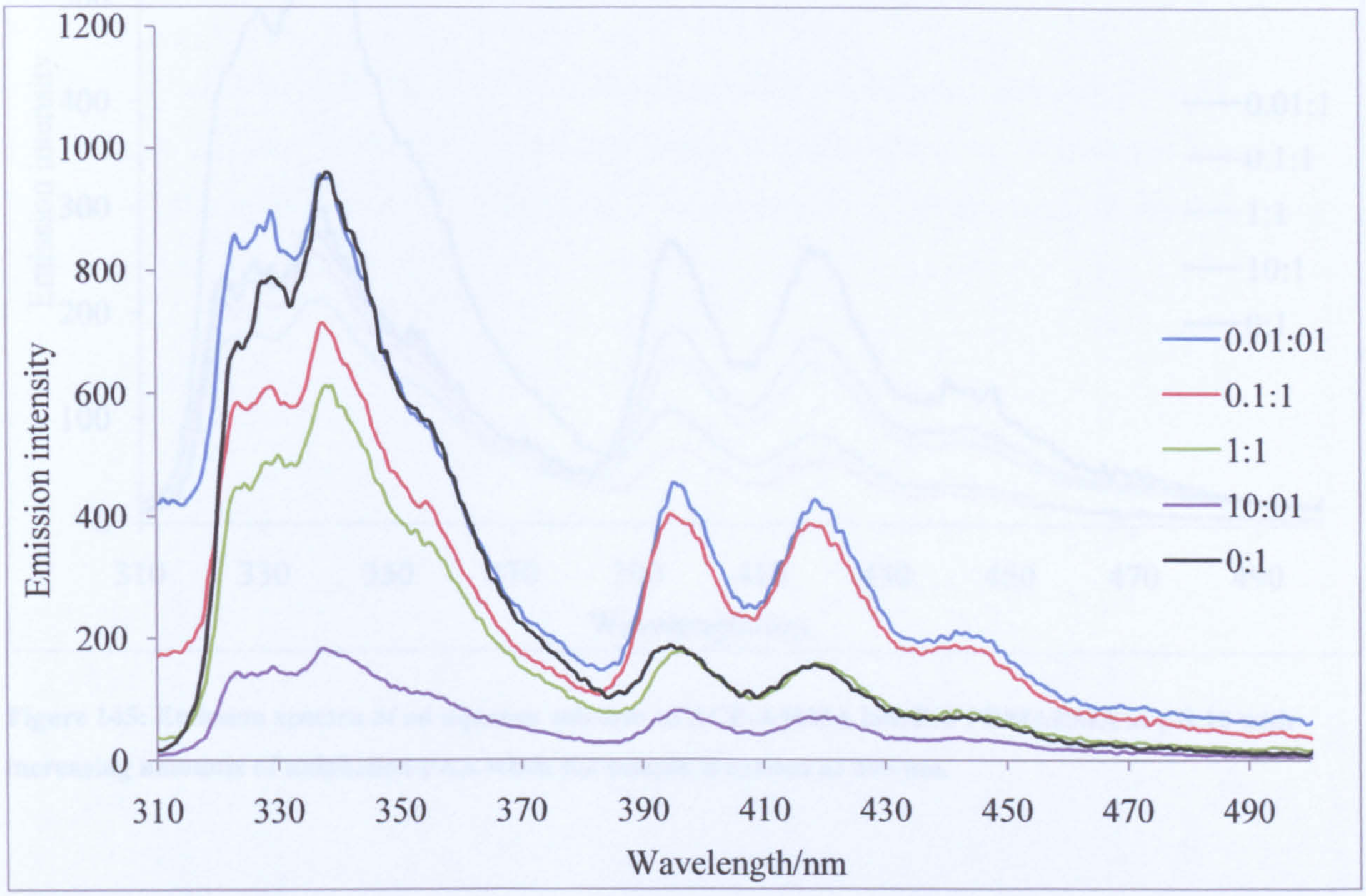

Figure 144: Emission spectra of an aqueous solution of ACE-AMMA labelled PDMAEMA att pH 3 with increasing amounts of unlabelled PAA when the sample is excited at 290 nm.

PDMAEMA can be expected to be uncoiled and not self quenched, causes an increase in emission intensity from the AMMA label indicating that the polymer system is collapsed. Further addition of PAA to the system causes the overall emission intensity to drop. This may simply indicate that at high stoichiometric ratios of polyacid the interpolymer complex is unstable and precipitation occurs.

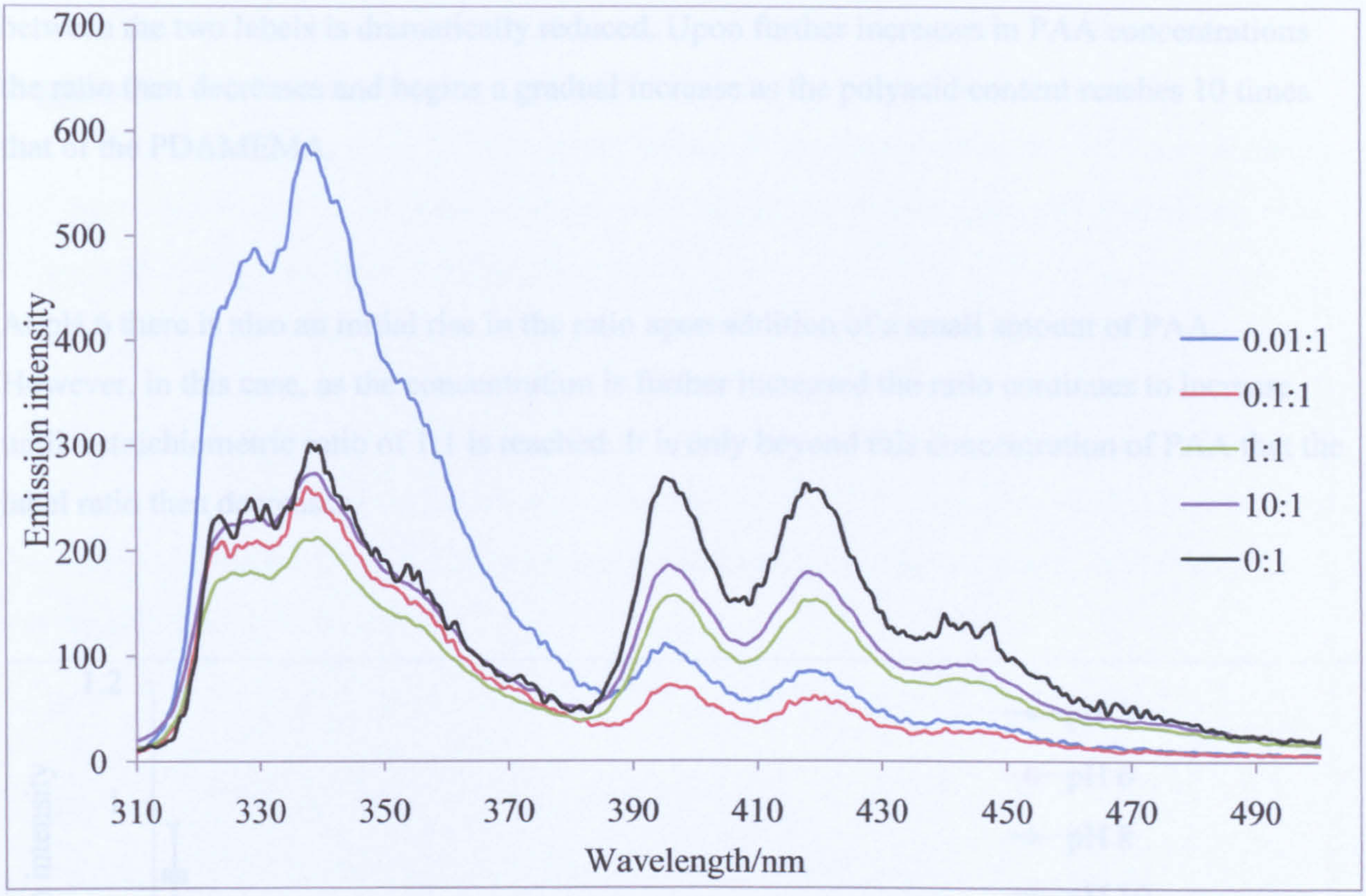

Figure 145: Emission spectra of an aqueous solution of ACE-AMMA labelled PDMAEMA at pH 10 with increasing amounts of unlabelled PAA when the sample is excited at 290 nm.

The emission spectra of the same polymer system at pH 10 (see figure 145) shows an initial increase in the ACE fluorescence with a corresponding decrease in the AMMA emission upon addition of 10^{-4} wt% of PAA. This may reflect that the polymer system uncoils upon addition of PAA. As the PAA concentration increases further the labelled PDMAEMA again shows an increase in the emission from AMMA with a corresponding decrease in the naphthyl fluorescence. This may reflect the fact that the PDMAEMA component adopts a collapsed conformation in the complex.

The AMMA to ACE emission ratio for the double labelled PDMAEMA system with increasing amounts of unlabelled PAA was calculate and is plotted in figure 146. At pH 3 addition of PAA at low concentrations to PDMAEMA greatly increases the ratio which indicates that the distance

between the two labels is dramatically reduced. Upon further increases in PAA concentrations the ratio then decreases and begins a gradual increase as the polyacid content reaches 10 times that of the PDAMEMA.

At pH 6 there is also an initial rise in the ratio upon addition of a small amount of PAA. However, in this case, as the concentration is further increased the ratio continues to increase until a stoichiometric ratio of 1:1 is reached. It is only beyond this concentration of PAA that the label ratio then decreases.

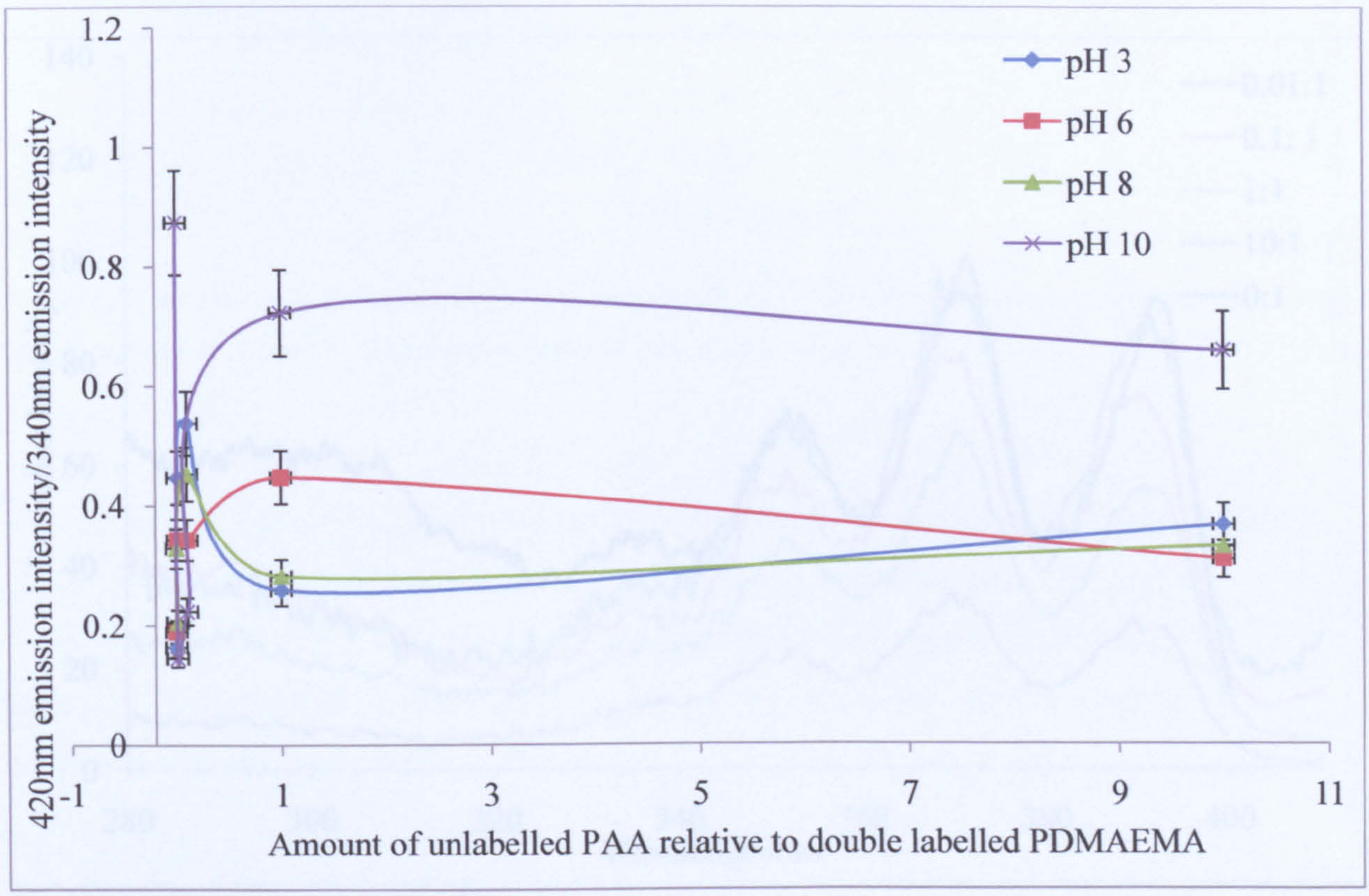

Figure 146: A plot of the emission intensity ratio between the AMMA emission at 420 nm and the ACE emission at 340 nm for ACE-AMMA-PDMAEMA in aqueous solution when excited at 290 nm with increasing concentrations of unlabelled PAA at four different pH values.

The situation at pH 8 matches that at pH 6 addition of PAA to PDMAEMA dramatically increases the ratio between (see figure 146) which indicates that the distance between the two labels is dramatically reduced. Upon further increase in the PAA content the ratio then decreases and begins a slow rise as the polyacid concentration reaches 10 times that of the polybase. The ratios at pH 3 and 8 are also very similar in magnitude.

At pH 10, where PDMAEMA would be expected to form a collapsed conformation, addition of PAA to the polybase causes a large drop in the AMMA/ACE ratio which indicates expansion of the labelled polymer. As the PAA concentration increases, the ratio increases, which implies further collapse of the polybase.

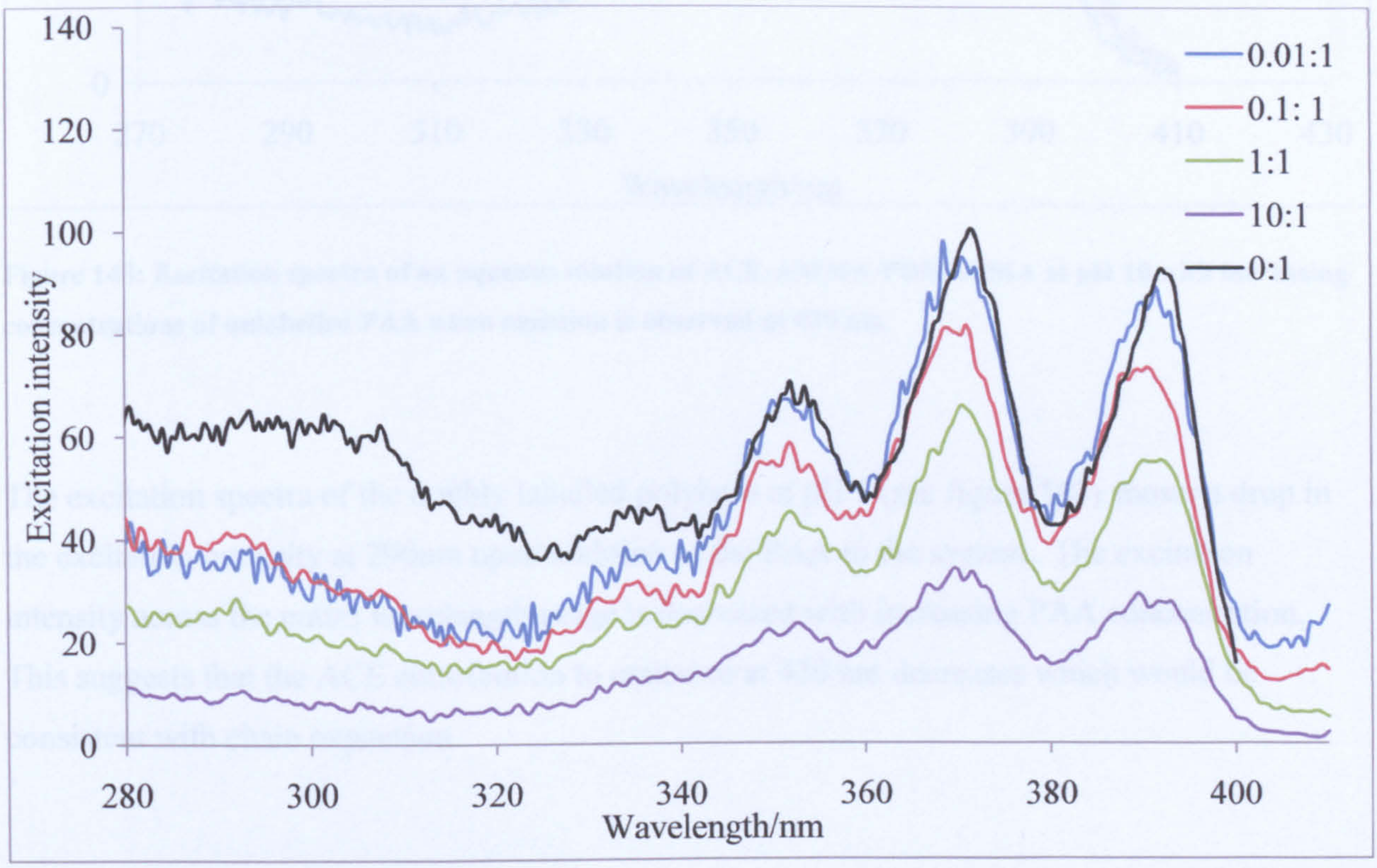

Figure 147: Excitation spectra of an aqueous solution of ACE-AMMA-PDMAEMA at pH 3 with increasing concentrations of unlabelled PAA when emission is observed at 420 nm.

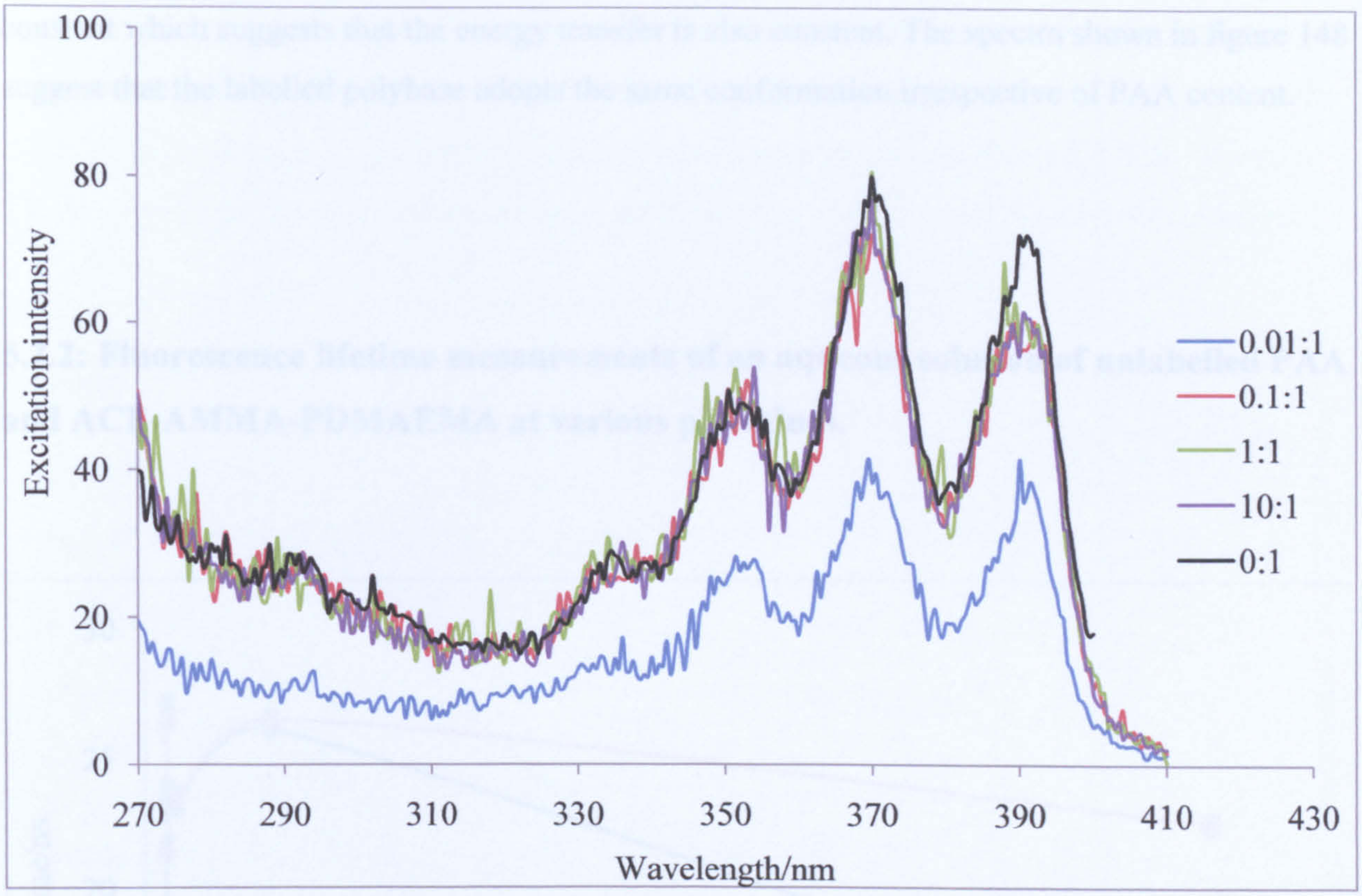

Figure 148: Excitation spectra of an aqueous solution of ACE-AMMA-PDMAEMA at pH 10 with increasing concentrations of unlabelled PAA when emission is observed at 420 nm.

The excitation spectra of the doubly labelled polybase at pH 3 (see figure 147) shows a drop in the excitation intensity at 290nm upon addition of the PAA to the system . The excitation intensity across the entire wavelength range is decreased with increasing PAA concentration. This suggests that the ACE contribution to emission at 420 nm decreases which would be consistent with chain expansion.

At pH 10 (figure 148) there is an initial drop in the excitation intensity of the polymer system across the entire wavelength range. At concentrations of 10^{-3} wt% or above of PAA the excitation intensity again increases across the entire wavelength range, there is then no further increase. This suggests that the ACE contribution to the emission samples at 420 nm remains

constant which suggests that the energy transfer is also constant. The spectra shown in figure 148 suggest that the labelled polybase adopts the same conformation irrespective of PAA content.

5.2.2: Fluorescence lifetime measurements of an aqueous solution of unlabelled PAA and ACE-AMMA-PDMAEMA at various pH values.

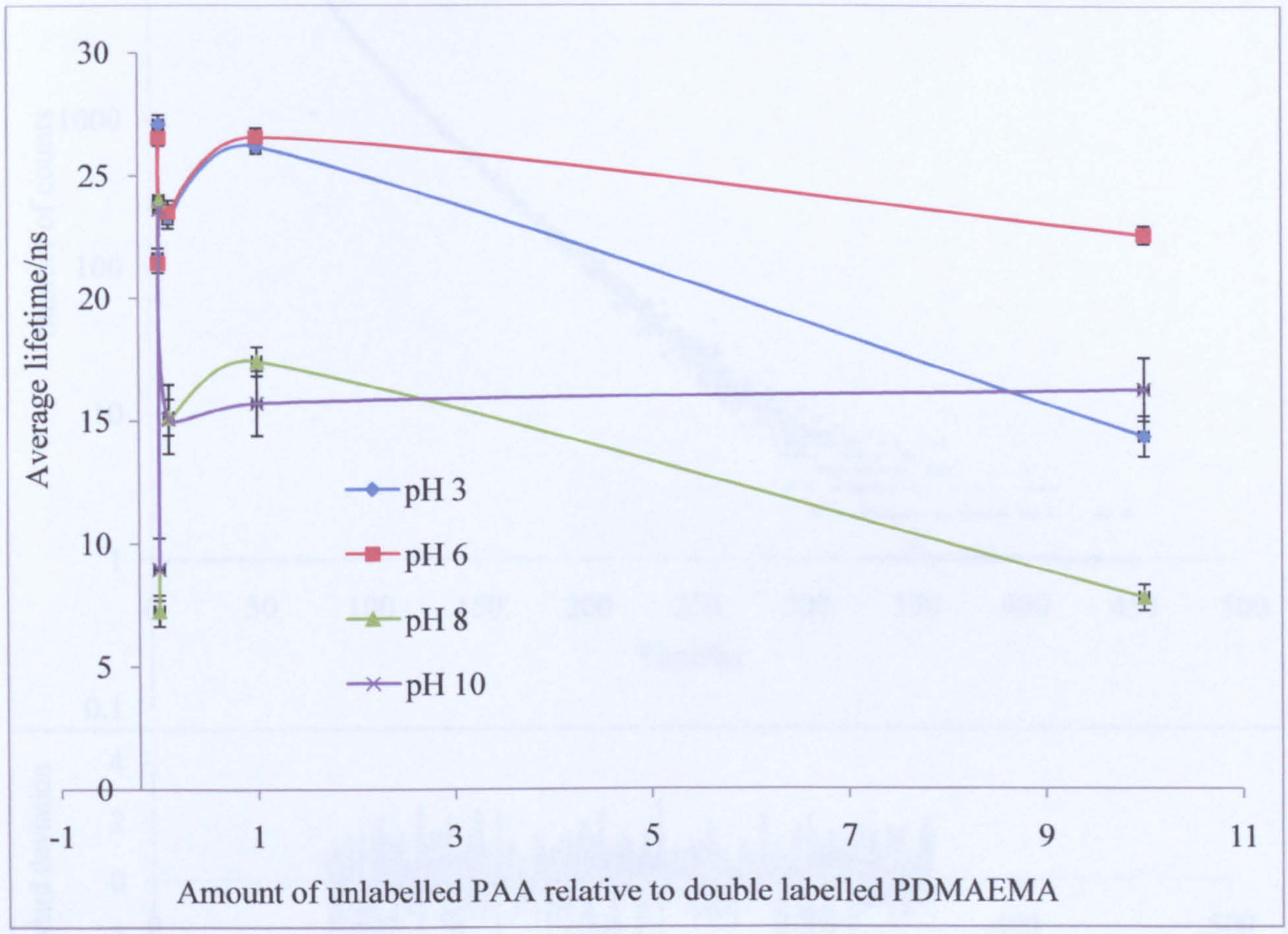

Figure 149: A plot of ACE average lifetime values for ACE-AMMA-PDMAEMA in aqueous solution with increasing concentrations of unlabelled PAA across a range of pH values when excited at 290 nm and observed at 340 nm.

As with all the previous lifetime work the best statistical fit to the lifetime data, providing good χ^2 values and evenly distributed residuals, was achieved with using a triple exponential fit to the decay as in equation 1.3. The lifetime values shown above are averages derived from equation 1.4 to show a relative overview of the polymer behaviour which is undoubtedly very complex.

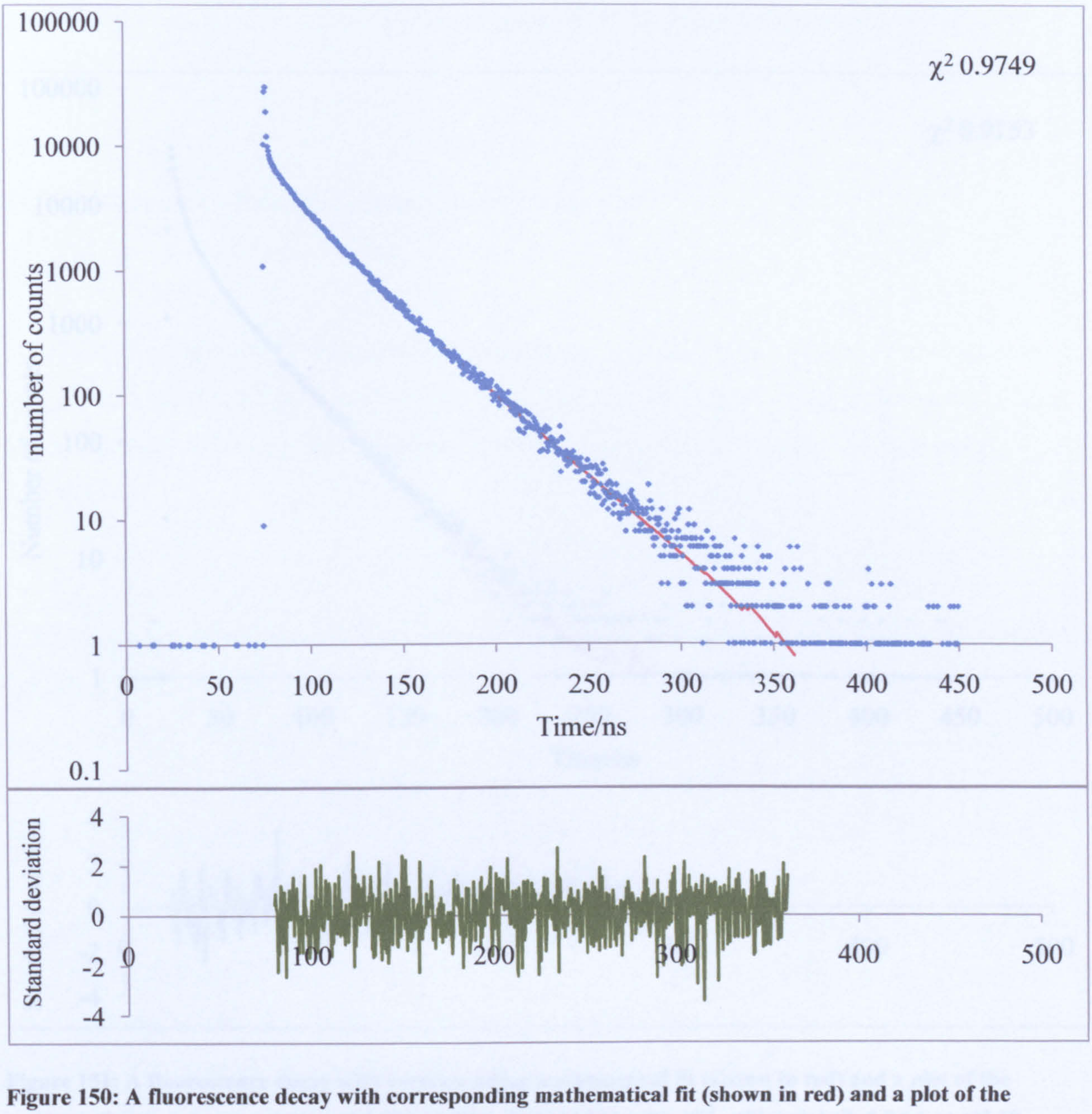

Figure 150: A fluorescence decay with corresponding mathematical fit (shown in red) and a plot of the resulting residuals for an aqueous solution of ACE-AMMA-PDMAEMA with 10^{-4} wt% unlabelled PAA at pH 3.

Clearly, from consideration of figure 149, at all pH values the addition of 10^{-4} wt% of PAA causes a substantial increase in the average lifetime of the ACE label which indicates a decrease in quenching, this may be due to polymer collapse or at least some shielding of the label from aqueous medium, this effect is more pronounced at higher pH values.

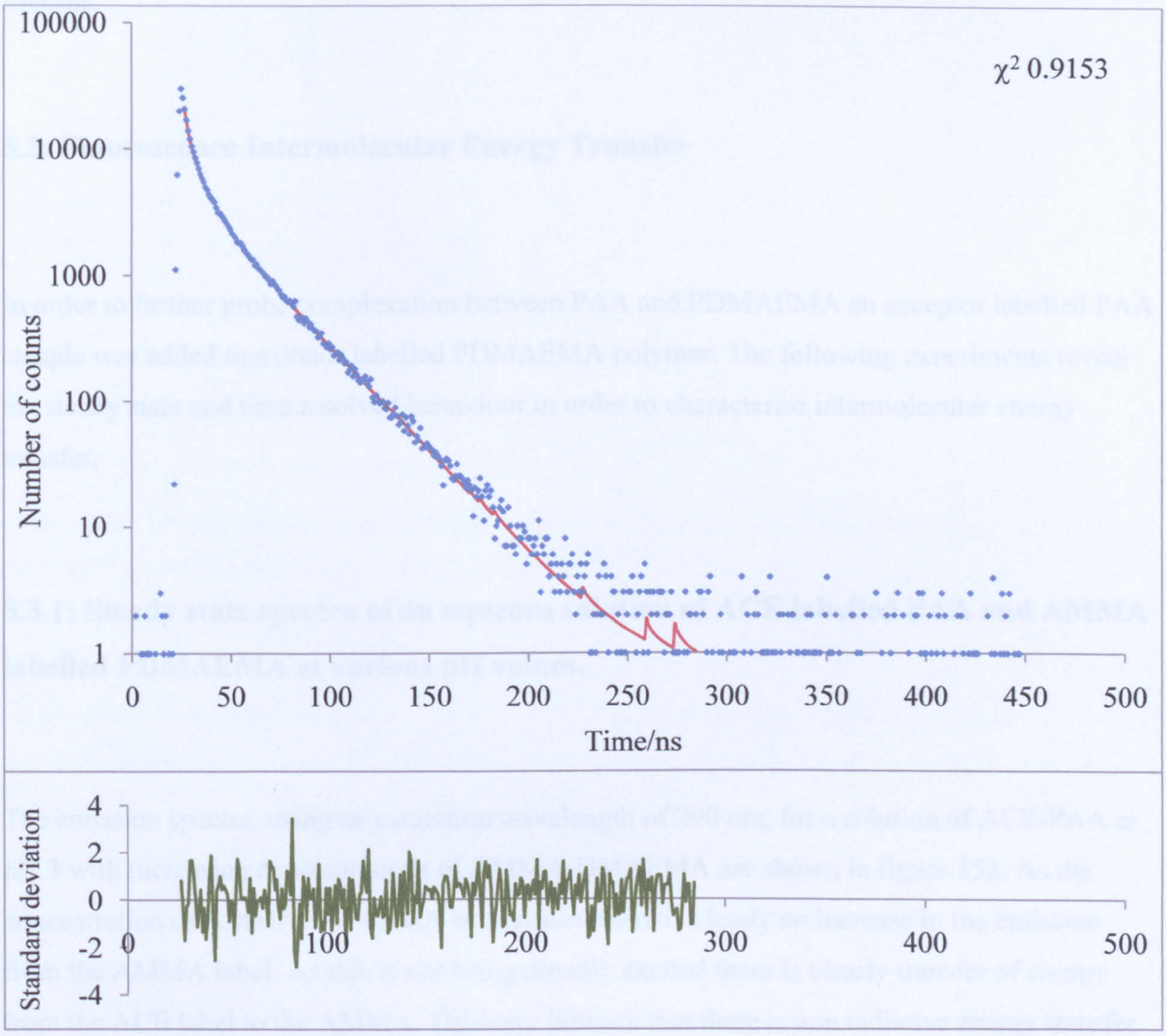

Figure 151: A fluorescence decay with corresponding mathematical fit (shown in red) and a plot of the residuals for an aqueous solution of ACE-AMMA-PDMAEMA with 10^{-1} wt% unlabelled PAA at pH 10.

Further examination of figure 149 reveals that all pH values then show a decrease in the lifetime at 10^{-3} wt% of PAA which suggests that the polymer is contracting or the fluorescence is at least being quenched more effectively. With still further increasing PAA content unusual behaviour is observed. At pH 3 and 8 the lifetime increases slightly to a PAA concentration of 10^{-2} wt%. Beyond this, where the weight percentage of the PAA exceeds that of the DMAEMA, the lifetime decreases. At pH values of 6 and 10 however, this decrease in the lifetime at high polyacid contents is not as marked, or, in the case of pH 10, there is even a slight increase in lifetime.

5.3: Fluorescence Intermolecular Energy Transfer

In order to further probe complexation between PAA and PDMAEMA an acceptor labelled PAA sample was added to a donor labelled PDMAEMA polymer. The following experiments reveal the steady state and time resolved behaviour in order to characterise intermolecular energy transfer.

5.3.1: Steady state spectra of an aqueous solution of ACE labelled PAA and AMMA labelled PDMAEMA at various pH values.

The emission spectra, using an excitation wavelength of 290 nm, for a solution of ACE-PAA at pH 3 with increasing concentrations of AMMA-DMAEMA are shown in figure 152. As the concentration of AMMA-DMAEMA is increased there is clearly an increase in the emission from the AMMA label. As this is not being directly excited there is clearly transfer of energy from the ACE label to the AMMA. This may indicate that there is non radiative energy transfer occurring in the system, it could also however be due to excitation of the AMMA from the emission of the ACE and so radiative energy transfer.

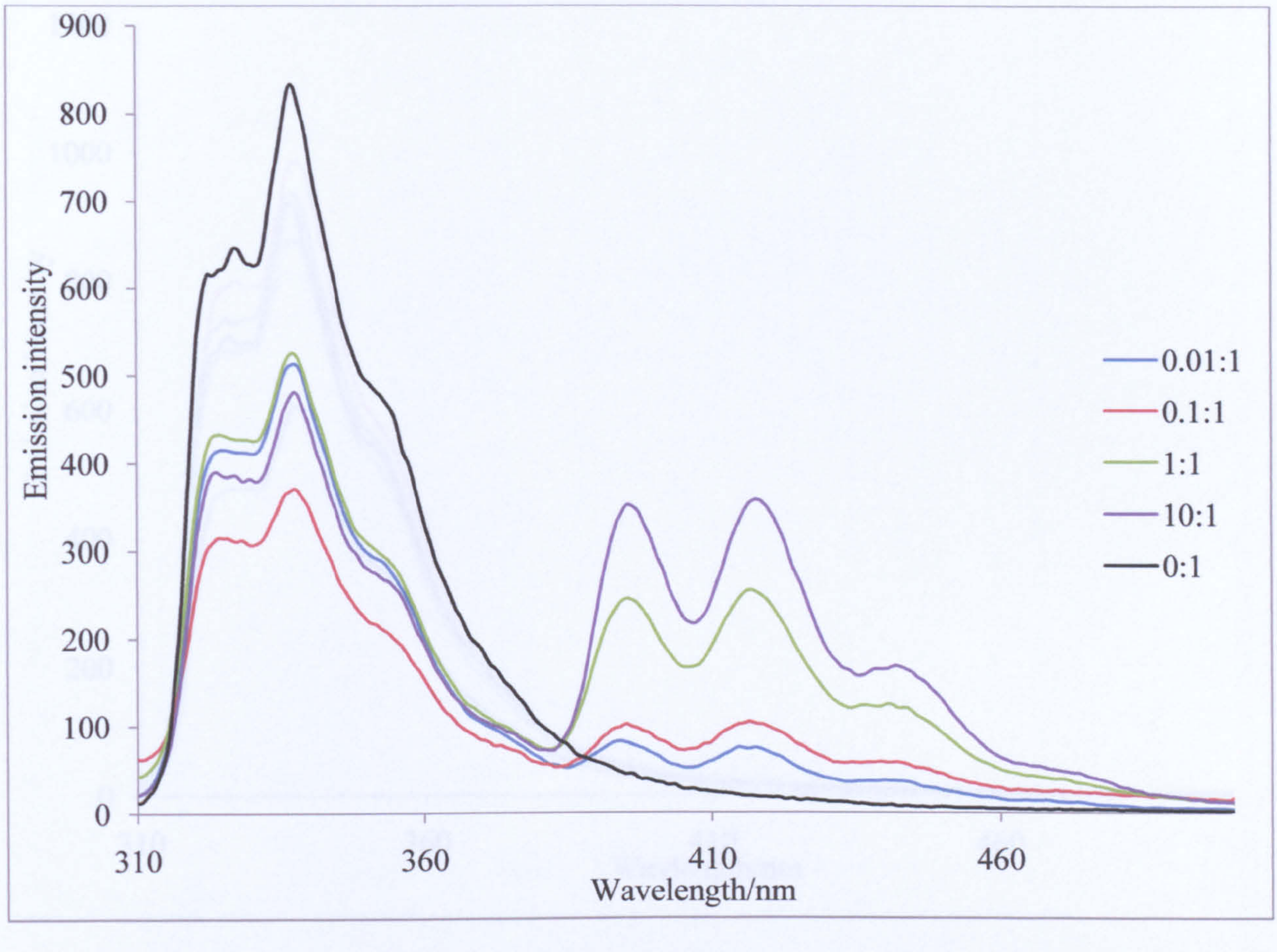

Figure 152: Emission spectra for an aqueous solution of ACE-PAA with increasing amounts of AMMA - PDMAEMA at pH 3 when excited at 290 nm.

At pH 10 on the other hand, the same polymer system shows an increase in the emission intensity of the ACE label and no emission at all from the AMMA label. (see figure 153) This indicates that under these conditions the AMMA label is outside the critical distance from ACE for sufficient energy transfer from ACE to occur. However because of the increase of the ACE emission clearly the addition of DMAEMA is having some effect on the polyacid.

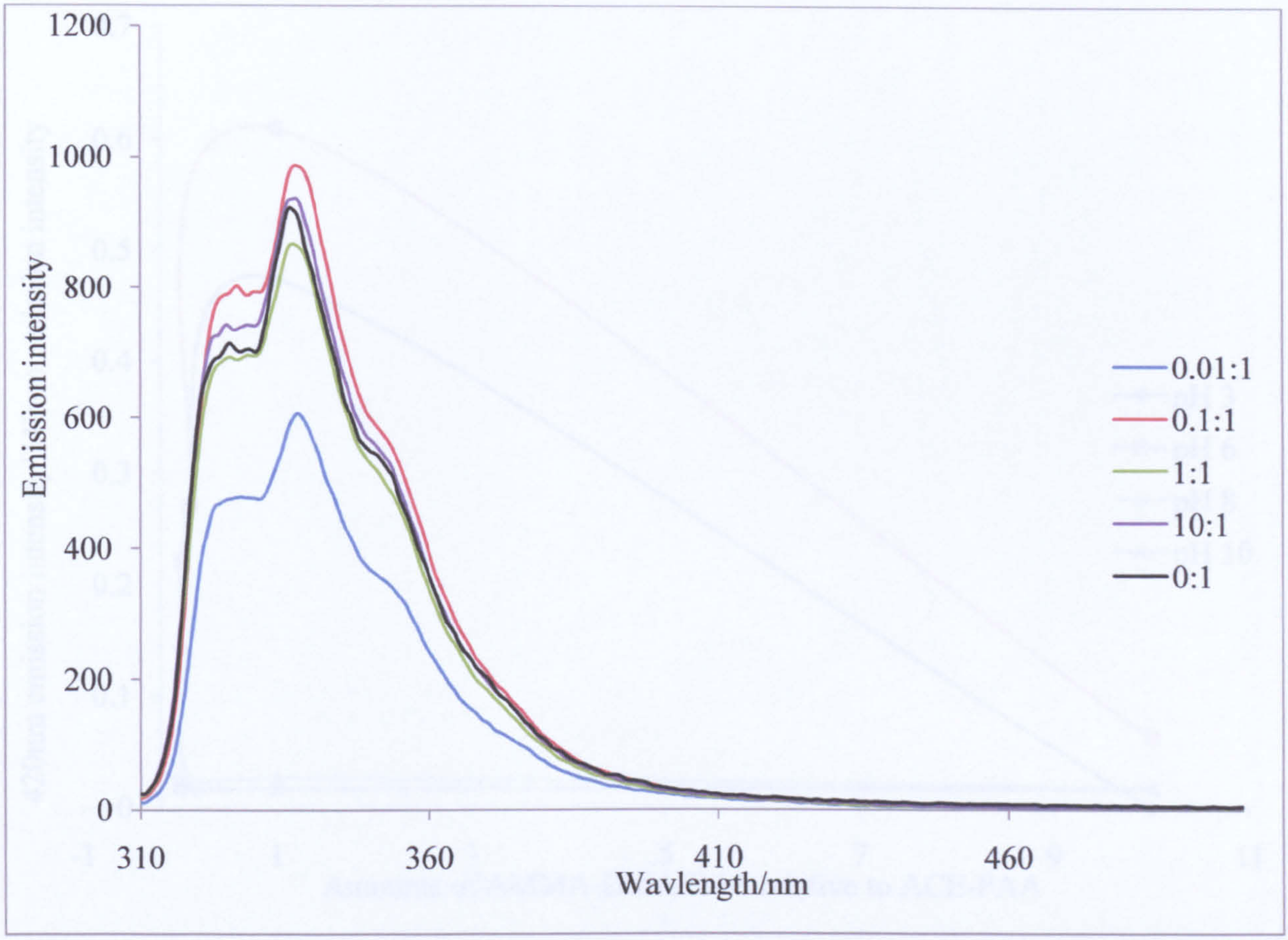

Figure 153: Emission spectra for an aqueous solution of ACE labelled PAA with increasing amounts of AMMA labelled PDMAEMA at pH 10 when excited at 290 nm.

The emission intensity ratio sampled at 420 nm and 340 nm was calculate for each polybase content and pH condition and is shown in figure 154.

At pH 3 and 6 the emission ratios for the PAA-ACE and AMMA-DMAEMA system show a sharp increase as the PDMAEMA concentration increases to 10^{-2} wt%. Once this concentration is exceeded there is a dramatic reduction in the intensity ratio which implies a greater sepraration distance between D and A.

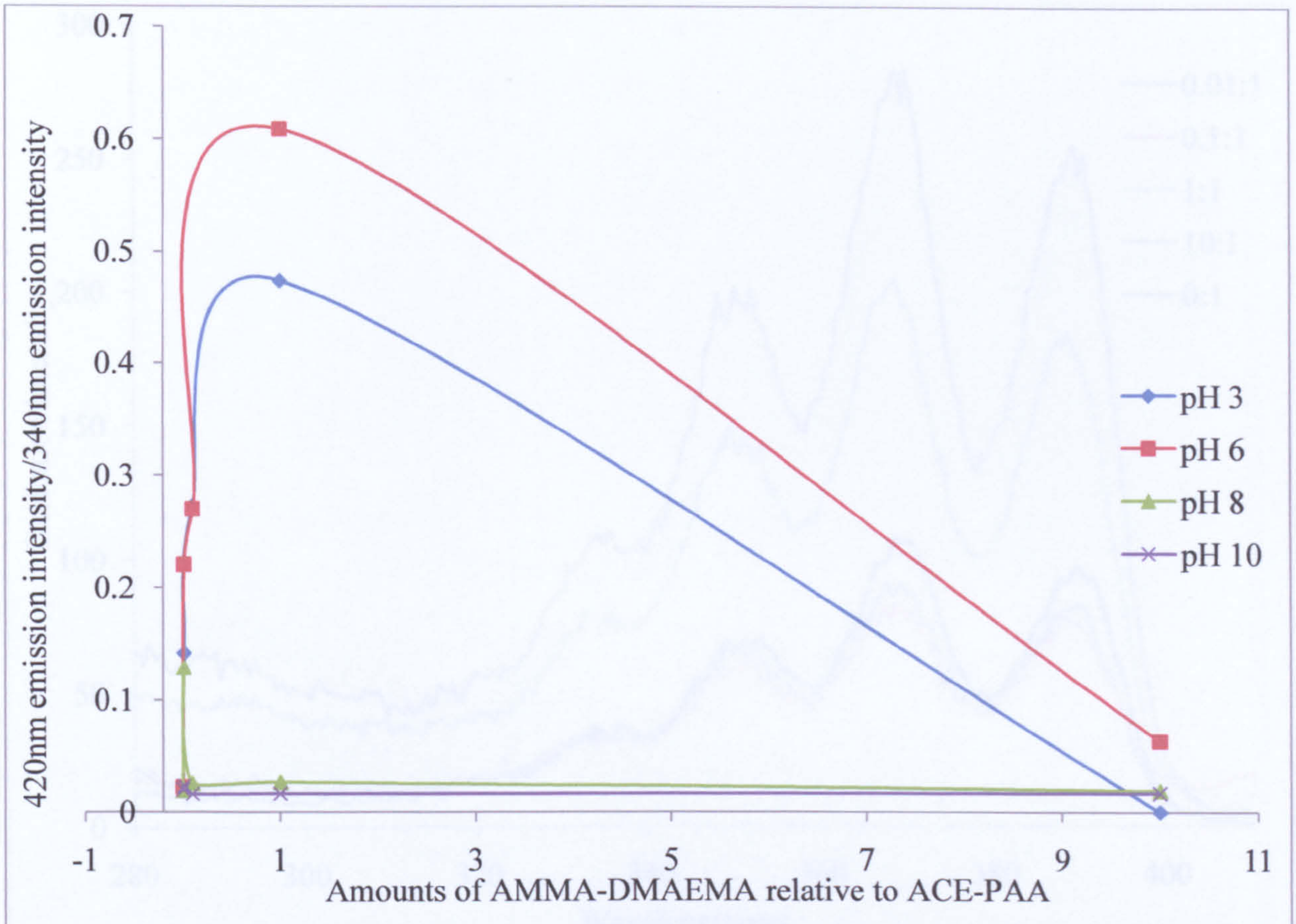

Figure 154: A plot of the emission intensity ratio between the AMMA emission at 420 nm and the ACE emission at 340 nm for an aqueous solution of ACE labelled PAA with increasing concentrations of an AMMA labelled PDMAEMA when excited at 290 at four different pH values.

Further examination of figure 154 reveals that at pH 8 and 10 there appears to be little change in the emission ratio with increasing PDMAEMA concentration. This suggests that at these pH values the ACE label is inaccessible to the AMMA acceptor.

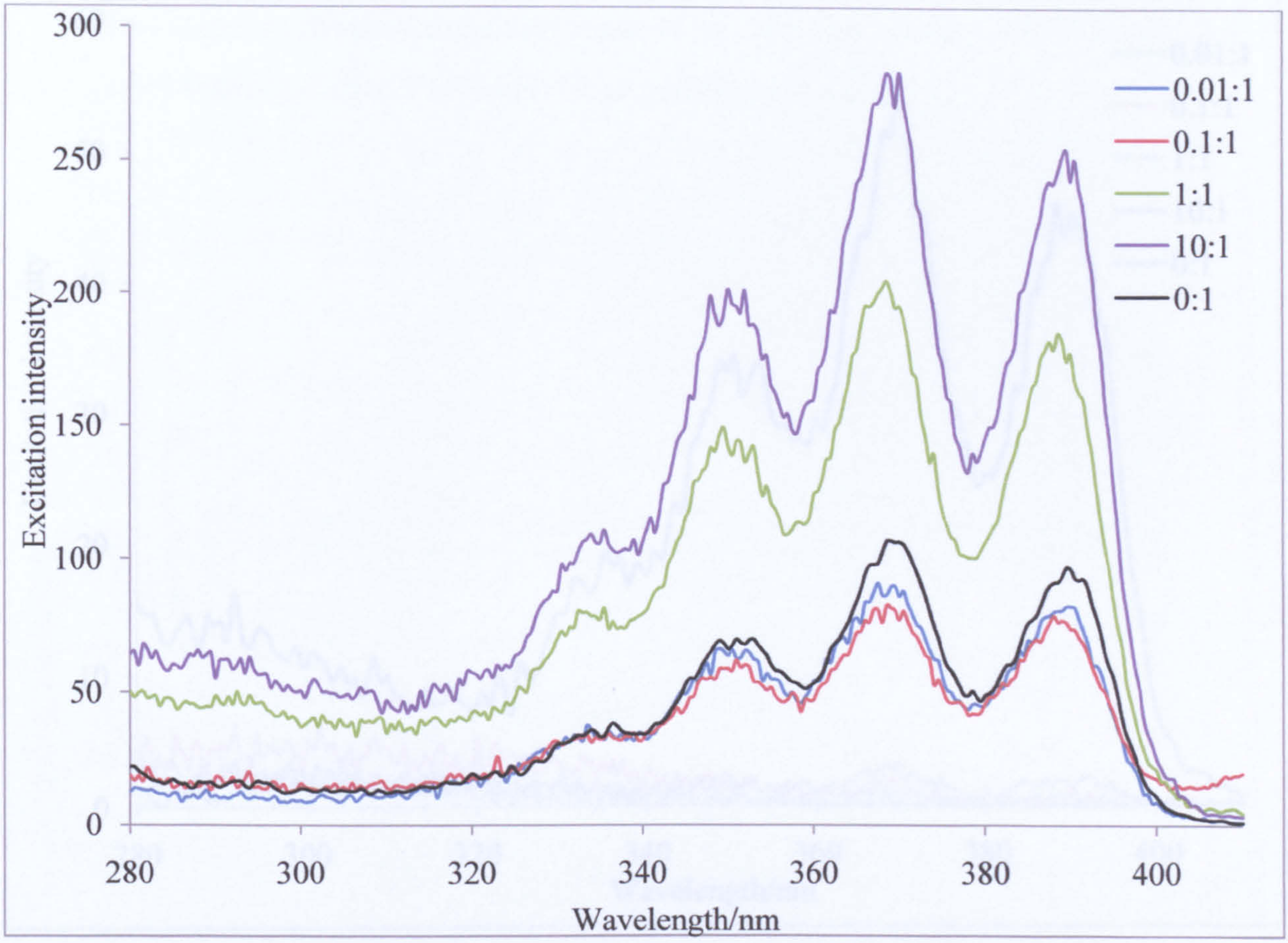

Figure 155: Excitation spectra for an aqueous solution of ACE labelled PAA with increasing amounts of AMMA labelled PDMAEMA at pH 3 when observed at 420 nm.

Figure 155 shows the effect of increasing concentrations of acceptor labelled polybase on the excitation spectra samples at 420 nm. Once a critical PDMAEMA content is reached (1:1 stoichiometric ratio) an enhanced contribution to the anthryl emission is apparent at ca. 300 nm. This suggests that there is an increase in energy transfer from ACE to AMMA which is consistent with the formation of an interpolymer complex.

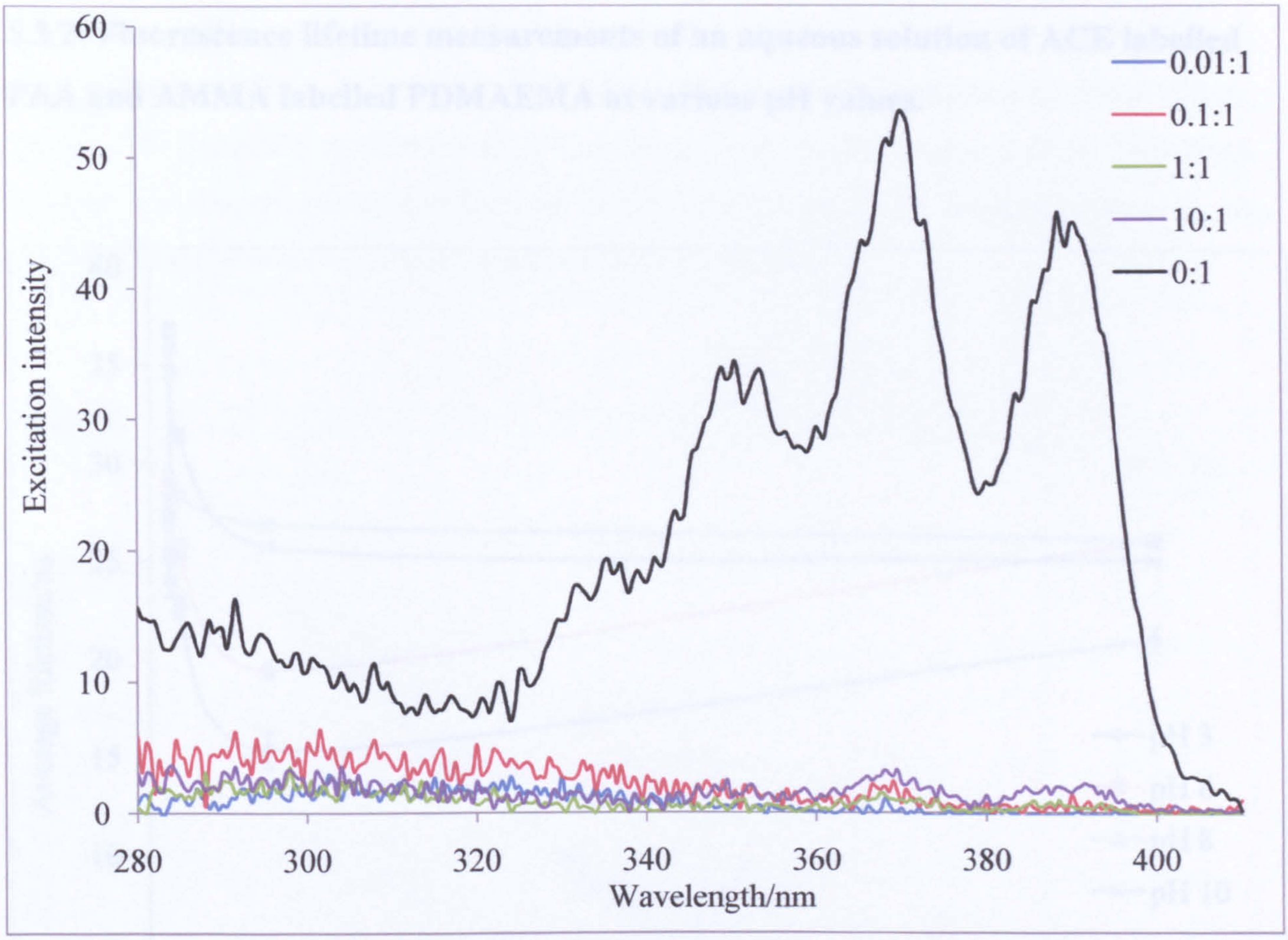

Figure 156: Excitation spectra for an aqueous solution of ACE labelled PAA with increasing amounts of AMMA labelled PDMAEMA at pH 10 when observed at 420 nm.

Consideration of the excitation spectra at pH 10 (figure 156) reveal that the situation is quite different compared to that at pH 3. For the PAA-ACE PDMAEMA-AMMA system the excitation of AMMA has almost entirely vanished, this is a much greater reduction than was seen in the ACE-AMMA-PDMAEMA system. It could be that addition of the unprotonated amine from the PDMAEMA acts as a quencher of the ACE-PAA fluorescence which interferes with the energy transfer experiment.

5.3.2: Fluorescence lifetime measurements of an aqueous solution of ACE labelled PAA and AMMA labelled PDMAEMA at various pH values.

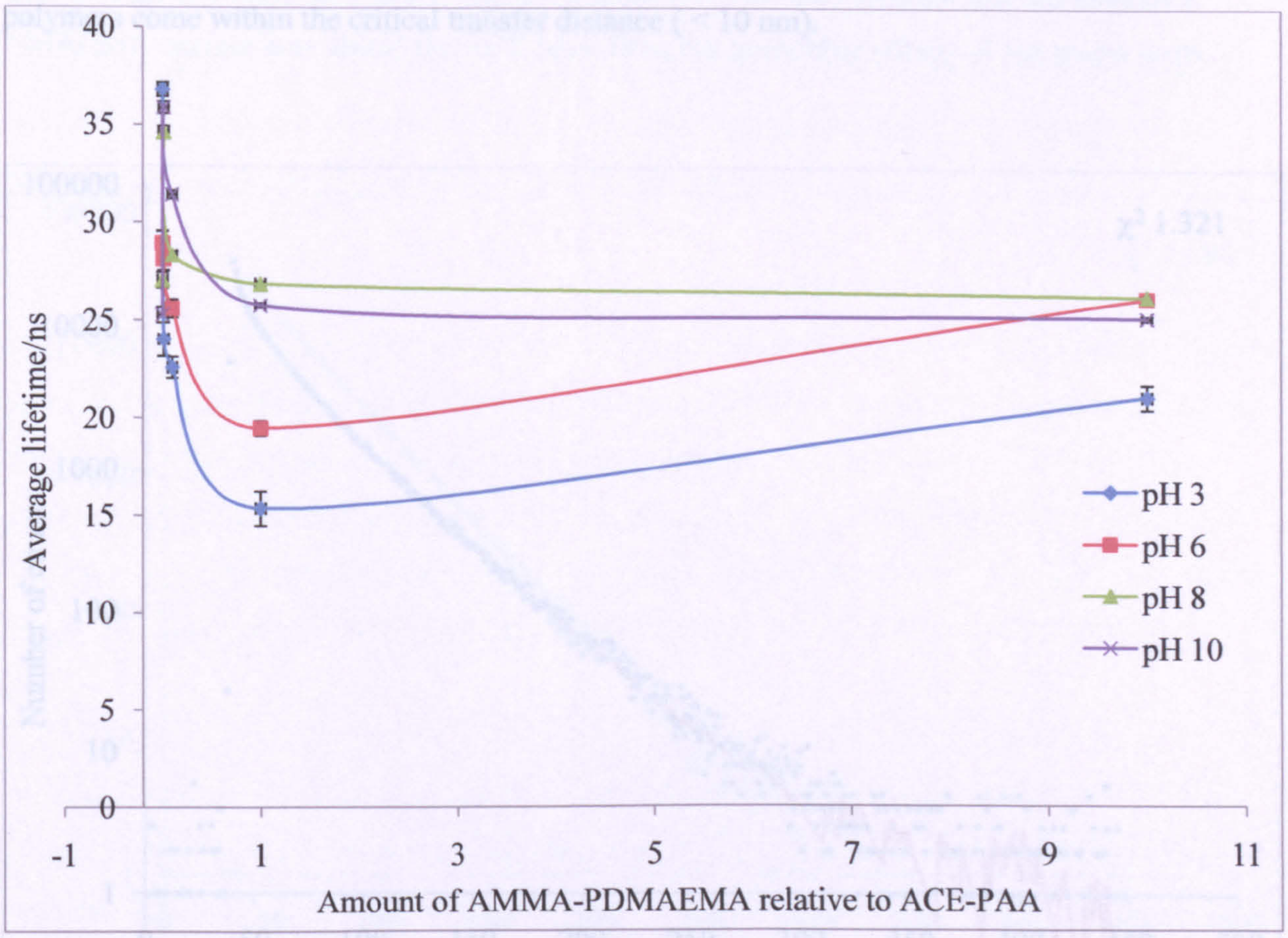

Figure 157: A plot of the average lifetime values of the ACE label in an aqueous solution of ACE-PAA with increasing amounts of AMMA-DMAEMA at four different pH values when excited at 290 nm and observed at 340 nm.

The lifetime data for the ACE labelled PAA with increasing concentration of AMMA labelled PDMAEMA was best fit with a triple exponential as in equation 1.3. This gave good statistical fits with χ^2 values close to unity, small standard deviations and randomly spread residuals. (for examples see figures 158 and 159.) The above plot shows the average lifetime obtained from equation 1.4 for the data for ease of comparison.

All values of pH show a decrease in the lifetime of the ACE label as the AMMA-PDMAEMA concentration is increased up to 10^{-2} wt%. This is consistent with the fact that the PDMAEMA can not only potentially quench the ACE fluorescence with the amine groups of the DMAEMA units but also through energy transfer from ACE to AMMA should the distance between the two polymers come within the critical transfer distance (< 10 nm).

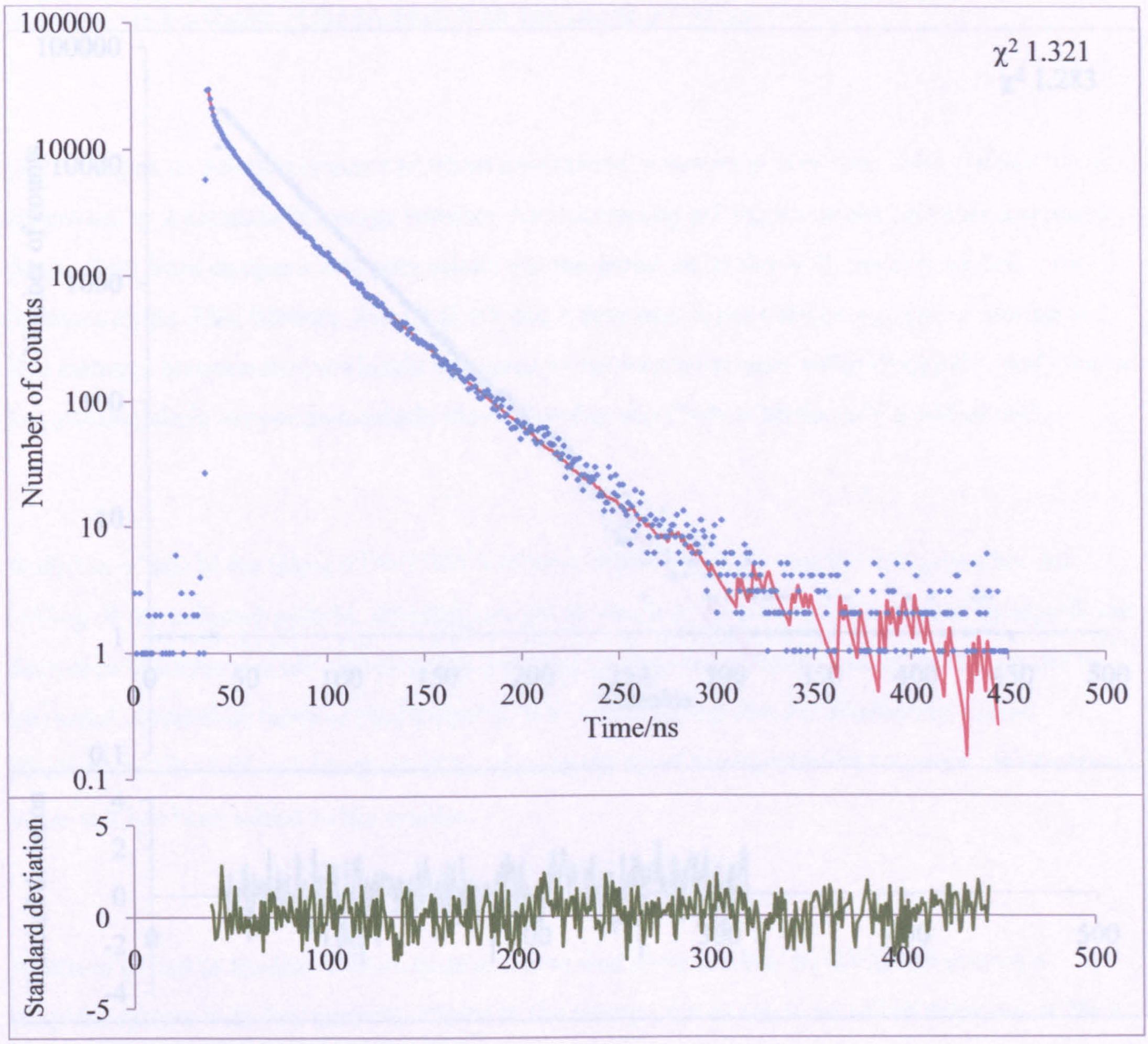

Figure 158: A fluorescence decay with corresponding mathematical fit (shown in red) and a plot of the resulting residuals for an aqueous solution of ACE-PAA with 10^{-4} wt% AMMA-PDMAEMA at pH 3.

Upon increasing the concentration of PDMAEMA further at pH 8 and 10 no change in the ACE lifetime is noted. This could indicate that the PAA-ACE sample is fully complexed by this stage. Further reference to figure 157 shows that at pHs 3 and 6 an increase in the lifetime of the ACE label at high concentrations of DMAEMA is apparent. This may indicate that the increased DMAEMA content may shield the ACE label from the quenching effects of the amine units.

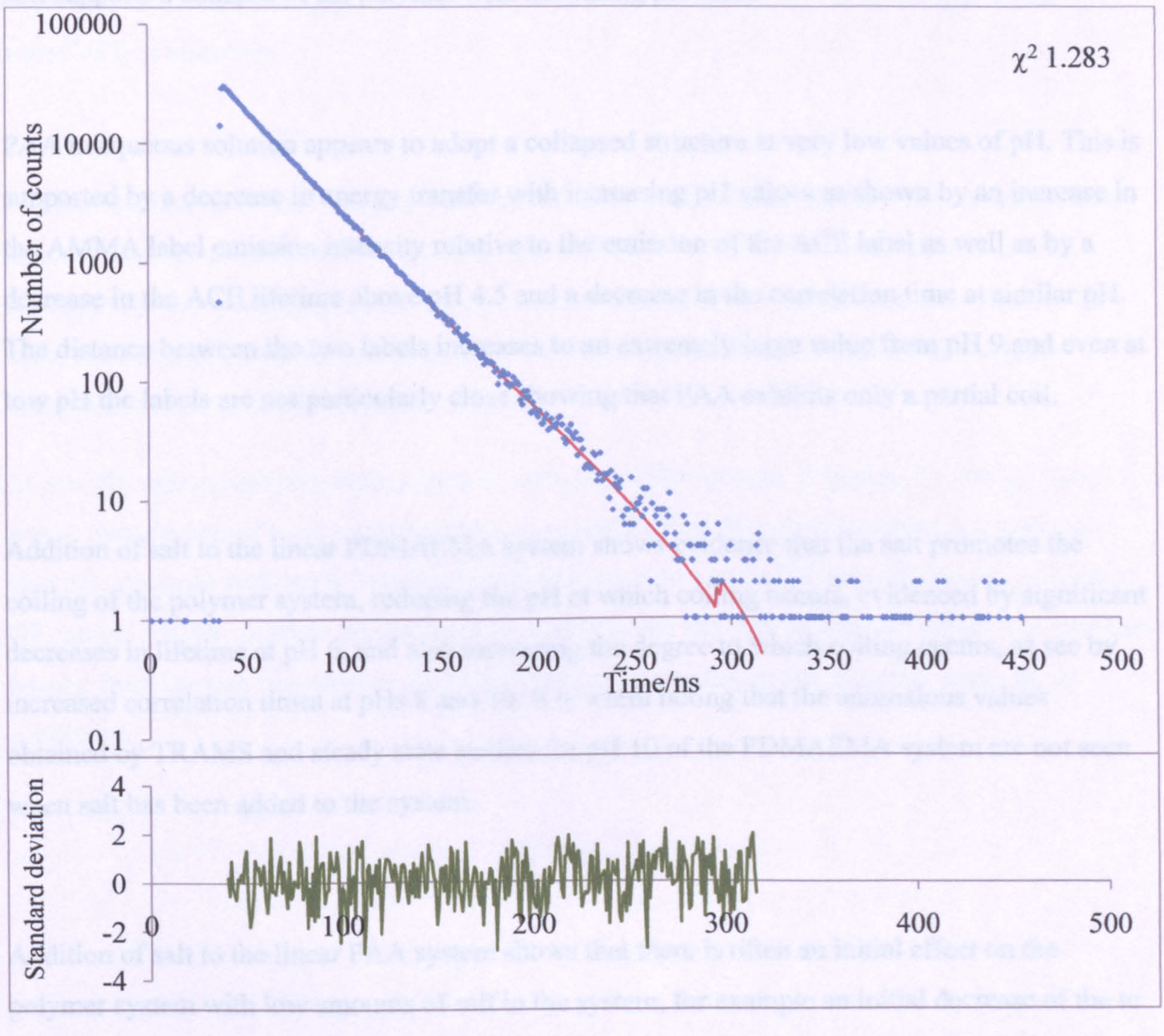

Figure 159: A fluorescence decay with corresponding mathematical fit (shown in red) and a plot of the resulting residuals for an aqueous solution of ACE-PAA with 10^{-1} wt% AMMA-PDMAEMA at pH 10.

Chapter 6: Conclusions.

PDMAEMA in aqueous solution shows an increase in the amount of energy transfer between ACE and AMMA labels with increasing pH. This collapse of the PDMAEMA backbone is supported by TRAMs studies which show a decrease in segmental mobility at the same pH range. Both fluorescence studies show an interesting decrease at a pH value of 10 that is as yet unexplained. This strange change is not seen in the fluorescence decay lifetime results, which still supports a collapse of the polymer with increasing pH value.

PAA in aqueous solution appears to adopt a collapsed structure at very low values of pH. This is supported by a decrease in energy transfer with increasing pH values as shown by an increase in the AMMA label emission intensity relative to the emission of the ACE label as well as by a decrease in the ACE lifetime above pH 4.5 and a decrease in the correlation time at similar pH. The distance between the two labels increases to an extremely large value from pH 9 and even at low pH the labels are not particularly close showing that PAA exhibits only a partial coil.

Addition of salt to the linear PDMAEMA system shows evidence that the salt promotes the coiling of the polymer system, reducing the pH at which coiling occurs, evidenced by significant decreases in lifetime at pH 6, and also increasing the degree to which coiling occurs, as see by increased correlation times at pHs 8 and 10. It is worth noting that the anomalous values obtained by TRAMS and steady state studies for pH 10 of the PDMAEMA system are not seen when salt has been added to the system.

Addition of salt to the linear PAA system shows that there is often an initial effect on the polymer system with low amounts of salt in the system, for example an initial decrease of the tc value, which is then is reversed as the salt concentrations increase further. This would seem to indicate that salt has two effects. One in small amounts, perhaps an ordering of the water molecules around the polymer system shielding the polymer to a degree from hydrophobic

effects, and another effect at high salt concentrations where coiling of the polymer system is significantly increased suggesting that it is possible that in normally uncoiled states ions alone the polymer backbone are effectively neutralised by association with salt ions promoting polymer collapse as the hydrophobic interacts dominate.

Both polymers show an increased affect from $CaCl_2$ than from NaCl, whether this is from a larger number of ions being present in the system or from the greater ionic strength introduced with $CaCl_2$ is unknown.

The interactions between PAA and PDMAEMA in double polymer systems are complex. Data indicates that the presence of a polyacid in the PDMAEMA system or a polybase in a PAA system definitely have an effect on the polymer conformations. Precipitation and other factors make the exact effect difficult to determine but there appears to be two different complex structures formed under differing conditions.

At low pH values both polymers appear to form a coil like system indicating by energy transfer levels, they do appear to be conjoined and it is possible that the actual structure is a loops and tails like structure with PAA forming loops complexed to a coiled PDMAEMA core. At higher pH values, ≥ 6 the structure appears to have changed and the data indicates a ladder like structure formed from the two polymers is the more likely conformation of the complex under these conditions.

Chapter 7: Future work.

Based off the work in this thesis there are many directions that research can be taken, including taking paths that were deemed too tangential for this piece of work.

Polymer brushes fluorescence: Although brushes of PDMAEMA labelled with a fluorophore were attempted the results were poor at best. It could be that the nature of the surface upon which the brush is grown is having an effect and causing large amounts of reflection in the fluorescence spectrophotometers. If a sufficiently optical transparent material with a low reflectivity can be found then further investigation in to the segmental motion of polymer brushes could be justified.

Similar polymer systems: Polydiethylaminoethyl methacrylate and polydimethylaminoethyl acrylate were both attempted for the work shown here however neither were obtained in a usable form, both polymers being difficult to isolate. Optimisation of the conditions for the radical initiated polymerisation for these two systems could provide two further polymers that can be investigated in comparison with PDMAEMA.

Further fluorescence: There are many further fluorescence measurements that could be taken on the polymer systems used above. Further techniques such as observing fluorescence quenching of the systems upon addition of a small molecule quencher could be used on the same polymer systems used above. Additionally labelling of the polymers with a fluorophore positioned at the end of the polymer chain could provide further insights in to the segmental motions of the polymers. Additionally given the observed behaviours of the polymer systems with increasing concentrations of salt and different ratios of two polymer systems further spectroscopy of these systems with intermediate concentrations of the salts and/or polymers could prove beneficial as could readings taken on two polymer systems in the presence of increasing concentrations of one or more salts.

References:

1. Gil, E.S. and Hudson, S.M., Progress is Polymer Science, 2004. **29**: p. 1173-1222.
2. Jeong, B. and Gutowska, A., Trends Biotechnol, 2002. **20**: p. 305-11.
3. Feng, Q.;Li, F.;Yan, Q.-Z.;Zhu, Y.-C. and and Ge, C.-C., Colloid Polym Sci, 2010(288).
4. Chee, C.K.;Ghiggino, K.P.;Smith, T.A.;Rimmer, S.;Soutar, I. and and Swanson, L., Polymer, 2001. **42**: p. 2235-2240.
5. Chee, C.K.;Rimmer, S.;Soutar, I. and and Swanson, L., Polymer, 1996. **38**: p. 483-486.
6. Cristiano, C.M.Z.;Soldi, V.;Li, C.;Armes, S.P.;Rochas, C.;Pignot-Paintrand, I. and Borsali, R., Macromol. Chem. Phys. , 2009(210): p. 1726-1733.
7. Wang, P.;He, J.;Wang, P.-N. and and Chen, J.-Y., Photomedicine and Laser Surgery, 2010. **28**(2).
8. Ishida, N. and and Biggs, S., Macromolecules, 2010.
9. Hu, X.;Tong, Z. and Lyon, L.A., 2010.
10. Dai, S.;Ravi, P. and Tam, K.C., Soft Matter, 2008. **4**: p. 435-449.
11. Kita, Y.;Futagawa, H.;Inaki, Y. and and Takemoto, K., Polymer Bulletin 2, 1980: p. 195-199.
12. Pelet, J.M. and and Putnam, D., Macromolecules, 2009. **42**: p. 1494-1499.
13. Pamell, A.J.;Martin, S.J.;Dang, C.C.;Geoghegan, M.;Jones, R.A.L.;Crook, C.J.;Howse, J.R. and J., a.R.A., Polymer, 2009. **50**: p. 1005-1014.
14. Flint, N.J.;Haywood, R.;Soutar, I. and And Swanson, L., Journal of fluorescence 1998. **8**: p. 327-333.
15. Anghel, D.F.;Toca-Herrera, J.L.;Winnik, F.M.;Rettig, W. and and Klitzing, R., Langmuir, 2002. **18**: p. 5600-5606.
16. Soutar, I.;Jones, C.;Lucas, D.M. and and Swanson, L., Journal of photochemistry and photobiology A: Chemistry, 1996. **102**: p. 87-92.
17. Sternberg, M. and and Hershberg, D., Biochimica et biophysica acta, 1974. **342**: p. 195-206.
18. Takakgishi, T.;Hosokawa, T. and Hatanaka, Y., Journal of Polymer Science; Part A: Polymer Chemistry, 1989. **27**: p. 1-13.
19. Přadnỳ, M. and Ševčik, S., Makromol Chem

1985. **186**: p. 111-121.

20. PolySciences Inc, *Technical datasheet 213: N,N Dimethylaminoethyl methacrylate*.
21. Přadnỳ, M. and Ševčik, S., Rapid Commun, Makromol Chem, 1984. **5**: p. 37-41.
22. Morawetz, H., Macromolecules, 1996(29): p. 2689-2690.
23. Ruiz-Perez, L.;Pryke, A.;Sommer, M.;Battaglia, G.;Soutar, I.;Swanson, L. and and Geoghegan, M., Macromolecules, 2008. **41**: p. 2203-2211.
24. Peterson, C.M.;Lu, J.M.;Sun, Y.;Peterson, C.A.;Shiah, J.G.;Straight, R.C. and Kopecek, J., Cancer Res, 1996. **56**: p. 3980-3985.
25. Murthy, N.;Campbell, J.;Fausto, N.;Hoffman, A.S. and Stayton, P.S., J. Controlled Release, 2003. **89**: p. 365-374.
26. Liu, M.;Kono, K. and Frechet, J.M.J., J. Controlled Release

2000. **65**: p. 121-131.

27. Torchilin, V.P. and Weissig, V., J. Controlled Release, 2001. **73**: p. 137-172.

28. Monsky, W.L.;Fukumura, D.;Gohongi, T.;Aneukiewez, M.;Weich, H.A.;Torchilin, V.P. and Jain, R.K., Cancer Res, 1999. **59**: p. 4129-4135.
29. Jain, R.K., J. Controlled Release, 2001. **74**: p. 7-25.
30. Yuan, F.;Dellian, M.;Fukumura, D.;Leuning, M.;Berk, D.D.;P., T.V. and Jain, R.K., Cancer Res, 1995. **55**: p. 3752-3756.
31. Nishiyama, N.;Okazakim S;Cabral, H.;Miyamoto, M.;Kato, Y.;Sugiyama, Y.;Nishio, K.;Matsumura, Y. and Kataoka, K., Cancer Res, 2003. **63**: p. 8977-8983.
32. Kwom, G.;Naito, M.;Yokoyama, M.;Okano, T.;Sakurai, Y. and Kataoka, K., J. Controlled Release, 1997. **48**: p. 195-201.
33. Yokoyama, M.;Fukushima, S.;Uehara, R.;Okamoto, K.;Kataoka, K.;Sakurai, Y. and Okana, T., J. Controlled Release, 1998. **50**: p. 79-92.
34. Potineni, A.;Lynn, D.M.;Langer, R. and Amiji, M.M., J. Controlled Release, 2003. **86**: p. 223-234.
35. Mori, H.;Walther, A.;Andre, X.;Lanzendorfer, M.G. and Muller, A.H.E., Macromolecules, 2004. **37**: p. 2054-2066.
36. Butun, V.;Armes, S.P. and Bilingham, N.C., Polymer, 2001. **42**: p. 5993-6008.
37. Katchalsky, A.;Mazur, J. and Spitnik, P., J. Polymer Sci, 1957. **23**.
38. Zaslawsky, J.Z. and Fischer, E., J. Phys. Chem, 1963. **67**.
39. Bolto, B.A., Prog Polym Sci, 1995. **20**: p. 987-1041.
40. Oliverira, P.C.;Guimaraes, A.;Cavaille, J.V.;Chazeau, L.;Gilbert, R.G. and Santos, A.M., Polymer, 2005. **46**: p. 1105-1111.
41. Zhang, X.;Xia, J. and Matyjaszewski, K., Macromolecules, 1998. **31**: p. 5167-5169.
42. Cho, S.H.;Jhon, M.S.;Yuk, S.H. and and Lee, H., J. Polym. Sci. Part B: Polym Phys, 1997. **35**.
43. Hui, H.;Xiao-dong, F. and Zhong-lin, C., Polymer, 2005. **46**: p. 9514-9522.
44. Siegel, R.A. and Firestone, B.A., Macromolecules, 1988. **21**.
45. Cornejo-Bravo, J.M. and Siegel, R.A., Biomaterials, 1996. **17**.
46. Hariharan, D. and Peppas, N.A., Polymer, 1996. **37**.
47. Siegel, R.A.;Falmarzian, M.;Firestone, B.A. and Moxley, B.C., J. Controlled Release, 1988. **8**
48. Shahalom, S.;Tong, T.;Emmett, S. and Saunders, B., Langmuir, 2006. **22** p. 8311-8317.
49. Baines, F.L.;Armes, S.P.;Billingham, N. and Tuzar, Z., Macromolecules, 1996. **29**.
50. Chen, W.Y.;Alexandridis, P.;Su, C.K.;Patrickios, C.S.;Hertler, W.R. and Hatton, T.A., Macromolecules, 1995. **28**.
51. Patrickios, C.S.;Hertler, W.R.;Abbot, N.L. and Hatton, T.A., Macromolecules, 1994. **27**.
52. Zhang, Z.;Liu, G. and Bell, S., Macromolecules, 2000. **33**: p. 7877-7883.
53. Zhang, X. and Matyjaszewski, K., Macromolecules, 1999. **32**.
54. Pitsikalis, M.;Sakali-Kioulafa, E. and Hadjichristidis, N., J Polym Sci, Part A: Polym Chem, 2004. **42**.
55. Sanjuan, S.;Perrin, P.;Pantoustier, N. and and Tran, Y., Langmuir, 2007. **23**: p. 5769-5778.
56. Kobayashi, M.;Yamaguchi, H.;Terayama, Y.;Wang, Z.;Ishihara, K.;Hino, M. and and Takahara, A., Macromol. Symp, 2009. **279**: p. 79-87.

57. Ghiggino, K., P.; and Tan, K.L., *Polymer Photophysics*. 1985, London: Phillips,D: Chapman and Hall:.
58. Soutar, I.;Swanson, L.;Imhof, R.E. and Rumbles, G., Macromolecules, 1992. **25**: p. 4399-4405.
59. Vasilescu, M. and and Anghel, D.F., Langmuir, 1997. **13**: p. 6951-6955.
60. Seixas de Melo, J.;Costa, T.;Miguel, M.;Lindman, B. and and Schillen, K., J. Phys. Chem. B, 2003. **107**: p. 12605-12621.
61. Soutar, I. and And Swanson, L., Macromolecules, 1992. **25**: p. 4399-4405.
62. Heyward, J.J. and Ghiggino, K.P., Macromolecules, 1989. **22**.
63. Soutar, I. and Swanson, L., Macromolecules, 1990. **23**.
64. Blay, G.A.;Borjas, R.E.;Hughes, S.;Maddox, P.;Rice, K.;Stansbury, W. and and Laurel, N., Journal of Applied Polymer Science, 1999. **73**: p. 1097-1115.
65. Kriz, J.;Masar, B.;Plestil, J.;Tuzar, Z.;Pospisil, H. and Doskocilova, D., Macromolecules, 1998. **31**: p. 41-51.
66. Treat, N.D.;Ayres, N.;Boyes, S.G. and Brittain, W.J., Macromolecules, 2006. **39**: p. 26-29.
67. Milner, S.T., Science, 1991. **251**.
68. Topham, P.D.;Howse, J.R.;Crook, C.J.;Parnell, A.J.;Geoghegan, M.;Jones, R.A.L. and Ryan, A., Polym Int, 2006. **55**: p. 808-815.
69. Iwata, H.;Hirata, I. and Ikada, Y., Macromolecules, 1998. **31**.
70. Huber, D.L.;Manginell, R.P.;Samara, M.A.;Kim, B.-I. and Bunker, B.C., Science, 2003. **301**.
71. Zeng, F.;Shen, Y.;Zhu, S. and Pelton, R., Macromolecules, 2000. **33**.
72. Zeng, F.;Shen, Y.;Zhu, S. and Pelton, R., J. Polym. Sci. Part A. Polym Chem, 2000. **38**.
73. Lakowicz, J.R., *Principles of Fluorescence Spectroscopy. Third ed.* 2006, Singapore: Springer.
74. Soutar, I., Polymer international, 1991. **26**: p. 35-49.
75. Olea, A.;Rosenbluth, H. and Thomas, J., Macromolecules, 1999. **32**: p. 8077-8083.
76. Kalyanasundaram, K. and Thomas, J., Journal of the American chemical society, 1977. **99**.
77. Soutar, I. and Swanson, L., Macromolecules, 1994. **27**.
78. Chee, C.K.;Rimmer, S.;Soutar, I. and Swanson, L., Polymer, 2001. **42**: p. 5079-5087.
79. Stryer, L., Ann. Rev. Bochem, 1978. **47**: p. 819-846.
80. Forster, T. and Translated by Knox. R. L. , Ann Phys, 1948. **2**: p. 55-75.
81. Guillet, J.E. and Liu, G., Macromolecules, 1990. **23**: p. 1388-1392.
82. Guillet, J.E.;Liu, G.;Al-Takrity, E.T.B.;Jenkins, A.D. and Walton, D.R.M., Macromolecules, 1990. **23**: p. 1393-1401.
83. Guillet, J.E. and Liu, G., Macromolecules, 1990. **23**: p. 2969-2973.
84. Guillet, J.E. and Liu, G., Macromolecules, 1990. **23**: p. 2973-2977.
85. Guillet, J.E.;Liu, G.;Al-Takrity, E.T.B.;Jenkins, A.D. and Walton, D.R.M., Macromolecules, 1990. **23**: p. 4164-4167.
86. Guillet, J.E.;Liu, G.;Al-Takrity, E.T.B.;Jenkins, A.D. and Walton, D.R.M., Macromolecules, 1991. **24**: p. 68-74.
87. Swanson, L., Private Internal Communication, University of Sheffield.
88. Huang, K.H.;Fairclough, R.H. and Cantor, C.R.J., Mol. Biol, 1975. **97**.
89. Papadakis, N. and Hammes, G.G., Biochemistry, 1977. **16**.

90. Chee, C.K.;Rimmer, S.;Rutkaite, R.;Soutar, I. and And Swanson, L., Journal of photochemistry and photobiology A: Chemistry, 2006. **180**: p. 1-8.
91. Flint, N.J.;Gardebrecht, S. and And Swanson, L., Journal of Fluorescence, 1998. **8**: p. 343-353.
92. Chee, C.K.;Rimmer, S.;Soutar, I. and and Swanson, L., Reactive and functional polymers, 2006. **66**: p. 1-11.
93. Soutar, I. and And Swanson, L., Polym Int, 2006. **55**: p. 729-739.
94. Rutkaite, R.;Swanson, L.;Li, Y. and and Armes, S.P., Polymer, 2008. **49**: p. 1800-1811.
95. Soutar, I.;swanson, L.;Thorpe, G.F. and and Zhu, C., Macromolecules, 1996. **29**: p. 918-924.
96. Soutar, I. and and Swanson, L., Macromolecules, 1994. **27**: p. 4304-4311.
97. Marsh, A.J.;Rumbles, G.;Soutar, I. and Swanson, L., Chemical Physics Letters, 1992. **195**.
98. Hall, N.F. and Sprinkle, M.R., J Am Chem Soc, 1992. **54**.
99. Chen, H.L. and Morawetz, H., Macromolecules, 1982. **15**.
100. Bednar, B.;Li, Z.;Huang, Y.;Chang, L.C.P. and Morawetz, H., Macromolecules, 1985. **18**: p. 1829-1833.
101. Oyama, H.T.;Tang, W.T. and Frank, C.W., Macromolecules, 1987. **20**.
102. Wang, Y. and Morawetz, H., Macromolecules, 1989. **22**: p. 164-167.
103. Tsuchida, E. and Nishide, H., Adv Polym Sci, 1977. **24**: p. 1-87.
104. Chen, H.L. and Morawetz, H., Eur Polym J, 1983. **19**: p. 923-928.
105. Thalhammer, A., *Unpublished internal report*. 2002, The University of Sheffield.
106. Chen, X.Y. and Armes, S.P., Langmuir, 2004. **20**: p. 587-595.
107. Winnik, M.A.;Bystryak, S.M. and Lie, Z., Macromolecules, 1998. **31**: p. 6855-6864.
108. Sysocki, S.;Karolczak, S. and Fouracre, R.A., Radiation physics and chemistry, 1999. **54**: p. 189-191.
109. Webber, S., Chem Rev, 1990. **90**: p. 1469-1482.
110. Lee, N.K. and and Obukhov, S., Europhys. Lett, 2004. **66**: p. 350-356.

Appendix A: NMR

DMAEMA-ACE

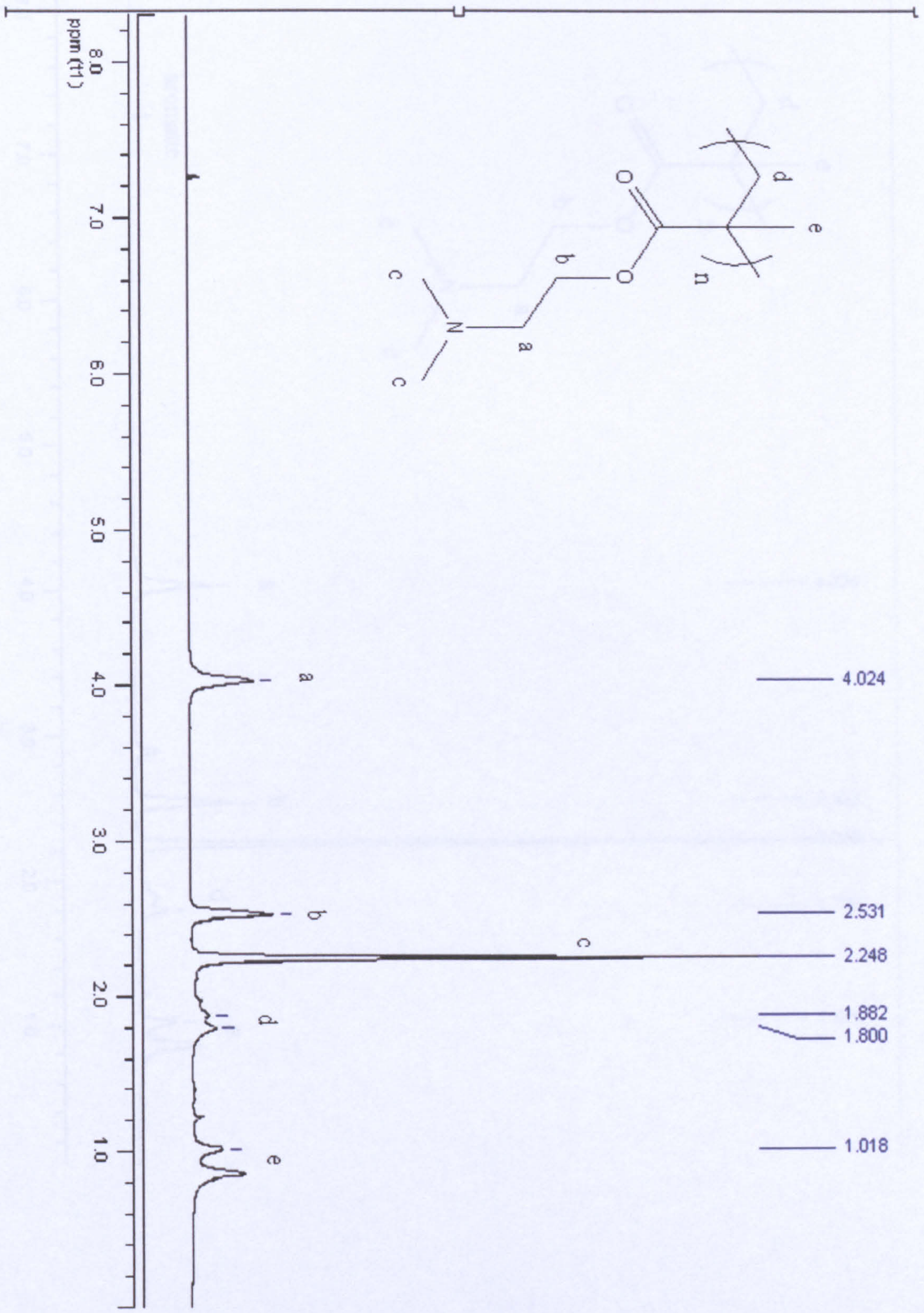

DMAEMA-ACE-AMMA

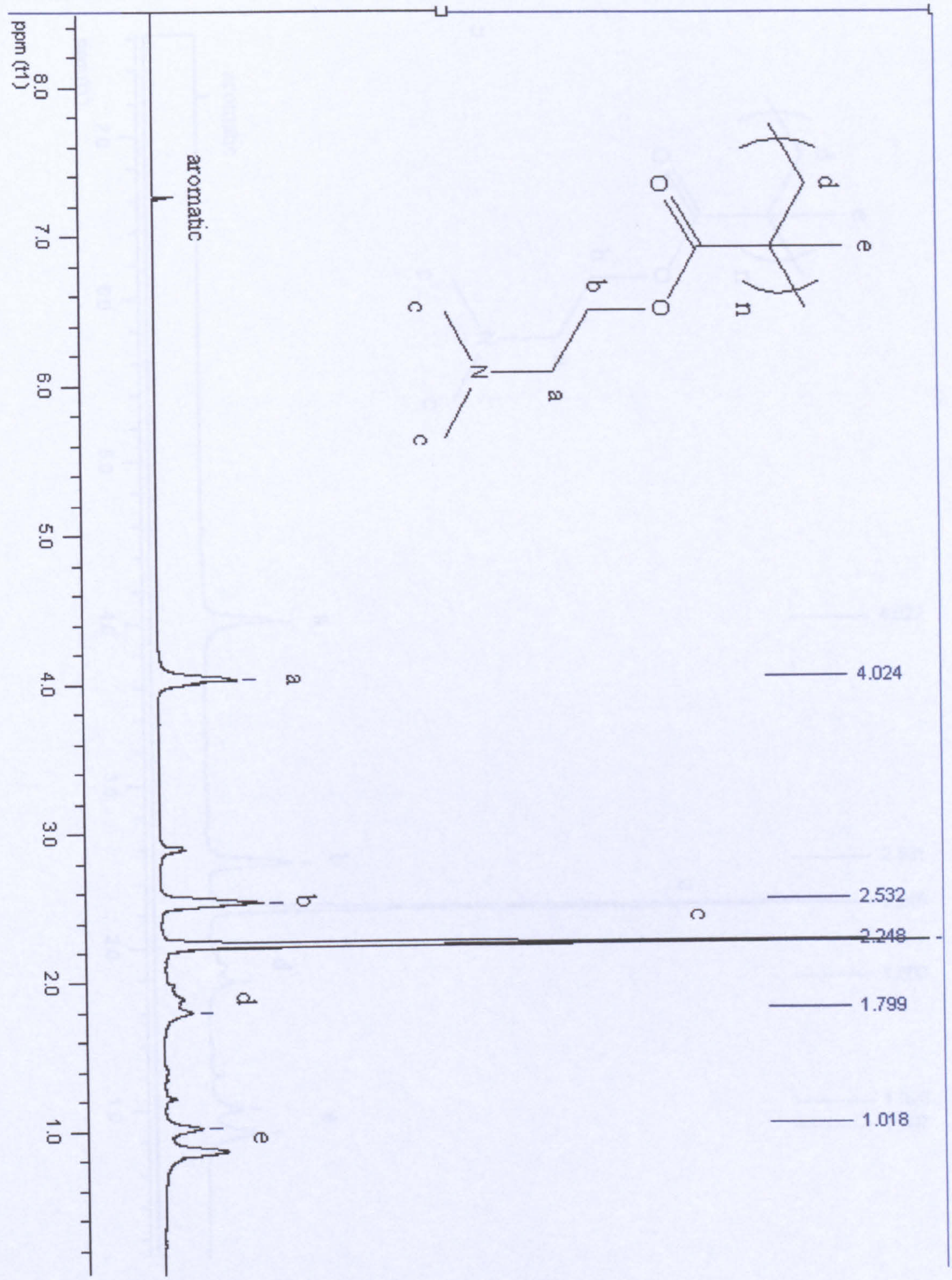

DMAEMA-AMMA

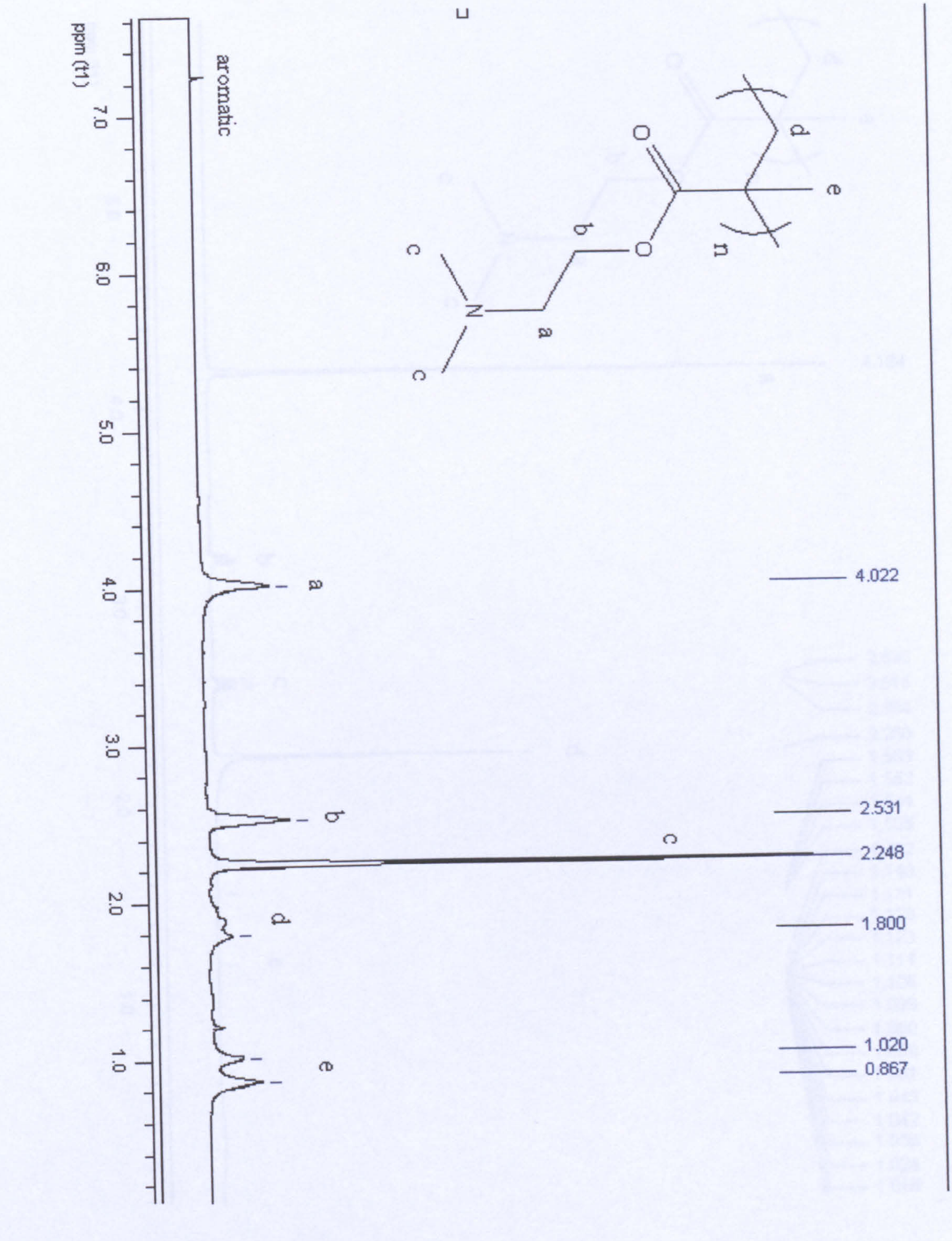
aromatic
ppm (t1)
7.0
6.0
5.0
4.0
3.0
2.0
1.0
a
b
c
d
e
4.022
2.531
2.248
1.800
1.020
0.867

DMAEMA-no label

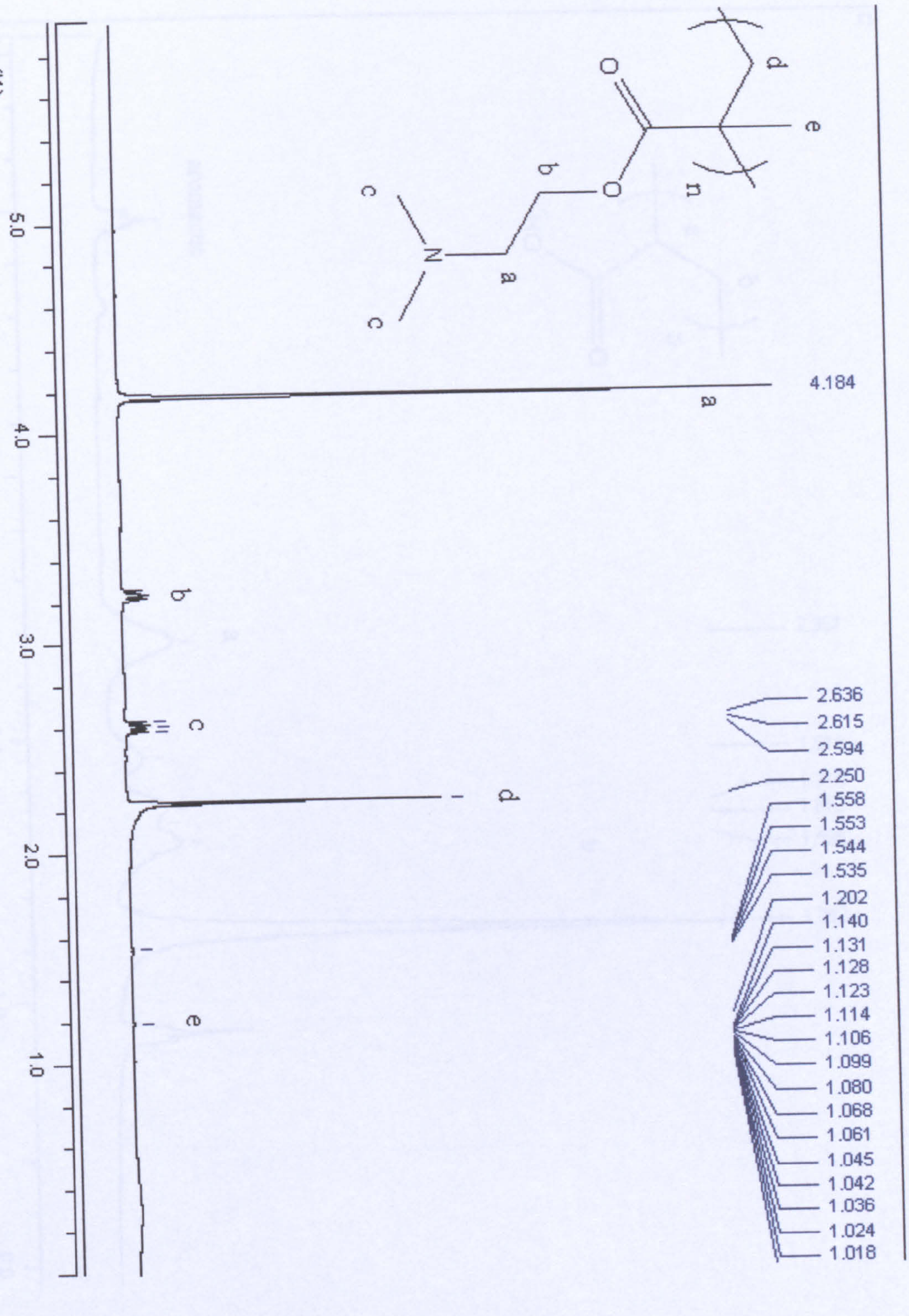

PAA-ACE

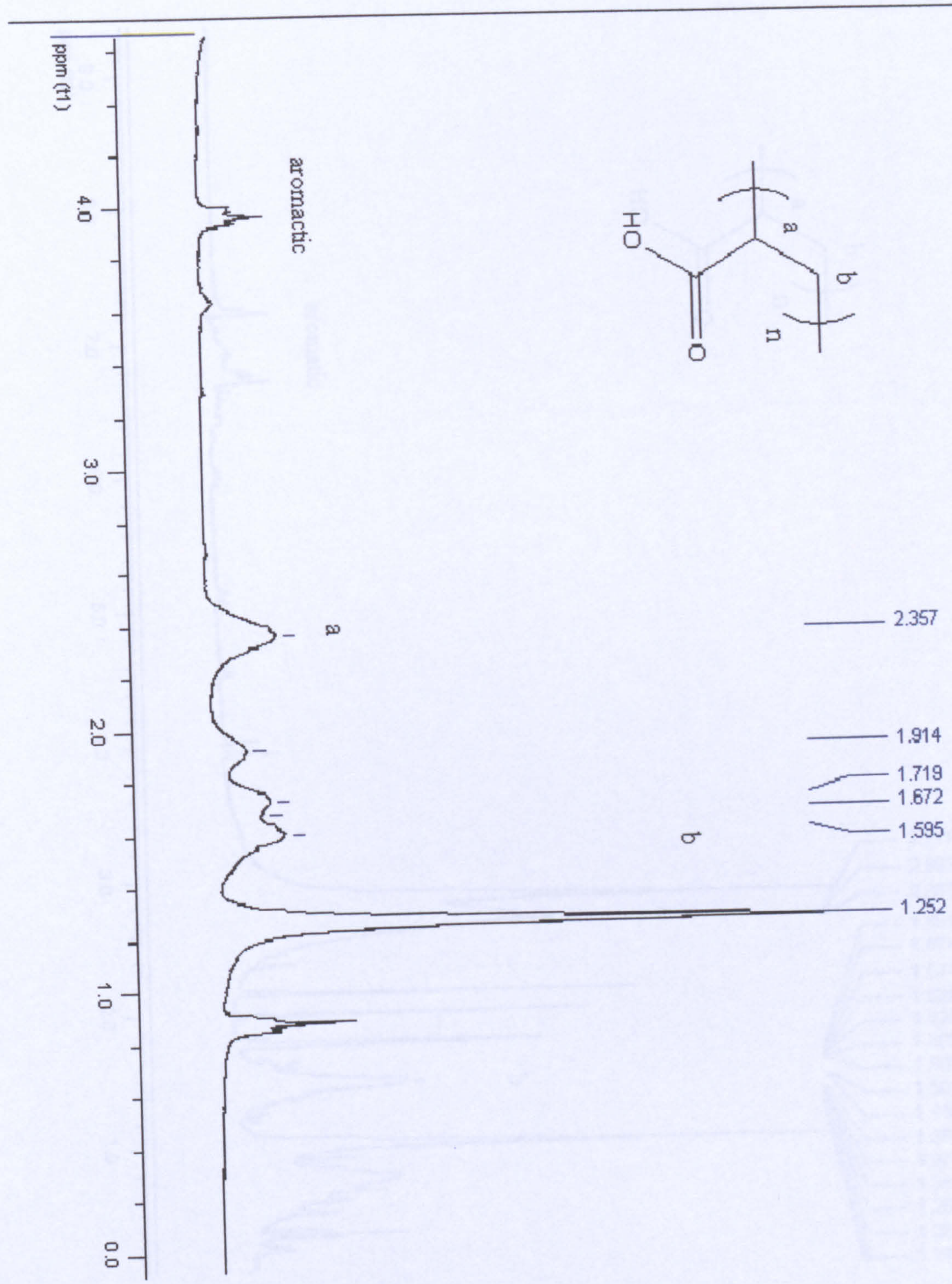
HO
a
b
n
C=O
aromactic
a
b
σ
2.357
1.914
1.719
1.672
1.595
1.252
ppm (t1)
4.0
3.0
2.0
1.0
0.0

PAA-ACE-AMMA

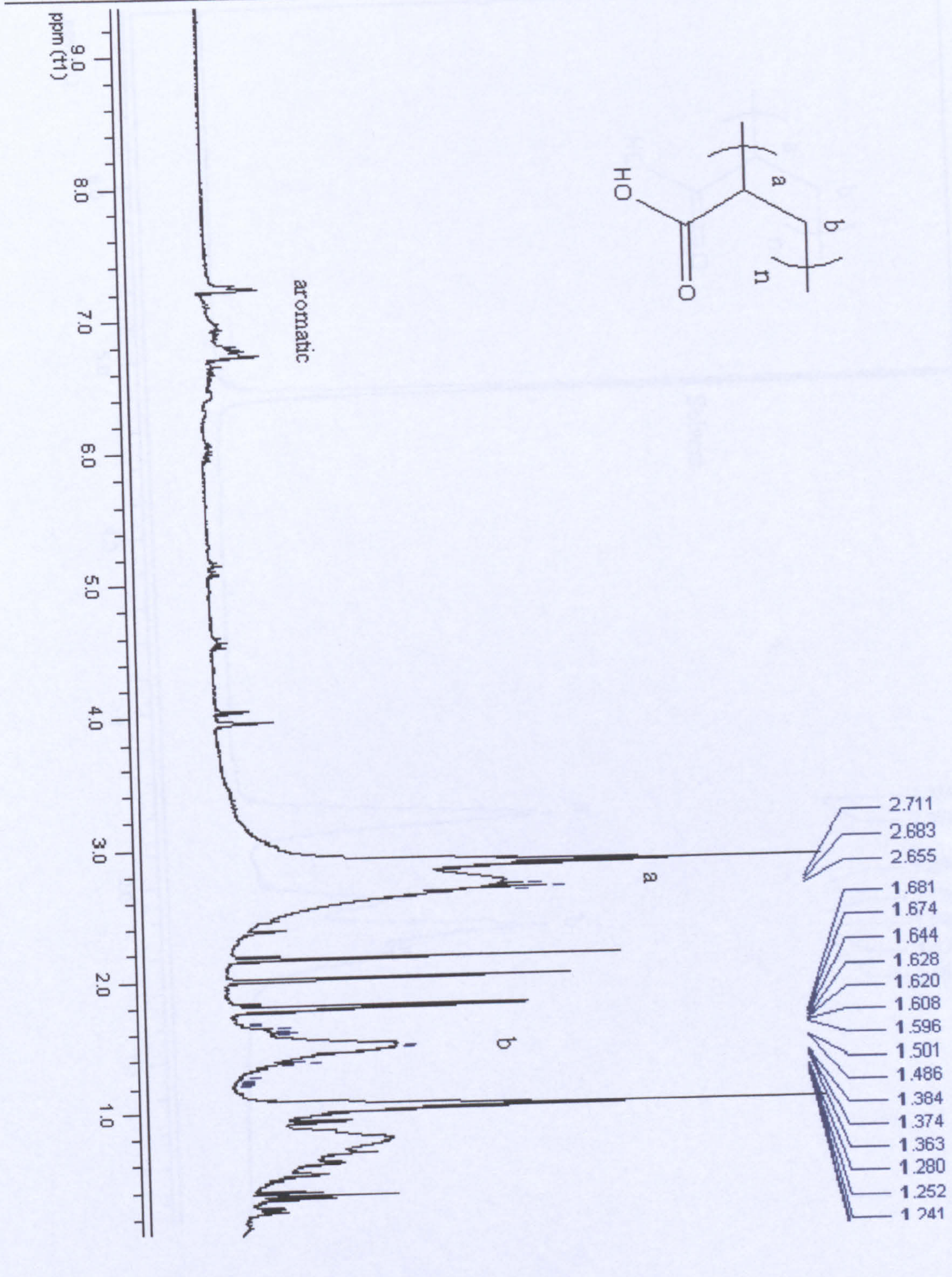
HO
O
a
b
n
aromatic
ppm (t1)
9.0
8.0
7.0
6.0
5.0
4.0
3.0
2.0
1.0
2.711
2.683
2.655
1.681
1.674
1.644
1.628
1.620
1.608
1.596
1.501
1.486
1.384
1.374
1.363
1.280
1.252
1.241

PAA-no label

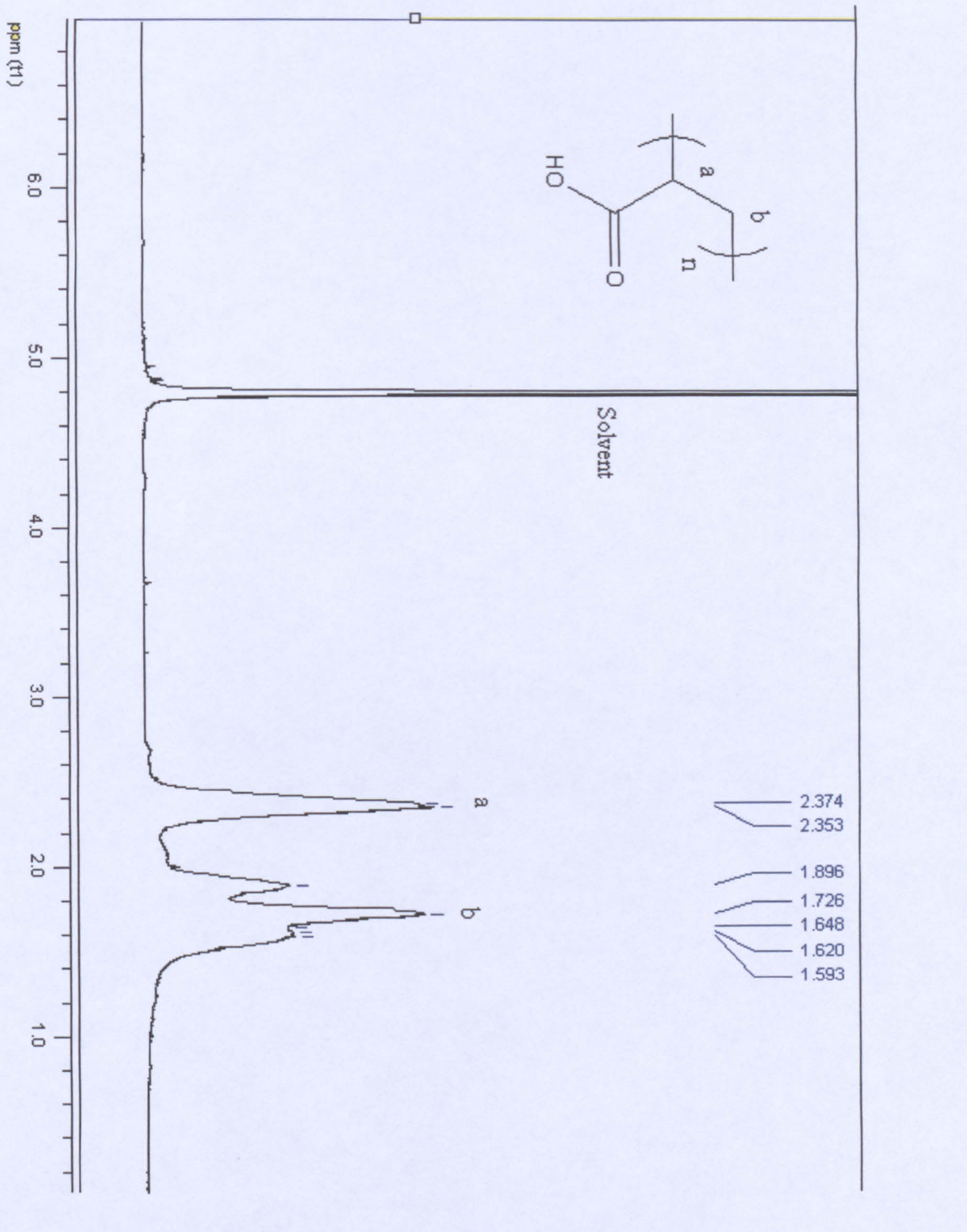
ppm (t1)
6.0
5.0
4.0
3.0
2.0
1.0
HO
O
a
b
n
Solvent
a
b
2.374
2.353
1.896
1.726
1.648
1.620
1.593